

SIDE AIR BAG OUT-OF-POSITION TESTING OF RECENT MODEL YEAR VEHICLES

Allison E. Loudon

National Highway Traffic Safety Administration

United States

Paper Number: 07-213

ABSTRACT

Side air bags are becoming more of a standard feature in the emerging vehicle fleet. These systems appear to offer superior protection in side crashes. Vehicle manufacturers are increasingly adding larger curtains that cover the entire window and two or three rows of seating. Currently, there are not any Federal Motor Vehicle Safety Standards (FMVSS) performance requirements related to the side out-of-position (OOP) performance with respect to side air bags. Therefore, the National Highway Traffic Safety Administration (NHTSA) conducted research tests to monitor this performance in both the front seat and rear seat positions where side air bags deploy.

The NHTSA has been monitoring this performance in recent model years, guided by the Technical Working Group (TWG) Procedures, a document that describes a voluntary set of OOP procedures with the main focus on side air bags, primarily in the front seats. This study uses the Hybrid III 3-year-old, 6-year-old and SID-II_s (5th percentile adult female side impact dummy) dummies in different OOP test modes for all rows in the vehicle. The dummy responses from tests of side air curtains were all below the injury assessment reference values (IARVs). The dummy responses from tests of door and seat-mounted side air bags were also generally below the IARVs, but some OOP orientations in some vehicles did result in responses that were elevated or exceeded the IARVs.

As more vehicles add side air bags as standard features, the NHTSA is monitoring vehicles through Vehicle Safety Research (VSR) and the New Car Assessment Program (NCAP). The agency will continue to monitor how the air bags are affecting the OOP occupants in all near-side seating positions as air bag technology changes resulting from voluntary and federal upgrades. Currently, the NHTSA relies on the manufacturers to provide voluntary feedback on whether they have passed the TWG procedures, in addition to the testing done by VSR and NCAP.

INTRODUCTION

Side air bags started emerging in the vehicle fleet in the mid-to-late 1990s for side occupant protection. In 1999, the NHTSA asked the Alliance of Automobile Manufacturers (Alliance) and the Association of International Automobile Manufacturers (AIAM) to develop a guideline for vehicle manufacturers to assess the risks associated with side air bags and children. The procedures they produced, along with the Insurance Institute of Highway Safety (IIHS) and the Automotive Occupant Restraints Council (AORC), were the "Recommended Procedures for Evaluating Occupant Injury Risk from Deploying Side Air Bags" [1]. This set of guidelines was released to the public in August of 2000.

The NHTSA studied these procedures by procuring several vehicles and conducting numerous tests in both the front and rear seating positions along with various child restraints. The original study used a Hybrid III 3-year-old, 6-year-old, 12-month-CRABI, and a SID-II_s Build Level C dummy. The NHTSA used the Technical Working Group (TWG) procedures as a guideline and recommended several changes to the TWG. These results were documented in the 2001 ESV paper of reference 2. In July of 2003, the TWG document was updated with some of the changes and is currently being used as a guideline by both the NHTSA and the manufacturers for side air bag OOP testing.

In December of 2003, the Auto Alliance announced a voluntary commitment to enhance protection for occupants in side-struck vehicles by improving head protection, which includes making side curtains standard features in most vehicles [3]. In May of 2004, a Notice of Proposed Rulemaking (NPRM) was issued to upgrade the current FMVSS Number 214 "Side Impact Protection". The proposed rule will upgrade the current test procedure and also add an additional side impact test, the oblique pole test.

Manufacturers may need to add or enhance the current side occupant protection designs. This may or may not include side air bags, including roof rail or curtain air bags.

The NHTSA is monitoring these changes to vehicles, especially in the second and third rows of the vehicles. The results presented in this paper are from a small sample of the vehicle fleet from MY2000, MY2004, and MY2005. The OOP tests were conducted by using the TWG procedures as a baseline for the testing and adding additional tests where deemed necessary.

TEST MATRIX

Vehicle Selection – Table 1 shows the vehicles chosen for this study and the styles of air bags and their location.

**Table 1.
Vehicle Selection**

Seat Mounted		Door Mounted	Roof Mounted
Thorax bags	Head/Thorax bags	Thorax bags	Head Bags
2004 Honda Accord	2005 Subaru Forester	2000 BMW 528i (Front and rear)	2000 BMW 528i (Front only)
2004 Volvo XC90	2005 Saab 93 Convertible		2004 Honda Accord
2004 Toyota Sienna			2004 Volvo XC90*
2005 VW Jetta			2004 Toyota Sienna*
2005 Honda CRV			2005 VW Jetta
2005 Toyota Corolla			2005 Honda CRV
2005 Ford 500			2005 Toyota Corolla
			2005 Ford 500

* These vehicles have curtain air bags that cover the 3rd row.

The MY2004 and 2005 vehicles chosen were based on sales, style and safety features. The 2000 BMW

528i used in this study was an original test vehicle used in the previous 2000 study.

All of the vehicles had air curtains and thoracic bags, except for the 2005 Subaru Forester and 2005 Saab 93 convertible. These two vehicles were equipped with combination (head and thorax) air bags.

The 2004 Volvo XC90 and 2004 Toyota Sienna were the only two vehicles in the test matrix that had a third row and that had an air curtain that reached its third row occupant area.

MY2000

The 2000 BMW 528i had thoracic door-mounted air bags in both the front and rear seats. The roof-mounted air bag was a tubular inflatable head protection system that only deployed in the front occupant area. This vehicle was tested using only the SID-II's dummy because the previous study tested with the Hybrid III 3- and 6-year old dummies. [2]

MY2004

There were three vehicles in the MY2004 test matrix: Honda Accord, Toyota Sienna, Volvo XC90. The focus of the testing was to compare how the TWG positions could be used in other rows. All three vehicles had thoracic seat mounted air bags in the front seats and roof-mounted air bags that spanned all of the rows. The 2004 Toyota Sienna had 2nd and 3rd rows with adjustable seat backs. The curtain spanned all three rows. The Volvo XC90 had 2nd and 3rd rows with non-adjustable seat backs. The curtain spanned the front and 2nd rows, and it also had a separate curtain that covered the 3rd row only.

MY2005

The vehicles used in the MY2005 test matrix were a Volkswagen Jetta, Honda CRV, Toyota Corolla, Ford 500, Subaru Forester and Saab 93 convertible. The testing conducted with the MY2005 vehicles focused on the rear seats and how the roof rail mounted air bags affected the occupants. The thoracic air bags in the front seats were also tested. Four of the six vehicles used in the study had an air curtain. The other two vehicles had a combination seat-mounted air bag.

Test Setup

All of the TWG procedures were used, except the thoracic seat-mounted position for a Hybrid III 3-year-old, TWG 3.3.3.4 - Lying on the seat. This test mode was not tested because the thoracic bags would only slightly touch the dummy when fully inflated and were therefore deemed unnecessary for this testing.

**Table 2.
Test Matrix**

			Vehicles									
			2004 Honda Accord	2004 Volvo XC90	2004 Toyota Sienna	2005 Subaru Forester	2005 VW Jetta	2005 Honda CRV	2005 Toyota Corolla	2005 Ford 500	2005 Saab 93 Conv.	2000 BMW 528i
Right Front Seat Thoracic Air Bag	3YO	TWG 3.3.3.1 Fwd Facing on Booster Block	X	X	X	X	X	X	X	X	X	n/a
	3YO	TWG 3.3.3.2: Rwd Facing (peek-a-boo)	X	X	X	X	X	X	X	X	X	n/a
	3YO	TWG 3.3.3.3: Head on Armrest	X	X	X	n/a	n/a	n/a	n/a	n/a	n/a	n/a
	3YO	TWG 3.3.3.4: Lying on Seat	n/a	n/a	n/a	n/a	n/a	n/a	n/a	n/a	n/a	n/a
Right Front Seat Thoracic Air Bag	6YO	TWG 3.3.3.5: Fwd Facing on Booster Block	X	X	X	X	X	X	X	X	X	n/a
	SIDIIs	TWG 3.3.3.6: Inboard Facing	X	X	X	X	X	X	X	X	X	X
Roof Rail Front Seat Air Bag	6YO	TWG 3.3.5.1: Inboard Facing on Booster Block	X	X	X	n/a	X	X	X	X	n/a	n/a
	SIDIIs	TWG 3.3.5.2: Fwd Facing on Raised Seat	X	X	X	n/a	X	X	X	X	n/a	X
	SIDIIs	TWG 3.3.5.3: Inboard Facing on Raised Seat	X	X	X	n/a	X	X	X	X	n/a	X
Roof Rail 2nd Row Seating	3YO*	Back Against Door	n/a	n/a	X	n/a	X	X	X	X	n/a	n/a
	3YO*	On Knees Looking Out	n/a	n/a	X	n/a	X	X	X	X	n/a	n/a
	3YO*	Leaning Sideways on Booster	n/a	n/a	n/a	n/a	X	X	X	X	n/a	n/a
	6YO	TWG 3.3.5.1: Inboard Facing on Booster Block	X	X	X	n/a	n/a	n/a	n/a	n/a	n/a	n/a
	6YO*	Leaning Sideways on Booster	n/a	n/a	n/a	n/a	X	X	X	X	n/a	n/a
	SIDIIS	TWG 3.3.5.2: Fwd Facing	X	X	X	n/a	n/a	n/a	n/a	n/a	n/a	X
Roof Rail 3rd Row Seating	3YO*	Back Against Door	n/a	n/a	X	n/a	n/a	n/a	n/a	n/a	n/a	n/a
	3YO*	On Knees Looking Out	n/a	n/a	X	n/a	n/a	n/a	n/a	n/a	n/a	n/a
	6YO	TWG 3.3.5.1: Inboard Facing on Booster Block	n/a	X	X	n/a	n/a	n/a	n/a	n/a	n/a	n/a
	SIDIIs	TWG 3.3.5.2 Fwd Facing	n/a	X	X	n/a	n/a	n/a	n/a	n/a	n/a	n/a

*NHTSA Procedures

The setup for the right front passenger seat followed the TWG guidelines as follows: Seat in the lowest and rearmost position unless there was interference with the B-Pillar, in which case the seat was moved forward to avoid this interference. The seat back angle was set at the manufacturer's design or 25 degrees. The Toyota Sienna had adjustable seat backs in the 2nd and 3rd rows, which were adjusted 3 notches rearward when testing with the SID-II's dummy. Otherwise, they were tested in the full upright position.

Test Positions - The test configurations were based on the TWG document, July 2003. When the TWG guidelines were written, they focused mainly on the front seat occupant and thoracic style of air bags. Curtain air bags were relatively new when the procedures were first written. They now are common features in the existing fleet and deploy into more than one row. This study looked at the front passenger seat as well as the 2nd and 3rd rows.

The TWG procedures were slightly modified when used in the 2nd and 3rd rows of the vehicles. Table 2 shows the test matrix, and Appendix A has a brief summary of the TWG test procedures.

NHTSA Positions – The TWG document does not have any recommended test procedures for the roof rail system with a Hybrid III 3-year old and is limited to only one test mode for the Hybrid III 6-year-old. In order to fully evaluate the roof rail systems, the NHTSA tested using a few more seating positions. The new seating positions were based on the TWG thoracic seating positions.

The new positions were for the roof rail system for the 2nd and 3rd rows were as follows:

3YO Back Against Door on Booster Block:

Sitting perpendicular to the vehicle door on a foam booster block with the back against the door and with the center of gravity of the head aligned with roof rail air bag opening (Figure 1).



Figure 1. 3YO Back Against Door on Booster Block.

3YO On Knees Looking Out Side Window:

Kneeling, facing out the window, and leaning against door or side window with the center of gravity of the head aligned with the roof rail air bag opening (Figure 2).



Figure 2. 3YO On Knees Looking Out Side Window.

3YO Leaning Sideways on Booster Block:

Sitting on a foam booster block with back against the seat back, with the dummy's head leaning sideways, aligning the center of gravity of the head with the roof rail air bag opening (Figure 3).



Figure 3. 3YO Leaning Sideways on Booster Block.

6YO Leaning Sideways on Booster Block:

Sitting on a foam booster block with back against the seat back, with the dummy’s head leaning sideways, aligning the center of gravity of the head with the roof rail air bag opening (Figure 4).



Figure 4. 6YO Leaning Sideways on Booster Block.

The objective was to gather more information on how small occupants react with the curtain style air bags in various positions in the rear seats. See Appendix A for the details of the new seating positions.

Dummy Instrumentation

The Hybrid III 3- and 6-year-old dummies are frontal impact dummies, and the SIDIIs is a side impact dummy. There are no federalized 3-or 6-year-old side impact dummies available. These are the dummies suggested for use in the TWG guidelines.

The Hybrid III 3- and 6-year-old dummies used in the testing had the following instrumentation: accelerometers in the head, shoulder, chest, ribs,

spine and pelvis; upper and lower 6-axis neck load cells; and a chest displacement potentiometer.

The SID-IIs dummy was instrumented with the following: accelerometers in the head, shoulders, chest, ribs, spine, and pelvis; load cells in the upper and lower neck and shoulder; and displacement potentiometers in the ribs and chest. The study started with the FRG (floating rib guide) dummy (tests SIDIIs_001-018) and finished with Build Level D dummy (SIDIIs_019-037).

Injury Criteria (IARVs)

Table 3 shows the corresponding injury assessment reference values (IARVs) used to determine the probability for injury for each of the dummies. The values represent approximately a 5 percent risk of AIS 4 or greater injury for the head and thorax and an AIS 3 or greater injury for the neck [1]. For each test, the calculated values for 15ms Head Injury Criterion (HIC) and Neck Injury Criterion (Nij), along with the measured peak values for chest deflection, rib deflection, and neck tension and compression were evaluated based on their respective IARV. See the Tables in Appendix B for the normalized dummy responses for each dummy and test configuration.

TABLE 3. Injury Assessment Reference Values (IARV)

	15ms HIC	Chest/Rib* Def. (mm)	Nij	Neck Tension (N)	Neck Comp. (N)
3YO	570	36	1.0	1130	1380
6YO	723	40	1.0	1490	1820
SIDIIs	779	34	1.0	2070	2520

*Rib Deflection used for SIDIIs

TEST RESULTS

There were 96 tests conducted on ten vehicles using three dummies, and three test configurations exceeded one or more IARV. These results were with the Hybrid III 3-year-old and/or 6-year old dummies, and all of these were from the thoracic air bags. There were seven other tests that had elevated responses (above 80% of the normalized IARV), but did not exceed an IARV. The test data with the normalized responses are shown in Appendix B.

Thoracic Air Bags (seat and door mounted):

All of the vehicles used in this study had a type of thoracic air bag for the front occupant. Seven of the ten vehicles had a thoracic only seat mounted air bag that was located in the front seats. One vehicle, the

2000 BMW 528i, had thoracic door mounted air bags in the front and rear doors (Figure 5). The other two vehicles, a 2005 Subaru Forester and 2005 Saab 93 convertible had a combination air bag located in the front seat (Figure 6). Of the 42 tests conducted with thoracic air bags, only three tests exceeded the IARV and seven tests had elevated responses in the chest and/or rib deflection or with the neck injury. All of the 15ms HIC values were negligible.



Figure 5. 2000 BMW 528i Door Mounted Air Bag.



Figure 6. 2005 Subaru Forester Combination Air Bag.

TWG 3.3.3.1 (Figure 7) places the Hybrid III 3-year-old against the seat edge with its head/neck junction at the top edge of the air bag module. This test mode produced neck responses that were elevated or exceeded the IARV in one of the nine vehicles tested in this mode. The Hybrid III 3-year-old exceeded the neck tension IARV and had an elevated Nij response in the test mode TWG 3.3.3.1 for the 2005 Honda CRV. As the air bag deployed it punched through the seat cover and caused direct loads onto the neck.



Figure 7. Hybrid III 3-year-old Position TWG 3.3.3.1.

TWG 3.3.3.2 (Figure 8) places the chest at the top edge of the air bag module. It also produced higher responses, with four of the nine vehicles having chest

deflections, Nij, or Neck Tension responses that were elevated or that exceeded the IARV.



Figure 8. Hybrid III 3-year-old Position TWG 3.3.3.2.

The Hybrid III 3-year old exceeded the chest deflection IARV in the 2005 Subaru Forester test with a normalized response of 1.03. The 2004 Volvo XC90 had elevated response in the front passenger seat for the chest deflection, Nij, and neck tension with normalized response values of 0.88, 0.87, and 0.97, respectively. The 2005 Ford 500 had an Nij response of 0.84, while the chest deflection for the 2004 Toyota Sienna was 0.90. As the air bag emerges from the seat, the dummy's chest is directly loaded causing higher responses.

TWG 3.3.3.5 places the Hybrid III 6-year-old dummy's neck/torso junction with the top edge of the air bag module. The 2005 Subaru Forester exceeded the Nij response and the 2004 Honda Accord had an elevated response with this test mode. As the air bag was deployed, the torso moved forward and the neck was put into extension. Figure 9 shows the Hybrid III 6-year-old during the Subaru Forester test. Similar dummy kinematics were also seen with the Hybrid III 3-year-old in the test mode of TWG 3.3.3.1.



Figure 9. Hybrid III 6YO (Test no. 6YO_015) With Deploying Air Bag.

The 2000 BMW 528i was only tested with the SID-IIs dummy, which resulted in elevated responses of the rib deflection for both the front and rear door mounted air bags, test condition TWG 3.3.4.5.

The two vehicles that exceeded the IARV responses were 2005 Subaru Forester and 2005 Honda CRV. These vehicles were certified by the manufacturer, and reported to the NHTSA, as meeting all of the qualified TWG guidelines [6]. Further research and comparison testing would be needed to explain the different results.

Curtain Air Bags (roof rail mounted):

There were 54 tests conducted on eight vehicles with the roof rail systems resulting in low response values (below 70% of all of the IARVs). Thirty-two tests were conducted with the Hybrid III 3-year-old and 6-year old dummies. Twenty-two of the tests were conducted with the SID-IIs dummy. The 15ms HIC responses were negligible for all three dummies.

The new NHTSA procedures used with the Hybrid III 3-year-old and 6-year-old dummies, positioned the heads in various locations. All the normalized responses were below 60% of the Nij IARV values. The 2004 Toyota Sienna Hybrid III 3-year-old NHTSA position “Back against door” in the second row had the highest response with a 0.60 Nij response value.

The Hybrid III 6-year-old and SID-IIs dummies were tested in all three rows of the 2004 Volvo XC90 and Toyota Sienna. The test modes were TWG 3.3.5.1 and TWG 3.3.5.2. The dummies were positioned according to the TWG guidelines in all three rows, which typically placed the head in the same lateral plane in all three rows. The air bag produced similar responses when tested with the same dummy and same seating positions for the various rows.

The 2004 Toyota Sienna had a curtain that spanned all three rows. The Nij responses for the Hybrid III 6-year-old dummy were similar for all three rows. When tested with the SID-IIs dummy, the 2nd row produced slightly lower responses for both the Nij and Neck Compression. (Figure 10)

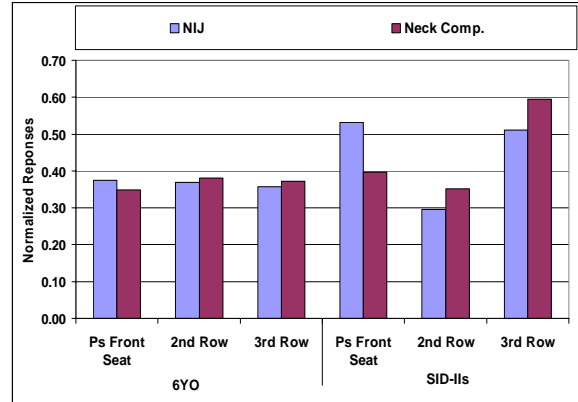


Figure 10. Hybrid III 6YO TWG 3.3.5.1 and SID-IIs TWG 3.3.5.2 Responses for the 2004 Toyota Sienna.

The 2004 Volvo XC90 produced similar findings except that the 3rd row positions produced higher results than the 1st and 2nd rows (Figure 11). There is an individual curtain for the 3rd row that is deployed at the same time as the 1st and 2nd row curtain. See Figures 12 and 13.

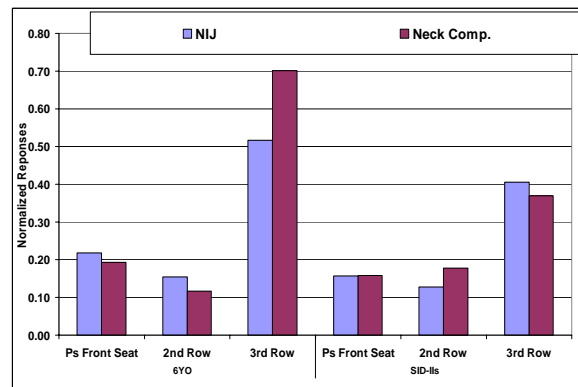


Figure 11. Hybrid III 6YO TWG 3.3.5.1 and SID-IIs TWG 3.3.5.2 Responses for the 2004 Volvo XC90.



Figure 12. 2004 Volvo XC90 2nd row curtain.



Figure 13. 2004 Volvo XC90 3rd row curtain.

Five vehicles were tested by positioning the SID-IIs dummy in the test condition TWG 3.3.5.2 with the curtain and the thoracic air bags both deployed. This resulted in one vehicle, the 2000 BMW 528i, with an elevated response in the rib deflection. This elevated

response was from the thoracic bag and not the curtain bag.

In some instances, the curtain pushed the dummy toward the side window, which placed the dummy in between the side window and the curtain (Figure 14). This occurred in approximately 30% of the roof rail tests conducted. The vehicles in which this result occurred were the 2004 Honda Accord, 2005 Toyota Corolla, 2005 VW Jetta, and 2005 Honda CRV.

This may be a finding that will require further investigation of OOP testing conditions and how the dummy is positioned for the curtain test. Currently, the center of gravity of the dummy's head is aligned with the deployment path of the roof rail module. Therefore, the trajectory of the dummy upon curtain deployment may be sensitive to the precise impact location relative to the dummy head center of gravity. In that case, just slight variations in dummy positioning or the direction of curtain deployment may affect the outcome.



Figure 14. Curtain deployments in different vehicles with the different dummies.

OBSERVATIONS

Even though there is not an FMVSS performance requirement for side air bags, the out of position testing showed these air bags generally should not produce serious injury to small occupants in all rows of the vehicle. Ninety-seven percent (97%) of the

tests conducted met or passed all of the proposed injury values.

Of the 42 tests conducted with thoracic air bags, only three tests exceeded an IARV, and seven other tests had elevated responses in the chest and/or rib deflection or with the neck injury.

Two of the three tests that exceeded an IARV were with the Hybrid III 3-year-old in the 2005 Honda CRV and the 2005 Subaru Forester. The third was with the Hybrid III 6-year-old, also in the Forester.

The curtain or roof rail mounted air bags produced relatively low numbers in all rows with all three dummies. The 15ms HIC values were negligible in this testing for all three dummies. The neck injury values were somewhat higher, but still relatively low. The highest Nij and neck tension values were 60% and 70% of the IARV, respectively.

The curtain air bags in the 2004 Volvo XC90 and Toyota Sienna generally produced similar results between the rows when tested with the SID-IIs and Hybrid III 6-year-old dummies. The exception was the 3rd row air curtain in the Volvo, which was a separate bag than that for the first two rows. It produced neck responses somewhat higher than the curtain for the front rows.

The TWG seating procedure guidelines can be used in all the rows with little or no modifications. Additional test positions for the roof mounted air bags, such as the NHTSA procedures with the Hybrid III 3- and 6-year-old dummies introduced in this paper, would provide a more thorough OOP evaluation.

REFERENCES

1. The Side Air Bag Out-of-Position Injury Technical Working Group (TWG), Adrian Lund (IHS) Chairman, "Recommended Procedures for Evaluating Occupant Injury Risk from Deploying Side Air Bags", August 2000 and July 2003.
2. Prasad, Alope, Samaha, Randa, Loudon, Allison "Evaluation of Injury Risk from Side Impact Air Bags", Paper Number 331, ESV Conference 2001.
3. Alliance of Automotive Manufacturers, "Automakers Compatibility Commitment: Improving Everyone's Safety Through Voluntary Industry Cooperation", December 2003.

4. Department of Transportation Federal Register, “Federal Motor Vehicle Safety Standards; Side Impact Protection; Side Impact Phase-In Reporting Requirements”, May 17, 2004.

5. NHTSA FMVSS 214, Side Impact Protection, <http://nhtsa.gov/cars/rules/standards/FMVSS-Regs/pages/TOC.htm>

6. NHTSA website, <http://safercar.gov/NCAP/>

APPENDIX A: SEATING GUIDELINES

The Technical Working Group Guidelines: “Recommended Procedures for Evaluating Occupant Injury Risk from Deploying Side Air Bags”, July 2003 revision document was used in this research study. The following is a brief seating summary for reference purposes.

Tests Conducted following TWG guidelines:

Hybrid III 3YO

- TWG 3.3.3.1: Sitting on seat edge on a booster, with head neck junction aligned with the top edge of the air bag module
- TWG 3.3.3.2: Kneeling on seat edge facing rearward, upper rib aligned with the top edge of the air bag module
- TWG 3.3.3.3: Lying on seat, perpendicular to the door, with the head on the armrest, with the center of gravity of the head aligned with the vertical centerline of the air bag module.

Hybrid III 6YO

- TWG 3.3.3.5: Sitting on seat edge on a booster, with the lower neck junction aligned with the top edge of the air bag module
- TWG 3.3.5.1: Sitting on foam booster perpendicular to door, with the center of gravity of the head aligned with the deployment path of the roof mounted air bag

SID-IIs

- TWG 3.3.3.6: Sitting on the outboard seat edge, perpendicular to the door, with the center of the first rib aligned with the top of the air bag module.
- TWG 3.3.5.2: Sitting on the outboard seat edge facing forward, with the center of gravity of the head aligned with the deployment path of the roof mounted air bag; dummy may be leaning slightly outboard.
- TWG 3.3.5.3: Sitting perpendicular to the door at the outboard edge of seat, with the center of gravity of the head aligned with the deployment path of the roof module at the forward most point to minimize the vertical distance.

The new NHTSA Test Procedures were created using the TWG seating as a baseline. The following is a brief summary of how the dummies were seated.

Hybrid III 3YO and 6YO:

3YO Back Against Door on Booster Block: Sitting on a foam booster block, perpendicular to the vehicle door, with the back resting against the door, and with the center of gravity of the head aligned with the roof rail air bag opening.

3YO On Knees Looking Out Side Window: Kneeling, facing outward, and leaning against the door or side window with center of gravity of the head aligned with the roof rail air bag opening.

3YO Leaning Sideways on Booster Block: Sitting on a foam booster block, with back against the seat back and leaning sideways, with the center of gravity of the head aligned with the roof rail air bag opening.

6YO Leaning Sideways on Booster Block: Sitting on a foam booster block, with back against the seat back and leaning sideways, with the center of gravity of the head aligned with the roof rail air bag opening.

APPENDIX B: NORMALIZED RESPONSE TABLES

Table A: Hybrid III 3YO Normalized Test Results

Vehicle	Test Number	Test Position	Air bag deployed	Seating position	15ms HIC	Chest Def.(mm)	NIJ	Neck Tension(N)	Neck Comp.(N)
04 Honda Accord	3YOSOOP_01	TWG 3.3.3.1	Thoracic	Ps Front Seat	0.10	0.06	0.32	0.53	0.25
04 Toyota Sienna	3YOSOOP_07	TWG 3.3.3.1	Thoracic	Ps Front Seat	0.01	0.07	0.32	0.16	0.16
04 Volvo XC90	3YOSOOP_04	TWG 3.3.3.1	Thoracic	Ps Front Seat	0.11	0.08	0.57	0.37	0.28
05 Ford 500*	3YO_036	TWG 3.3.3.1*	Thoracic+Curtain	RT FR Seat	0.04	0.06	0.52	0.58	0.16
05 Honda CRV	3YO_038	TWG 3.3.3.1	Thoracic	RT FR Seat	0.12	0.13	0.95	1.04	0.17
05 Saab 93	3YO_028	TWG 3.3.3.1	Combination	RT FR Seat	0.04	0.09	0.53	0.59	0.15
05 Subaru Forester	3YO_035	TWG 3.3.3.1	Combination	RT FR Seat	0.09	0.11	0.73	0.54	0.22
05 Toyota Corolla*	3YO_031	TWG 3.3.3.1*	Thoracic+Curtain	RT FR Seat	0.03	0.03	0.28	0.19	0.07
05 VW Jetta	3YO_033	TWG 3.3.3.1	Thoracic	RT FR Seat	0.01	0.04	0.28	0.25	0.04
04 Honda Accord	3YOSOOP_02	TWG 3.3.3.2	Thoracic	Ps Front Seat	0.00	0.37	0.32	0.29	0.04
04 Toyota Sienna	3YOSOOP_08	TWG 3.3.3.2	Thoracic	Ps Front Seat	0.00	0.90	0.36	0.42	0.06
04 Volvo XC90	3YOSOOP_05	TWG 3.3.3.2	Thoracic	Ps Front Seat	0.12	0.88	0.87	0.97	0.14
05 Ford 500	3YO_037	TWG 3.3.3.2	Thoracic	RT FR Seat	0.02	0.70	0.84	0.74	0.01
05 Honda CRV	3YO_039	TWG 3.3.3.2	Thoracic	RT FR Seat	0.00	0.15	0.25	0.17	0.05
05 Saab 93	3YO_030	TWG 3.3.3.2	Combination	RT FR Seat	0.01	0.48	0.58	0.37	0.03
05 Subaru Forester	3YO_015	TWG 3.3.3.2	Combination	RT FR Seat	0.04	1.03	0.49	0.64	0.06
05 Toyota Corolla	3YO_032	TWG 3.3.3.2	Thoracic	RT FR Seat	0.00	0.08	0.19	0.10	0.02
05 VW Jetta	3YO_034	TWG 3.3.3.2	Thoracic	RT FR Seat	0.01	0.36	0.67	0.45	0.16
04 Honda Accord	3YOSOOP_03	TWG 3.3.3.3	Thoracic	Ps Front Seat	0.02	0.01	0.10	0.10	0.10
04 Toyota Sienna	3YOSOOP_09	TWG 3.3.3.3	Thoracic	Ps Front Seat	0.00	0.00	0.05	0.06	0.03
04 Volvo XC90	3YOSOOP_06	TWG 3.3.3.3	Thoracic	Ps Front Seat	0.01	0.01	0.13	0.24	0.07
04 Toyota Sienna -	3YO_011	Back against Door	Curtain	2nd Row Seat	0.01	0.01	0.60	0.04	0.48
04 Toyota Sienna -	3YO_010	Back against Door	Curtain	3rd Row Seat	0.00	0.01	0.22	0.03	0.19
05 Ford 500	3YO_025	Back against Door	Curtain	RT RR Seat	0.01	0.01	0.30	0.01	0.11
05 Honda CRV	3YO_019	Back against Door	Curtain	RT RR Seat	0.01	0.01	0.14	0.03	0.17
05 Toyota Corolla	3YO_022	Back against Door	Curtain	RT RR Seat	0.01	0.01	0.14	0.05	0.18
05 VW Jetta	3YO_016	Back against Door	Curtain	RT RR Seat	0.01	0.00	0.08	0.03	0.07

Exceeds IARV

Elevated Response (80% to 99% of IARV)

Under 80% of IARV

APPENDIX B: NORMALIZED RESPONSE TABLES

Table A: Hybrid III 3YO Normalized Test Results Continued

Vehicle	Test Number	Test Position	Air bag deployed	Seating position	15ms HIC	Chest Def.(mm)	NIJ	Neck Tension(N)	Neck Comp.(N)
05 Ford 500	3YO_027	Leaning Sideways on Booster	Curtain	RT RR Seat	0.00	0.06	0.20	0.00	0.28
05 Honda CRV	3YO_021	Leaning Sideways on Booster	Curtain	RT RR Seat	0.01	0.01	0.07	0.00	0.01
05 Toyota Corolla	3YO_024	Leaning Sideways on Booster	Curtain	RT RR Seat	0.00	0.00	0.10	0.05	0.08
05 VW Jetta	3YO_018	Leaning Sideways on Booster	Curtain	RT RR Seat	0.00	0.01	0.25	0.02	0.21
04 Toyota Sienna -	3YO_012	On knees looking out	Curtain	2nd Row Seat	0.01	0.00	0.28	0.03	0.31
04 Toyota Sienna -	3YO_013	On knees looking out	Curtain	3rd Row Seat	0.00	0.00	0.11	0.04	0.12
05 Ford 500	3YO_026	On knees looking out	Curtain	RT RR Seat	0.00	0.00	0.14	0.01	0.14
05 Honda CRV	3YO_020	On knees looking out	Curtain	RT RR Seat	0.02	0.02	0.54	0.16	0.36
05 Toyota Corolla	3YO_023	On knees looking out	Curtain	RT RR Seat	0.02	0.01	0.32	0.04	0.43
05 VW Jetta	3YO_017	On knees looking out	Curtain	RT RR Seat	0.00	0.00	0.18	0.08	0.17

Exceeds IARV

Elevated Response (80% to 99% of IARV)

Under 80% of IARV

APPENDIX B: NORMALIZED RESPONSE TABLES

Table B: Hybrid III 6YO Normalized Test Results

Vehicle	Test Number.	Test Position	Air Bag Deployed	Seating position	15ms HIC	Chest Def.(mm)	NIJ	Neck Tension(N)	Neck Comp.(N)
04 Honda Accord	6YOSOOP_02	TWG 3.3.3.5	Thoracic	Ps Front Seat	0.01	0.05	0.80	0.28	0.27
04 Toyota Sienna	6YOSOOP_08	TWG 3.3.3.5	Thoracic	Ps Front Seat	0.00	0.04	0.25	0.04	0.12
04 Volvo XC90	6YOSOOP_03	TWG 3.3.3.5	Thoracic	Ps Front Seat	0.01	0.05	0.67	0.22	0.31
05 Ford 500	6YO_027	TWG 3.3.3.5	Thoracic	RT FR Seat	0.01	0.04	0.66	0.37	0.15
05 Honda CRV	6YO_028	TWG 3.3.3.5	Thoracic	RT FR Seat	0.01	0.02	0.64	0.20	0.12
05 Saab 93	6YO_024	TWG 3.3.3.5	Combination	RT FR Seat	0.01	0.04	0.46	0.33	0.06
05 Subaru Forester	6YO_015	TWG 3.3.3.5	Combination	RT FR Seat	0.07	0.09	1.20	0.47	0.39
05 Toyota Corolla	6YO_025	TWG 3.3.3.5	Thoracic	RT FR Seat	0.01	0.03	0.41	0.13	0.16
05 VW Jetta	6YO_026	TWG 3.3.3.5	Thoracic	RT FR Seat	0.00	0.01	0.22	0.04	0.15
04 Honda Accord	6YOSOOP_01	TWG 3.3.5.1	Curtain	Ps Front Seat	0.01	0.01	0.47	0.00	0.43
04 Honda Accord	6YOSOOP_05	TWG 3.3.5.1	Curtain	Ps Rear Seat	0.00	0.13	0.16	0.01	0.21
04 Toyota Sienna	6YOSOOP_07	TWG 3.3.5.1	Curtain	Ps Front Seat	0.04	0.01	0.38	0.01	0.35
04 Toyota Sienna	6YOSOOP_09	TWG 3.3.5.1	Curtain	2nd Row	0.01	0.01	0.37	0.20	0.38
04 Toyota Sienna	6YOSOOP_10	TWG 3.3.5.1	Curtain	3rd Row	0.00	0.00	0.36	0.00	0.37
04 Volvo XC90	6YOSOOP_06	TWG 3.3.5.1	Curtain	Ps Front Seat	0.00	0.00	0.22	0.01	0.19
04 Volvo XC90	6YOSOOP_04	TWG 3.3.5.1	Curtain	2nd Row	0.00	0.00	0.15	0.00	0.12
04 Volvo XC90	6YOSOOP_11	TWG 3.3.5.1	Curtain	3rd Row	0.05	0.01	0.52	0.00	0.70
05 VW Jetta	6YO_016	Back against Door	Curtain	RT RR Seat	0.00	0.01	0.19	0.06	0.16
05 Honda CRV	6YO_018	Back against Door	Curtain	RT RR Seat	0.01	0.01	0.27	0.01	0.24
05 Toyota Corolla	6YO_020	Back against Door	Curtain	RT RR Seat	0.00	0.01	0.17	0.04	0.23
05 Ford 500	6YO_022	Back against Door	Curtain	RT RR Seat	0.01	0.00	0.34	0.01	0.35
05 VW Jetta	6YO_017	Leaning Sideways on Booster	Curtain	RT RR Seat	0.01	0.01	0.22	0.02	0.25
05 Honda CRV	6YO_019	Leaning Sideways on Booster	Curtain	RT RR Seat	0.00	0.01	0.23	0.01	0.25
05 Toyota Corolla	6YO_021	Leaning Sideways on Booster	Curtain	RT RR Seat	0.01	0.01	0.20	0.01	0.29
05 Ford 500	6YO_023	Leaning Sideways on Booster	Curtain	RT RR Seat	0.00	0.00	0.43	0.01	0.51

Exceeds IARV

Elevated Response (80% to 99% of IARV)

Under 80% of IARV

APPENDIX B: NORMALIZED RESPONSE TABLES

Table C: SID-IIs Normalized Test Results

Vehicle	Test Number	Test Position	Air Bag	Seating position	15ms HIC	Rib Def. (mm)	NIJ	Neck Tension(N)	Neck Comp.(N)
04 Honda Accord	SOOP_SID2S_003	TWG 3.3.3.6	Thoracic	Ps Front Seat	0.00	0.22	0.18	0.06	0.08
04 Toyota Sienna	SOOP_SID2S_010	TWG 3.3.3.6	Thoracic	Ps Front Seat	0.00	0.29	0.09	0.06	0.06
04 Volvo XC90	SOOP_SID2s_018	TWG 3.3.3.6	Thoracic	Ps Front Seat	0.00	0.39	0.15	0.10	0.14
05 Subaru Forester	SIDIIIs_036	TWG 3.3.3.6 (LSC)	Combination	Ps Front Seat	0.00	0.39	0.22	0.18	0.07
05 Subaru Forester	SIDIIIs_037	TWG 3.3.3.6 (LSC)	Combination	Ps Front Seat	0.00	0.39	0.21	0.13	0.08
05 Ford 500	SIDIIIs_031	TWG 3.3.3.6 (LSC)	Thoracic	Ps Front Seat	0.00	0.05	0.10	0.06	0.06
05 Honda CRV	SIDIIIs_033	TWG 3.3.3.6 (LSC)	Thoracic	Ps Front Seat	0.00	0.30	0.09	0.07	0.08
05 Saab 93	SIDIIIs_032	TWG 3.3.3.6 (LSC)	Thoracic	Ps Front Seat	0.01	0.57	0.12	0.15	0.07
05 Toyota Corolla	SIDIIIs_035	TWG 3.3.3.6 (LSC)	Thoracic	Ps Front Seat	0.00	0.23	0.12	0.06	0.11
05 VW Jetta	SIDIIIs_034	TWG 3.3.3.6 (LSC)	Thoracic	Ps Front Seat	0.00	0.21	0.08	0.04	0.08
00 BMW 528i	SIDIIIs_019	TWG 3.3.4.5 (RSC)	Thoracic Door	Ps Front Seat	0.00	0.93	0.07	0.09	0.10
00 BMW 528i	SIDIIIs_020	TWG 3.3.4.5 (RSC)	Thoracic Door	Ps Rear Seat	0.05	0.88	0.21	0.51	0.17
04 Honda Accord	SOOP_SID2S_001	TWG 3.3.5.2	Curtain	Ps Front Seat	0.00	n/a	0.48	0.00	0.70
04 Toyota Sienna	SOOP_SID2S_008	TWG 3.3.5.2	Curtain	Ps Front Seat	0.01	n/a	0.53	0.02	0.40
04 Volvo XC90	SOOP_SID2s_005	TWG 3.3.5.2	Curtain	Ps Front Seat	0.00	n/a	0.16	0.01	0.16
04 Volvo XC90	SOOP_SID2s_013	TWG 3.3.5.2	Curtain	2nd Row	0.00	n/a	0.13	0.00	0.18
04 Volvo XC90	SOOP_SID2s_014	TWG 3.3.5.2	Curtain	3rd Row	0.02	n/a	0.41	0.01	0.37
04 Toyota Sienna	SOOP_SID2S_011	TWG 3.3.5.2	Curtain	2nd Row	0.00	n/a	0.30	0.02	0.35
04 Toyota Sienna	SOOP_SID2S_017	TWG 3.3.5.2	Curtain	3rd Row	0.02	n/a	0.51	0.00	0.59
05 Ford 500	SIDIIIs_029	TWG 3.3.5.2 (R S C)	Curtain + Thoracic	Ps Front Seat	0.00	0.13	0.09	0.05	0.21
05 Honda CRV	SIDIIIs_023	TWG 3.3.5.2 (R S C)	Curtain + Thoracic	Ps Front Seat	0.02	0.31	0.29	0.05	0.63
05 Toyota Corolla	SIDIIIs_025	TWG 3.3.5.2 (R S C)	Curtain + Thoracic	Ps Front Seat	0.01	0.01	0.11	0.14	0.25
05 VW Jetta	SIDIIIs_027	TWG 3.3.5.2 (R S C)	Curtain + Thoracic	Ps Front Seat	0.01	0.17	0.29	0.06	0.66
04 Honda Accord	SOOP_SID2S_015	TWG3.3.5.2	Curtain	Ps Rear Seat	0.00	n/a	0.14	0.01	0.16
04 Honda Accord	SOOP_SID2S_016	TWG3.3.5.2	Curtain	Ps Rear Seat	0.00	n/a	0.14	0.02	0.15
00 BMW 528i	SIDIIIs_021	TWG 3.3.5.2 (RSC)	Curtain + Thoracic	Ps Front Seat	0.02	0.88	0.34	0.02	0.63
04 Honda Accord	SOOP_SID2S_002	TWG 3.3.5.3	Curtain	Ps Front Seat	0.01	n/a	0.46	0.00	0.43
04 Toyota Sienna	SOOP_SID2S_009	TWG 3.3.5.3	Curtain	Ps Front Seat	0.07	n/a	0.28	0.01	0.34
04 Volvo XC90	SOOP_SID2s_006	TWG 3.3.5.3	Curtain	Ps Front Seat	0.00	n/a	0.18	0.01	0.25
00 BMW 528i	SIDIIIs_022	TWG 3.3.5.3 (RSC)	Curtain	Ps Front Seat	0.01	0.04	0.31	0.00	0.68
05 Ford 500	SIDIIIs_030	TWG 3.3.5.3 (RSC)	Curtain	Ps Front Seat	0.00	0.00	0.10	0.00	0.14
05 Honda CRV	SIDIIIs_024	TWG 3.3.5.3 (RSC)	Curtain	Ps Front Seat	0.01	0.01	0.16	0.04	0.28
05 Toyota Corolla	SIDIIIs_026	TWG 3.3.5.3 (RSC)	Curtain	Ps Front Seat	0.02	0.01	0.45	0.23	0.65
05 VW Jetta	SIDIIIs_028	TWG 3.3.5.3 (RSC)	Curtain	Ps Front Seat	0.01	0.01	0.27	0.01	0.62

Exceeds IARV

Elevated Response (80% to 99% of IARV)

Under 80% of IARV

Status of NHTSA's Hydrogen and Fuel Cell Vehicle Safety Research Program
Barbara C. Hennessey
Nha T. Nguyen

National Highway Traffic Safety Administration
USA
Paper No. 07-0046

Abstract

The FreedomCAR and Fuel Initiative is a cooperative automotive research partnership between the U.S. Department of Energy, the U.S. Council for Automotive Research (USCAR), and fuel suppliers. It was initiated in 2002 as part of the President's goal to reduce U.S. dependence on foreign oil, improve vehicle efficiency, reduce emissions, and make hydrogen fuel cell vehicles (HFCVs) a practical and cost-effective choice for large numbers of Americans by 2020.

Following the announcement of the FreedomCAR program, NHTSA began collecting information on the status of hydrogen vehicle technology and drafting a research plan to address the impact of fuel cell and hydrogen fuel systems on vehicle safety. In 2004 NHTSA published the plan in the Federal Register for public comment and issued a voluntary request to manufacturers asking them to provide written information on their strategies to ensure that hydrogen fueled vehicles attain a level of safety comparable to that of conventionally fueled vehicles [1]. Additionally, NHTSA published an updated version of this plan for the 19th Enhanced Safety of Vehicles Conference [2].

Funding to initiate NHTSA's hydrogen safety research program was not made available until 2006. This paper provides a status report on several projects assessing hydrogen fuel system safety that were initiated that year, and the follow-on work that will be conducted in 2007.

Introduction

NHTSA's mission is to save lives, prevent injuries, and reduce vehicle related crashes, which it does through a variety of means including testing and statistical research, regulation and enforcement, and educational programs. Often a safety problem will be identified through statistical analysis of real world crash data or reported failures, and then a test program is executed to determine the cause and to assess remedial strategies.

Previous reports have identified fuel system integrity as the unique safety challenge in hydrogen and fuel cell vehicles [1,2]. Current Federal Motor Vehicle Safety Standards (FMVSS) for fuel system integrity set performance criteria to limit crash induced leakage in vehicles powered by liquid fuels and compressed natural gas, and impose post-crash electrical isolation and electrolyte spillage limits for electric vehicles [3]. However, no analogous regulations currently exist in the U.S. to ensure fuel system integrity for hydrogen or fuel cell systems because crash integrity information does not exist to support data-driven performance requirements. Research is required to assess the unique characteristics of hydrogen and fuel cell propulsion system safety performance in crashes.

Hydrogen is colorless, odorless and difficult to contain when compared to conventional fuels like gasoline, diesel, and compressed natural gas. Its flammability, buoyancy, and dispersion properties are different; and it can cause embrittlement of some metals, which could lead to failure of fuel lines and other components. Hydrogen storage methods range from very high-pressure gas storage to cryogenic liquid, and chemical and solid metal hydrides. Each of these storage methods presents specific hazards should the containment fail due to a crash or defect in fail-safe design. Because fuel cells are electrical devices they operate at high voltage and currents so that electrical shock, isolation, and ignition of surrounding materials are issues to be considered in a safety assessment.

In addition to the challenges presented above concerning fuel handling and fuel system architecture of hydrogen and fuel cell vehicles, there are more practical concerns that set them apart from conventionally fueled vehicles in terms of safety assessment.

First, there is a lack of real world safety performance data because the vehicle population is very small. Hydrogen fuel cell vehicles number only in the hundreds worldwide, are used under strictly controlled conditions in demonstration fleets, and are typically accompanied by trained personnel from the manufacturers that build them. The vehicles are

prototypes and preproduction prototypes for which very few of a given model exists. Because they are experimental vehicles, they are also usually over-engineered to meet more stringent safety factors than those to which a typical production vehicle would be built. If any particular safety issue comes up in the demonstration of the vehicle, the manufacturer is on hand to pull it out of service and repair or retire it immediately based on assessment of the problem. Because these vehicles are managed so closely, there is no history associated with them of real world driving experience, maintenance, aging, or crash exposure.

A second issue which affects the practical aspect of assessing hydrogen fueled vehicle safety is the cost and availability of components and vehicles to test. Vehicles are not currently available on the open market for purchase and testing. Other than testing conducted in-house by manufacturers, the results of which are proprietary, there is no opportunity at this time for an independent safety assessment of vehicle crashworthiness.

A third concern is the relevance of any safety assessment that is conducted on prototype vehicles or their components. As mentioned earlier, prototypes are expensive, low production vehicles that may be over-designed for safety and utilize components, materials, and packaging architectures that are not representative of designs that will eventually be mass-produced for the market.

Despite these challenges, a strong interest in effecting a safe transition to hydrogen and fuel cell vehicles is supported by government and industry worldwide. This support has been critical to the implementation of NHTSA's research program. Collaboration and cooperation is essential to promoting a comprehensive safety initiative that will provide benefits to consumers, the economy, and the environment.

Objective

The objective of this research program is to assess fuel system integrity of hydrogen and fuel cell vehicles through real world data collection, research testing, and analysis. This assessment will ultimately support promulgation of FMVSS and Global Technical Regulations (GTRs) that afford an equivalent level of safety to vehicle occupants, emergency response personnel, and the public, to that provided by enforcement of the existing fuel system integrity requirements for conventionally fueled vehicles.

Status of 2006 Research Projects

Four safety assessment projects were initiated in 2006 for hydrogen and fuel cell vehicles. These projects were selected in conjunction with market research consisting of collaborative talks with stakeholders in government and industry on the scope of near-term research topics, the state of recommended practices ensuring fuel system safety performance, and the availability of test articles from which useful test protocols could be developed and executed to assess a subset of fuel system safety issues at the component and subsystem levels. It is anticipated that the results of these projects form a foundation for a future assessment of fuel system integrity and fire safety at the full vehicle level.

Projects are discussed in the order of their initiation:

Project 1: Evaluation and Comparative Assessment of the Fuel System Integrity Performance Requirements of Existing Industry Standards and Government Regulations

NHTSA is actively working with other countries and international communities to develop GTRs for vehicle safety under a Program of Work of the 1998 Global Agreement administered by the United Nations World Forum for the Harmonization of Vehicle Regulations. Consequently, NHTSA has been collaborating with international partners to develop a GTR for hydrogen fuel cell vehicles. The effort, which was formally kicked off in FY 2006, seeks to ensure the development of a comprehensive, performance-based and data driven GTR that would ensure the integrity and safety of hydrogen fuel cell powered passenger vehicles. A GTR is desirable because it would enable manufacturers to build vehicles for a global market, easing the economic burden of producing vehicles designed to meet divergent national and regional regulatory safety requirements.

There are several Standards Developing Organizations (SDOs) and regulatory bodies that have issued final or draft requirements for hydrogen fuel cell vehicle safety. During the development of a GTR or FMVSS, these standards and regulations can be used as the basis for technical discussion. In order to better understand these requirements, NHTSA is conducting a comparative assessment of those standards, directives and regulations specific to onboard vehicle fuel system safety and crashworthiness at the component, system, and full vehicle levels. Table 1 shows a list of the standards

under consideration at this time. Culmination of this project will result in a final report detailing similarities, redundancies, and differences in performance and design restrictive requirements of

each standard. This study is being conducted by Battelle Memorial Institute under NHTSA contract. The final report will be made available in 2007.

Table 1: Standards for Fuel System Integrity of HFCVs

Standard	Title/Description
SAE J2578	Recommended Practice for General Fuel Cell Vehicle Safety
SAE J2579	Recommended Practice for Fuel Systems in Fuel Cell and Other Hydrogen Vehicles (draft)
ISO 23273-1	Fuel Cell Road Vehicles – Safety Specifications – Part 1: Vehicle Functional Safety
ISO 23273-2	Fuel Cell Road Vehicles – Safety Specifications – Part 2: Protection Against Hydrogen Hazards for Vehicles Fueled with Compressed Hydrogen
ISO/DIS 23273-3	Fuel Cell Road Vehicles – Safety Specifications – Part 3: Protection of Persons Against Electrical Shock
WP.29 Draft Standard for Compressed Gaseous Hydrogen	Proposal for a New Draft Regulation for Vehicles Using Compressed Hydrogen
WP.29 Draft Standard for Liquid Hydrogen	Proposal for a New Draft Regulation for Vehicles Using Liquid Hydrogen
Japanese HFCV Regulations	Attachment 17, 100, 101
CSA HGV2	Standard Hydrogen Vehicle Fuel Containers (Draft)
CSA HPRD1	Standards for Basic Requirements for Pressure Relief Devices for Compressed Hydrogen Vehicle Fuel Containers (Draft)

Project 2: Failure Modes and Effects Analysis (FMEA) for Compressed Hydrogen Fuel Cell Vehicles

A failure modes and effects analysis is a tool through which potential failures, and remedial fail-safe strategies may be assessed and ranked in terms of consequence to assist engineers in reiterative design to mitigate hazards. Prior to conducting any physical testing of HFCVs, NHTSA decided that a structured, high-level FMEA would be helpful in determining potential areas of concern for assessment of HCFV crashworthiness and fuel system safety.

This assessment formalizes the process through which NHTSA determines how best to implement its test plan to generate data that evaluates fuel system safety performance under the current front, side, and rear impact conditions specified in the FMVSS.

The first task under this project, which is being conducted by Battelle under consultation with NHTSA and vehicle manufacturers, is development of a generic, high-level schematic of a compressed HFCV fuel system. This schematic is not representative of any one vehicle design. It identifies and links the components that are expected to be common in all vehicle architectures. This includes multiple hydrogen storage tanks, (assuming around 4 kilograms of onboard hydrogen storage), fill port, the fuel delivery system, coolant system components, fuel cell stack, humidifier, valves, pressure relief devices, regulators, pumps, and hydrogen sensors.

From this schematic, a table is being developed that lists each of the critical components in the vehicle schematic, which at this point number around thirty, and applies the seven descriptors shown in Table 2 below, to each:

Table 2: FMEA Table Outline and Example Entries (Work in progress)

N	Subsystem/ Component	Component Description	Component Function	Potential Failure Modes	Failure Mode Consequence	Counter measure	Relative Risk
1	Compressed Hydrogen Storage Tanks	Type III, IV Rated to 10,000 psi Temp 20 - 180 F	Store and deliver hydrogen fuel to fuel system				
2	Thermally activated Pressure Relief Device (PRD)	Thermally activated valve that employs thermal expansion or melting to activate	Release pressure in case of extreme temperature exposure				
n							

Upon completion of populating Table 2 through the sixth descriptor, “Countermeasures,” a panel of experts will convene to prioritize and rank each failure mode in terms of the risk and hazard imposed by that failure.

The final report from this assessment will be available in 2007.

Project 3: Electrical Isolation Test Procedure for Hydrogen Fuel Cell Vehicles

Fuel cells generate electricity through a catalytic chemical reaction between hydrogen and oxygen. Current FMVSS 305 *Electric-Powered vehicles; electrolyte spillage and electric shock protection*, sets post-crash requirements for electrical isolation of the high voltage system for electric vehicles, but is written specifically for vehicles utilizing high voltage batteries. In the case of a crash, FMVSS 305 requires that electrical isolation be maintained between the charged traction battery system and the vehicle chassis. Unlike a battery, which is an electrical storage device, the operating voltage of a fuel cell stack is dependent upon the hydrogen flow through the system. The goal of this project is to develop an analogous test procedure for evaluating electrical safety of high voltage fuel cell systems under the same front, side and rear crash conditions prescribed in FMVSS 305.

Of concern is the fire safety of conducting crash tests with a combustible fuel onboard the vehicle. Currently, NHTSA conducts FMVSS compliance crash tests using non-flammable surrogate “fuels” to

detect post-crash fuel system leakage. In the case of liquid-fueled vehicles, such as those utilizing gasoline or diesel, a replacement called Stoddard solvent is used. Stoddard solvent has a specific gravity close to that of liquid fuels, but is much more difficult to ignite. For testing compressed natural gas (CNG) vehicles, nitrogen is used as the surrogate to detect fuel leakage through a pressure drop in the system. NHTSA has not yet promulgated a standard for crash testing hydrogen fueled vehicles, but it would be likely, given the recommendations of current industry practices (i.e., those being reviewed under project 1) that helium would be used as a surrogate fuel to assess fuel leakage in crashes.

Since a hydrogen supply is necessary to provide the electron flow through the high voltage propulsion system of a fuel cell vehicle, determining electrical safety in a crash test using helium as the surrogate energy carrier would not keep those portions of the propulsion system that are dependent upon the fuel cell for power generation active. Therefore, NHTSA is exploring different methods for testing post-crash electrical isolation in a laboratory setting that minimize the risk to the technicians conducting the tests.

Under this contract, Battelle, in consultation with NHTSA and vehicle manufacturers, is developing a generic schematic of an HFCV electrical system and tabulating isolation hazards and requirements in conjunction with a review of applicable industry standards for shock prevention. The standards under review are listed in Table 3.

Table 3: Standards for Electric Shock Protection

Standard	Title
ISO 23273-3:2006	Fuel cell road vehicles – Safety specifications – Protection of persons against electric shock
ISO 6469-3:2001	Electric road vehicles – Safety specifications – Protection of persons against electric hazards
SAE J1766 June 1998	Recommended Practice for Electric and Hybrid Electric Vehicle Battery Systems Crash Integrity Testing
SAE J1766 April 2005	Recommended Practice for Electric, Fuel Cell and Hybrid Electric Vehicle High Voltage Power Generation and Energy Storage Systems Crash Integrity
FMVSS 305	Electric-powered vehicles; electrolyte spillage and electrical shock protection
SAE J2579	Recommended Practice for Fuel Systems in Fuel Cell and Other Hydrogen Vehicles
IEC 60479-1 & 2	Effects of current on human beings and livestock

Several test methods are under consideration for measuring post-crash electrical isolation at this time, both with and without hydrogen onboard the vehicle at the time of the test. Following selection of the most appropriate of these methods, the contractor will draft a test procedure and validate its efficacy through bench top testing. A draft work plan will also be developed for potential full scale demonstration testing at a later date. The results will be documented in a comprehensive report which will be published in 2007.

Project 4: Compressed Hydrogen Fuel Container Integrity Testing

As a key early step in its strategy for ensuring safety of hydrogen fuel cell vehicles, NHTSA desires to conduct component level integrity testing of the cylinders used to store high pressure hydrogen on HFCVs. FMVSS 304 *Compressed natural gas fuel container integrity*, specifies performance, labeling, and inspection requirements for compressed natural gas (CNG) motor vehicle fuel containers [3]. Typically CNG containers are rated up to 3,600 psi service pressure. Hydrogen containers are typically rated from 5,000 to 10,000 psi service pressure, but, although industry standards exist, NHTSA currently imposes no regulatory requirements on their performance.

In order to generate performance data on HFCV storage integrity, research oriented testing of hydrogen cylinders will be performed in general accordance with FMVSS 304, and any applicable or draft industry standards and test specifications analogous and/or supplemental to those requirements, and specific to hydrogen storage. Testing is being conducted at Southwest Research Institute by the Department of Fire Technology under contract to

NHTSA, and the proposed test matrix is currently under review.

As mentioned earlier, hydrogen vehicle components, including the storage cylinders used on prototype vehicles, are not readily available on the open market. However, four different models of “off the shelf” cylinders have been identified for NHTSA’s first round of integrity testing. It is hoped that as the HFCV safety program progresses, more test articles that are actually in use on state-of-the-art vehicles will become available.

The four models that will be tested initially are NGV2-2000 certified cylinders of type 3, composite metallic full wrapped, or type 4, composite non-metallic full wrapped.

The draft test matrix is shown below in table 4.

Table 4: Hydrogen Cylinder Test Matrix

Test Type	Pass/Fail Criteria	Test Description	Reference Std/Reg	Test condition/ comments	
Bonfire	20 minutes or vent	Position longitudinal axis of cylinder horizontally over uniform fire source 1.65 meters in length, > 430 degrees Celsius	FMVSS 304	100% fill	10% fill
Pressure Cycling	No leakage	13,000 cycles between 100% and ≤10% SP, and 5,000 cycles between ≤ 10% and 125% SP	FMVSS 304	Fleet cycle, 4 refuelings/day, 300 days, 15 years.	
Penetration Test	No rupture	Penetration of at least one cylinder wall with a .30-in. caliber bullet	ISO 15865	100% fill	10% fill
Hydrostatic Burst	2.25x service pressure	Increase pressure to minimum prescribed burst pressure at a rate up to and including 200 psi per second and hold constant for 10 seconds	FMVSS 304	Test to failure	
				Cylinders that survive other tests will be tested to failure	

Tests may include instrumentation beyond the requirements of the certification test procedures, e.g., addition of strain gauges, pressure transducers, thermocouples, and any cylinders that pass the test criteria will be hydrostatically burst-tested to failure.

Testing will be documented in a final report that should be made available in May 2007.

Plans for FY 2007 HFCV Research and Testing

HFCV technology is developing rapidly as evidenced by the recent announcements by GM and Honda that they will be releasing wholly new vehicles for demonstration in the near future. GM plans to begin placing its new Equinox FCV with customers in the fall of 2007, and Honda plans limited introduction in 2008 of a new FCV based on its FCX Concept.

To aid in planning follow-on research to the projects discussed in this paper, NHTSA published a Request for Information (RFI) in December 2006, to identify potential sources, costs, and schedule estimates for obtaining hydrogen and fuel cell vehicles, fuel system components, and test facilities with the capabilities to conduct fuel system integrity research testing.

Specifically, this RFI sought the following information:

- Availability and cost of hydrogen fueled vehicles and fuel system components for destructive testing.

- Availability of facilities, personnel, expertise, material and equipment to perform fuel system integrity testing and evaluation of hydrogen fuel systems and fuel system components.
- Schedule estimates and costs for component, systems level, and full scale vehicle fuel system integrity testing.
- Information concerning likely fuel system packaging configurations and test methods to assess failure mitigation strategies for hazards imposed by crash or fire exposure.
- Information concerning the value of using purpose-built, generic hydrogen fuel systems to collect baseline performance data in crash or fire exposure testing.
- Suggestions for evaluating fuel system safety in prototype or preproduction vehicles, through non-destructive assessment or testing.

The responses to this RFI are being analyzed and will help define the scope and scheduling of near and long term projects assessing HFCV safety. In the near term, NHTSA plans on expanding physical testing from single cylinders to plumbed cylinder assemblies to assess deceleration and crash performance at the subsystem level. It also plans to subject cylinders and plumbed arrays to flame impingement testing to assess pressure relief device performance with remote, localized heating. NHTSA also hopes to obtain vehicles from manufacturers for testing, which could include non-destructive assessments such as hydrogen sensor sensitivity testing, leak detection

while garaged or parked, and electrical isolation testing during normal operation.

Future Work

As the industry matures, NHTSA will continue to monitor the progress of vehicle and standards development, and assess each through testing and analysis. Although most manufacturers are utilizing high pressure hydrogen storage at this time, it is likely that the industry will continue to explore cryogenic and low pressure hydrides as options for the future, so that as those systems come closer to utilization, they will have to be assessed for safety performance as well.

References

[1] U.S. Department of Transportation Docket Management System,
<http://dms.dot.gov/search/searchFormSimple.cfm>,
Docket No. NHTSA-2004-18039

[2] Hennessey, B., Hammel-Smith, C., Koubek, M.,
“NHTSA’s Four-Year Plan for Hydrogen, Fuel Cell,
and Alternative Fuel Vehicle Safety Research,” 19th
International Conference on the Enhanced Safety of
Vehicles, Washington, DC, 2005

[3] CFR 49 Transportation, Chapter V - National
Highway Traffic Safety Administration, Part 571—
Federal Motor Vehicle Safety Standards, §571.301,
§571.303, §571.304, §571.305,
http://www.access.gpo.gov/nara/cfr/waisidx_05/49cfr571_05.html

A STUDY OF US CRASH STATISTICS FROM AUTOMATED CRASH NOTIFICATION DATA

Mukul K. Verma

Robert C. Lange

Daniel C. McGarry

General Motors Corporation

USA

Paper Number 07-0058

ABSTRACT

This paper analyzes data available as part of telematics-based automatic collision notification in vehicles so equipped for all cases of frontal impact that generated the collision notification. Such data are transmitted as part of collision notification system and intended to enhance the effectiveness of emergency services in providing timely and appropriate care to vehicle occupants. Only the information related to vehicle kinematics is used for the present study and any information that may uniquely identify vehicle customers was removed.

The correct values of maximum velocity change during these crashes are presented here. It was also possible from this data to generate estimates of the time period over which these velocity changes occurred. Since injury parameters measured in tests are related to the rate of dissipation of the vehicle's kinetic energy, the availability of the information regarding the time period for maximum velocity change greatly enhances the value of crash data in defining crashes and thus in setting research priorities for improving traffic safety.

INTRODUCTION

Knowledge of parameters defining automobile crashes is of great significance in developing priorities and countermeasures for reducing societal harm associated with such crashes. Historically, in order to generate such information, motor vehicle safety researchers examined selected vehicles involved in crashes, measured residual deformation patterns, applied conventional modeling techniques along with known algorithms and calculated various collision parameters such as dissipated kinetic energy, post-collision vehicle motion and change in velocity. Such post-crash reconstructions are known to be limited in terms both of the amount of information that can be generated as well as the precision of the results. For example, crashes are quantified by estimates of maximum change in vehicle's velocity (ΔV) by these techniques. It is

shown in this paper that it is possible to obtain a more complete and accurate description of crashes by using the limited data used by a telematics-based advanced automatic crash notification system (AACN).

The capability to automatically provide information about a crash to a central source was introduced by OnStar several years ago. This system, known as ACN, uses airbag sensors in the car along with a GPS system to determine the car location and notifies an operator when an airbag is deployed. The operator, in turn, contacts emergency services to get proper services to respond to the vehicle crash.

The Advanced Automatic Crash Notification (AACN) system was introduced by OnStar in General Motors vehicles to further improve the existing capabilities of the automatic airbag deployment notification system [1]. This AACN system provides an automatic call to the OnStar Center when any of the following occur during a crash:

- a) an airbag is deployed;
- b) maximum change in velocity (ΔV) of the vehicle exceeds pre-determined crash severity criteria;
- c) a vehicle rollover is detected by a rollover sensor.

The AACN system thus enhances the capability of the previous system by also providing notifications in other types of crashes where a possibility of significant injury may exist.

In this paper, AACN data for the period from May 2005 to May 2006 are utilized for study of front impact crashes. These crashes are divided into two categories – (a) those with airbag deployment and, (b) those where the crash severity was not sufficient to deploy airbags but exceeded a predetermined maximum change in velocity (ΔV). The cases corresponding to condition 'b' are referred to as 'non deployment' cases in this paper.

The determination of ΔV of the vehicle is made from crash sensors which are present in the vehicle for

deployment of restraint systems (e.g. airbags, seatbelt pretensioners, etc). These sensors usually measure acceleration of the vehicle and ΔV is obtained by integration of the acceleration, beginning from the instant a crash is determined by pre-programmed algorithms. For purposes of AACN and for getting an indication of crash severity for communication to emergency services, the maximum change in velocity (ΔV) calculated from the vehicle crash sensors is utilized. The vehicle velocity is calculated during a 300 millisecond window with 15 discrete data points each separated by 20 milliseconds. For deployment events, three ΔV samples are taken prior to deployment, one sample is approximately at deployment and eleven samples are after deployment. For non-deployment events, the ΔV samples start at the time the impact is detected. Since there are sensors present for longitudinal as well as for lateral impacts, estimates of ΔV are available in all crash directions. In addition, an estimate of the direction of impact is made from the x- and y-components of ΔV .

It should be noted here that the AACN system uses the acceleration records in the sensing and diagnostic module (SDM) in the vehicle and the calculated ΔV approximates the change in velocity at the center of gravity of the vehicle. Other accelerometers that may be present for detection of localized impacts (e.g. front sensors mounted near the radiator front) are not utilized in the calculation of ΔV in the present study, although they are utilized in determining the deployment of restraints in the automobile.

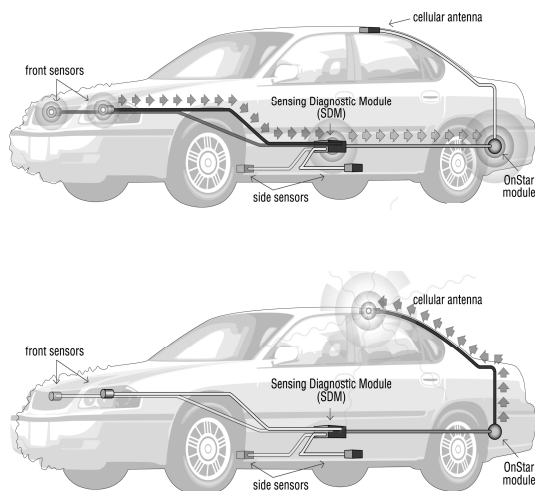


Figure 1: Schematic Representation of AACN System

In the event of a front-, rear- or side-impact crash exceeding the crash severity criteria, the SDM transmits crash information to the vehicle's OnStar

module. In cases of rollover, the rollover sensor also provides the data for transmission to OnStar. The following data are transmitted:

- a) Identification of the deployed airbag and if any were suppressed because of suppression systems;
- b) Identification of a non-deployment event meeting or exceeding crash severity criteria;
- c) Maximum change in velocity (ΔV) of the vehicle and the time step at which this occurs (if the maximum ΔV occurs later than the above-mentioned window of 300 milliseconds, its value is transmitted but the time step count remains at 15);
- d) The principle direction of impact at maximum ΔV ;
- e) Identification of a vehicle rollover when rollover sensors are present;
- f) Identification of single or multiple impacts if they occur within the 300 millisecond window.

Upon receipt of this crash information, the OnStar module sends a signal to OnStar Center through a cellular connection, informing the advisor that a crash has occurred. A voice connection between the OnStar advisor and the vehicle occupant is established and the advisor can then contact the appropriate emergency services (e.g. ambulance, rescue, etc) and provide these with crash information that can help estimate the severity of the crash and determine the appropriate rescue and medical services. This pre-determination of likely crash severity and direction of impact, as well as vehicle location determined by GPS system (as part of OnStar system), may help reduce the time taken for appropriate response as well as for the readiness of appropriate medical care. Previous studies [2, 3] have shown that the time taken from the moment of injury to the administration of medical care in the proper facility is a critical factor in determining post-crash outcome for the automobile occupant and the AACN system may provide a significant reduction in this total time taken.

The present study is based only on the above-mentioned transmitted records from the selected crashes and does not contain other data about the vehicle or its occupants. Although the data utilized in this study are a subset of those studied elsewhere [4, 5], the large number of cases that can be included in the present methodology provide a wider perspective than is possible from smaller sample sizes.

ANALYSIS OF AACN DATA FOR FRONT IMPACTS

For the present study, vehicle-related data from frontal crashes with AACN notifications from May 2005 to May 2006 was analyzed. During this period,

there were 1045 recorded frontal crashes with frontal airbag deployment in the AACN-equipped vehicles. In addition, there were 356 cases of ‘non deployment’ frontal crashes where the predetermined thresholds for AACN in frontal impact were reached or exceeded. For these events, the maximum changes in velocity (ΔV) were analyzed as follows.

For each of the 1045 events of frontal impact accompanied by deployment of one or both front airbags, the maximum change in velocity (ΔV) is shown in Figure 2.

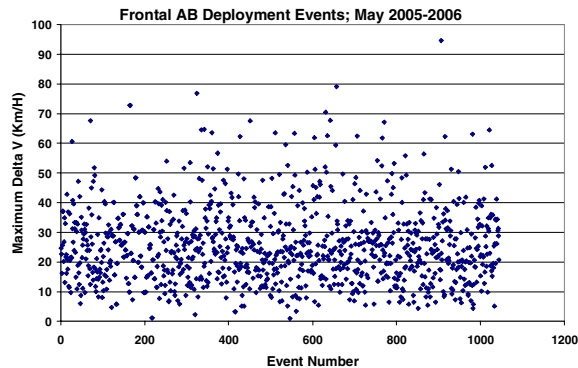


Figure 2: Maximum ΔV for Frontal Crashes with Airbag Deployment

It is observed that maximum ΔV in these crashes has a wide distribution, with most of the cases being below 40 kilometers per hour. The frequency distribution of ΔV is shown in Figure 3, indicating that 95% of these crashes have maximum velocity change of less than 50 kilometers per hour.

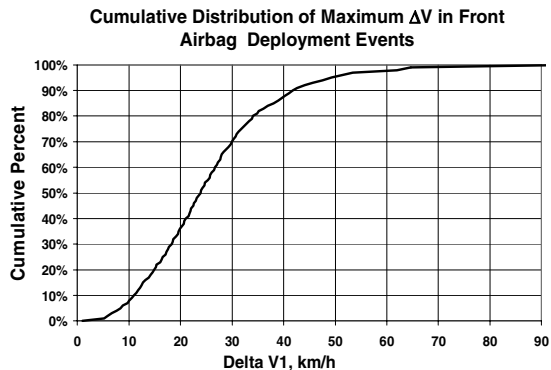


Figure 3: Distribution of Maximum ΔV in Front Crashes with Airbag Deployment

The maximum change in velocity in the 356 cases of ‘non deployment’ in front impacts is shown in Figure 4. It is observed that these ΔV values are bounded at the lower end by the AACN deployment threshold for the system.

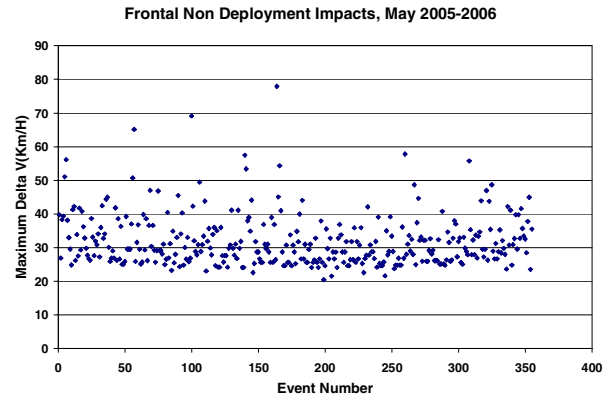


Figure 4: Maximum ΔV for Frontal Non-Deployment’ Events

Definition of Crash Severity for Front Impacts

In existing literature, statistical information on crash severity has been presented as estimates of maximum velocity change during the crash, without any estimates of the time period over which such velocity changes occur. This lack of information about time period is due to the fact that accident reconstruction techniques utilized by researchers for post-crash investigation are capable of generating only limited information with some degree of reliability. This knowledge of maximum change in velocity provides information of the pre-impact kinetic energy of the vehicle dissipated during the impact but not about the rate of such energy dissipation.

However, as is well understood, the probability of injury during an impact is proportional not to the energy dissipated but to the rate at which energy is dissipated (defined as mechanical ‘power’). This is illustrated by two simple examples of considering a moving body traveling at a given initial velocity and impacting two different surfaces – one being a stiff surface with little energy dissipation and the other being a soft surface with significant energy dissipation. An example of the first type of surface would be a thick steel plate and an example of the second type would be expanded metal honeycomb of low stiffness. The injury suffered by the moving body impacting a hard surface with little energy dissipation capability is likely to be of much higher severity than the same body impacting a softer surface with significant energy dissipation, all other variables being the same in both impacts.

As another example, a crash of a certain ΔV over a longer duration (for example, an impact into a soft embankment) is of lower severity (less likely to cause

injuries) than another crash with the same ΔV in a shorter duration (e.g. an impact into a rigid barrier).

The relationship between injury probability and the rate of energy dissipation can be expressed as the functional relationship:

Injury Probability \propto Rate of Energy Dissipation

Therefore, defining crash severity by only the maximum ΔV value is not likely to reliably estimate the injury probability in the crash. It is therefore highly desirable that crashes be described not just by the maximum ΔV but also by the duration over which this velocity change occurred in the crash. Such information is available when detailed time history of the crash event is obtained [4] from devices such as the data recorders available in some vehicles.

This detailed velocity-versus-time record in crashes was not available for the present study (since it is not part of the data utilized in AACN transmission) and therefore, an attempt is made here to estimate these from the available data. As described earlier, the transmitted data provides 15 values of ΔV every 20 milliseconds arranged such that the first three values of ΔV are prior to the event (airbag deployment or AACN deployment) and 12 samples are after the event (in the case that the maximum ΔV in the crash occurs later than 12 time steps from the deployment, the maximum ΔV is available but the time step count stops at 15 as described above). Thus, each value of ΔV is associated with a counter which enables the estimation of time duration from airbag or AACN deployment to the maximum ΔV in the crash. This distribution of maximum ΔV and the time calculated for all the front crashes with front airbag deployment is shown in Figure 5.

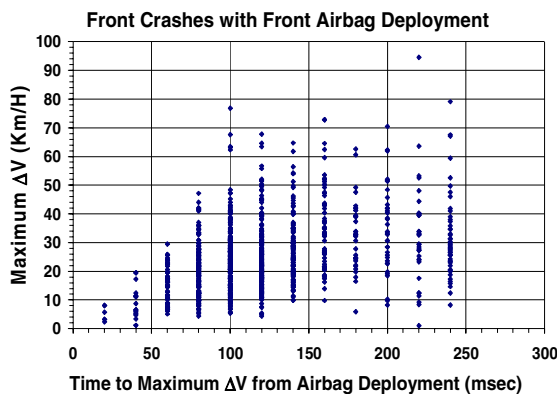


Figure 5: Maximum ΔV versus Time in Front Crashes with Airbag Deployment

To compare this data from field events to similar data from crash tests, the velocity versus time plot from a 64 kilometer/hour front impact test against a rigid barrier (US NCAP test) is shown in Figure 6. The maximum ΔV in such tests is usually higher than the nominal test speed due to the ‘rebound’ of the vehicle during the test (approximately 5 to 10 km/h).

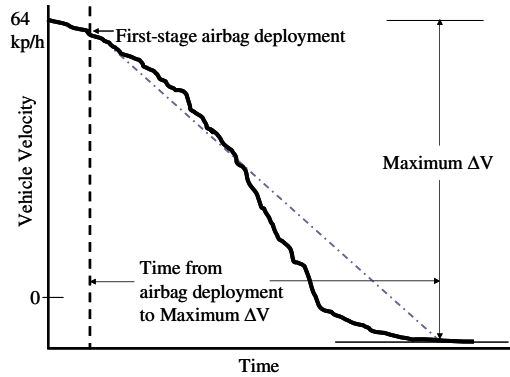


Figure 6: Vehicle Velocity versus Time in 64 km/h front rigid barrier impact

Front airbag sensing systems are designed to predict crash severity in time to inflate airbags and restrain the occupants, and a ‘typical’ ΔV associated with the airbag deployment command in the above test (64 km/h front impact into a rigid barrier) may be at 4-8 km/h (this is dependent on the vehicle and is likely to be somewhat different for each vehicle depending on design parameters).

It is then possible to compare the severity of frontal crashes observed in the field to that in existing tests such as the one described above. In order to do this, NCAP test data for the vehicle groups in the AACN

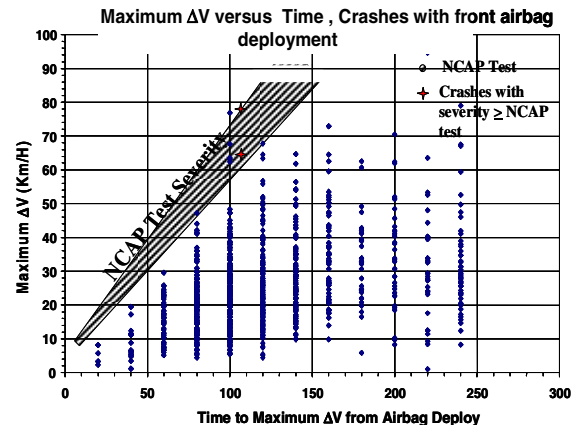


Figure 7: Comparison of Front Crashes with Airbag Deployment to 56 km/h NCAP Tests

data set were analyzed to obtain the time and the value of maximum ΔV as well as the time and the ΔV

of front airbag deployment. This ‘corridor’ of crash severity for NCAP tests is shown in Figure 7. Also shown in this figure are crashes where the crash severity would meet or exceed the NCAP test severity of the corresponding vehicle showing only two cases whose crash severity as measured by the averaged deceleration would meet or exceed the severity of the NCAP tests.

A similar evaluation was done to compare the severity of the 1045 frontal crashes with airbag deployment to the crash severity of front offset crashes into a deformable barrier with an impact speed of 64 km/h. The calculated severity of the offset deformable barrier tests for the same family of vehicles is shown in Figure 8 along with those crashes in the field whose severity (as defined by the ‘averaged’ severity described above)

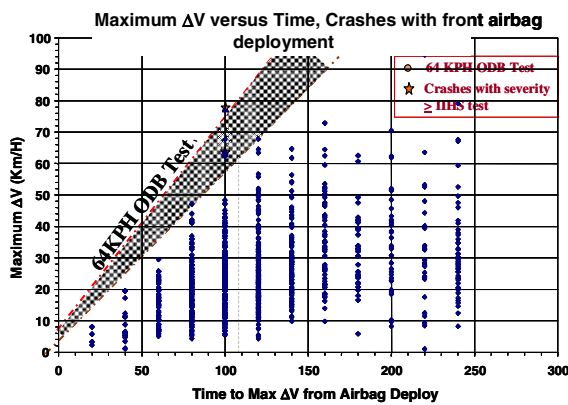


Figure 8: Comparison of Front Crashes with Airbag Deployment to 64 km/h ODB tests

would meet or exceed that of the severity of the 64 km/h offset deformable barrier test for the corresponding vehicle. It is noted that there are only two such crashes among the 1045 frontal impacts in the crash database of frontal impacts with airbag deployment.

CONCLUSIONS

A methodology for obtaining crash statistics from advanced automated crash notification (AACN) data has been described in this paper. With this methodology, it is possible to obtain correct values of maximum ΔV as well as estimates of the time scale associated with the ΔV in a crash. Data for the correct direction of impact (principal direction of force) are also available but are not shown here. Results have been presented for front crashes with airbag deployment as well for front crashes without airbag deployment but with maximum ΔV exceeding

predetermined values. Almost all (99.8%) of the front airbag deployment crashes observed were less severe (based on averaged deceleration) than the 56 km/h NCAP test and the 64 km/h ODB test, two of the front impact tests currently used in the US to assess and rate vehicle crashworthiness. It is also observed that large number of crashes occur with lower values of maximum ΔV and over longer time durations.

The significance of the present study is that all crashes of vehicles equipped with AACN or similar systems can be analyzed without need for detailed investigations and that crash severity can be obtained in terms of velocity change, associated time duration as well as direction of impact (not presented here). Such enhanced description of crashes by a complete set of parameters relevant to injuries is important since it provides a better description of the field conditions than is possible by classical methods and is therefore valuable in setting research priorities for improvement of automotive safety.

ACKNOWLEDGEMENT

We are grateful to Thomas Mercer for the technical guidance and support in these studies and to Joseph Lavelle for the statistical analyses and interpretations.

REFERENCES

1. Butler D., “Launching Advanced Automatic Crash Notification (AACN): “A New Generation of Emergency Response”, Paper 2002-21-0066, Convergence International Congress, 2002.
2. Stewart R.D., “Pre-Hospital Care of Trauma”, Ch 3, p 24, Management of Blunt Trauma, Williams and Wilkins, Baltimore, 1990.
3. Champion H. et al, “Reducing Highway Deaths and Disabilities with Automatic Wireless Transmission of Serious Injury Probability Ratings from Crash Recorders to Emergency Medical Service Providers”, paper 406, 18th ESV Conference, 2003
4. Gabler H., et al “Crash Severity: A Comparison of Event Data Recorder Measurements with Accident Reconstruction Estimates”, Paper 2004-01-1194, SAE Annual Congress, 2004.
5. Niehoff P., et al , “Evaluation of Event Data Recorders in Full Systems Crash Tests“, 19th Enhanced Safety of Vehicles Conference, Paper No. 05-0271, June 2005.

INVESTIGATION FOR NEW SIDE IMPACT TEST PROCEDURES IN JAPAN

-Effect of Various Moving Deformable Barriers and Male/Female Dummies on Injury Criteria in Side Impact Test-

Yasuhiro Matsui

Naruyuki Hosokawa

Shunsuke Takagi

Hideki Yonezawa

National Traffic Safety and Environment Laboratory

Koji Mizuno

Nagoya University

Hidenobu Kubota

Ministry of Land, Infrastructure and Transport

Japan

Paper Number 07-0059

ABSTRACT

The International Harmonization Research Activities Side Impact Working Group (IHRA-SIWG) focused on a new barrier face such as the Advanced European Moving Deformable Barrier (AE-MDB), which reflects recent car characteristics. Since the proportion of females severely or fatally injured in vehicle-to-vehicle crashes was greater than in males in the USA and Europe, a difference of injury criteria between male and female dummies should be investigated. Therefore, the purpose of the present study is to investigate the effect of AE-MDB on the injury criteria in male (ES-2) and female (SID-IIs) in the front seat and in female (SID-IIs) in the rear seat. In the present study, the ECE/R95 MDB or AE-MDB or car was impacted into the side of the same type of small passenger car. The present study also describes the results of the pole side impact test against the small passenger car used in the above test series according to the impact conditions proposed by the FMVSS/214 draft and E-NCAP.

INTRODUCTION

Japan introduced a side impact regulation⁽¹⁾ in 1998 for occupant protection in side collisions. As a result, the number of fatal and serious injuries in side collisions has been reduced. However, there are still many side collision accidents, and further effective countermeasures are needed to reduce fatalities and serious injuries in side impacts. It is known that occupants in cars are inclined to sustain serious injuries when struck by vehicles with high front stiffness and high ground clearance such as Sport Utility Vehicles (SUVs), Multi-Purpose Vehicles (MPVs) and minivans⁽²⁾⁽³⁾. It is also necessary to consider improving the protection of occupants against side collisions with narrow objects such as trees and poles in single collisions.

The proportion of females severely or fatally injured in vehicle-to-vehicle crashes was greater than in males⁽²⁾ in the USA and Europe. A difference of injury criteria between male and female dummy should be investigated.

In this paper, new side impact test procedures using AE-MDB were investigated, which have been discussed in IHRA SIWG and EEVC/WG13. The side impact test procedure using pole proposed by the United States and E-NCAP was also investigated. These tests consist of (1) MDB-to-car test: AE-MDB test in which the current vehicle specifications and front stiffness are taken into consideration, ECE/R95 MDB test and car-to-car test, and (2) Car-to-pole test: procedure of FMVSS/214 draft and E-NCAP.

In the tests of the present research, SID-IIs and ES-2 were used in order to investigate the difference in injury criteria between female and male.

TEST CONDITIONS

Moving Deformable Barriers-to-Car Test

Table 1 shows the test configurations and conditions in the moving deformable barriers (MDBs) to car test and the car-to-car. In the present study, one type of Japanese bonnet-type 4 door sedan was used as the struck car. The specification of the tested car is listed as Table 2. This car is one of the representative models of the small car fleet in Japan. The striker (MDB or car) impact velocity was 50 km/h.

The test configuration of Test No. 1 and 2 was according to the ECE/R95 test procedure. In Test No.1, the ECE/R95 MDB was used, and the ES-2 was placed in the front seat and SID-IIs in the rear seat. In Test No. 2, only the SID-IIs was placed in the front seat.

In Test No. 3, 4 and 5, the AE-MDB version 2⁽⁴⁾ was used as an MDB. The AE-MDB is an MDB that was developed based on the car dimensions, mass and front stiffness in the current vehicle fleet⁽⁵⁾. It also considers both-vehicle traveling and loading

of the rear seat occupants. The AE-MDB face was made in Japan according to the specification⁽⁴⁾ required by EEVC/WG13. The AE-MDB tests were conducted under two conditions: The center line of the AE-MDB was aligned with the driver Seat Reference Point (SRP) (Test No. 3), 250 mm behind the front seat SRP (Test No.4 and 5).

In Test No. 3, the two SID-IIs were placed in a front seat and a rear seat, respectively. The center line of the AE-MDB was aligned with the driver Seat Reference Point (SRP). In Test No. 4, the two SID-IIs were placed in the front and rear seat, respectively. In Test No. 4, the two ES-2 were placed in the front and rear seat, respectively. The center line of the AE-MDB was 250 mm behind the driver SRP. In Test No. 5, the two SID-IIs were placed in the front and rear seat, respectively. The center line of the AE-MDB was 250 mm behind the SRP.

In Test No. 6, a car was used as a striker. The specifications of the car are the same as those used for the struck car. The two ES-2 were placed in the front and rear seat, respectively. The center line of the striking car was aligned with the driver SRP in the front seat.

Car-to-Pole Test

Table 3 shows the test configurations and conditions in the car to pole test. The same type of car employed in the moving deformable barrier to car test was used (Table 2) except for the optional

equipment with curtain air bag. In Test No. 7, 8 and 9, a curtain airbag was installed in the tested car.

The test configuration of Test No. 7 and 8 was according to the car-to-pole test proposed by NHTSA (FMVSS/214 Draft), where the impact velocity is 32 km/h and the impact angle is 75 degrees. The pole diameter is 254 mm. The ES-2 was placed in the front seat in Test No. 7 according to the FMVSS/214 Draft. When the ES-2 is used, the seat was set in the midway position in the seat slide range. In Test No. 8, the SID-IIs was placed in the front seat in order to investigate the injury criteria difference between the ES-2 and SID-IIs. When the SID-IIs is used, the seat was set in the forward most position in the seat slide range (hereafter referred to forward-most). In both tests, the gravity center of the dummy head in a front seat was in alignment with the center of the pole.

The test configuration of Test No. 9 was according to the car-to-pole test proposed by Euro-NCAP, where the impact velocity is 29 km/h and the impact angle is 90 degrees. The pole diameter is 254 mm. The ES-2 was placed in the front seat. The gravity center of the dummy head in the front seat was aligned with the center of the pole.

Table 2. Specification of tested car

Kurb Mass	1100 kg
Wheel base	2600 mm
Engin Displacement	1498 cc
Passenger	5

Table 1. Impact conditions in moving deformable barriers or car-to-car test

Test No.		1	2	3	4	5	6
Test config.							
Impact Verocity		50 km/h					
Impact Point	Striker	Vehicle C/L					
	Struck Car	SRP	SRP	SRP	SRP+250 mm	SRP+250 mm	SRP
Striker	Type	ECE/R95 MDB	ECE/R95 MDB	AE-MDB	AE-MDB	AE-MDB	Car
	Mass	948 kg	948 kg	1503 kg	1503 kg	1503 kg	1269 kg
	Ground Height	300 mm					
Struk Car	Curtain air bag	without	without	without	without	without	without
	Mass	1194 kg	1249 kg	1251 kg	1304 kg	1256 kg	1317 kg
	Front Dummy	ES-2	SID-IIs	SID-IIs	ES-2	SID-IIs	ES-2
	Rear Dummy	SID-IIs	-	SID-IIs	ES-2	SID-IIs	ES-2

C/L: Center line
SRP: Seat reference point of driver in front seat
SRP + 250 mm: 250 mm behind the SRP

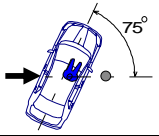
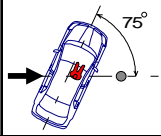
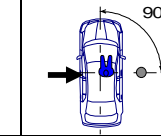


Figure 1. ECE/R95 MDB.



Figure 2. AE-MDB ver.2.

Table 3. Impact conditions in car-to-pole test

Test No.		7	8	9
Test configuration				
Impact Velocity		32 km/h	32 km/h	29 km/h
Impact Point		Pole center to Front Dummy Head center	Pole center to Front Dummy Head center	Pole center to Front Dummy Head center
Pole	Size	254 mm (10 in)	254 mm (10 in)	254 mm (10 in)
	Impact Angle	75°	75°	90°
Struck Car	Curtain air bag	with	with	with
	Mass including Dummy	1194 kg	1161 kg	1195 kg
	Front Dummy	ES-2	SID-IIs	ES-2
	Rear Dummy	—	—	—

Exterior



MDB



Test No. 1
(ECE/R95)

Test No. 2
(ECE/R95)

Figure 3a. Deformation (Test No. 1 and 2).

TEST RESULTS

1. Moving Deformable Barriers To Car Test Car and MDB Deformation - The deformations of struck car (outer panel) and striker (MDB or car) in all test cases (Test No.1, 2, 3, 4, 5 and 6) are presented in Figures 3a, 3b and 3c.

Exterior



MDB



Test No. 3
(AE-MDB)

Test No. 4
(AE-MDB, SRP+250 mm)

Figure 3b. Deformation (Test No. 3 and 4).

Exterior



MDB or car (striker)



Test No. 5
(AE-MDB SRP+250 mm)

Test No. 6
(Car-to-car)

Figure 3c. Deformation (Test No. 5 and 6).

The deformations of the outer door panel of the struck car at the level of (a) dummy thorax, (b) dummy hip point and (c) side sill in moving deformable barriers-to-car test with ECE/R95 MDB (Test No.1), AE-MDB (Test No. 3), AE-MDB SRP+250 (Test No. 4) and car-to-car test (Test No. 5) are shown in Figure 4. The door panel deformation shapes struck by car, AE-MDB and AE-MDB SRP+250 are similar. Especially, the deformation of rear door panel struck by AE-MDB SRP+250 is larger than that by car or AE-MDB at thorax level. On the other hand, the door panel deformation shapes struck by ECE/R95 are different from those by AE-MDB, AE-MDB SRP+250 and car. The door panel deformation did not create the cavity shape due to impact with the B-pillar in the car struck by the ECE/R95. Thus, the MDB characteristics at the location contacting the B-pillar are more rigid than the AE-MDB characteristics or car.

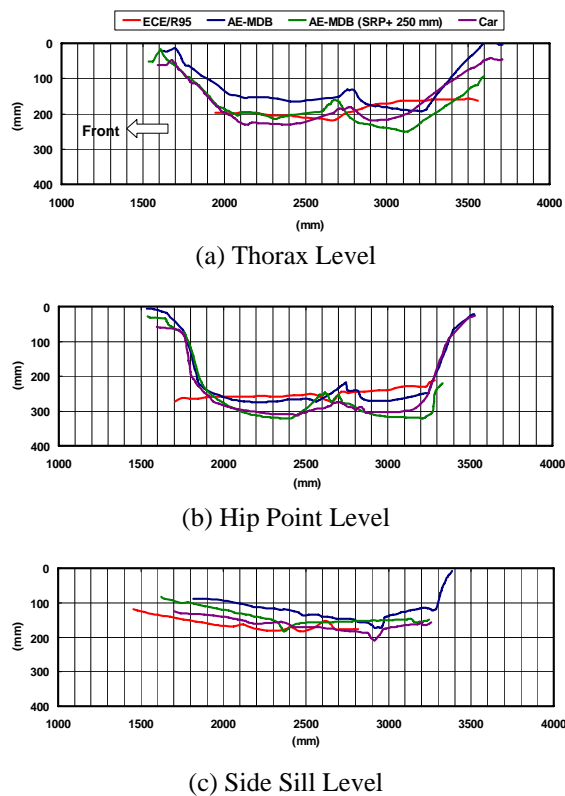


Figure 4. Deformation of outer door panel of struck car in moving deformable barriers-to-car test and car-to-car test (Test No. 1, 3, 4 and 6).

Velocity-time histories of the struck car at the gravity center, front door, MDB and dummy upper and lower rib deflections in Test No. 1 (ECE/R95 MDB, ES-2), No. 3 (AE-MDB, SID-IIs), No. 4 (AE-MDB, SID-IIs) and No. 6 (Car-to-car, ES-2) are shown in Figure 5.

The maximum velocities of the front door are different in each test case. Furthermore, the time of

the maximum velocity of the front door and dummy rib deflection are different. Especially, the timing of the maximum dummy rib deflections in the car-to-car test is faster than in moving deformable barrier tests, because the bumper equipped in the striking car front might intrude into the struck car door at the level of the dummy chest.

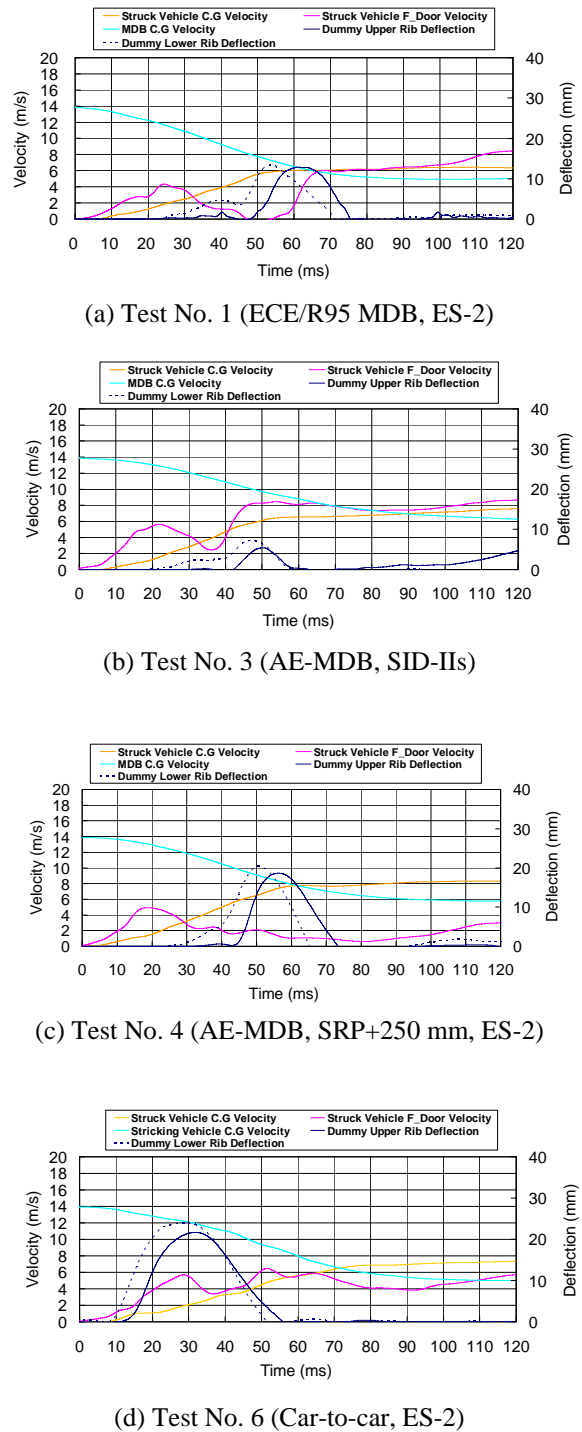


Figure 5. Velocity-time histories of struck car and striker (MDB or car).

Dummy Injury Criteria

Front seat dummy (ES-2) - Using the results of Test No. 1, 4 and 6, the injury criteria of ES-2 sit in a driver seat in the struck car by ECE/R95 MDB, the AE-MDB SRP+250 and actual car were compared.

HPC (head performance criteria) of ES-2 in each test are shown in Figure 6. The HPC of the dummy in three test cases were close to 700, due to the fact that the dummy head grazed the edge of the roof-side-rail. The HPC 700 is under the injury threshold of 1000.

Thoracic rib deflections at upper, middle and lower of the ES-2 are shown in Figure 7. The thoracic deflections are in descending order of lower, middle and upper rib in the AE-MDB SRP+250 test and car-to-car test. The thoracic rib deflection is the smallest in the test using ECE/R95 MDB. When we focus on the maximum deflection, the thoracic deflections are in descending order of car-to-car test, AE-MDB SRP+250 test, and ECE/R95 MDB test.

The thoracic rib V*C of ES-2 are shown in Figure 8. The V*C are in descending order of lower, middle and upper rib in the ECE/R95 MDB test and car-to-car test. The V*C in middle rib is the smallest in the test using AE-MDB SRP+250 test. When we focus on the maximum V*C, the thoracic rib V*C are in descending order of car-to-car test, AE-MDB SRP+250 test, and ECE/R95 MDB test.

The abdominal force and pubic force of ES-2 are shown in Figure 9. The abdominal force shows similar values among the three tests, whereas the pubic force is higher in the AE-MDB SRP+250 test than the ECE/R95 MDB test and car-to-car test.

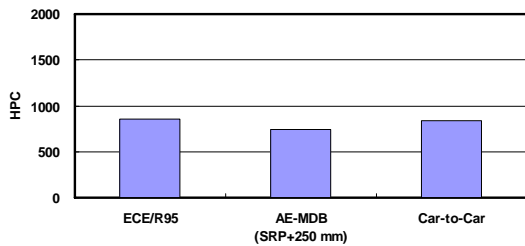


Figure 6. HPC of ES-2 sit in front driver seat in struck car by ECE/R95 MDB, AE-MDB SRP+250 and car.

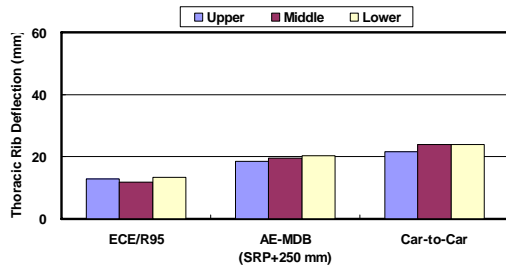


Figure 7. Thoracic rib deflection of ES-2.

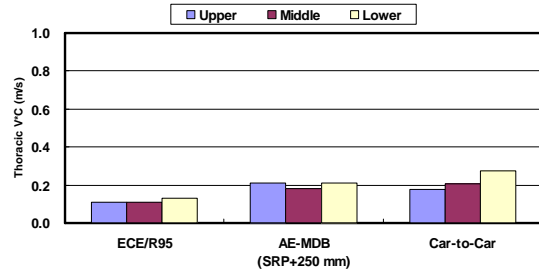


Figure 8. Thoracic rib V*C of ES-2.

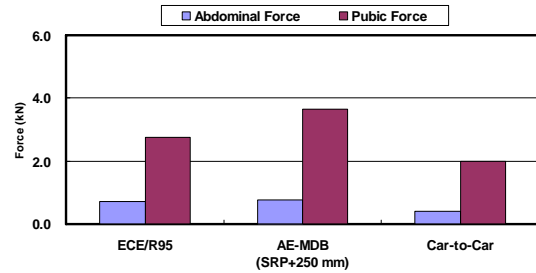


Figure 9. Abdominal and pubic forces of ES-2.

Front seat dummy (SID-IIs) - Using the results of Test No. 2, 3 and 5, the injury criteria of SID-IIs sit in a driver seat in the struck car by ECE/R95 MDB, AE-MDB (AE-MDB center was aligned with the target car front seat SRP), and AE-MDB SRP+250 were compared.

HPC of SID-IIs in each test are shown in Figure 10. The HPC in AE-MDB test is higher in three test cases. However, they were less than 500, due to the fact that the dummy head did not impact the interior. Thus, the HPC of SID-IIs are smaller than that of ES-2.

Thoracic rib deflections at upper, middle and lower of the SID-IIs are shown in Figure 11. When we focus on the maximum deflection, the thoracic deflections are in descending order of ECE/R95 MDB test, AE-MDB SRP+250 test, and AE-MDB test. The order is different from that observed in HPC results.

The thoracic rib V*C of SID-IIs are shown in Figure 12. When we focus on the maximum V*C, the thoracic rib V*C are in descending order of ECE/R95 MDB test, AE-MDB test and AE-MDB SRP+250 test.

The pubic force of SID-IIs is shown in Figure 13. The pubic forces are in descending order of AE-MDB SRP+250 test, AE-MDB test and ECE/R95 MDB test.

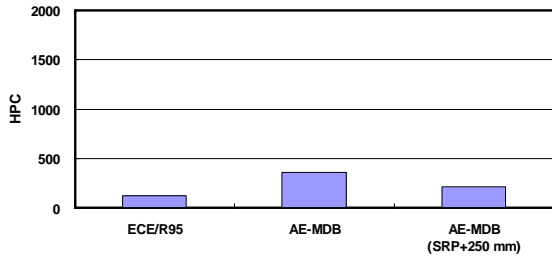


Figure 10. HPC of SID-IIIs sitting in front driver seat in struck car by ECE/R95 MDB, AE-MDB and AE-MDB SRP+250.

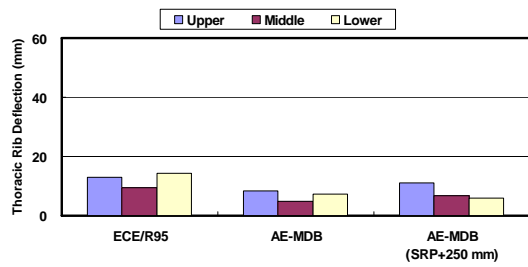


Figure 11. Thoracic rib deflection of SID-IIIs.

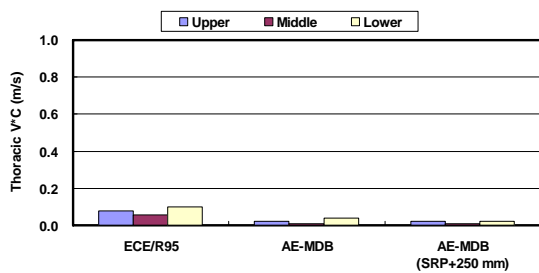


Figure 12. Thoracic rib V*C of SID-IIIs.

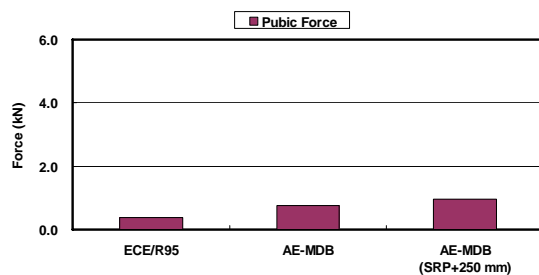


Figure 13. Pubic force of SID-IIIs.

Rear seat dummy (SID-IIIs) - The injury criteria of the rear seat dummy (SID IIIs) in struck car by ECE/R95 MDB, AE-MDB and AE-MDB SRP+250 were compared from the results of Test No. 1, 3 and 5.

HPC of SID-IIIs in each test is shown in Figure 14. The HPC are in descending order of AE-MDB SRP+250 test, AE-MDB test and ECE/R95 MDB test.

Thoracic rib deflections at upper, middle and lower SID-IIIs are shown in Figure 15. The thoracic deflections are in descending order of AE-MDB SRP+250 test and AE-MDB test as with the order

observed in HPC results. In the present study, thoracic rib deflections were not measured in ECE/R95 MDB test.

The thoracic rib V*C of SID-IIIs are shown in Figure 16. The V*C are in descending order of AE-MDB SRP+250 test and AE-MDB test as with the order observed in HPC and thoracic rib deflection results. In the present study, V*C were also not measured in ECE/R95 MDB test.

The pubic forces of SID-IIIs are shown in Figure 17. The pubic forces are in descending order of AE-MDB SRP+250 test and AE-MDB test as with the order observed in HPC, thoracic rib deflection and thoracic rib V*C results.

In the impact configuration in the present research, the distance between the dummy in rear seat and left edge of the MDB are close order of AE-MDB SRP+250 test, AE-MDB test and ECE/R95 MDB test, which would affect the injury criteria of the dummy in the rear seat.

In ECE/R95 MDB test, thoracic rib deflections were not measured, on the other hand, thoracic rib accelerations were measured (Figure 18). When we focus on the maximum acceleration, the thoracic accelerations are in descending order of AE-MDB SRP+250 test, AE-MDB test and ECE/R95 MDB test. Since thoracic rib deflections would connect to the thoracic rib accelerations, the descending order of the thoracic rib deflections could be the same as for thoracic rib accelerations.

Overall, the injury criteria measured in SID-IIIs in rear seat are in descending order of AE-MDB SRP+250 test, AE-MDB test and ECE/R95 MDB test.

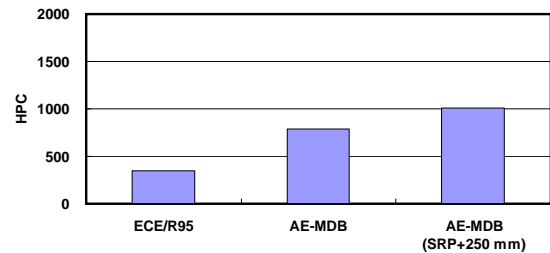


Figure 14. HPC of rear seat dummy (SID-IIIs) in struck car by ECE/R95 MDB, AE-MDB and AE-MDB SRP+250.

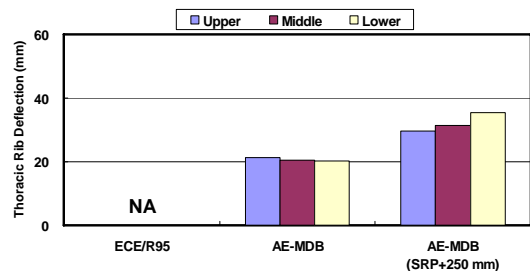


Figure 15. Thoracic rib deflection of rear seat dummy (SID-IIIs).

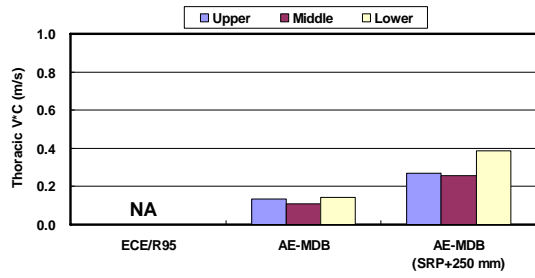


Figure 16. Thoracic rib V*C of rear seat dummy (SID-IIs).

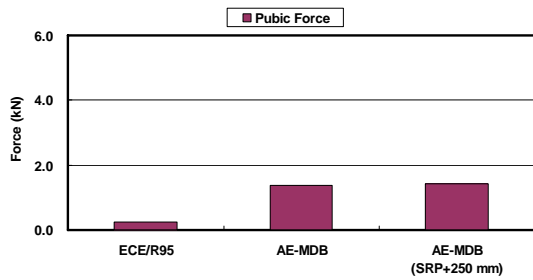


Figure 17. Abdominal and pubic forces of rear seat dummy (SID-IIs).

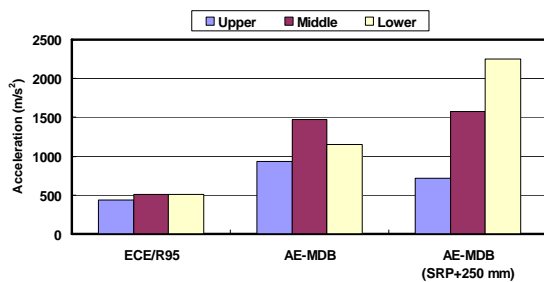


Figure 18. Thoracic rib acceleration of rear seat dummy (SID-IIs).

2. Car-To-Pole Test

Car Deformation - The deformations of struck car in all test cases (Test No. 7, 8 and 9) are presented in Figures 19a and 19b. ES2 dummy heads contacted the curtain airbag in Test No. 7 and 9. On the other hand, in Test No. 8, the SID-IIs dummy head did not contact the curtain air bag as shown in Figure 19b right.

The deformation of outer door panel of struck car at the level of (a) dummy thorax, (b) dummy hip point and (c) side sill in a car to pole test are shown in Figure 20. The intrusions are in descending order of Test No. 7 (32 km/h, 75 degrees, ES-2), Test No. 8 (32 km/h, 75 degrees, SID-IIs) and Test No. 9 (29 km/h, 90 degrees, ES-2). Thus, the intrusion in the car-to-pole test conducted at 32 km/h (Test 7 and 8) are larger than that in the car-to-pole test conducted at 29 km/h. The contact location of the outer door panel to the pole in Test 8 (SID-IIs in forward-most seating position) is 250 mm forward comparing to the location in Test 7 (ES-2 in middle seating

position), since the contact location of the dummy head was aligned with the center of the pole.

Exterior



Interior



Test No.7

(ES-2)

Test No.8

(SID-IIs)

Figure 19a. Deformation of test car struck by pole at 32 km/h and 75 degrees.

Exterior



Interior



Test No.9

(ES-2)

Figure 19b. Deformation of test car struck by pole at 29 km/h and 90 degrees.

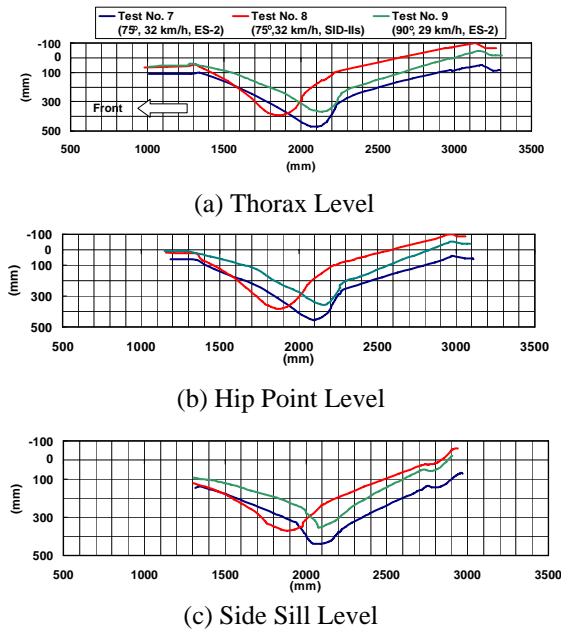


Figure 20. Deformation of outer panel of struck car in the pole test (Test No. 7, 8 and 9).

Dummy Injury Criteria - The injury criteria of ES-2 (Test No. 7 and 9) and SID-IIs (Test No. 8) in a driver seat in the car struck by a pole were compared.

HPC measured in each test are shown in Figure 21. Although the equipped curtain airbag deployed in all tested cars, the HPC of the SID-IIs dummy (Test No. 8) was far higher (over 7832) in the car-to-pole test compared with the other two tests with ES-2 (Test No. 7 and 9). At the moment of impact, the curtain airbag did not cover the SID-IIs dummy head, due to the forward-most seating position.

Although the curtain airbag deployed, the HPC in ES-2 measured in Test No. 7 (75 degrees, 32 km/h) was 1964. The HPC in ES-2 in Test No. 9 (90 degrees, 28 km/h) measured 783.

Thoracic rib deflections at upper, middle and lower are shown in Figure 22. When we focus on the maximum deflection, the thoracic deflections are in descending order of Test No. 9 (ES-2, 90 degrees, 29 km/h), Test No. 7 (ES-2, 75 degrees, 32 km/h) and Test No. 8 (SID-IIs, 75 degrees, 32 km/h). Furthermore, the thorax upper, middle and lower rib deflections were larger in the car-to-pole test than in the ECE/R95 MDB test or AE-MDB test because the door intrusion at the thorax was large in the car-to-pole test (Figures 4 and 20).

The thoracic rib V*C are shown in Figure 23. When we focus on the maximum V*C, the thoracic rib V*C are in the same descending order of the one observed in thoracic rib deflections.

The abdominal and pubic forces are shown in Figure 24. The pubic forces are in descending order of Test No. 7 (ES-2, 75 degrees, 32 km/h), Test No. 9

(ES-2, 90 degrees, 29 km/h) and Test No. 8 (SID-IIs, 75 degrees, 32 km/h).

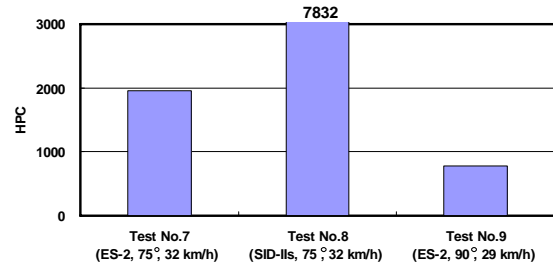


Figure 21. HPC of ES-2 (75 degrees, 32 km/h), and SID-IIs (75 degrees, 32 km/h) and ES-2 (90 degrees, 29 km/h) in car-to-pole test.

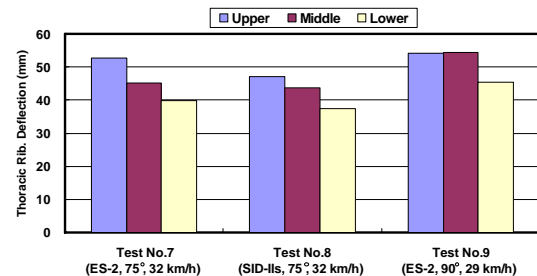


Figure 22. Thoracic rib deflection in car-to-pole test.

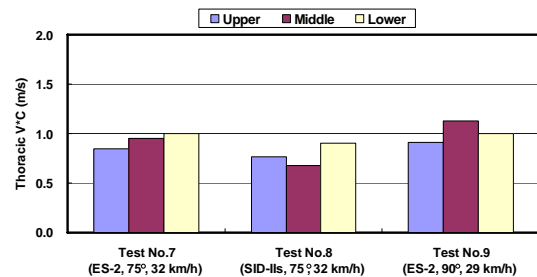


Figure 23. Thoracic rib V*C of ES-2 in car-to-pole test.

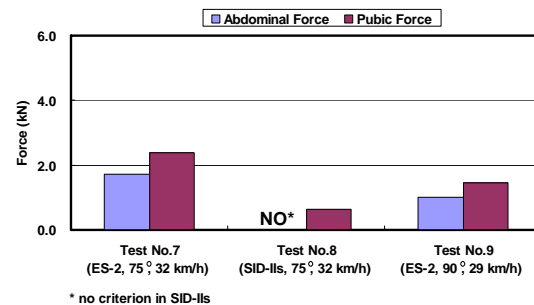


Figure 24. Abdominal and pubic forces in car-to-pole test.

DISCUSSION

In the moving deformable barriers-to-car test, the injury criteria measured in SID-IIs (Figures 6, 7, 8 and 9) were lower than in ES-2 (Figures 10, 11, 12 and 13). Following reasons could be considered.

1) Stiffness of impacted area in car: Fundamentally, the seating position of the SID-IIs was set to the forward-most, while the ES-2 was set to the middle position. Since the door panel corresponding to the SRP was impacted by the MDB, the impact position of the car using SID-IIs was different from the impact position of car using ES-2. For example, when the MDB is impacted against the door using SID-IIs, the cabin stiffness could be more rigid than the cabin stiffness using ES-2 test (Figure 20). Furthermore, the seat back can prevent intrusion of the door in the test using SID-IIs. On the other hand, the door intruded directly toward the dummy in ES-2 test.

2) Distance between dummy and door inner panel: A distance between dummy and door inner panel using ES-2 was smaller than that using SID-IIs. Thus, greater force was applied to the ES-2 than the SID-IIs. Therefore, the distance between dummy and door inner panel also affected the injury criteria in ES-2 and SID-IIs.

Regarding the injury criteria of ES-2 in the front seat, the thoracic deflection and thoracic rib V*C measured in car-to-car test are larger than those in the AE-MDB SRP+250 test or AE-MDB test. On the other hand, the abdominal force and pubic force in the AE-MDB SRP+250 test or AE-MDB test were larger than those in car-to-car test. Each MDB has different compressive characteristics in height. Hence, the above-mentioned phenomena could be owing to different force distribution due to the type of MDB.

In moving deformable barriers-to-car test, the present study used AE-MDB version 2. On the other hand, the AE-MDB has been under development and the current version of AE-MDB was 3. When the development of AE-MDB is finished, the present research should be modified using the final version.

In a car-to-pole test, although the curtain airbag deployed, the HPC measured by ES-2 in Test No. 7 (75 degrees, 32 km/h) was higher (HPC 1964) than by ES-2 (HPC 783) in Test No. 9 (90 degrees, 28 km/h). The first reason for this phenomenon was the different impact energy in these tests. The impact energy of Test No. 7 is roughly 22% higher than that of Test No. 9. The second reason was the different air bag deployment timing due to the different impact angle in these tests. Therefore, the deployment timing and volume of the curtain air bag may be the key factors influencing the driver injury criteria.

In a car-to-pole test with an impact angle of 75 degrees and impact velocity of 32 km/h, the thoracic rib deflection, thoracic rib V*C and pubic force measured by ES-2 (Test No. 7) were higher than those measured by SID-IIs (Test No. 9). The main reason was the different intrusion in these tests. The

intrusion in the pole test at thorax level, hip joint level, and side sill level conducted with ES-2 were larger (471 mm, 455 mm, 440 mm) than those with SID-IIs (391 mm, 381 mm, 371 mm), respectively. Those intrusion differences were due to different impact locations on the door panel in these tests. The contact locations of the outer door panel in relation to the pole in Test 8 (SID-IIs in forward-most seating position) is 250 mm forward of the location in Test 7 (ES-2 in middle seat position), since the contact location of the dummy head was aligned with the center of the pole.

SUMMARY

In the present study, the ECE/R95 MDB or AE-MDB was impacted onto the side of one Japanese small passenger car which was not equipped with a curtain air bag. The injury criteria in ES-2 and SID-IIs on the front passenger seat, and the injury criteria in SID-IIs on the rear passenger seat were investigated. Pole side impact tests against the same type of small passenger car equipped with a curtain air bag were conducted according to the FMVSS/214 draft (75 degrees, 32 km/h) to investigate the injury criteria in ES-2 and SID-IIs. Furthermore, a pole side impact test according to E-NCAP (90 degrees, 29 km/h) was conducted to investigate the injury criteria in ES-2. The results are summarized as follows.

(1) Moving Deformable Barriers-To-Car Test

- (i) Regarding the injury criteria of ES-2 in front seat, the thoracic deflection and thoracic rib V*C measured in the car-to-car test are larger than those in the AE-MDB SRP+250 (AE-MDB test with rearward target point) test or AE-MDB test. On the other hand, the abdominal force and pubic force in the AE-MDB SRP+250 test or AE-MDB test were larger than those in car-to-car test.
- (ii) The injury criteria, HPC, thoracic deflection and thoracic rib V*C measured in SID-IIs in front seat were smaller than those measured in ES-2 in front seat.
- (iii) The injury criteria, HPC, thoracic deflection and thoracic rib V*C and pubic force of SID-IIs in rear seat, are in descending order of AE-MDB SRP+250 test, AE-MDB test and ECE/R95 MDB test.

(2) Car-To-Pole Test

- (i) The injury criteria of the head and chest of the dummy in the pole test were far higher than in the MDB test.
- (ii) Although the curtain airbag deployed, the HPC measured by ES-2 in the test according to the FMVSS/214 draft (75 degrees, 32 km/h) was higher (HPC 1964) than the injury reference value HPC 1000. On the other hand, the HPC

measured by ES-2 in the test according to the E-NCAP (90 degrees, 29 km/h) was 783.

- (iii) The injury criteria of thoracic rib deflection, thoracic rib V*C, abdominal force and pubic force measured by ES-2 in the test according to the FMVSS/214 draft (75 degrees, 32 km/h) were higher than by ES-2 in the test according to the E-NCAP (90 degrees, 29 km/h).
- (iv) Although the curtain airbag deployed, the HPC of the SID-IIs dummy was far higher (over 7832) in the pole test compared with the other two tests using ES-2. At the moment of impact, the curtain airbag did not cover the SID-IIs dummy head, due to the forward-most seating position of the SID-IIs dummy. On the other hand, the HPC in ES-2 measured in the test (75 degrees, 32 km/h) was 1964.
- (v) In the test according to the FMVSS/214 draft (75 degrees, 32 km/h), the injury criteria of thoracic rib deflection, thoracic rib V*C, abdominal force and pubic force measured by SID-IIs dummy were lower than those measured by ES-2.

In Japan, a side impact regulation for occupant protection in side collisions was introduced in 1998. As a result, the side protection safety performance of current production cars has reached the level five score according to the J-NCAP (Japan New Car Assessment Program). On the other hand, the current barrier face employed in ECE/R95 side impact test procedure referred to in European regulation, Japanese regulation and J-NCAP, was developed based on the front characteristics of production cars in the 1970s. Since the stiffness of front characteristics and mass of recent cars have increased drastically compared to those of cars in the 1970s, it is necessary to develop a new barrier face reflecting the current car accident situation.

In the present study, we used the Advanced European Moving Deformable Barrier (AE-MDB) version 2, which was developed by IHRA-SIWG. The AE-MDB was developed based on the current accident situation in several countries. Our research objective is to continue fundamental research^{(6) (7) (8)} in order to introduce a new Japanese side impact test procedure reflecting the current accident situation with a high level of occupant protection.

In the present study, we used the SID-IIs, because the proportion of females severely or fatally injured in vehicle-to-vehicle crashes has been greater than for male⁽²⁾ in the USA and Europe.

In addition to car-to-car collisions, occupant protection in single-car crashes is also important. In the present research, the pole test proposed by NHTSA was carried out, and the influences of the curtain air bag on the dummy injury criteria were investigated. In Japan, basic research on occupant protection in side collisions will be continued, and

side impact test procedures will be developed in the near future.

ACKNOWLEDGEMENT

This study project was carried out under contract between the Japan Ministry of Land, Infrastructure and Transport (Japan MLIT) and National Traffic Safety and Environment Laboratory (NTSEL).

The authors are indebted to Mr. Hisao Itoh, Mr. Masanori Ueno, Mr. Takeshi Harigae, Manager Masami Kubota and General manager Minoru Sakurai, Japan Automobile Research Institute (JARI), Prof. Masaaki Morisawa, Musashi Institute of Technology (MI-Tech), Mr. Shinji Azami, NAC Image Technology Inc., Mr. Yutaka Takahashi and Mr. Osamu Masada, Japan Automobile Transport Technology Association (JATA), Mr. Tokujirou Miyake, Mr. Mitsuteru Murai, Mr. Akinori Watanabe and Mr. Etsuo Tokuda, National Traffic Safety and Environment Laboratory (NTSEL), for their valuable assistance in the moving deformable barrier-to-car tests and a car-to-pole test.

REFERENCES

1. ECE Regulation No. 95, "Uniform provisions concerning the approval of vehicles with regard to the occupants in the event of a lateral collision" (1995)
2. Newland C., "International Harmonized Research Activities Side Impact Working Group Status Report" 19th ESV, Paper Number 05-0460 (2005)
3. Seyer, K., "International Harmonized Research Activities Side Impact Working Group Status Report," 18th ESV, Paper Number 579 (2003)
4. Ellway J., "The Development of an Advanced European Mobile Deformable Barrier Face (AE-MDB)" 19th ESV, Paper Number 05-0239 (2005)
5. Roberts A., "Progress on the Development of the Advance European Mobile Deformable Barrier Face (AE-MDB)" 19th ESV, Paper Number 05-0126 (2003)
6. Yonezawa, H., et al "Investigation of New Side Impact Test Procedures in Japan" 19th ESV, Paper Number 05-0188 (2005)
7. Yonezawa, H., et al. "Investigation of New Side Impact Test Procedures in Japan," 18th ESV, Paper Number 328 (2003)
8. Yonezawa, H., et al. "Japanese Research Activity on Future Side Impact Test Procedures," 17th ESV, Paper Number 267 (2001)

INJURY OUTCOMES IN SIDE IMPACTS INVOLVING MODERN PASSENGER CARS

Ruth Welsh

Andrew Morris

Vehicle Safety Research Centre

Loughborough University

UK

Ahamedali Hassan

Birmingham Automotive Safety Centre

The University of Birmingham

UK

Paper Number 07-0097

ABSTRACT

This study examines some characteristics of side impact crashes involving modern passenger cars. The UK National Accident Database (STATS 19) and UK In-depth Accident Database (CCIS) were analysed to determine crash characteristics and injury outcomes in side impacts. UK national accident data (300,000 road crash records per year) shows clear improvements in injury outcomes in side impacts when a sample of 'older' vehicle designs are compared to 'newer' vehicle designs. In-depth accident data was analysed to understand the nature and circumstances of crashes in which injury occurred.

Analysis of the characteristics of such crashes which resulted in serious injury suggests that the conditions in terms of collision speed and height of impact (on the struck vehicle) do not usually match those of the UNECE R95 test specification, but impact angle is in agreement.

In terms of AIS2+ injury outcomes in modern vehicles, head (28% of AIS2+ injuries to front seat occupants) and chest injuries (22%) still predominate although injuries to the abdomen (10%), upper extremity (14%) and lower extremity (including pelvis 19%) are also observed. When only AIS4+ injuries are considered, head (36%), chest (41.3%) and abdomen injuries (30.5%) comprise the overwhelming majority of injuries. The type of injury (in terms of anatomical location) was then considered together with injury contact source.

In conclusion, rates of serious injury outcome are highest in non-oblique impact modes, in accordance with the current regulatory test. The in-depth data indicate that serious injury occurs at speeds exceeding those in the current regulatory test and that a sizable proportion of bullet vehicles engage at a height above that used for the MDB in the regulatory test. Modifications to the current regulatory test procedure should be considered in order to ensure that regulation is more representative of the real world accident situation.

INTRODUCTION

Struck side impacts have always presented an engineering design challenge in terms of provision of good protection to vehicle occupants. In the main, this is because there is generally so little space between the occupant and the striking object which reduces the scope for providing crash energy management unlike the situation in frontal impacts. Therefore in many cases, the occupants can be subjected to a very severe impact to the side of the vehicle. The seat belt can offer only reduced protective benefits compared to frontal impacts simply because of the lack of ride-down space and the seat belt geometry; occupants can slip easily out of the seat belt in side impacts. Additionally, because of the seated position of the occupants, there is potential for ejection of the head through the side window aperture and consequent exterior head contact.

Regulations governing design of vehicles for side impact crashes were introduced in the European Union in 1996 (UNECE R95). In many cases, the regulation implied a change of vehicle design so that acceptable levels of protection were provided specifically to the head, chest and pelvis. As a consequence, vehicles manufactured after the introduction of the regulation were generally somewhat structurally different to vehicles manufactured earlier. In the UNECE R95 test procedure, the Mobile Deformable Barrier (MDB) impacts the test vehicle at 50km/h and at 90-degrees. No attempt is made to simulate the movement of the target vehicle. The lateral striking position is aligned with the occupant seating position rather than the vehicle wheelbase with the MDB centred on the R-point. The introduction of the EuroNCAP programme has also contributed to a change in design because in order to obtain a maximum 5-star occupant protection rating, vehicles are required to undergo a pole impact test. In order to perform well in the pole impact test, such vehicles need to be equipped with an effective head protection device (such as side curtain, Inflatable Tubular System (ITS)) designed to prevent head contacts directly on the pole. Since

the introduction of the regulation and also EuroNCAP, some studies have examined the changes that have been introduced from an injury perspective. However, lack of field data in the UK has prevented a rigorous examination of effectiveness.

This study examines UK field data to explore a number of specific issues;

- What has been the overall change in struck-side casualty figures in the UK as a result of the changes in vehicle design;
- How do injury rates vary between regulatory and non-regulatory struck-side crash characteristics?
- What are the most common AIS2+ injuries (and their respective contact sources) that occur in struck side impact crashes to occupants of modern European passenger cars.

METHODOLOGY

Two data sources have been used in this study:

In the first part an analysis has been made of the UK National Accident Data (STATS 19). The STATS 19 data contains information relating to UK accidents resulting in human injury or death but does not contain any information relating to non-injury accidents. The data gives a full representation of the accident situation within the UK but is limited in respect of detailed vehicle damage and casualty injury information. Data for the years 2001-2003 were used for this analysis and cars selected for inclusion based upon their year of manufacture. Two distinct groups were defined; old vehicles manufactured 1990-1992 (distinctly pre regulation and new vehicles manufactured 2001-2003 – distinctly post regulation. An exploration was made of the relative Killed or Seriously Injured (KSI) rates for drivers in the two scenarios, car to car and car to non-car struck-side impacts. The impact type was necessarily categorised according to the STATS 19 variable ‘first point of impact’ and is subjective to the attending police officer; it does not imply but gives an indication of the direction of force (DoF) of the impact. The occupant severity is as judged by the attending police officer at the time of the accident unless death subsequently occurs within 30 days of the accident.

The results shown in parts 2 and 3 involve analysis of UK in-depth crash injury data (CCIS). The data for these analyses were collected between June 1998 and February 2005. The CCIS data use a stratified sampling criterion to identify crashes to be investigated; 100% of fatal, 80% of serious and 10-15% of slight injury crashes (according to the UK Government’s accident classification) that occur within specified geographical regions

throughout the UK are investigated. The sampling criteria also specify that injury must have occurred in at least one car that was at most 7 years old at the time of the accident. All vehicles in the study were towed away from the crash scene and an in-depth examination of each vehicle was made in recovery-yards and garages within a few days of the accident. All injuries were coded using the Abbreviated Injury Scale (AIS) 1990 revision. Data were obtained from medical records held by hospitals to which the crash casualties were admitted. For the purposes of the analyses presented, the data were selected so that vehicles sustained only one impact in order to more accurately relate the injury outcome to the specific impact event. Furthermore, selection was made on the age of the vehicle so that consideration was given only to those manufactured 1998 onwards. Data on only restrained front seat occupants was considered. Where appropriate, data on drivers and front seat passengers were combined to provide a larger sample of ‘struck-side’ occupants for analysis.

RESULTS

PART 1 – UK National Data (STATS 19) analysis

In this section an analysis has been made of the STATS 19 data for the years 2001-2003. Data are recorded for injured occupants and although information can be derived from the data for uninjured drivers, this is not the case for front seat passengers (FSP). Thus, in order to best comprehend how injury rates have changed with vehicle design modification, the analysis is restricted to drivers in right-side crashes. The data are still limited in respect of the population under consideration; an injury has to have occurred to a road user for inclusion in the STATS19 database. Hence the analysis does not support conclusion relating towards complete injury mitigation.

Two scenarios, car to car impacts (generally covered by regulation) and car to non-car impacts (not generally covered by regulation), are considered. The car-to-non-car impacts exclude impacts with vulnerable road users. It is not possible to determine restraint use or airbag deployment from the STATS19 data but it is considered that patterns of belt use would not have changed significantly during the three years worth of data analysed in the study. This is supported by observational studies carried out in the UK (TRL 2002, 2004). The effect that belt use has in side impact protection is also somewhat limited.

The population sizes for this analysis are given in Table 1.

Table 1.
Population size struck-side crashes STATS 19 2001-2003

	DRIVER	
	Old cars	New cars
Car to Car	7,841	6,800
Car to non-car	6,130	5,940

Table 2 shows how the proportion of drivers killed or seriously injured in struck-side impacts has changed with vehicle age. Struck side impacts are defined as right side impacts for drivers (assuming vehicles to be right hand drive). The KSI rate is lower in the new cars for both of the impact scenarios considered.

Table 2.
KSI rates in struck-side crashes STATS 19 2001-2003

	DRIVER	
	Old cars	New cars
Car to Car	4.9%	3.8%
Car to non-car	7.0%	4.8%

Table 3 shows the percentage reduction in the KSI rates comparing the post-regulatory cars to those manufactured earlier.

Table 3.
Percentage reduction in KSI rates for struck-side crashes STATS 19 2001-2003

	DRIVER
Car to Car	22.4%
Car to non-car	31.4%

There is some variation in the amount of benefit that has been seen in the scenarios considered. Whilst the reduction for car to car impacts is 22.4%, the benefit in car to non car impacts is even greater at 31.4%.

Table 4.
Fatality rates in struck-side crashes STATS 19 2001-2003

	DRIVER	
	Old cars	New cars
Car to Car	0.6%	0.4%
Car to non-car	1.5%	0.7%

Table 5.
Percentage reduction in KSI rates for struck-side crashes STATS 19 2001-2003

	DRIVER
Car to Car	33.3%
Car to non-car	53.3%

When fatalities alone are considered, the rates among injured occupants are shown in Table 4 and the percentage reduction in the rate of fatality in Table 5.

Table 4 shows that the fatality rates have also dropped in post-regulatory cars compared with earlier design for both car to car and car to non-car impacts. The percentage reduction in fatalities is more marked than when considering those also seriously injured. Of note here is the broad categorisation of injury outcome used within the STATS19 data. Whilst a life saved reduces the fatality count, reducing a severe injury to a moderate or serious injury (e.g. bi-lateral rib fractures with hemothorax to simple unilateral rib fractures) does not alter the 'serious' casualty classification, thus improvements within the 'serious' injury outcome category are difficult to gauge.

It is apparent from these results that newer vehicle design has benefited drivers in struck-side impacts. It also clear that for this impact type, in the event of injury, KSI outcome and indeed fatality is more likely in impacts other than car-to-car impacts, such impacts are not currently being considered in compulsory regulatory testing.

PART 2 – In-depth data analysis - struck side impacts in relation to the regulatory test procedure

This analysis uses the UK in-depth accident data (CCIS) to examine injury severity by body region to front seat occupants in car-to-car struck side crashes in newer model vehicles (1998 onwards). These are considered in relation to some characteristics of the ECE R95 crash test procedure, the direction of force of the impact and the closing speed of the impact. Some examination of the impacting height of the bullet vehicle in relation to the target vehicle's sill height is also made.

(a) Direction of Force (DoF) Three scenarios were analysed; all Directions of Force including side-swipe type impacts (158 occupants), non-oblique impacts (3 o'clock and 9 o'clock - 36 occupants) and oblique frontal angles (2 o'clock and 10 o'clock - 40 occupants).

Table 6.
MAIS – struck side front occupants – all body regions

	All Dof	Non-Oblique	Oblique
MAIS 0,1	72.8 %	58.3 %	72.5 %
MAIS 2,3	17.1 %	27.8 %	17.5 %
MAIS 4+	5.7 %	13.9 %	5.0 %
Not Known	4.4 %	0 %	5.0 %

Table 6 shows the MAIS score across all body regions. The lowest rate of MAIS 0, 1 injury outcome occurs in crashes in which a non-oblique direction of force and consequently there is a higher rate of Serious injury outcome (MAIS 2, 3 – 27.8%) and MAIS 4+ (13.9%).

Injuries to the different body regions were then considered, specifically those to the head, chest and pelvis. Table 7 shows the Maximum AIS score to the head.

Table 7.
Max AIS head – struck side front occupants

	All Dof	Non Oblique	Oblique
Max AIS 0,1	83.5 %	80.6 %	77.5 %
Max AIS 2,3	10.1 %	13.8 %	17.5 %
Max AIS 4+	1.9 %	5.6 %	0 %
Not Known	4.5 %	0 %	5 %

Serious head injury is most prevalent in non-oblique impacts, followed by oblique impacts; both rates are higher than when all directions of force are considered together.

For chest injury (Table 8) the rate of MAIS 2+ injury is considerably higher in non oblique impacts (27.8%) than for the oblique (7.5%) and when all directions of force are considered together (11.3%).

Table 8.
Max AIS chest – struck side front occupants

	All Dof	Non Oblique	Oblique
Max AIS 0,1	84.2 %	72.2 %	87.5 %
Max AIS 2,3	7.0 %	16.7 %	2.5 %
Max AIS 4+	4.3 %	11.1 %	5.0 %
Not Known	4.5 %	0 %	5.0 %

A similar situation occurs for pelvic injuries (Table 9). Here, the rate of serious injury in non oblique impacts is 13.9% compared with 5% in oblique impacts and 6.3% for struck side impacts in general.

It is evident from the data presented in Tables 6-9 that more serious injury outcome occurs in impacts with a purely perpendicular lateral component.

Table 9.
Max AIS pelvis– struck side front occupants

	All Dof	Non Oblique	Oblique
Max AIS 0,1	89.2 %	86.1 %	90.0 %
Max AIS 2,3	5.7 %	11.1 %	5.0 %
Max AIS 4+	0.6 %	2.8%	0 %
Not Known	4.5 %	0 %	5.0 %

(b) Closing speed As a measure of the impact severity, the closing speeds (km/h) for side impacts in which there was a car to car impact have been calculated (where the data allowed). The closing speeds for crashes involving 73 struck side occupants in newer model cars are shown in Table 10.

Table 10.
Closing speeds, struck side occupants (N=73)

	25 th percentile	50 th percentile	75 th percentile
All severities	34.5 km/h	46 km/h	65.0 km/h
MAIS 2+	43.5 km/h	62 km/h	76 km/h
MAIS 3+	46 km/h	70 km/h	81 km/h
Fatalities	71 km/h	76 km/h	90.8 km/h

When all occupant severities are considered, the 50th percentile closing speed is a little lower than the current test speed (50 km/h). However, when considering occupants with ‘Serious’ injury outcome (MAIS 2+ and MAIS 3+) a higher closing speed distribution is observed and the 25th percentile is closer to the current test speed. The closing speed for fatalities far exceeds the current test speed.

It should be noted that the sample size used here is small (73 struck side occupants) since substantial pre-selection on a data set comprising only newer cars has been made and both cars in the accident needed to have a recorded Delta-V in order to calculate the closing speed. However the results are in accordance with previous work (Thomas et al, 2003). Both this and the previous study indicate that Serious injury is prevalent and more frequent at impact speeds exceeding the current test speed and consideration should be given to increasing the test speed in order to better reflect the crash circumstances under which Serious injury still occurs in newer cars.

(c) Impact Height An analysis was then made of car-to-car impacts where the impact on the struck side was into the passenger compartment i.e.

middle third of the car (266 occupants). The analysis was made on an occupant basis to establish the proportion of occupants exposed to conditions where the sill has been overridden.

In 64% of cases, there was direct contact upon the sill, however the variable used in the analysis does indicate whether there was or was not an override of the sill at the same time. In 88 out of the 266 cases examined the bottom of the direct contact of the bullet car was clearly above the sill height for the struck side occupant, a third of cases. This is considered an underestimate of the number of cases since this represents full override and does not include cases where partial override may have occurred. In those cases where full override occurred, over two thirds of the bullet cars have a reported effective stiff structure height greater than 390mm the current height of the MDB used in European regulation. It is important to note that the lower stiff structures on car fronts may be set more rearwards so it is possible that considerable intrusion can occur from override even when there is good later stage structural engagement.

Part 3 – AIS 2+ injuries in struck side impacts in newer vehicles

Front seat occupants of post regulatory cars in struck side crashes, irrespective of direction of force, are considered in this section. The data comprise 317 occupants with an overall injury outcome as shown in Table 11.

Table 11.

Front occupant injury outcome in struck side impacts

	N	%
Fatal	27	8.5%
Serious	74	23.3%
Slight	177	55.8%
Uninjured	39	12.3%
Total	317	100

The KSI rate in this data set is somewhat higher than presented in part 1 (STATS19 data) since the CCIS data are biased towards serious injury outcome. However, the purpose of the analysis in this section is to examine the *type* of serious injury experienced by struck side occupants and so the sample bias does not affect the conclusions in this case.

In the subsequent analysis, the 350 AIS2+ injuries sustained by the 317 front seat occupants in struck side crashes are examined in more detail. Table 12 shows the breakdown according to AIS injury severity of the AIS 2+ injuries. A little under half of the AIS 2+ injuries are in fact AIS 2, a further

29.7% are AIS 3 and the remaining 23.8% are AIS 4 and above.

Table 12.

Severity of injuries to front occupants in struck side impacts

	N	%
AIS 2	163	46.6
AIS 3	104	29.7
AIS 4	50	14.3
AIS 5	24	6.9
AIS 6	9	2.6
Total	350	100

The distribution of the 350 AIS 2+ injuries across the various body regions is shown in figure 1. The largest proportion occurs to the head followed by the chest then the lower extremity.

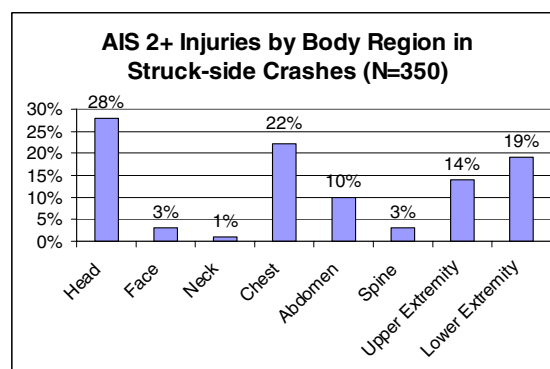


Figure 1. AIS 2+ Injuries by body region in struck-side crashes.

The data were then studied to examine injured body region by AIS score. Injuries to the head, chest, abdomen, upper and lower extremity (including pelvis) only have been included in this analysis since they are the only body regions which contribute more than 10% of the total number of AIS2+ injuries. This analysis is as shown in Table 13.

Table 13.

AIS2+ injuries to body regions

	AIS 2,3 N=267	AIS 4+ N=83
Head (N=97)	64%	36%
Chest (N=80)	58.8%	41.2%
Abdomen (N=36)	69.5%	30.5%
Upper limb (N=48)	100%	-
Lower limb (N=67)	100%	-

It can be seen from Table 13 that injuries to the upper and lower extremity are not particularly life-threatening since they are all rated as AIS 3 and below. However, the debilitating effects of AIS 2 and AIS 3 lower limb and in particular foot/ankle injuries should not be under-estimated (Morris et

al, 2006). For head, chest and abdominal injury, of those rating AIS2+, a further 30-40% rate as 4+. AIS 4+ injuries represent a greater threat-to-life particularly when multiplicity of injury occurs. The next analysis examines injury types for the main body regions injured. These are as shown in Tables 14 to 18.

Table 14.
Head injury typology in struck-side impacts

INJURY TYPE	N	% (OF ALL AIS2+ INJURIES)
Cerebrum injury (including contusion, laceration, haematoma, cerebral oedema, etc)	44	12.6
Skull fracture (including fracture to skull base and vault)	26	7.4
Unconsciousness for more than 1 hour	14	4.0
Other injury (including brain-stem, cerebellum etc)	13	3.7
Total	97	

Table 14 shows that injuries to the cerebrum are a particularly common injury in struck-side impact crashes followed by skull fractures. In many cases, these injuries occur simultaneously but this study has not examined multiplicity of injury. In total, cerebrum injuries comprise almost 13% of the total number of AIS 2+ injuries in struck-side impacts.

Table 15.
Chest injury typology in struck-side impacts

INJURY TYPE	N	% (OF ALL AIS 2+ INJURIES)
Up to 3 fractured ribs	17	4.9
More than 3 fractured ribs	14	4.0
Sternum fracture	7	2.0
Lung injury (including contusion, laceration)	27	7.7
Aorta laceration	5	1.4
Other injury	10	2.9
Total	80	

As can be seen from Table 15, fractures to the ribs in struck-side impacts (at all severities) comprise 9% of the total number of AIS2+ injuries in struck-side impacts. However, lung injuries (including particularly laceration and contusion) are also relatively frequent. Again, rib fractures and lung injuries do occur simultaneously but this effect has not been considered in this study.

Table 16.
Abdomen injury typology in struck-side impacts

INJURY TYPE	N	% (OF ALL AIS2+ INJURIES)
Liver injury (including laceration, contusion)	16	4.6
Spleen injury (including laceration, rupture)	12	3.4
Other injury	8	2.3
Total	36	

In Table 16, AIS 2+ abdominal injuries do not occur nearly as frequently in struck-side impacts when compared to injuries in other body regions. However, injuries to this body region do comprise over 10% of the total numbers of injuries in side impacts. Furthermore, just under one-third of abdominal injuries are rated as AIS 4+ and are thus associated with a relatively high risk of mortality.

Table 17.
Upper extremity injury typology in struck-side impacts

INJURY TYPE	N	% (OF ALL AIS 2+ INJURIES)
Clavicle fractures	16	4.6
Ulna/radius fracture	15	4.3
Humerus fracture	6	1.7
Metacarpus/carpus	5	1.4
Other	6	1.7
Total	48	

Whilst AIS 2+ upper extremity injuries are relatively common in side impacts, they are not usually rated above AIS 3 in terms of threat-to-life. Clavicle, radius and ulna fractures were found to be the most common injury types in side impacts as shown in Table 17.

Table 18.
Lower extremity injury typology in struck-side impacts

INJURY TYPE	N	% (OF ALL AIS 2+ INJURIES)
Pelvic fracture	25	7.1
Femur fracture (shaft, trochanter, condylar)	19	5.4
Tibia	8	2.3
Fibula	7	2.0
Other	9	2.6
Total	67	

Table 18 shows that pelvic and femur fractures make up the majority of AIS 2+ lower extremity

injuries in side impacts comprising 12.5% of the total number of AIS 2+ injuries. Below-knee injuries were relatively uncommon in comparison and foot/ankle fractures were found to be very rare in side impacts. However, all of the lower extremity injuries were rated as AIS 2 or 3 and are thus associated with a low probability of mortality. The injuries described above make up 94% (from Tables 14-18) of the total injuries that were sustained by struck-side front-seat occupants in side impact crashes.

Contact sources for these AIS2+ injuries were then analysed in order to establish the most frequent source of contact in (or exterior to) the vehicle. These are as shown in Table 19, which shows a number of interesting findings. Firstly, AIS 2+ head injuries were found to be associated with contacts on exterior objects usually the exterior surfaces of bullet vehicles and also direct contact on poles and trees. When head contact on the vehicle interior surface occurred, it usually involved interaction with the A or B pillar or the header-rail. Chest injuries tended to occur as a result of contact with the door which was also the case for abdominal injury in high severity crashes. The door region was also responsible for injuries to the upper and lower extremity. It is interesting to note that the airbag (both side/frontal) was thought to be responsible for approximately 10% of injuries to the upper extremity although whether this is due to direct interaction with the airbag or through 'fling' onto interior surfaces is uncertain.

Table 19.
Contact sources for AIS 2+ injuries in struck-side impacts

MAIN INJURY CONTACT SOURCES	1	2	3
Head	External contact (54%)	B-Pillar (19%)	A-Pillar (10%)
Chest	Door/B-pillar (68%)	Seatbelt (10%)	External contact (8%)
Abdomen	Door/B-pillar (56%)	Not known (22%)	External contact (17%)
Upper Extremity	Door (63%)	Not known (13%)	Airbag restraint (10%)
Lower Extremity	Door/footwell (68%)	Footwell/Facia (30%)	-

DISCUSSION

This paper highlights the success of regulation and also EuroNCAP in improving vehicle design for better crash protection. Benefits are clearly seen for drivers involved in struck side impacts. Changes that have been made and have given an apparent benefit to drivers in struck side in car-to-car impacts have also benefited drivers in struck side car-to-non-car impacts.

Despite the enormous improvements to vehicles in terms of safety, most vehicle occupants who are killed in side impact crashes die as a result of sustaining head or chest injury. Whilst there is some activity on-going in terms of head protection (e.g. EEVC proposed test procedure, optional pole-test as part of EuroNCAP, head protection airbags/side curtains), there is no specific procedure to exclusively consider chest protection, although side airbag technology is available. Additionally, a recent study by Morris et al (2005) indicated that whilst head bags seemed to offer increased protection in struck-side impacts, the same was not evident for chest bags, particularly those that were seat mounted.

The remaining problem for chest injury is somewhat surprising since the vehicle industry can meet the requirements of the current regulations governing side impact (i.e. UN-ECE R95) relatively easily and no issues concerning chest injury are detected in compliance testing. This could be because many vehicles are designed such that loading is applied directly from the vehicle B-pillar/door structure to the pelvis thereby removing the potential for loading via intrusion to the thorax by pushing the dummy sideways. However, the same will only apply in real-world situations if the transfer of load from the pelvis to the chest through the lumbar spine is correctly represented in the test dummy. This is probably not achieved in the EuroSID dummy but could be better predicted by the WorldSID dummy.

The analysis of injury severity in relation to the direction of force confirms that, in newer model cars, higher rates of Serious injury outcome for struck side occupants are apparent in non oblique impacts compared with oblique impacts and struck side impacts on the whole (irrespective of the direction of force). This is particularly the case for the chest, abdomen, pelvis and struck side limbs but not the case for head impacts.

With respect to the impact speed, it is evident that in newer model cars 'Serious' injury outcome occurs at crash speeds above that used in the current crash test. In order to predict and monitor these Serious injuries, consideration should be given to modifying the existing side impact test speed to better reflect that in which Serious injury occurs in real world crash situations.

A sizeable proportion of bullet cars contact the case car above sill height. It is anticipated that this proportion will grow as SUV/MPV type vehicles become increasingly more prevalent in the fleet. Consideration should be given to the structure and point of impact of the Mobile Deformable Barrier (MDB) in the side impact test procedure in light of the changing vehicle fleet.

Current test procedures only represent car-to-car impacts - however car to pole impacts are an important consideration (highlighted here in the analysis of injury contact sources, particularly for head injuries). EEVC have developed a pole-test procedure which could be used to monitor the situation for head protection but further modifications would be required to address chest protection in pole impacts.

Serious chest and abdominal injuries are however more likely to occur through direct contact with the intruding side door. Devices such as door and seat mounted chest air bags have been introduced to cushion the effects. However, as previously mentioned, there is no evidence to show that these have been effective. Continued monitoring of the effectiveness of side airbags is required including an assessment of the situation for out of position occupants with a view to the development of pre-crash sensing that would allow for early deployment. Additional countermeasures could include increased bolstering/padding of the interior door surfaces.

A further consideration, though not examined in the analysis presented here, is the interaction effect on struck-side occupants of non-struck side and rear seat occupants. The European regulation only requires a dummy in the front struck-side position. There is potential to make better use of other empty seats in order to monitor occupant interaction in the current test.

CONCLUSIONS

- Post regulatory vehicles offer improved protection for front occupant in struck-side crashes
- Rates of serious injury outcome are highest in non-oblique impact modes, in accordance with the current regulatory test.
- However, the CCIS data indicate that serious injury occurs at speeds exceeding those in the current regulatory test and that a sizeable proportion of bullet vehicle engage at a height above that used for the MDB in the regulatory test.
- Serious head and chest injuries continue to present a threat to life in post regulatory vehicles, for head injuries the major contact source is with an external object

(bullet vehicle, tree, pole) whilst for chest injuries the most prevalent contact source is the side door.

- A continued monitoring of the effectiveness of side airbag protection is required.
- Modifications to the current regulatory test procedure should be considered in order to ensure that the test best represents the real world accident situation that reflects more involvement of newer cars with improved safety.

REFERENCES

- [1] UNECE Regulation 95 – *Protection of Occupants Against Lateral Collision* <http://www.unece.org/trans/main/wp29/wp29regs81-100.html>
- [2] TRL Leaflet LF2087. Restraint use by car occupants, 2000-2002
- [3] TRL Leaflet LF2092. Restraint use by car occupants, 2002-2004
- [4] Morris, A; Welsh, R, Kirk, A and Thomas, P. Head and Chest Injury Outcomes in Struck-side Crashes. Proceedings IRCOBI Conference, Prague, Czech Republic, Sept 2005.
- [5] Morris, AP; Welsh, R H; Barnes, J S and Frampton, R. *The Nature Type and Consequences of Lower Extremity Injuries in Front and Side Impacts in Pre and Post-Regulatory Passenger Cars* Proceedings of IRCOBI Conference, Madrid Spain, 2006 (in press)
- [6] Thomas, P, Frampton R *Real-world Crash Performance of Recent Model Cars – Next Steps in Injury Prevention* Proceedings IRCOBI Conference, Lisbon, Portugal, 2003

ACKNOWLEDGEMENTS

The authors would like to acknowledge the financial support of the Department for Transport. This paper uses accident data from the United Kingdom Co-operative Crash Injury Study. CCIS is funded by the Department for Transport (Vehicle Standards and Engineering Division), Autoliv, Daimler Chrysler, Ford Motor Company, LAB, Nissan Motor Europe, Toyota Motor Europe and Visteon.

Further information on CCIS can be found at <http://www.ukccis.com/>

INVESTIGATION INTO A RESTRAINT SYSTEM DEVICE ADDRESSING DIFFERENT OCCUPANT SEATING POSITIONS AND REAL WORLD ACCIDENT SCENARIOS

Jörg Hoffmann

Toyoda Gosei Europe N.V.

Germany

Kazuaki Bito

Masanari Sakamoto

TOYODA GOSEI CO., LTD.

Japan

Paper Number 07-0173

ABSTRACT

The development of occupant restraint systems continues to evolve in response to new government regulations and consumer demand. Traditional seatbelt and airbag designs are giving way to more complex and intelligent systems that respond to crash and occupant conditions. In regulated vehicle compliance safety tests, restraint performance is usually judged against injury criteria that differ with respect to occupant size. On the basis of NASS/CDS accident data investigations, it can be observed that vehicle occupants on the passenger side sit predominantly on neutral to most-rear seat position. This paper discusses the approach of a multi-surface passenger airbag devised to enhance the protection of passenger occupants under different frontal collision scenarios in a range of varying occupant seating positions and occupant sizes. A wide range of experiments was carried out that adjusted parameters of the restraint system including seatbelt load limits, inflator outputs and various airbag shapes. This paper documents a new approach to a restraint system component as it looks behind specific test requirements to real world accident scenario comparisons.

Keywords: Airbag, Seating position, Adaptive

INTRODUCTION

Modern restraint systems for passenger cars are developed to protect occupants in the vehicle that is involved in an accident. A frontal protection system mainly consists of the seatbelt, the belt pretensioner,

the load limiter and the airbag. This system is developed to address low loads to the occupants under different accident conditions. Corresponding to the different occupant sizes, the restraint system is designed to AF05 seated in frontal position, AM50 seated in neutral position and finally rear position of AM95 dummies. But do these regulated seating positions reflect actual passenger seating positions in the real world?

NASS/CDS (National Automotive Sampling System / Crashworthiness Data System) accident data supplies information about the seating position of passengers during accidents. Based on the size of the occupant which has been defined by the body weight, the seating position can be allocated. A classification of occupant sizes has been made as follows: small-size occupants of 31 to 60 kg representing AF05 dummies, mid-size occupants with a body mass of 61 to 90 kg representing AM50 dummies and finally those occupants with a weight above 90 kg representing AM95 dummies. The seating positions were defined by the possible seat notches on the passenger seat: front-most, neutral and rear-most as well as both front-most/neutral and neutral/rear-most positions.

From the data evaluated it can be seen that many occupants on the passenger side do not sit in the position for which the restraint system was designed. More than 80 % of small passengers sit in the neutral to rear-most position, while more than 60 % of large occupants do not sit in the rear-most position for which the seatbelt and passenger airbag were designed. In the following Figure 1, the seating positions of the different occupant sizes are shown as

derived from NASS/CDS data. The investigation is based on 12,733 accidents in which passengers were injured between 1995 and 2004. Accidents involving busses, medium and heavy trucks have not been considered for this evaluation.

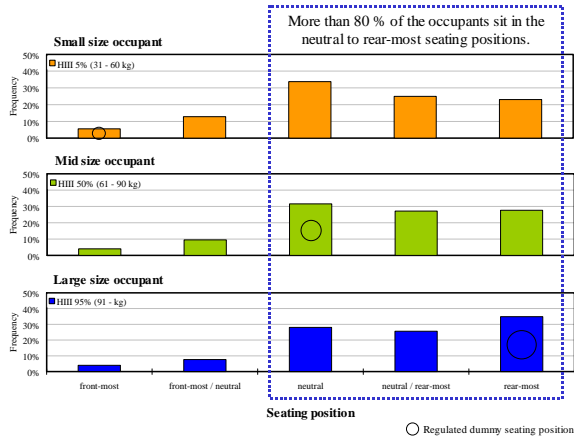


Figure 1. Seating position of occupants on the passenger side in real world

When evaluating NASS/CDS [1] accident data according to the injury area and injury levels on the passenger side, the following Figure 2 can be derived. The chart is based on 1,316 accident cases between 1995 and 2005 in which belted passengers were injured. Chest, head, lower and upper extremities are the most frequently injured body parts when evaluating the accident data according to AIS2+ injury level. The data also demonstrates that chest, head and abdomen injuries are most severe. Injuries of AIS4+ level occur.

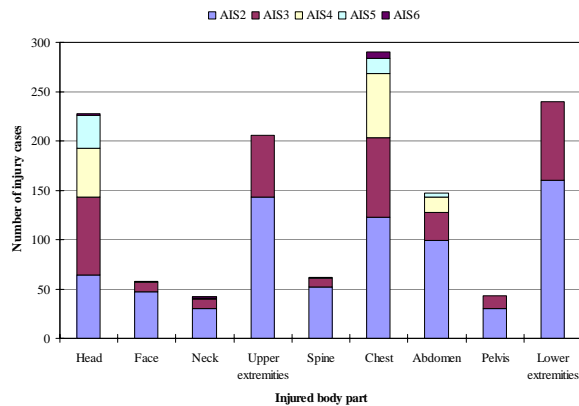


Figure 2. Injured body parts of front-seat passengers and their injury levels according to the abbreviated injury system ASI

When evaluating the same accident data, the cause of abdomen injuries of front-seat passengers can be derived. The data clearly shows that the lap belt

affects AIS2+ injuries disproportionately highly compared to armrest, instrument panel or passenger airbag. Figure 3 presents the derived accident data.

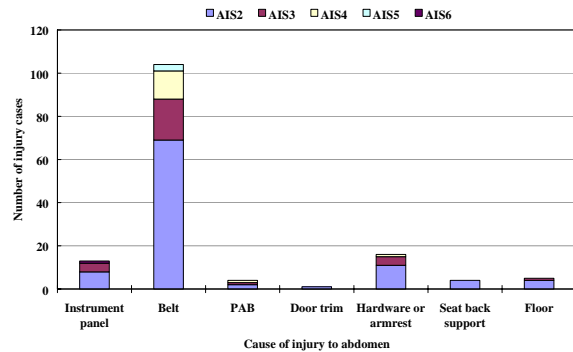


Figure 3. Cause of abdomen injuries of front-seat passengers and their injury levels according to the abbreviated injury system ASI

DESIGN CONCEPT

Nowadays, most passenger airbag cushion designs are of a simple 3-D triangular shape. In interaction with the seatbelt, they represent state-of-the-art technology for protecting passengers in both regulation and consumer test scenarios. Head and neck loads of AF05 and AM50 hybrid dummies are the scales used to determine the performance of such a restraint system, whereby the contact area between the dummy and the airbag front is characterised by the nose and chin as well as the concentrated contact load on the chest.

Based on the above information, it was decided that the development process for the multi-surface passenger airbag (MSA) would first be designed to address a low injury level of the AM50 dummy. If the injury levels in the head and neck area were too high, the loads would then be partly distributed to the chest area by a suitable change to the airbag design. It was recognised that in some cases, this change in airbag cushion design might lead to an increase of the head and neck injury level of AM50 dummies. To prevent these phenomena, a compromise between AM50 dummy head restraint performance and AF05 dummy neck injury level would have to be made.

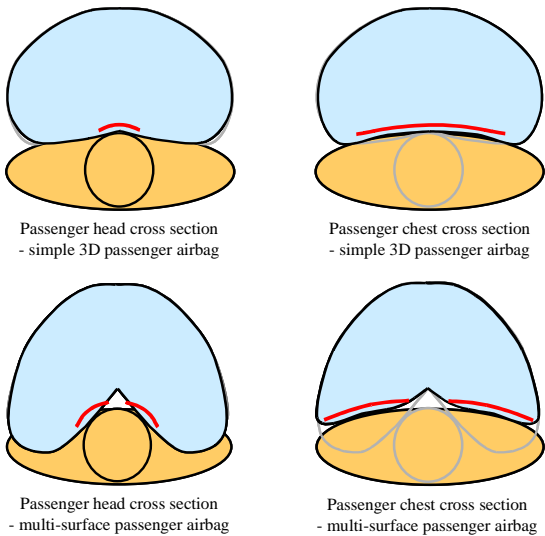


Figure 4. Comparison between simple 3-D passenger airbag and multi-surface airbag concept concerning contact force areas

Fortunately, multi-surface passenger airbags can be used to avoid the necessity of such a compromise and to counteract increased AF05 head and neck loads. In contrast to the simpler 3-D triangular cushion shape, this new airbag design technology provides distributed contact loads in the head and chest areas during the restraint phase. By causing the cushion to bulge out in two separate and specific contact zones to support the left and right areas of the chest, the resulting dent between the zones provides lateral contact of the head with the bag and supports longitudinal head movement during intrusion into the airbag, while also preventing the head from making direct contact with other hard points of the car, such as the A-pillar. The above Figure 4 shows the main differences in airbag cushion design between simple 3-D triangular shape and multi-surface airbags.

In a previous study [2], the occupant injury levels in frontal crashes with simple 3-D triangular and multi-surface passenger airbags were investigated. By using multi-body simulations with Madymo and performing sled tests, the effect on restraint performance of the different airbag design concepts was evaluated. In addition, simulations with the human simulation model THUMS were performed to analyse more deeply the protection effect of this safety device on loads experienced by the fifty percentile male. The study demonstrates that both airbag concepts, simple 3-D and multi-surface airbag, have an overall similar restraint performance which was confirmed by performing validated numerical simulations and conducting sled tests. Furthermore, the study of the multi-surface passenger airbag

showed that there is a potential increase in restraint performance for the AF05 dummy under unbelted conditions. Neck loads described by the normalised neck injury value can be reduced significantly. Reasons for this potential restraint improvement are, on one hand, the wide support of the upper torso and head during intrusion of the dummy into the airbag cushion and, on the other hand, the lateral stabilisation of the dummy head by the two dents of the cushion.

In the future, vehicle innovations will lead to an increase in information available both before and during collision, for instance the size and velocity of the obstacle, the direction of the crash, the characteristics and size of the passenger-side occupant and more details about the occupant's seating position. Based on this information, the restraint performance for real-life scenarios could be advanced if the restraint device can be controlled. This new information would in the future allow adaptation of restraint performance of safety devices to whichever occupant might be seated inside the car at any given moment.

Nowadays, it is possible to detect the position in which the occupant is sitting. Thus, it would be possible to adapt the performance of the passenger airbag to offer the best protection to the occupant in any seating position.

A bag shape optimised for one seating position would not be the best option for all possible positions. If information about where the occupant is sitting were available, it would be possible to adapt the shape of the multi-surface airbag – using variable bag technology – to offer the best protection to the occupant in a wider range of incidents [3].

The concept to adapt the multi-surface passenger airbag (adaptive multi-surface airbag – AMSA) is based on the ability to adjust the length of the airbag tethers during bag deployment, maintaining the concave frontal surface. By adjusting the length of the airbag tethers initially, three shapes of the airbag, i.e. A-shape, B-shape and C-shape, can be generated. The shapes correspond to the passenger seat positions. Respectively for the front-most seat position, the airbag will deploy in A-shape, for the neutral seat position in B-shape and for the rear-most seat position in C-shape. The superimposition of the three different airbag deployment shapes of the adaptive multi-surface airbag is indicated in Figure 5 as outlines.

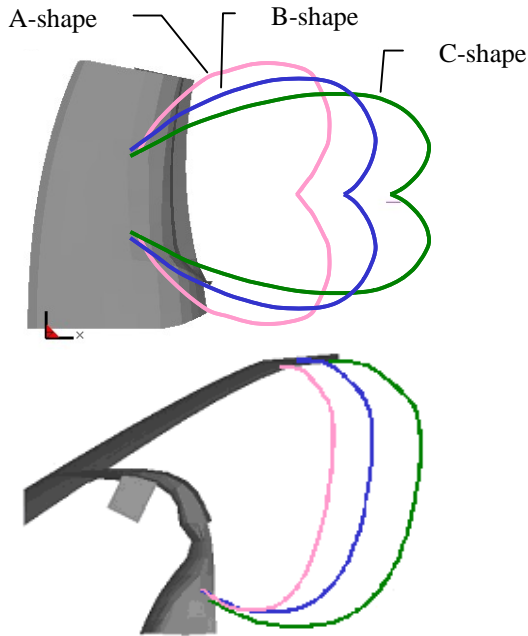


Figure 5. Superimposition of three different deployment shapes in cross-section of the adaptive multi-surface airbag for different seating positions on the passenger side; top – top view; bottom – side view

Selectable inflator gas output and variable vents complement the advanced airbag concept to supply the optimum airbag inner pressure for any occupant seating position.

NUMERICAL SIMULATION

The aim of the investigation was to assess the potential passenger restraint improvement by the application of an adaptive multi-surface airbag under the belt conditions of US-NCAP test procedure.

During the study, several multi-body simulations with Madymo [4] and tests, based on frontal crash scenarios with seatbelts and using an adaptive multi-surface passenger airbag, allowed us to evaluate the kinematics and injury level of the occupant sitting on the passenger side of the car. In addition, three different seating positions, front-most, neutral and rear-most for AF05, AM50 and AM95 dummies were investigated. To compare the restraint performance, a multi-surface passenger airbag with a volume of 130 litres and two constant vent holes each of 60 mm in diameter was selected as baseline technology. Also, a constant seatbelt force limit of 4 kN was applied. One of the variable parameters of the AMSA concept was the bag volume, which varies between

120 and 150 litres. Another parameter was the variable venting corresponding to the dummy size and seating position. The effectiveness of this airbag system was complemented by a seatbelt system that is able to adjust a belt force of 3, 4 and 5 kN. The varied parameters of the adaptive multi-surface passenger airbag are shown in Tables 1 and 2.

Table 1. AMSA parameters

	MSA	AMSA
Bag volume	130 litres	120 to 150 litres
Inflator	dual stage	dual stage
Vent size	Constant	Variable
Belt force limiter	4 kN	3, 4 and 5 kN

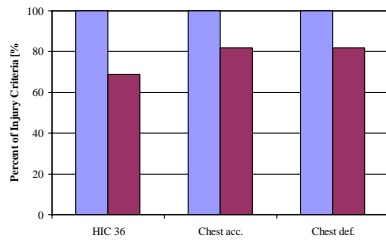
Table 2. Seat position versus AMSA shape

Front-most position	Neutral position	Rear-most position
A-shape	B-shape	C-shape

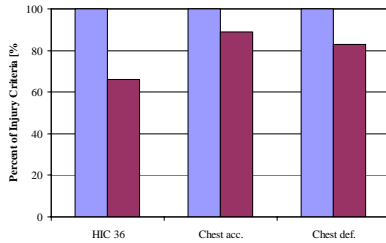
When evaluating the simulation results of the AF05 dummy, presented in the following Figure 6 as a normalised value, it is obvious that the adaptive multi-surface airbag is able to enhance the head loads compared to the MSA passenger airbag in its regulated seating position. In fact, a reduction of the head injury criteria (HIC_{36}) by 31 % was achieved. Even under the same crash scenario but seated in the neutral or rear-most position, the protection of the head through the adaptable bag technology with its variable vent was significant, improving the HIC value by 34 to 41 %. The advancement of chest acceleration $a_{3\text{ms}}$ by 11 to 19 % and chest deflection by 17 to 26 % can be ascribed to the concurrence of the AMSA and the adapted belt force limit.

The results of the study indicate that the optimisations of passenger airbag shape and seatbelt force limiters are viable measures for injury reduction of the occupant. Among them, the AF05 dummy representing small adults showed significant injury mitigation on its chest.

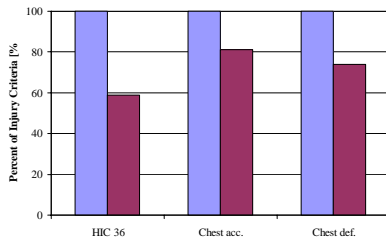
AF05 on front-most seating position



AF05 on neutral seating position



AF05 on rear-most seating position



■ Current Airbag ■ AMSA Airbag

Figure 6. Simulation results – comparison of injury levels of AF05 dummy standard versus AMSA in different seating positions

The results of head and chest loads, obtained from multi-body simulations with the three different dummy sizes and three different seating positions, are indicated in Table 3. It can be clearly seen that the loads were reduced for AM50 and AM95 dummies as well. It should be noted that the injury level of seating positions for which the MSA passenger airbag is not designed was substantially reduced.

Table 3. Simulation results – comparison of all injury levels of AF05, AM50 and AM95 dummies with MSA airbag versus AMSA in different seating positions

		Improvement [%]		
		Front-most	Neutral	Rear-most
AF05	HIC ₃₆	31*	34	41
	Chest a _{3ms}	18*	11	19
	Chest def.	18*	17	26
AM50	HIC ₃₆	39	29*	37
	Chest a _{3ms}	8	9*	8
	Chest def.	12	5*	19
AM95	HIC ₃₆	31	32	34*
	Chest a _{3ms}	6	7	4*
	Chest def.	4	9	5*

*: Dummy in regulated seating position

The superimposition of the three AMSA shapes and the AF05 dummy in front-most and neutral and rear-most seating positions is shown in Figure 7.

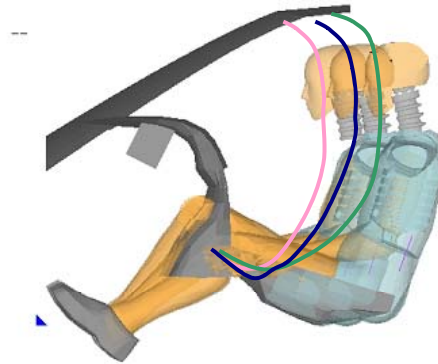


Figure 7. Superimposition of AF05 front-most/neutral/rear-most simulation model

Depending on the seating position, the response of the head acceleration under MSA and adaptive multi-surface airbag is presented in the following Figure 8 as normalised value plots for the AF05 dummy. In the design case for the small female dummy, which represents a tough requirement for the restraint system, the head acceleration response in front-most seating position is well pronounced. By applying the

AMSA, the limited forward displacement space of the occupant can be utilised to lower the head acceleration peak value under the same conditions. Airbag and seatbelt can be adjusted more gently. The effect of the adaptive multi-surface airbag under the remaining two seating positions is similar. By means of early contact between the head and the cushion during the restraint phase, the load level of the head can be kept much lower compared to the level experienced with the base airbag.

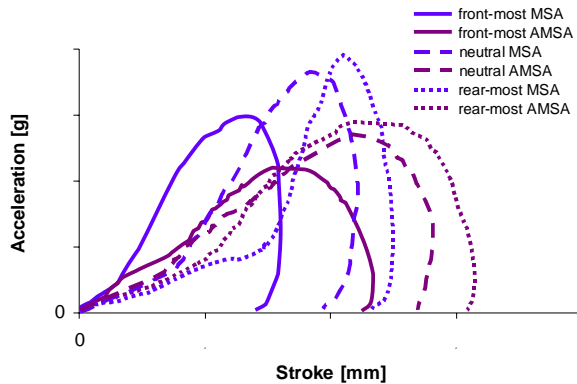


Figure 8. Head acceleration plot of AF05 in front-most, neutral and rear-most seating position with MSA and AMSA technology

Three different effects mitigating the injury criteria can be derived from these simulation results.

As already demonstrated in a previous study [1], the specific shaped passenger airbag is able to reduce dummy loads in the head and chest area due to the distributed contact forces between the dummy and the airbag. When this multi-surface airbag adapts to the seating position occupied by the dummy, earlier restraint is achieved. The loads on the human body can be reduced. – First effect.

During the restraint phase of the dummy, its kinetic energy will be absorbed mainly by belt elongation, by the force limiter of the seatbelt system and the venting of the airbag. Variable vent holes are able to adjust the damping behaviour by changing the inner pressure of the cushion, shaped according to the dummy size and its seating position and thus, forward displacement can be optimised. – Second effect.

The third effect attributed to the AMSA is the possibility to introduce a variable seatbelt force limiter to manage the different dummy sizes in their various seating positions and thus to optimise the load acting on the occupant’s chest.

THE EFFECT ON ABDOMEN INJURY MITIGATION

As confirmed by the multi-body simulation, the AMSA for the passenger side could reduce the loads on head and chest, accounting for the early restraint of the dummy during the crash and for the ability to adapt energy absorption. But when reviewing the results of the evaluation in Figure 8, the protection potential for the abdomen using AMSA also needs to be validated.

Dummies like Hybrid III are not the appropriate measures for valuing and judging the injuries of the abdomen which often turn into higher AIS injury levels subsequently.

A dummy’s dimensions are based on statistical and biomechanical values and are used to evaluate the performance of a restraint system according to defined injury limits. These measurements are an essential tool for the development process of a restraint system. However, numerical simulation with the human simulation model THUMS can be performed in order to assess the restraint performance concerning local loads on the human body.

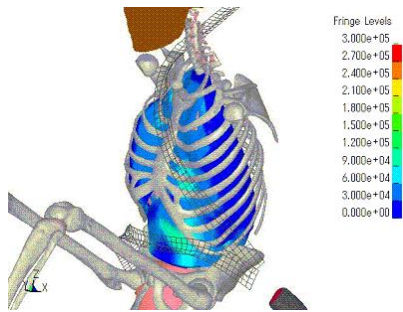
The THUMS is a family of human models created by Toyota Central R&D Labs that represent a fifty percentile male. The THUMS LS-Dyna model has been validated by four different test scenarios [5] and [6]: thoracic frontal impact [7] and [8], thoracic side impact [9], pelvic side impact [9] and abdominal frontal impact [10].

Using the fifty percentile male human model THUMS, a sled test simulation model was created in LS-Dyna based on the same vehicle environment parameters as in Madymo. The restraint components are the same as the validated components used in the multi-body simulations. The analysis was based on the same crash scenario: 56 km/h US-NCAP crash specification under belted conditions.

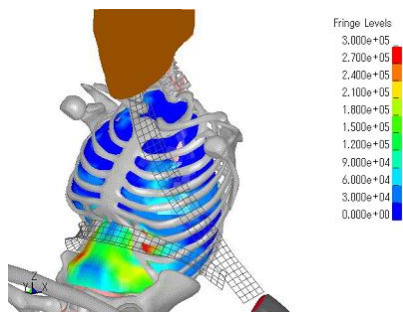
By applying the human body simulation model THUMS, the effect on abdomen injuries of the adaptive multi-surface airbag and the corresponding belt force limit was investigated

Four scenarios were set up and investigated. The basic set up involves the fifty percentile male human body seated in neutral position with MSA passenger airbag and a backrest inclination regulated per the US-NCAP specification. A second simulation model was set up with the same airbag and seating position but with a flattened backrest. The third scenario

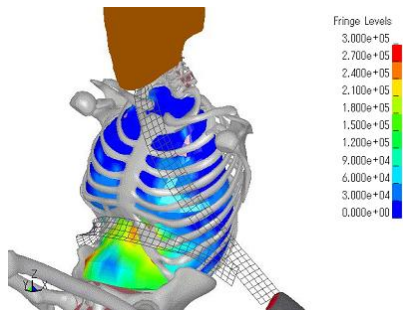
featured a flattened backrest and the adaptive multi-surface airbag. The fourth scenario was the sled model with AMSA and knee airbag.



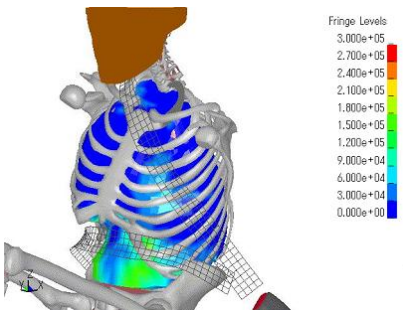
MSA passenger airbag under US-NCAP conditions



MSA passenger airbag with flattened backrest



AMSA with flattened backrest



AMSA and KAB with flattened backrest

Figure 9. Comparison of belt loads on the abdomen under different restraint conditions and backrest inclinations

The analysis of the results in Figure 9 with the MSA passenger airbag showed moderate loads on the abdomen. The results with the same airbag but with the flattened backrest showed an increase of the abdominal loads which can be attributed to the changed occupant kinematics. During the restraint phase of the occupant, the lap belt in the seat belt system slips from the pelvis to the abdomen. This results in a strong forward movement of the occupant's pelvis and results in increased abdomen loads.

The AMSA allows to set the seat belt load limiter at a lower force level. Thanks to early restraint of the occupant during the restraint phase, there is a slight reduction in pelvis displacement as well as lap belt slippage. Hence, local forces on abdomen can be attenuated. However, slippage of the lap belt off the pelvis sill occurs. The analysis of the results with AMSA airbag in combination with a knee airbag under the same crash conditions indicates an improvement in the occupant kinematics. By introducing the knee airbag, the effect on the occupant's pelvis displacement is further enforced. Thus, the abdominal loads on the occupants under flattened backrest conditions could be further mitigated. In the following Figure 9, the loads on the abdominal area are presented as normalised contour plots.

CONCLUSION

Simple 3-D passenger airbags are able to prevent the passenger-side occupant from experiencing high injury loads during a head-on collision. This study demonstrates that the adaptive multi-surface passenger airbag concept has an overall improved restraint performance under advantage of seating positions, which was confirmed by performing validated numerical simulations. This study confirms that the adaptive multi-surface airbag is a viable means of reducing occupant injuries in the conditions.

Furthermore, the multi-body simulation of the adaptive multi-surface passenger airbag showed that there is a potential increase in restraint performance for the AF05 dummy under belted conditions seated in different positions. Head loads described by the head injury criteria can be reduced significantly. The reasons for this potential restraint improvement are the early and wide support of the upper torso and head by the shape adaptation to the occupant's seating position in combination with seatbelt force limits and variable vents.

In addition to numerical development tools with dedicated software, and empirical development tools such as crash and sled tests, simulation with human models complements the development process by allowing a better understanding of the protection mechanism of a restraint device. It also complements the information that is derived from a frontal dummy, making it possible to obtain data about loads on bones and organs. The numerical simulations with the human body model THUMS were also useful for gaining a better understanding of the detailed protection mechanism of the adaptive multi-surface airbag. It was observed that local stress acting on the abdomen could be reduced by a adaptive multi-surface design in combination with the variable force limiter of the seatbelt system. In addition, it was found that the restraint of knees by a knee airbag can add to the reduction of pelvis forward displacement and thus to reduce abdomen loads under backrest flattened conditions.

REFERENCES

- [1] NASS/CDS: National Automotive Sampling System / Crashworthiness Data System, 1995-2004.
- [2] Hoffmann J., Sakamoto M., Freisinger M., Shiga I., "Potential passenger restraint system improvement by the application of a multi-surface airbag.", 8th International Symposium and Exhibition on Sophisticated Car Occupant Safety Systems, airbag 2006, Karlsruhe, Germany, December 2006.
- [3] Richert J., Coutellier D., Götz C., Eberle W., "Advanced smart airbags: The solution for real life safety?", VDI-Berichte Nr. 1967, 2006.
- [4] Madymo 6.2.2 Reference / Theory Manual. TNO Madymo BV. Delft, The Netherlands, August 2006.
- [5] LSTC, LS-DYNA User's Manual. 2006.
- [6] Toyota Central R&D Labs THUMS User's Manual, 2006.
- [7] Kroell C. K., Schneider D. C. and Nahum M., "Impact tolerance and response of the human thorax.", SAE Paper No. 710851, 1971.
- [8] Kroell C. K., Schneider D. C. and Nahum M., "Impact tolerance and response of the human thorax II.", SAE Paper No. 741187, 1974.
- [9] Bouquet R., Ramel M., Bermond F. and Cesarii, D., "Thoracic and pelvis human response to impact." Proceedings of the 14th International Technical Conference on the Enhanced Safety of Vehicles, pp. 100-09, 1994.
- [10] Nusholtz G. S., Kaiker P. S. and Lehman R. J., "Steering system abdominal impact trauma.", MVMA Report UMTRI-88-19, 1988.

RESEARCH INTO NEW SIDE IMPACT TEST BASED ON ACCIDENTS IN EUROPE AND JAPAN

Taisuke Fujiwara

Hiroyuki Murayama

Toyota Motor Corporation

Japan

Paper Number 07-0219

ABSTRACT

The current test procedures described in European and Japanese side impact regulations and ratings are conducted so that a non-crabbed Mobile Deformable Barrier (MDB) strikes a stationary test vehicle. However, in real-world accidents, many struck vehicles are not stationary but moving when the collision occurs. In consequence, it is advantageous to consider the velocity of the struck vehicles as well as that of the striking vehicles.

Accordingly, data of accidents occurring in Europe and Japan was analyzed. This accident data analysis showed that in both regions, more accidents occurred when struck vehicles were moving than when stationary. Consequently, car-to-car side impact tests were conducted using a moving target vehicle to comprehend the real-world deformation characteristics of the struck vehicle. Two side impact tests were then conducted using the Advanced European - Mobile Deformable Barrier (AE-MDB) Ver. 3.3, which represents the front-end stiffness of vehicles in Europe and Japan. The tests were conducted so that the AE-MDB struck both stationary and moving vehicles to compare the differences between the two scenarios. The test results indicated that larger and more severe peak intrusion level can be seen on stationary vehicles, but different types of deformation mode were seen between the stationary and moving vehicles. Based on these results, a new side impact test procedure using AE-MDB Ver. 3.3 was devised. The AE-MDB trolley was moved at a crabbed angle to reflect the moving condition of the target vehicle. This procedure represents a more common accident scenario that occurs in the real-world, and it allows for the direction of load applied to the struck vehicle to be taken into consideration. Such a test procedure that represents a more common real-world accident scenario is useful to further advance vehicle safety in side impacts.

INTRODUCTION

Since the fatalities in side impact accidents have not decreased in comparison with that of frontal impact accidents, many research institutes and vehicle manufacturers are examining various aspects of vehicle safety in side impacts. As one of these aspects, it can be stated that the existing ECE regulatory side impact test procedure (R95) is becoming less representative of the impact severity

observed in recent accident data [1]. It has also been stated that side impact tests should be made more severe than the R95 procedure in order to represent a more severe side impact crash as found in real-world side impact accidents. Yonezawa [2] et al. investigated vehicle front-end characteristics and clarified the differences between them and the existing R95 barrier. Based on this data, the Japan Automobile Manufacturers Association, Inc. (JAMA) and the Japan Automobile Standards Internationalization Center (JASIC) developed AE-MDB Ver. 3.3 to represent the front-end stiffness of recent vehicle [3]. In addition, after researching accident data in the Co-Operative Crash Injury Study (CCIS) and considering the repeatability and reproducibility of tests, the European Enhanced Vehicle-safety Committee Working Group 13 (EEVC WG13) developed a new side impact test requirement using AE-MDB [1]. However, the CCIS accident data researched at that time was out of date and did not reflect recent accidents, additionally the accident data were not collected from other regions. For these reasons, this paper presents a new test procedure using AE-MDB Ver. 3.3. The procedure represents a more common side impact accident scenario based on real-world accidents and research into vehicle characteristics conducted in Europe and Japan.

ANALYSIS OF ACCIDENTS AND VEHICLE CHARACTERISTICS

The European and Japanese accident databases used in this research are from CCIS (2002/1-2005/12), the German In-Depth Accident Study (GIDAS: 2003/1-2005/12), and the Institute for Traffic Accident Research and Data Analysis (ITARDA: 1994/1-2003/12).

Research requirements:

1. Accident cases involving car-to-car side impacts, and resulting in fatality or injury (MAIS 2+) were extracted.
2. Regardless of fastening seatbelt or not.
3. Curb weight of striking and struck vehicles is 2500 kg or less.
4. Non-multiple accidents.
5. Cases resulting in fatality or injury due to side slipping were omitted.

Supplementary explanations:

In CCIS database, cases resulting in fatality or injury occurred in roundabout were omitted.

In CCIS and GIDAS data that correspond to the requirements listed above, based on investigations into the sketch, account, and photo of each accident, cases in which cabins of struck vehicles were not deformed, and collision configurations which were not considered as side impacts were omitted. In addition, accident data that did not contain the sketch nor account of each accident were also omitted.

Impact Direction

The impact direction in side impact accidents was analyzed. The angle at which the struck and striking vehicles are configured on impact is defined as the impact direction. In real-world accidents, vehicles are most likely to be struck from the directions around 3 or 9 o'clock (90 degrees) (Figure 1).

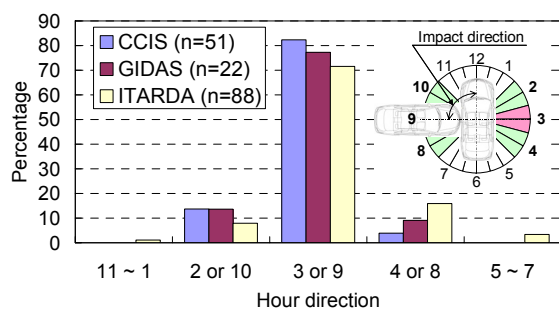


Figure 1. Frequency of Impact Direction in Side Impact Accidents.

Impact Velocity of Striking Vehicle

Next, the impact velocity of striking vehicles was analyzed. This data is available from GIDAS and ITARDA, since these databases have impact velocity data. The values from GIDAS are estimated or calculated, and those from ITARDA are based on evidence given by drivers or are estimated from brake marks. ITARDA, which contains a larger amount of data than GIDAS, shows that the highest percentage of fatality or injury can be seen when the impact velocity is approximately 55 km/h (Figure 2).

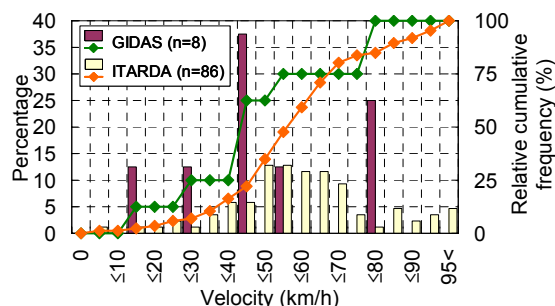


Figure 2. Velocity Distribution in Side Impact Accidents.

Accident Situation

Accident situations were also analyzed. The CCIS data shows that the highest percentage of side impact accidents occurred while the struck vehicle was

turning right or left. On the other hand, the GIDAS and ITARDA data show that the highest percentage of side impact accidents occurred while the struck vehicle was traveling in a straight line. The percentage of side impact accidents that occurred while the struck vehicle was stationary is low in all 3 databases (Figure 3).

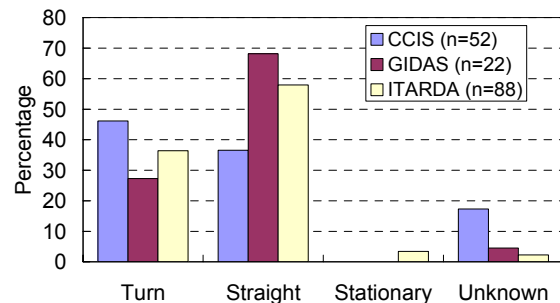


Figure 3. Frequency of Struck Vehicle Condition in Side Impact Accidents.

Velocity Ratio

As Figure 3 indicates, few accidents occurred when the struck vehicle was stationary. For this reason, the velocity ratio of the striking vehicles to the struck vehicles was analyzed. This was calculated based on the data from GIDAS and ITARDA, since these databases have impact velocity data. Consequently, a high percentage of velocity ratios between 1 and 3.73 were found in these databases (Figure 4). Converting the ratios to the direction of load applied to the struck vehicle obtained an angle of about 30 degrees. This direction is seen most often in real-world accidents.

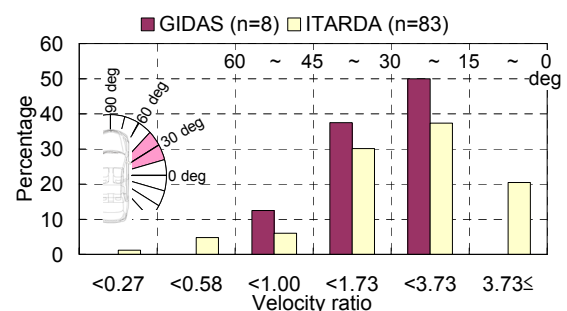


Figure 4. Frequency of Velocity Ratio of Striking Vehicle to Struck Vehicle.

Vehicle Weight

In order to obtain recent vehicle weights, weight data was researched based on vehicle sales data collected in each region. This research did not use accident data. (Research requirements - Europe: 2005 sales data from 19 countries, vehicle models ranked in the top 10 of sales volume of each segment; Japan: 2003 sales data, vehicle models that sold more than 20,000). The result shows that in both Europe and Japan, around 90 % of vehicles sold weighed 1500 kg or less (Figure 5). Accordingly, it can be said that most of the striking vehicles in real-world accidents

would also weigh 1500 kg or less.

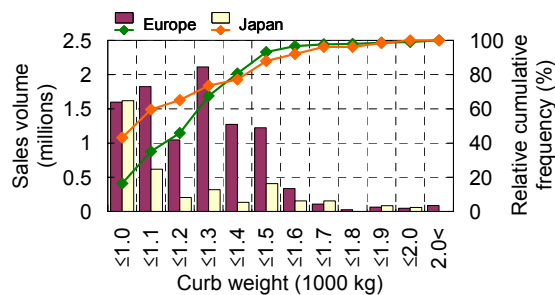


Figure 5. Relative Cumulative Frequency of Curb Weight.

REPRESENTING REAL-WORLD ACCIDENTS

Test Conditions

Car-to-car tests were conducted in order to reproduce real-world accidents. The test conditions were defined as follows based on previous research (Figure 6).

- 1. Impact Direction** - The longitudinal centerline of the bullet vehicle perpendicular to the longitudinal centerline of the target vehicle when the bullet vehicle strikes the target vehicle.
- 2. Impact Velocity of Striking Vehicle** - The velocity of the bullet vehicle was 55 km/h, which is the same velocity specified in J-NCAP. In addition, half of side impact accident fatalities and injuries in Japan occur when the striking vehicles were traveling at 55 km/h or less, as shown in Figure 2.
- 3. Velocity Ratio** - In the real-world, many struck vehicles are side impacted at an angle of 30 degrees in the direction of applied load. Therefore, the velocity ratio between the target and bullet vehicles was specified to be 1 to 2.
- 4. Vehicle Weight** - The bullet vehicle weight was specified to be 1500 kg.
- 5. Impact Point** - The impact point was specified at a position where the bumper beam of the bullet vehicle does not contact the front pillar and rear wheelhouse of the target vehicle during the impact development, in order to apply the most severe deformation to the target vehicle.

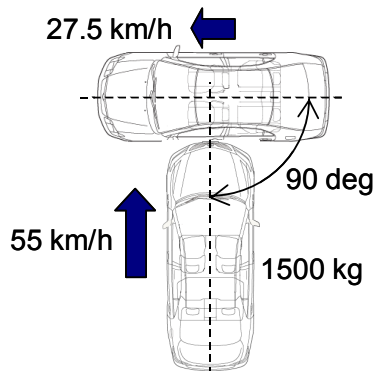


Figure 6. Test Conditions.

Conducting Representation Test

Bullet Vehicle Models - The 1500 kg Passenger Car (PC) was used as the baseline bullet vehicle. In addition, more severe tests using the 2000 kg PC and 2000 kg Sport Utility Vehicle (SUV) as the bullet vehicles were also conducted to obtain reference data. When the front-end stiffness of these three bullet vehicle models was examined, it was found to be close to the AE-MDB Ver. 3.3 corridor (Figure 7).

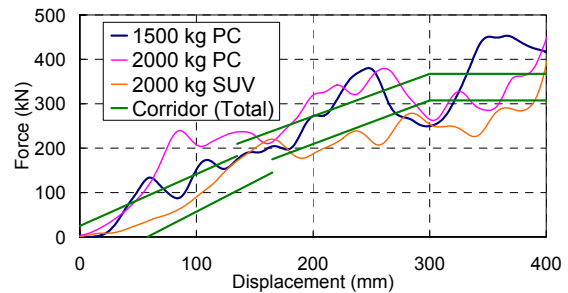


Figure 7. Vehicle Front-End Stiffness.

Target Vehicle Model - Another 1500 kg PC was used as the struck vehicle. The PC equipped with side airbags and curtain shield airbags.

Anthropometric Test Devices - Since the ES-2 dummy, which is seen as being an improvement over the EuroSID-1, is used in Euro-NCAP, it was also used in this research.

Test Observations - The deformation in the struck side of the target vehicle after the baseline test is shown in Figure 8. There was no indication that the bumper beam of the bullet vehicle intruded far enough to contact the front pillar and rear wheelhouse. This indicates that the test met test condition 5, "Impact Point".

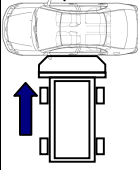
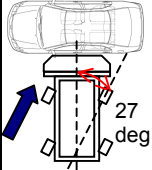
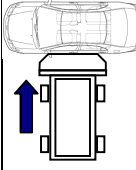


Figure 8. Struck Side of the Target Vehicle.

Representation with AE-MDB Ver. 3.3

Subsequently, three types of test procedures were considered to define their potential to help represent a severe real-world side impact accident using AE-MDB Ver. 3.3 (Table 1).

Table 1
AE-MDB Test Matrix

Name	MtM	CtS	MtS
Configuration			
Impact point (mm)	SRP-66.5	SRP-66.5	SRP+250
Velocity (km/h)	27.5 x 55	62	55

MtM = Moving trolley to moving vehicle
 CtS = Crabbed moving trolley to stationary vehicle
 MtS = Moving trolley to stationary vehicle
 SRP = Seating reference point

The trolley weight for the three tests was 1500 kg. A 1500 kg PC was used as the target vehicle. This was the same target vehicle as that used in the car-to-car test.

The ES-2 dummy was used.

MtM Test - The MtM test was conducted in accordance with the car-to-car test conditions previously explained. The impact point was arranged as the position where the beam element of the AE-MDB was deemed not to contact with the front pillar and rear wheelhouse of the target vehicle during the impact development.

CtS Test - In the CtS test, the crab angle was specified to be 27 degrees, reflecting the velocity ratio of 1 to 2. The impact velocity was calculated from the relative velocity of the MtM test condition. The impact point was the same as that of the MtM test.

MtS Test - In the MtS test, the impact velocity was specified to be 55 km/h. This is the same as that of the bullet vehicle specified in the MtM test. The impact point was specified to be SRP+250 mm, based on the research paper of Ellway [1] et al.

Vehicle Intrusion Profiles

In all of the tests conducted, the geometrical characteristics of each target vehicle were mapped before and after each impact. The measurement lines for these tests are shown in Figure 9. Regarding the front and rear door panels, the inner panels were measured.

The post-test deformation profiles for each line were shown in Figure 10. The data set contains the results of the six tests explained previously.

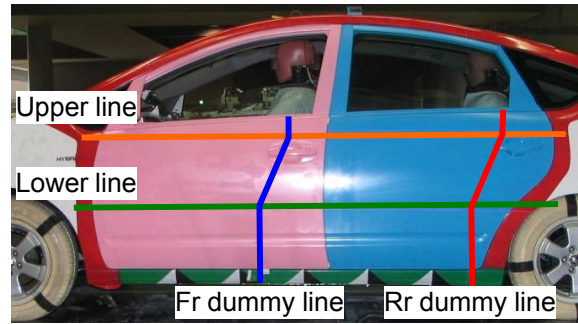


Figure 9. Measurement Lines of the Target Vehicle.

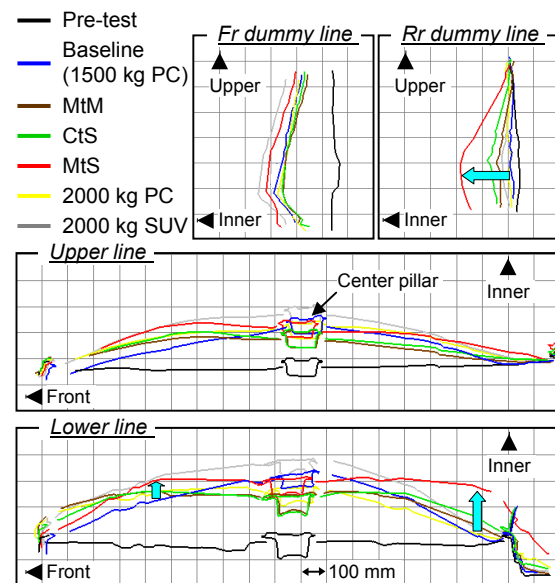


Figure 10. Intrusion Profiles of the Target Vehicle.

In the MtM test, although the peak intrusion level of the Fr dummy line was 36 mm smaller than that in the baseline test, the deformation mode was very similar.

In the CtS test, the intrusion level of the Fr dummy line was almost the same as that in the MtM test. This indicates the MtM test and the CtS test are essentially equivalent.

On the other hand, in the MtS test, the intrusion level of any point in the Fr dummy line was larger than that in the baseline test, and the peak intrusion level of the Rr dummy line was 192 mm larger than that in the baseline test. Especially, for the deformation at the lower lines, the center pillar intrusion level was almost the same as that in the baseline test, but the deformation mode at the front part of the front door inner and the rear part of the rear door inner was much different.

Front and Rear Dummy Responses

The percentages of measured injury values to injury criteria are shown in Figure 11. The injury criteria are defined in R95. The data set contains the results of the six tests explained previously.

In the MtM test, the values for pelvis injury in the

rear dummy were higher than those in the baseline tests, whereas the values for other body part injuries were at similar.

In the CtS test, the results were similar to those in the MtM test. There was no major difference between the results in the baseline test, except the value for pelvis injury in the rear dummy. However, in the MtS test, the values for pelvis injury in both the front and rear dummies were higher than those in the baseline test, and the maximum deflection at the thorax in the rear dummy was lower than that in the baseline test.

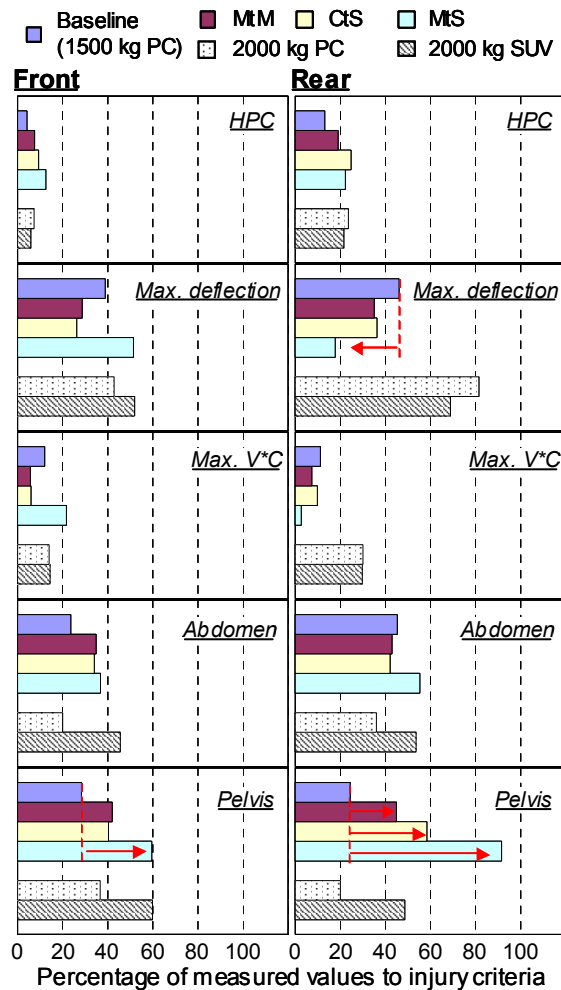


Figure 11. ES-2 Dummy Responses.

DISCUSSION

This paper integrates the results of research on real-world accidents and vehicles into test conditions to define their potential to develop a more representative test condition using AE-MDB Ver. 3.3.

In the case of the baseline test, the deformation mode at the door inner and center pillar on the target vehicle showed an arc. Similar results were seen after impact from different bullet vehicles. This result implies that the bullet vehicle does not

perpendicularly intrude into the target vehicle, but instead slides to the rear of the target vehicle and intrudes into the target vehicle in accordance with the velocity component of the target vehicle. In contrast, in the case of the three tests using AE-MDB Ver. 3.3 as the bullet vehicle, the door inner and the center pillar appeared to be intruded parallel to the pre-test configuration. Especially in the MtS test, larger deformation was seen at the rear part of the rear door. This result is totally different from the one in the car-to-car test. However, in the MtM and CtS tests, the velocity component of the target vehicle was considered, and the deformation mode was more similar to that in the car-to-car test.

In the MtM test, the dummy responses were more similar to those in the baseline test than those in the MtS test. In the CtS test, the dummy responses were similar to those in the MtM test.

In the MtS test, the value for pelvis injury was higher than that in the baseline test. This is assumed to be because a higher intrusion level at the door inner was seen in the MtS test than that in the baseline test.

According to analysis of Japanese accident data as researched by Yonezawa [2] et al., chest injuries occur more than pelvis injuries in side impact accidents. However, in the MtS test, the value for maximum deflection at thorax for the rear dummy was lower than that in the baseline test. This result is different from the trend of injured body part that occurred in real-world side impact accidents.

For these reasons, it is believed that the test conditions of the MtM or CtS tests, which represent the values for injury tendency seen in real-world accidents, are more effective than the those of the MtS test for occupant protection.

Since the CtS test considers the direction of load applied to the target vehicle of the MtM test, the vehicle intrusion level, deformation mode, and dummy responses are very similar in the two test conditions. This result indicates that the CtS test conditions can be used as a substitute for the MtM test conditions.

Tests were also conducted using AE-MDB Ver. 3.3. After the tests, it was found that the beam element of AE-MDB Ver. 3.3 was bent. This result caused a lower intrusion level at the center pillar than that in the baseline test. Consequently, JAMA and JASIC have developed a new generation barrier by applying a frontal plate to the beam element of AE-MDB Ver. 3.3 to increase the strength of the element. With the new generation barrier, it is thought that the intrusion level at the center pillar will be more similar to that found in the baseline test.

FUTURE RESEARCHES

In this research, only one vehicle model was used as a target vehicle. In the future, various types of vehicles should be investigated to verify the same tendency.

In addition, when the MtM and CtS tests were conducted, lateral bending and shear were found on the AE-MDB. In the car-to-car test, lateral bending was found at the front side rail on the bullet vehicle. Therefore, it is necessary to study to make the lateral mechanical properties of the AE-MDB correspond to those of the bullet vehicles.

CONCLUSIONS

1. Based on real-world accident analysis research in Europe and Japan, a side impact test procedure using AE-MDB Ver. 3.3 was devised.
2. In an MtM test using AE-MDB, the trends of deformation mode for the target vehicle and the injury values provide a more representative test condition than the MtS test condition, when compared to recent real-world accident data.
3. Based on the research completed, the CtS test can be conducted as a substitute for the MtM test.

REFERENCES

- [1] Ellway, J. D. (on behalf of EEVC WG13). 2005. "The Development of an Advanced European Mobile Deformable Barrier (AE-MDB)." The 19th International Technical Conference on the Enhanced Safety of Vehicles (ESV) (Washington D.C., Paper No. 05-0239).
- [2] Yonezawa, H. 2001. "Japanese Research Activity on Future Side Impact Test Procedures." The 17th International Technical Conference on the Enhanced Safety of Vehicles (ESV) (Amsterdam, The Netherlands, Paper No. 267).
- [3] Japan Automobile Standards Internationalization Center (JASIC). 2004. "Full-scale Side Impact Test Results in Japan." The 37th EEVC WG13.
- [4] Lowne, R. (on behalf of EEVC WG13). 2001. "Research Progress on Improved Side Impact Protection: EEVC WG13 Progress Report." The 17th International Technical Conference on the Enhanced Safety of Vehicles (ESV) (Amsterdam, The Netherlands, Paper No. 47).

ACKNOWLEDGMENTS

This paper uses accident data from the United Kingdom Co-operative Crash Injury Study (CCIS) collected during the period January 2002 to December 2005, from German In-Depth Accident Study (GIDAS) collected during the period January 2003 to December 2005, and from Institute for Traffic Accident Research and Data Analysis (ITARDA) collected during the period January 1994 to December 2003.

Currently CCIS is managed by TRL Limited, on behalf of the United Kingdom Department for Transport (DfT) (Transport Technology and Standards Division) who fund the project along with Autoliv, Ford Motor Company, Nissan Motor Company and Toyota Motor Europe. Previous sponsors of CCIS have included, Daimler Chrysler, LAB, Rover Group Ltd, Visteon, Volvo Car Corporation, Daewoo Motor Company Ltd and Honda R&D Europe (UK) Ltd.

Data was collected by teams from the Birmingham Automotive Safety Centre of the University of Birmingham; the Vehicle Safety Research Centre at Loughborough University; TRL Limited and the Vehicle & Operator Services Agency of the DfT

Further information on CCIS can be found at <http://www.ukccis.org>

The Medical University of Hannover study (MUH) is funded by the Federal Highway Institute (BASt). A second team was set up in Dresden (TUD) and is funded by the FAT (Forschungsvereinigung Automobiltechnik or Automotive Industry Research Association). The German In-Depth Accident Study (GIDAS) is co-operation between the two projects.

NEARSIDE OCCUPANTS IN LOW DELTA-V SIDE IMPACT CRASHES: ANALYSIS OF INJURY AND VEHICLE DAMAGE PATTERNS

Mark Scarboro

Rodney Rudd

National Highway Traffic Safety Administration
United States

Mark Sochor

University of Michigan Transportation Research Institute
United States
Paper Number 07-0225

ABSTRACT

Nearside occupants in side impact crashes often sustain severe injuries resulting in significant economic burden. Continual advancements in safety technology, including reinforced door structures, torso and head curtain air bags, compatibility improvements and other advancements, attempt to provide increased protection to occupants in these side impact crashes. Despite these advancements, serious injuries continue to occur at low delta-V's. In this paper, detailed analysis of field crash data will show which factors have the most influence on occupant outcome in these side impact crashes.

One-hundred and eighty-nine side impact crashes from the Crash Injury Research and Engineering Network (CIREN), National Automotive Sampling System/Crashworthiness Data System (NASS/CDS), and Special Crash Investigation (SCI) databases were selected based on crash criteria including a delta-V below 40 km/h and a principal direction of force (PDOF) between 2 and 4 o'clock or 8 and 10 o'clock. Cases were also restricted to those in which the front-row nearside occupant sustained an AIS 3+ injury to the head, torso, abdomen or lower extremity. Analyzing anatomical injury in conjunction with the vehicle damage patterns allows for the development of injury causation scenarios, which can speak directly to the interaction of the occupant and the components of the vehicle during the crash. These findings may identify trends which could be investigated for potential areas of improvement in future side impact testing and design of countermeasures.

INTRODUCTION

Nearside crashes have higher serious injury and fatality risks as compared to all crash modes [Samaha and Elliot, 2003]. Nearside occupants are at increased risk of significant injury due to their

limited ride down space and proximity to the intruding vehicle structures. The limited crush space and intervention time to protect the nearside occupant in a lateral crash makes the development of effective occupant protection features a difficult task. The challenges are even greater with recent shifts in the composition of the U.S. fleet towards a greater proportion of higher-riding trucks and utility vehicles. Dalmotas *et al* [2001] stated that passenger car occupants struck by vehicles with higher ride-heights put nearside occupants at elevated risk for head, chest and abdomen injuries.

Frontal collisions have long been the predominate type of crashes occurring on U.S. roadways. Occupant protection in frontal collisions has been aggressively pursued with mandated air bags, advanced seat belts, crumple zones and other energy absorbing technologies in the struck vehicle as well as in the striking vehicle [Barbat, 2005]. Nearside occupants involved in lateral crashes are currently protected by rigid structures in their door and possibly by some type of side air bag (SAB) designed to protect the occupant (or a body region of the occupant) in a lateral crash. A recent study of SAB effectiveness by the Insurance Institute for Highway Safety (IIHS) found that the presence of a SAB did indeed lower the risk of death to drivers in left-side impacts [McCartt and Kyrychenko, 2006]. Unfortunately, even with modern occupant protection features, serious injuries and fatalities are still occurring in a sizeable number of nearside crashes.

The NASS/CDS weighted data between 1999 and 2005 indicates that 16% of all crash occupants in the United States were in the nearside seating position of side impact crashes for the most significant (Rank 1) impact event. When the same nearside crashes are analyzed by the delta-V for the nearside impact event (Rank 1) using 40 kmph (25mph) as a threshold, the breakdown shows 62% of the crashes occurring with a delta-V less than or equal to 40 kmph and 14% over

40 kmph with the remaining 24% having unknown delta-V's as displayed in Table 1. For the nearside crashes occurring at or below 40 kmph, the incidence of AIS3+ injury is 3.33% (17,212 out of 516,165 occupants).

Table 1.
Nearside Delta-V Distribution
(NASS/CDS 1999-2005)

Delta V	Percent of Nearside Crashes
<= 40 kmph	62
> 40 kmph	14
Unknown	24

Due to the incidence of serious injuries to nearside occupants in side impacts at low speeds, this study was undertaken to better understand modern vehicle crash performance and occupant response. The objective was to identify trends in injury patterns in order to develop target areas for further side impact research.

METHODS

To maximize case count all of the NHTSA crash investigation data systems were queried for side impact cases matching the study's inclusion criteria. Cases were pulled from the NASS/CDS, CIREN and SCI databases.

The following inclusion criteria are utilized;

- AIS ≥ 3 injury to head, chest, abdomen or lower extremity
- Occupant age ≥ 16 years
- Rank 1 event is nearside to the study occupant
- Rank 1 event ≤ 40 kmph
- Model year of the study vehicle is ≥ 1998
- No rollover events are recorded for the study vehicle in subsequent crash events
- Row 1 occupants only
- All crash configurations are vehicle to vehicle
- The following Crash Deformation Classification (CDC) [SAE, 1980] values are used –
 - O'clock direction of force is 2-4 or 8-10 (CDC columns 1-2)
 - General area of deformation must equal Right or Left (CDC column 3)
 - Longitudinal damage location must equal P, Y, Z, D, F (CDC column 4)

The NASS and SCI data systems were queried from 1999 to 2004 and the CIREN data system was queried from 1998 to 2005. Since all three of these systems utilize the same investigation and coding standards the same crash and injury fields could be extracted from all systems in the same manner. Once the base variables were collected, all of the cases were reviewed individually to collect detailed injury and vehicle damage data not typically available in hard coded fields. The majority of the additional vehicle details were derived from inspection of the vehicle photos. The case occupant's radiology images/reports and operative reports in CIREN and the mannequin illustrations and annotation fields available in NASS and SCI were utilized to capture injury detail not otherwise coded.

Crash data were augmented by manual review of the case vehicle to classify several different aspects of the vehicle and the crash damage. The lower rocker panel or sill was evaluated on each case vehicle to evaluate any possible underride or override characteristics in the crash. Door deformation was reviewed on each vehicle to evaluate crush patterns. Patterns similar to those used by Tencer *et al* [2005] in their analysis of side impact crashes were utilized. The external crush pattern was also reviewed for engagement of the major structural pillars in the side plane. The vehicle interior photographs were also reviewed to establish the general geometry of the inside panel of each door as well as the existence of a row 1 center floor mounted console. If SAB(s) deployed during the crash event, these air bags were categorized into general protection types based on whether they were intended to protect the head, torso, or both.

The standard injury data were bolstered by a detailed review of the chest and pelvic injuries. The thoracic injury detail consisted of the actual number of fractured ribs, as well as the actual location of the rib fractures in the anterior-posterior direction along the curvature of the rib and in the inferior-superior direction by the anatomical rib number(s) fractured. Evidence and location of actual contact to the exterior chest wall was sought in all cases, but documented evidence was difficult to find in a majority of the cases. Evidence of thoracostomy procedures (chest tube) was also sought to determine whether pneumothorax (PTX) or hemothorax (HTX) injuries to the thorax were significant enough to warrant invasive intervention. Many times small amounts of blood and/or air in the thoracic cavity will be recorded, which can result in an increase in the severity of the injury coding. However, the presence

of a chest tube is a better indicator for aggressive evacuation of intra-thoracic air and/or blood which may be life threatening. Attempts to capture chest tube procedures on occupants sustaining a PTX and/or HTX proved quite difficult in the NASS and SCI data. Pelvic fractures were reviewed to extract fracture pattern detail as well as the actual location and number of fractures. Although the pelvis is usually referred to as a single bone, it is actually three separate bony structures connected by very strong ligaments. The symmetric hemi-pelves comprise two of the three bony structures and better known by their substructures, which are the pubic, ischium and iliac bone(s). The hemi-pelves establish the right and left aspects of the pelvic ring. The third component completing the pelvic ring, or girdle, is the sacrum, which constitutes the posterior part of the pelvic ring. Each of these bony structures was reviewed in each case for fractures and/or dislocations.

Several different approaches were taken in reviewing the data with regards to the occupant's injuries and their interaction with the vehicle and other crash parameters. Along with the detailed review of the study group, a general comparison was undertaken on the study group and the weighted NASS/CDS data for nearside crashes with delta-V's of 40 kmph or below. The weighted data reviewed included all nearside occupants from NASS/CDS 1999-2005 with a 3+ maximum abbreviated injury score (MAIS).

RESULTS

A total of 189 occupants meeting the inclusion criteria were extracted from NASS, CIREN and SCI. The general demographics of the study group are displayed in Table 2. Fifty-six percent of the occupants were female and the mean age was 47 years (range 16-93). The case occupants in the study group averaged 170 cm (67 in.) in height with an average weight of 76 kg (168 lbs). Gender differences indicated (as expected) taller and heavier males compared to females, with the male population being older by seven years on average.

**Table 2.
Demographic Data**

n	189	
	Mean	Range
Age	47 years	16-93 years
Height	170 cm 67 in	150-193 cm 59-76 in
Mass	76 kg 168 lb	39-133 kg 86-293 lb
Gender	Female	Male
n	105	84
% of group	56%	44%
Mean Age	44 years	51 years
Mean Height	165 cm 65 in	178 cm 70 in
Mean Mass	69 kg 153 lb	85 kg 187 lb

General crash and injury parameters are detailed in Table 3. The study occupant was the driver in 76% of the 189 cases captured for review. The delta-V's for the study group ranged from 5 kmph (3 mph) to 40 kmph (25 mph) with a mean of 29 kmph (18 mph). One-hundred and forty-five occupants (77%) were belted in 3-point manual belts. Thirty-one of the occupants (16%) had some form of deployed SAB at their seating position. In an additional four cases, SAB were available, but did not deploy. Impact angles were generally described as oblique or lateral. Left or driver's side impacts with a principal direction of force (PDOF) between 260 and 280 degrees and right or passenger's side impacts with a PDOF between 80 and 100 degrees are classified as lateral. All other cases are classified as an oblique impact. During the manual case review, intrusions were evaluated for each study vehicle. Intrusions at the study occupant's position were reviewed to determine the maximum value applicable to each case occupant. The vehicle component with the highest intrusion value for each of the study occupant positions was captured, and this value would override larger intrusion values that occurred at non-study seating positions. The mean maximum occupant intrusion measure for the study group was 25 cm (10 in.). Although the CIREN enrolls only occupants transported to a level 1 trauma center, the occupant intrusion measures and delta-V's were lower on average for the CIREN cases compared to the NASS/CDS and SCI cases. Intrusion averaged 23.6cm (9.3 in) in the CIREN cases and 26cm (10.2 in) for NASS/CDS and SCI. Delta-V's followed the same trend with the CIREN average at 27.8 kmph (17.3 mph) and the NASS/CDS and SCI average at 29.5 kmph (18.3 mph).

Table 3.
Crash and Injury Data

Occupant Seating Position	
Driver (Left Front)	143 (76%)
Restraint Status	
Belted	145 (77%)
Side air bag deployed	31 (16%)
Impact	
Mean Delta-V	29 kmph (18 mph)
<i>Impact angle</i>	
Oblique ¹	121 (64%)
Lateral ²	68 (36%)
<i>Crash Configuration</i>	
Car ³ -Car	76 (40%)
Car ³ -LTV	86 (45%)
LTV ³ -Car	7 (4%)
LTV ³ -LTV	20 (11%)
Mean maximum intrusion at occupant position	25 cm
1 – oblique crashes with PDOF between 30° -80° or 280° -330°	
2 – lateral crashes with PDOF between 80°-100° or 260° -280°	
3 – indicates study vehicle	

Injury Summary

All injury data were extracted on the study occupants and initially evaluated on the general categories of Maximum Abbreviated Injury Scale (MAIS), Injury Severity Score (ISS), and the individual AIS codes. The MAIS mean for the group was 3.7 and the mean ISS was 23, indicating significant injury in multiple body regions (Table 4).

Table 4.
Injury Severity

Mean ISS	23
Mean MAIS	3.7

The percent of AIS3+ injury by individual body regions indicated that the chest and lower extremity are the two most severely injured body regions in the study group. Sixty-three percent of the study group sustained an AIS3+ injury to the chest. The lower extremity body region ranked second with 42% sustaining AIS3+ injury. Interestingly, the head ranked third in our group with a 26% injury rate at an AIS3+ level. Figure 1 demonstrates the findings for all body regions in the current study. The abdomen was the only remaining body region with an injury rate in the double digits with a 17% occurrence.

Ribs and Pelvis

Utilizing the AIS and volume of coded injuries, the chest and lower extremities are the two most severely injured body regions in the study group. The distribution of injured organs within each of these body regions indicated a significant concentration of rib and pelvic fractures (Figures 2 and 3) within each of the general body regions.

Study Group vs. Weighted NASS/CDS

The NASS weighted data extract was compared to our study group by occupant age, fatality and MAIS. The age distribution from the weighted data is shown in Figure 4 along with that from the current study group. The NASS distribution was similar to that of the study group, with the exception of the 16-25 and the 36-45 groups.

The fatality rates for the weighted data were considerably lower than the study group. The weighted data indicates a 5.9% (16% unweighted) fatality rate for the nearside crashes below 40 kmph when a nearside occupant sustains an AIS3+ injury, whereas the study group had a 13% fatality rate. It is generally understood that weighted data from the NASS/CDS sampling underestimates actual fatality risk for a given group.

Study Group AIS 3+ Injury by Body Region

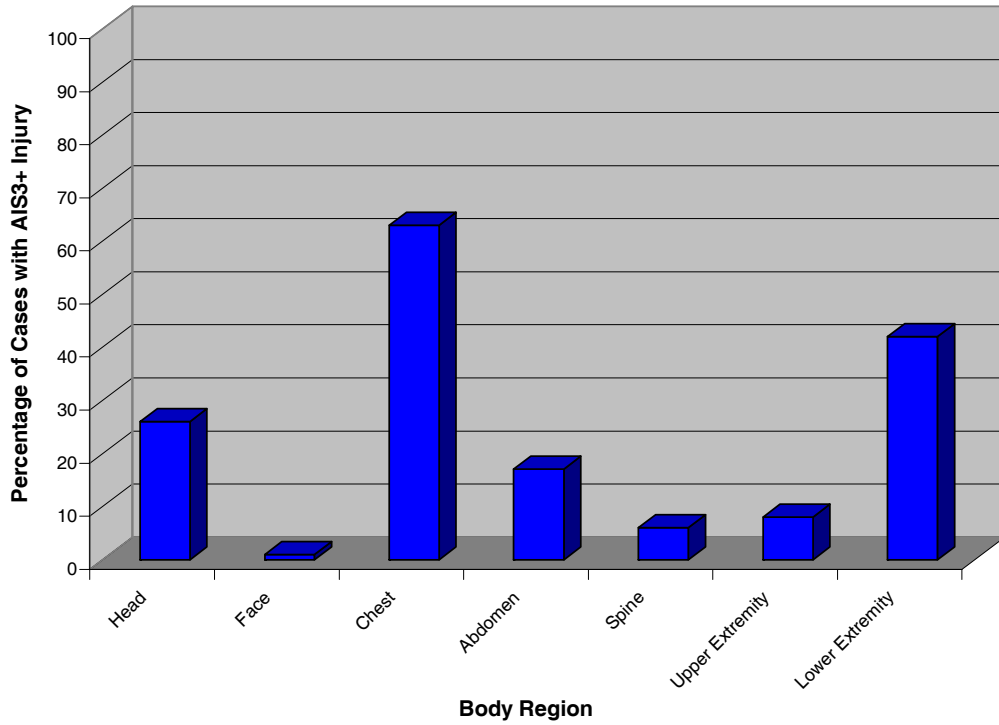


Figure 1. Percentage of cases with AIS 3+ injuries by body region.

Breakdown of AIS 3+ Chest Injuries

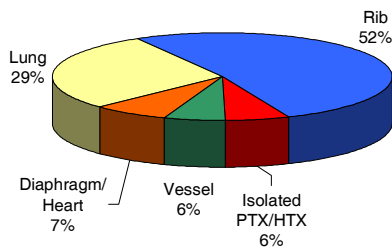


Figure 2. Breakdown of serious chest injuries by organ.

Breakdown of AIS 3+ Lower Extremity Injuries

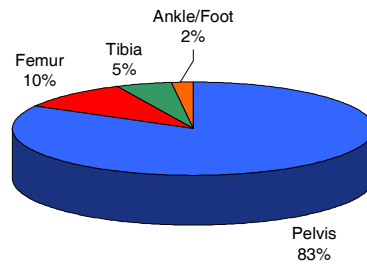


Figure 3. Breakdown of serious lower extremity injuries by organ.

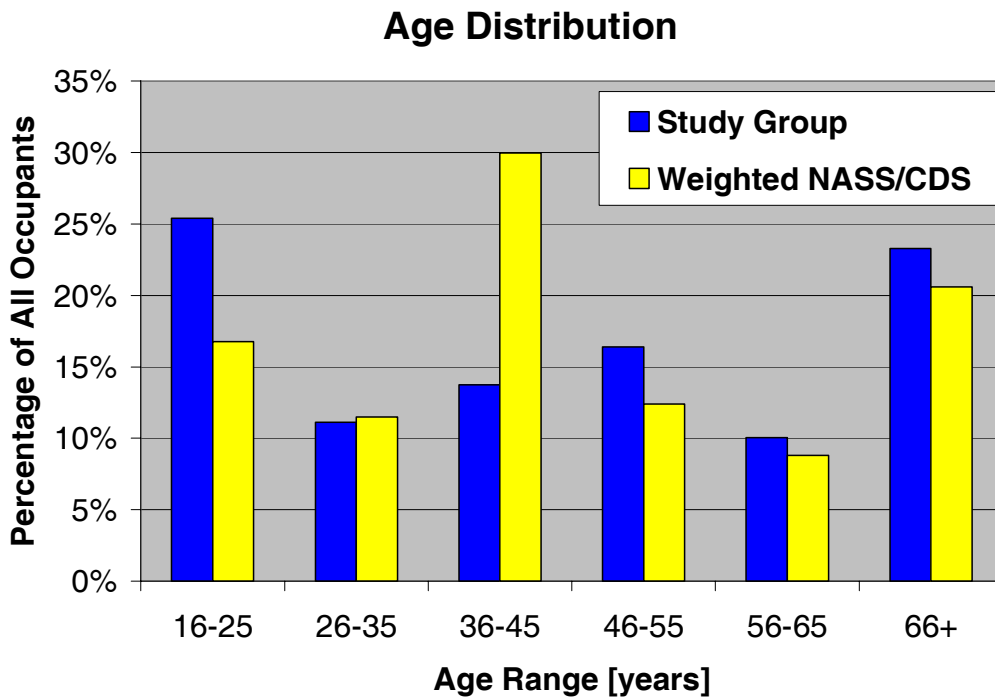


Figure 4. Age distribution of study group vs. weighted NASS/CDS.

Crash Compatibility

The effects of the geometry mismatch between passenger cars and light trucks were examined by looking at the prevalence of serious injuries for different crash configurations. Figure 5 shows the percentage of cases with AIS 3+ head, chest, abdomen and lower extremity injuries for passenger cars (PC) and light trucks (LTV), depending on their striking vehicle. The average ISS was also shown on the graph. The differences in ISS were small overall,

although the LTV occupants struck by passenger cars did have the highest average ISS of 23.7. Serious chest injuries were more common among passenger car occupants than LTV occupants, with those struck by LTVs having AIS 3+ chest injuries 71% of the time. The manual case reviews indicated over 25% of the case vehicles exhibited minimal to no rocker panel engagement. In the car struck by LTV group, the rate of minimal to no engagement was 26%.

Serious (AIS 3+) Injury by Body Region and Crash

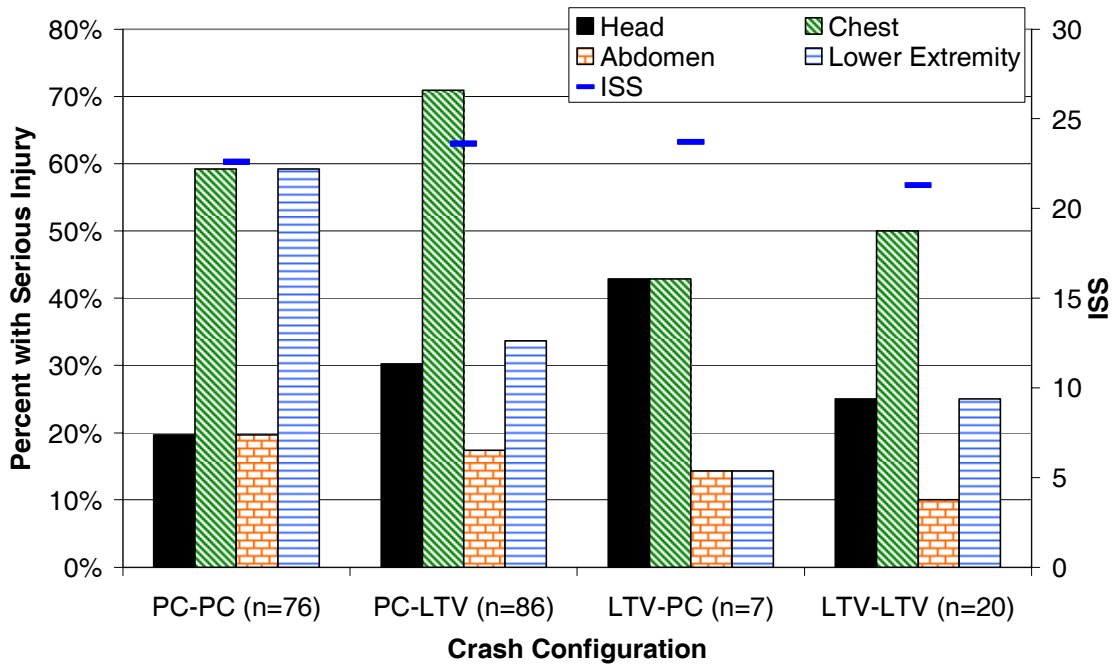


Figure 5. Percentage of occupants sustaining serious (AIS 3+) injuries by crash configuration and body region for current study group. The first vehicle type is the struck vehicle and the second is the striking vehicle. Some less-severely-injured body regions have been omitted for clarity.

Side Air Bags

A small subset of the study group (16%) had a SAB deploy to aid in mitigating the forces of the crash. Comparison of these thirty-one occupants to the remaining study group (without SAB deployment) indicates serious injury can still occur (see Table 5) in body regions with SAB protection.

The head injury group indicated 39% occurrence of AIS3+ injury when a SAB was deployed compared to only 23% when no SAB was present. The chest injury group indicated a slight advantage with SAB protection, with 55% AIS3+ injury compared to 65% when there was no SAB available.

Since the SAB type was captured during the manual case reviews, the injury analysis was revised to take into consideration the exact type of protection provided by each type of SAB in our study group. For example, if the SAB was intended to protect the head based on the position of the bag (head/thorax combo bag, head tube, or side curtain), it was considered to have a head SAB in the secondary analysis. Those cases with only a thorax bag were not considered to offer any head protection. The

findings did not show a big improvement for the head injury group with head SAB. Thirty-one percent of the cases with head SAB sustained an AIS3+ injury to the head. An analysis of the chest injury severity for cases with and without thorax SAB protection shows that 52% of the cases with chest protection sustained AIS3+ injury to the chest. These findings are detailed in Table 5.

Table 5.
Crash and Injury Data for Cases With and Without Side Air Bag (SAB) Deployment

	With SAB (n=31)	Without SAB (n=158)
Mean Age	52	46
Mean MAIS	3.8	3.6
Mean ISS	22	25
Mean Delta-V	29 kmph (18 mph)	29 kmph (18 mph)
<i>% of occupants with serious (AIS 3+) injury</i>		
Head	39%	23%
Face	3%	1%
Neck	0%	0%
Chest	55%	65%
Abdomen	19%	17%
Spine	13%	4%
Upper Extremity	0%	9%
Lower Extremity	48%	41%
<i>Head SAB¹</i>	<i>n=16</i>	<i>n=173</i>
Head	31%	25%
<i>Thorax SAB²</i>	<i>n=29</i>	<i>n=160</i>
Chest	52%	65%
1 – Cases with SAB intended for head protection (combination head/thorax, head tube or head curtain)		
2 – Cases with SAB intended for thorax protection (thorax, combination head/thorax)		

In an attempt to gain clarity into these perplexing results, the cases were further divided by the impact angle classifications previously described. When each of the two groups are sub-divided by impact angle of the striking vehicle (oblique vs. lateral), a more distinct pattern appears as shown in Table 6. The lateral impacts with SAB deployments appear to be more protective of the head and chest when compared to the oblique impacts. These new groups were again divided by the exact type of protection design available. The group with SAB designed to protect the head (N=10) indicated a 40% occurrence of AIS3+ head injury in oblique crashes while those in lateral crashes (N=6) sustained AIS3+ head injury at a rate of 17%. The chest injury group had less dramatic differences between impact angles with 58% of the oblique group sustaining AIS3+ chest injury compared to 40% in the lateral group. However, the difference may not be as impressive as the basic fact that 58% of the oblique and 40% of the lateral cases sustained an AIS3+ chest injury when an

advanced countermeasure was present in a crash of moderate severity.

Table 6.
Crash and Injury Data for Cases With and Without Side Air Bag (SAB) Deployment by Crash Configuration

	With SAB (n=31)		Without SAB (n=158)	
	O (n=20)	L (n=11)	O (n=101)	L (n=57)
Impact Angle ¹				
Mean MAIS	3.9	3.7	3.6	3.6
Mean ISS	25.5	24.4	22.9	21.9
<i>% of occupants with serious (AIS 3+) injury</i>				
Head	45%	27%	26%	19%
Face	5%	0%	1%	0%
Neck	0%	0%	0%	0%
Chest	60%	45%	65%	6% ³
Abd.	15%	27%	15%	21%
Spine	15%	9%	5%	4%
Up. Ext.	0%	0	12%	5%
Low. Ext.	40%	64%	36%	51%
<i>Head SAB²</i>	<i>n=10</i>	<i>n=6</i>	<i>n=111</i>	<i>n=62</i>
Head	40%	17%	28%	21%
<i>Thorax SAB³</i>	<i>n=19</i>	<i>n=10</i>	<i>n=102</i>	<i>n=58</i>
Chest	58%	40%	66%	64%
1 – O: oblique crashes 30° -80° or 280° -330°, L: lateral crashes 80°-100° or 260° -280°				
2 – Cases with SAB intended for head protection (combination head/thorax, head tube or head curtain)				
3 – Cases with SAB intended for thorax protection (thorax, combination head/thorax)				

Since the chest (ribs) and lower extremity (pelvis) comprised the highest percentage of AIS3+ injured body regions, the data were analyzed for severity by fracture count. When the fracture details for the ribs are broken down by number of fractured ribs, impact angle and the presence of a chest protection SAB, oblique crashes produced an overall higher degree of severity (Table 6). Although the n values were low, there were no rib fracture counts above five for any occupant with a SAB in a lateral crash. Conversely, for the occupants with a SAB designed to protect the chest and an oblique impact angle, 21% (4/19) sustained 6 to 12 rib fractures per occupant. Even in the cases where no SAB was available only 9% of the

lateral crashes sustained 6 or more rib fractures per occupant and 20% of the oblique crashes sustained 6 or more rib fractures per occupant. Of the four groups indicated in Table 7, it should also be noted that the highest percentage of occupants with no rib fractures (60%) was the lateral impact group with a deployed SAB. The lateral impact group without an available thorax SAB indicated only 34% of the occupants did not sustain any rib fractures.

Table 7.
Rib Fracture Count for Cases With and Without Thorax Side Air Bag (SAB) Deployment by Crash Configuration

	With Thorax SAB ² (n=29)		Without Thorax SAB (n=160)	
	O (n=19)	L (n=10)	O (n=102)	L (n=58)
Impact Angle¹				
Rib fx count	<i>% of occupants with rib fracture</i>			
0	42%	60%	44%	34%
1-2	16%	20%	11%	29%
3-5	16%	20%	16%	17%
6-12	21%	0%	15%	7%
13+	0%	0%	5%	2%
Multiple Unknown	5%	0%	10%	10%
1 – O: oblique crashes 30° -80° or 280° -330°, L: lateral crashes 80°-100° or 260° -280° 2 – Cases with SAB intended for thorax protection (thorax, combination head/thorax)				

The pelvic fracture detail indicates more fractures in the lateral impact group with a deployed SAB than any other group (Table 8). Only 30% of the lateral impact cases with a thorax SAB did not sustain a pelvic fracture. In contrast, the oblique impact group without a SAB indicated the best pelvic results with 57% sustaining no pelvic fracture.

Intrusion Level with Side Air Bag

Injury severity was evaluated relative to the maximum occupant intrusion level and whether or not a SAB deployed (Figure 6). Although there is a general trend of higher ISS for higher levels of intrusion, low severity scores were present in some of the more severely intruded cases and some cases with little or no intrusion produced relatively high injury severity scores. Cases with SAB deployment did not

produce a trend that was noticeably different except at intrusion levels below about 15 cm.

Table 8.
Pelvis Fracture Count for Cases With and Without Thorax Side Air Bag (SAB) Deployment by Crash Configuration

	With Thorax SAB ² (n=29)		Without Thorax SAB (n=160)	
	O (n=19)	L (n=10)	O (n=102)	L (n=58)
Impact Angle¹				
Pelvic fx count	<i>% of occupants with pelvis fracture</i>			
0	47%	30%	57%	41%
1-2	16%	40%	23%	34%
3+	37%	30%	21%	24%
1 – O: oblique crashes 30° -80° or 280° -330°, L: lateral crashes 80°-100° or 260° -280° 2 – Cases with SAB intended for thorax protection (thorax, combination head/thorax)				

Age Factor

The study group matched up well by age with the national data with the exception of the two age groups previously mentioned. The data analysis included the age of the study group in relation to injury severity. Figure 7 is a distribution of body region injury severity by age. Although an increasing level of severity is expected as age increases, several spikes in the plot were interesting. The highest percentage of serious head injuries was in the 16-25 year old group. The highest percentage of lower extremity injuries fell into the 56-65 year old group. Quite surprisingly, the highest percentage of chest injuries was in the 36-45 year old group at a rate of 85%. The same analysis was run on the weighted CDS data of nearside AIS 3+ occupants. The findings are detailed in Figure 8. The study group clearly demonstrates a greater level of severity than the weighted CDS data in almost every body region in every age group. The CDS data indicates the expected general rise in severity, with the majority of body regions, with age. There is a clear spike at age 36-45 for lower extremity injury. There is also a substantial spike at age 66+ for chest injury.

ISS vs. Intrusion and SAB

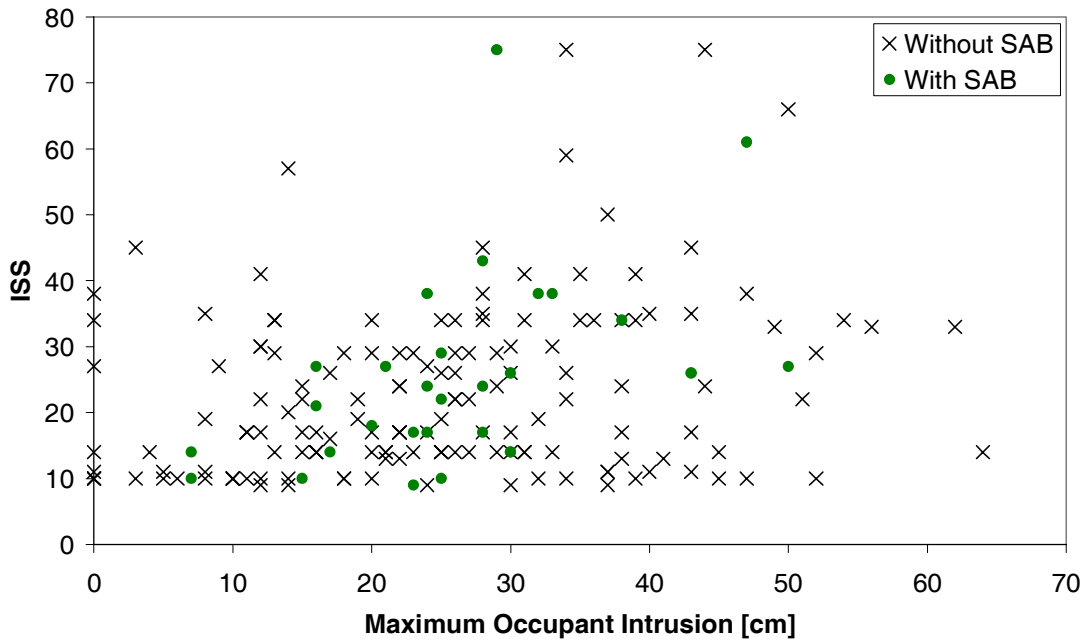


Figure 6. Injury Severity Score for occupants with and without side air bags by maximum intrusion at occupant seating position.

Serious (AIS 3+) Injury by Body Region and Age

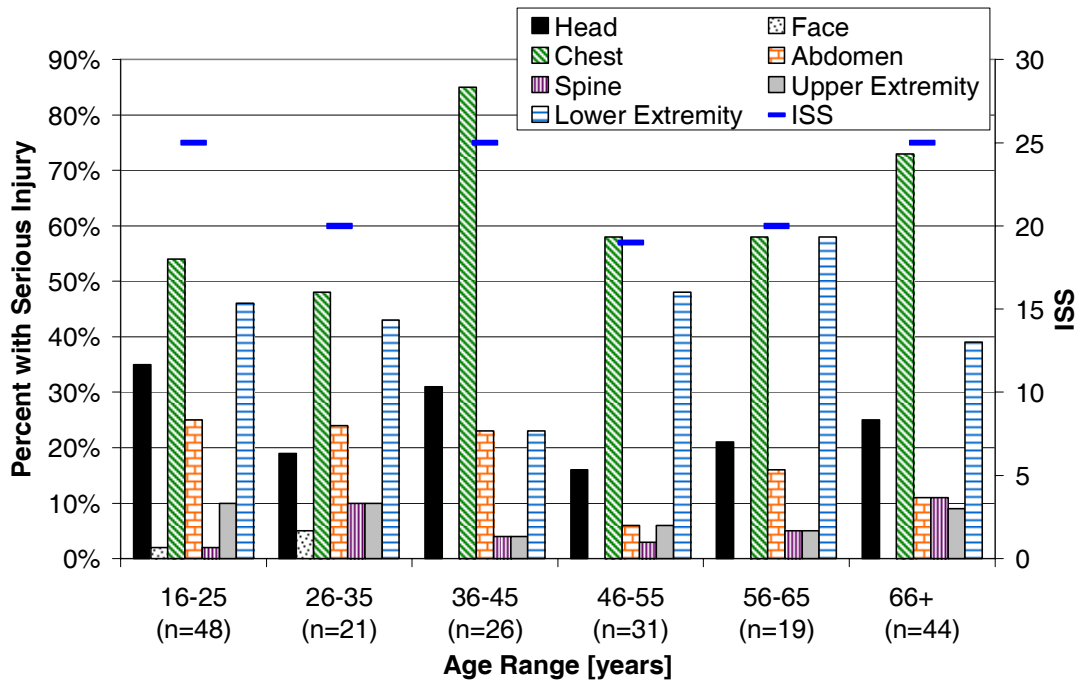


Figure 7. Percentage of occupants sustaining serious (AIS 3+) injuries by age group and body region for current study group. No occupants sustained AIS 3+ neck injuries.

Serious (AIS 3+) Injury by Body Region and Age

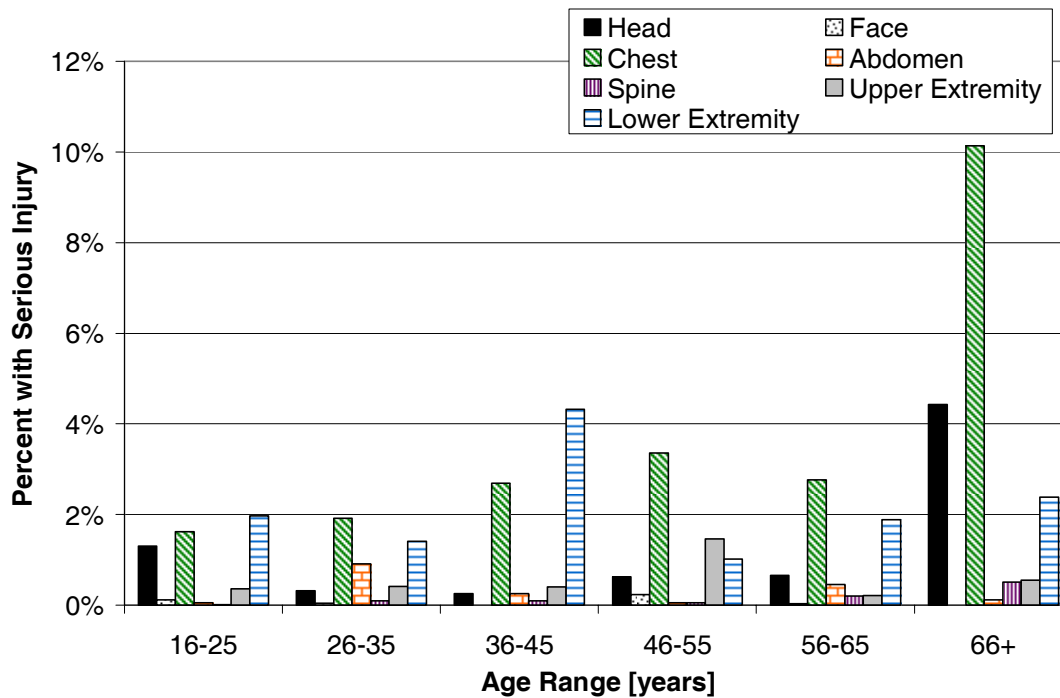


Figure 8. Percentage of occupants sustaining serious (AIS 3+) injuries by age group and body region for weighted NASS/CDS data.

Fatalities

The cause of death was determined for each of the 25 cases in which the occupant did not survive. The fatal cases were reviewed, and the injury region most likely responsible for the fatality was selected based on injury severity coding and rank as well as

biomechanical and clinical factors. The ages of the fatally-injured occupants are plotted in Figure 9 and grouped by the body region where the fatal injury occurred. Most of the older occupants died of thoracic injuries, while most of the younger occupants died of head trauma.



Figure 9. Body region linked to cause of death by age. Crash delta-V, SAB type, and ISS are shown in each bar.

DISCUSSION

The issue of side impact crashes continues to be a complicated problem with a multitude of factors contributing to occupant injury risk. The final study group was comprised of crashes with both pure lateral and oblique impact angles. The delta-V's, as calculated by the WinSmash algorithm place the study group at or below the delta-V's observed in sixty-two percent of nearside crashes in the United States.

Based on prior knowledge, it was expected that the analysis of the study group would yield certain facts about occupant injury and vehicle compatibility. These expected results included elderly drivers sustaining more severe thoracic injuries, an overall increase in injury severity with increased intrusion levels, greater injury for passenger car occupants struck by LTVs, distinct structural deformation differences among passenger cars struck by LTVs, less severe injuries in LTV occupants and an overall protective effect from SAB deployment. In general, these preconceived thoughts were supported by the results, but a number of unexpected results were also discovered throughout the analysis.

Because of changes in bone properties and skeletal structure, the chest tolerance of older persons decreases making them more susceptible to higher severity thoracic injuries [Kent *et al*, 2003]. The age-based incidence of serious chest injuries shown in Figure 7 does indicate an increase in prevalence with increasing age, but the 36-45 year old group stands out as having the greatest percentage of AIS 3+ chest injuries. While the data do support the expectation of increased severity with increased age, the spike shown for the 36-45 year old group was not well understood. Overall, AIS 3+ chest injuries occurred frequently. Serious chest injuries were seen in 63% of the cases, which is similar to findings in other side impact studies [Samaha and Elliot, 2003]. Attempts to break down the detail of the chest injuries proved difficult beyond the organ level. Although the count and general location of the rib fractures were available for most cases, it was evident from the occupant's outcome and minimal hospital stay that the chest injury may not have been quite as life-threatening as the AIS code would suggest. Rib fractures are coded in conjunction with or without the presence of PTX and/or HTX. When a PTX and/or HTX is present, the AIS severity is increased one level. Many of the PTX and HTX are quite small and warrant no intervention with the exception of a

follow-up radiological scan to determine if it has become worse. When a PTX and/or HTX are of sufficient size and severity, the medical intervention typically involves insertion of a chest tube to allow for decompression of the thoracic cavity. The lack of this data in the SCI and NASS cases hampered the ability to discern if the chest injuries scaled by AIS were truly as life-threatening as coded. The newest version of AIS [AAAM, 2005] has adopted a new method of separating the PTX/HTX diagnosis from the rib fractures which allows a greater level of sensitivity to the chest injury severity. Future use of the new AIS 2005 in crash investigation data systems would benefit this issue along with other injury research.

The head is typically the second most-seriously injured body region in nearside impacts [Samaha and Elliot, 2003]. The results of this study showed the lower extremity to be the second most-seriously injured region, with 42% of the cases resulting in an AIS 3+ lower extremity injury. More in-depth analysis showed that pelvic fractures were responsible for the high prevalence of lower extremity injuries in the study group.

Larger intrusion levels did tend to produce more serious injury, as evidenced by the upward trend in the ISS data in Figure 6. Although the crashes in this study group were considered of minimal to moderate severity based on delta-V, large amounts of intrusion and crush were seen in most of the vehicles. One finding of note is that the average maximum occupant intrusion of 10 inches is two inches less than the current American College of Surgeons Field Triage guidelines recommendation for immediate transport to a Level-1 trauma center [American College of Surgeons, 1999].

The study group consisted of a large number of passenger cars struck by LTVs, which was useful in attempting to evaluate compatibility issues. Injury results shown in Figure 5 indicate this group had the highest prevalence of serious chest injuries followed by the passenger cars struck by other passenger cars. This finding supports the original belief that passenger car occupants were more susceptible to thoracic injury, but the results for head injuries were not consistent. The group of LTV occupants struck by passenger cars showed the highest percentage of serious head injuries, although this group had a small n value which may have amplified the percentage. The manual case review involved extensive analysis of photographic evidence for the case vehicles in an attempt to determine whether compatibility played a role in the injury causation. These photograph-based

estimations were required due to a lack of hard coded measurements determining override/underide in the side plane from the current field investigation techniques. Although all crashes are coded with a CDC that describes the damage in a particular plane, this has limitations for researching override/underide scenarios. It would be advantageous to develop new measurement techniques or hard-coded fields to identify override/underide in side impacts.

Side impact air bags were only available in 16% of the case vehicles, but the comparison of cases with SAB deployment to those without produced some interesting results. Overall, considering all crash types together and all SAB types together, there did not appear to be a large benefit from SAB deployment for the cases under study. However, it should be noted that the small number of SAB cases made the percentages of serious injury much more sensitive than in the larger non-SAB group. The mean MAIS was slightly higher in the group with SAB deployment, and the head and lower extremities sustained a greater percentage of serious injuries in the SAB-protected group. The fact that head injuries were more prevalent in the group with SAB is counterintuitive. One possible explanation might be multi-trauma injury patterns where one body region may benefit from SAB availability, yet others are not protected. Yoganandan *et al* [2007] observed that chest injuries do not occur in isolation and are associated with a head injury in >90% of subjects with AIS ≥ 2 injuries in more than one body region. Once the SAB group is further sub-divided by defined head and/or chest protection, head injury declines from sixteen percent to six percent. Decreased prevalence of serious thoracic and abdominal injuries was observed in those cases with SAB deployment. After breaking the cases down by crash direction (lateral vs. oblique) and SAB type, the benefits and limitations of the SAB became more evident. The lateral impacts with SAB resulted in better head and chest injury outcome compared to the oblique impacts, possibly indicating the occupant is missing the bag or not getting full benefit because of the longitudinal motion when the impacting vehicle is approaching at angles greater than +/- 10 degrees from pure lateral. The portion of the study group with head-protective SAB had approximately two-thirds seat-mounted torso-head combo SAB that may not give the same amount of protection coverage as a curtain type SAB. Increased SAB size or improved position of the occupant by manual restraints may increase the effectiveness of SAB. With increasing amounts of vehicles entering the fleet with SAB installed, future research on this issue will benefit

through increased exposure and the resulting improved data capture.

The study population was assembled from every crash investigation data system available at NHTSA (NASS, CIREN and SCI). The breakdown of the study group compared to the weighted NASS/CDS data indicates a substantial bias towards serious injury for the study group. This discrepancy does not have a simple explanation. Attempts to compare the raw NASS/CDS data indicated a discrepancy in injury severity as well, just not as large. The most logical explanation for such a discrepancy is the study group is extremely biased toward serious multi-trauma, whereas the weighted data may be more representative of single system serious injury. Although the distribution of injury was quite different between the study group and the weighted data, chest and lower extremity injury ranked 1 and 2 respectively in both groups.

CONCLUSION

The side impact crash is a particularly harmful crash mode with many complicated factors creating a risky environment for the nearside occupant. Even at relatively low delta-V's, serious injuries and fatalities continue to occur in modern cars with side impact countermeasures. The chest, pelvis and head are the primary body regions sustaining such life-threatening injuries, and the chest, in particular, accounts for many of the injuries across a broad age-range. The current countermeasure of choice for this crash mode is a side impact air bag, which currently exists in several different forms. The limited SAB cases included in this study indicated improved protection improvements were evident in the lateral crashes. The findings suggest the need to further investigate the role the SAB plays in side impacts with longitudinal acceleration components that potentially force the occupant away from the SAB coverage area.

A small case study such as this one permits in-depth case review to determine SAB characteristics and compatibility factors, which are not hard-coded fields in the current data systems. The manual review undertaken in this study allowed for a more complete evaluation of the exact type of countermeasures available to each occupant and how the crash and vehicle dynamics contributed to the occupant's injury severity.

REFERENCES

- AAAM (2005) "Abbreviated Injury Scale 2005." Association for the Advancement of Automotive Medicine.
- Barbat, S. (2005) "Status of Enhanced Front-to-Front Vehicle Compatibility Technical Working Group Research and Commitments." 19th International Technical Conference on the Enhanced Safety of Vehicles, paper no. 463.
- Dalmotas, D., German, A., and Tylko, S. (2001) "The Crash and Field Performance of Side-Mounted Airbag Systems." 17th International Technical Conference on the Enhanced Safety of Vehicles, paper no. 442.
- Kent, R., Patrie, J., Poteau, F., Matsuoka, F., and Mullen, C. (2003) "Development of an Age-Dependent Thoracic Injury Criterion for Frontal Impact Restraint Loading." 18th International Technical Conference on the Enhanced Safety of Vehicles, paper no. 72.
- McCartt, A.T. and Kyrychenko, S.Y. (2006) "Efficacy of Side Airbags in Reducing Driver Deaths in Driver-Side Car and SUV Collisions." *Traffic Injury Prevention*, in press.
- SAE (1980) "Collision Deformation Classification." Surface Vehicle Standard J224 Revision MAR80.
- Samaha, R.R. and Elliot D.S. (2003) "NHTSA Side Impact Research: Motivation for Upgraded Test Procedures." 18th International Technical Conference on the Enhanced Safety of Vehicles, paper no. 492.
- Tencer, A.F., Kaufman, R., Huber, P. and Mock, C. (2005) "The Role of Door Orientation on Occupant injury in a Nearside Impact: A CIREN, MADYMO Modeling and Experimental Study." *Traffic Injury Prevention*, vol. 6, no. 4, pp. 372-378.
- Yoganandan, N., Pintar, F.A., Zhang, J., and Gennarelli, T.A. (2007) "Lateral Impact Injuries with Side Airbag Deployments – A Descriptive Study." *Accident Analysis and Prevention*, vol. 39, no. 1, pp. 22-27.
- American College of Surgeons Committee on Trauma. "Field Triage Decision Scheme." *Resources for Optimal Care of the Injured Patient: 1999*. Chicago, Illinois. American College of Surgeons. 1999 (www.facs.org)

Enhancement of side impact protection using an improved test procedure

**Marie-Laure Roussarie,
Richard Zeitouni,
Céline Adalian**

PSA Peugeot Citroën,
France
Paper number 07-0245

ABSTRACT

Several groups of research have been charged to enhance the current European regulatory side impact test procedure (ECE95). The Aprosys project, funded through the 6th Framework Programme of the European Commission, proposed in 2006 a new test procedure called AE-MDB (Advanced European Mobile Deformable Barrier) with:

- an updated barrier face representative of the current European fleet, including SUV,
- an increase in the mass of the trolley,
- a shift in the impact point,
- the addition of a rear occupant dummy.

Questions were raised, and not yet answered, on the added value of this new test procedure with respect to the current one, pointing out the current influence of the AE-MDB face. The purpose of our study is to highlight and quantify the extra-severity brought by AE-MDB and its consequences on occupant protection and car design in side impact. This research presents comparative study of ECE95 and AE-MDB procedure thanks to full scale crash tests, component tests but also virtual testing made on several vehicles of different size (small family and large family vehicles as well as MPV). The outcome shows a 30% extra-severity for AE-MDB with respect to ECE95 on dummy readings and car deformation. This is not only due to the increase in the trolley weight, but also because of the improvement in the barrier face (geometry and stiffness). It also highlights that vehicle design will be impacted if AE-MDB is chosen for regulation, on restraint systems (rear airbag, belt pretension, better design front airbag...) as well as on structural dimensioning.

This new procedure is representative of the last generation of European cars (its severity is clearly ranked between a test against an SUV and a passenger car). Its application on regulation and/or consumer tests will improve the protection in side impact of occupants on the roads.

INTRODUCTION - AIM OF THE STUDY

Several groups of research such as Aprosys and EEVC WG13 have been charged to enhance the current European regulatory side impact test procedure (ECE95) [1] in order to make it more representative of the average European vehicle fleet. The definition of a new side impact test procedure called AE-MDB (Advanced European Mobile Deformable Barrier) is therefore under progress since 2001.

Different versions of this new barrier AE-MDB have been tested by conducting and analyzing numerous crash tests against wall or against car. Barrier definition V3.9 is the version that fits the best to the initial outline "being representative of the average European vehicle fleet".

Therefore, PSA Peugeot Citroën decided to increase its knowledge of AE-MDB V3.9 version. Virtual testing has been carried out in order to understand the origin of the changes seen with the use of this new barrier. Full-scale testing was also conducted on several vehicle of different size to make a comparative study between the current regulatory procedure ECE 95 and this new AE-MDB V3.9 procedure.

BACKGROUND

The Aprosys Project was launched through the 6th Framework Program of the European Commission to study a new side impact barrier more representative of the average European vehicle fleet. According to the terms of references defined in the IHRA side working group for the 2003 ESV conference in Nagoya [2], this barrier should provide:

- an impact environment similar to that seen in car-to-car and small 4WD-to-car side impacts
- a sufficiently stringent test condition for the rear seat dummy while maintaining the same level of severity for the front seat dummy

A first version of barrier AE-MDB (Advanced European Mobile Deformable Barrier) was proposed and studied: AE-MDB V2.

It was based on:

- a 1500 kg trolley
- a corridor created with frontal test of cars to LCW (rigid) data (40 different vehicles crashed on rigid wall) [3] (see Figure 1)
- a definition made of 6 blocks: 3 upper blocks and 3 lower blocks (see Figure 2)

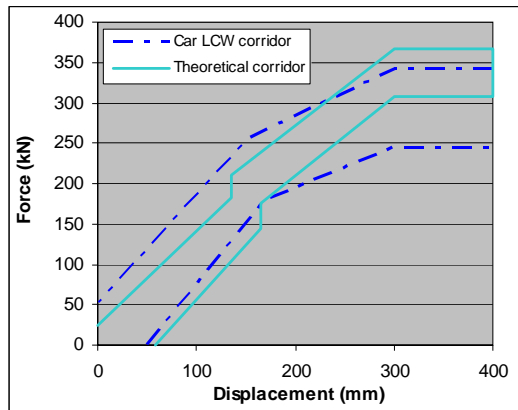


Figure 1. Effective force vs displacement corridor made with load cell wall test results and theoretical corridor as proposed to define AE-MDB.

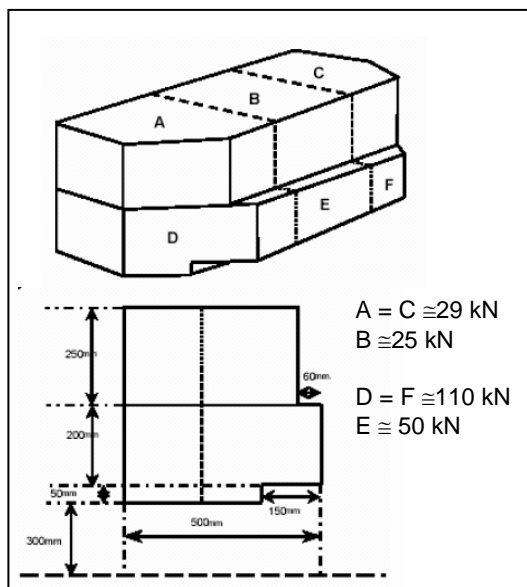


Figure 2. Theoretical characteristics of AE-MDB barrier face.

Its validation was done by comparing the results of a car-to-barrier side impact and two car-to-car tests (the bullet car being the LandRover Freelander or the Volkswagen Golf V).

ACEA (Association des Constructeurs Européens d'Automobiles) also contributed to this study (see Table 2).

After two years of studies, Aprosys and ACEA concluded that whereas the barrier V2 is in the LCW corridor, the comparison between the car-to-

barrier test in side impact and the "car-to-car" tests showed that it was not consistent to car-to-car deformation. Indeed, door intrusion was too high with the AE-MDB V2, and the distribution of deformation between doors and B-Pillar was not consistent with the distribution seen on car-to-car tests.

Since 2005, the members of EEEV WG13 discussed a series of modifications to the barrier face that could be further developed by Aprosys. All new versions (named V3.x, with x from 1 to 9) were based on V2 characteristics:

- all versions used the same definition by blocks (6 blocks, 3 upper and 3 lower blocks)
- the geometry remains unchanged with respect to V2
- each block stiffness is defined as a percentage of the initial V2 "block D" stiffness (block D is the lower exterior block)
- the barrier weight is still 1500 kg
- an additional bumper element was put in front of the barrier. The bumper definition is taken from the NHTSA FMVSS214 barrier (245 psi / 3+3 mm)

Version V3.9 was selected by the majority of the Aprosys member in 2006.

Its characteristics against version V2 are the following (see Table 1).

Table 1. Comparison between AE-MDB Version 2 and Version 3.9 in terms of stiffness and design.

AE-MDB Version	Block Stiffness	View
V2	$a = c = 29 \text{ kN}$ $b = 25 \text{ kN}$ $d = f = 110 \text{ kN}$ $e = 50 \text{ kN}$ no bumper element	
V3.9	$a, b \text{ and } c \text{ are unchanged with respect to V2}$ $d_{V3.9} = f_{V3.9} = 55\% * d_{V2}$ $e_{V3.9} = 60\% * d_{V2}$ Addition of a bumper element (245 psi / 3+3 mm)	

Part of the validation matrix conducted together by ACEA and the Aprosys project with this AE-MDB version V3.9 is shown in Table 2. Each target vehicle have been impacted by a car (car-to-car

test) or by a AE-MDB barrier (car-to-barrier test) with the V3.9 and sometimes with V2.

Table 2.

Test matrix of car-to-car or car-to-barrier tests carried out to compare V3.9 and V2 .

Target vehicle (project funding)	Freelander	Golf V	V3.9	V2
Golf V (Aprosys)	x	x	x	
Fiesta (Aprosys)	x	x	x	
Megane (ACEA)	x	x	x	x

Hence, in 2006, AE-MDB V3.9 barrier was selected by the Aprosys project as fulfilling the initial mandate. It was considered as:

- being in the stiffness corridor done with the frontal test of the 40 cars to LCW (rigid) data (See Appendix 1)
- being in between the severity of a car-to-car tests against Golf V and against Freelander

The selected side impact test procedure was the following (see Figure 3) :

- barrier AE-MDB V3.9
- trolley weight at 1500 kg
- the impact point is centered on R-Point + 250 mm rearward. This backward impact location point enables to take into account rear passengers protection as well as the movement of the 2 cars in a real front-to-side impact
- front and rear seat occupant: a 50th percentile dummies
- test speed: 50 +- 1 km/h

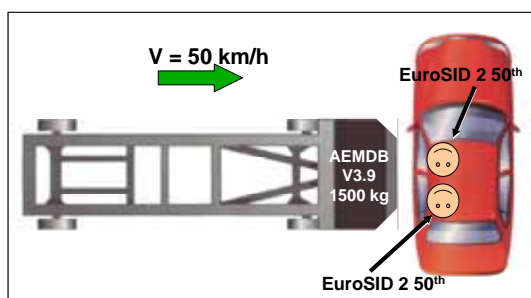


Figure 3. Test configuration for the AE-MDB side impact procedure.

COMPARATIVE STUDY BETWEEN AE-MDB AND ECE 95 TEST

This new side impact test procedure have been designed with the purpose to replace the current regulatory test (ECE regulation 95, also named Progress 950 kg in the remaining part of our study). Therefore PSA Peugeot Citroën decided to make physical and numerical comparative studies between the current ECE95 test and this new side impact procedure, with barrier AE-MDB V3.9. The first part of our study is a numerical study that has been performed to analyse separately the influence of each parameter (mass and stiffness). Thanks to modelling, it is relatively easy to understand very precisely the differences seen between old and new procedure and quantify the effect of each change.

The second part of our study has been to conduct full-scale tests on different vehicles in order to have a complete overview of the results with the future procedure and the current procedure on all different sizes of vehicles.

Parametric Study - influence of the two test parameters: increase in mass and increase in stiffness

The AE-MDB V3.9 procedure is carried out with two major evolutions with regard to the current ECE 95: A complete change in the barrier design (AE-MDB against Progress, with an increase in width and in stiffness), and a change in the trolley weight (1500 kg instead of 950 kg). Aprosys concluded from its studies that the procedure in overall was more severe. But, we can ask the following questions: is this increased severity the unique consequence of the increased trolley weight? Or is it the consequence of coupling both parameters in parallel: the increase in the trolley weight and a change in the deformable element?

To answer this question, PSA Peugeot Citroën has done a numerical study on a new large family car. This vehicle is therefore a last generation vehicle and its numerical model has been correlated to standard physical tests.

Three calculations have been performed:

- a Progress 50 km/h – Trolley Weight 950 kg
- a Progress 50 km/h – Trolley Weight 1500 kg
- an AE-MDB V3.9 50 km/h – Trolley Weight 1500 kg

Figure 4 presents the exterior intrusions at three different level heights for the three different modellings.

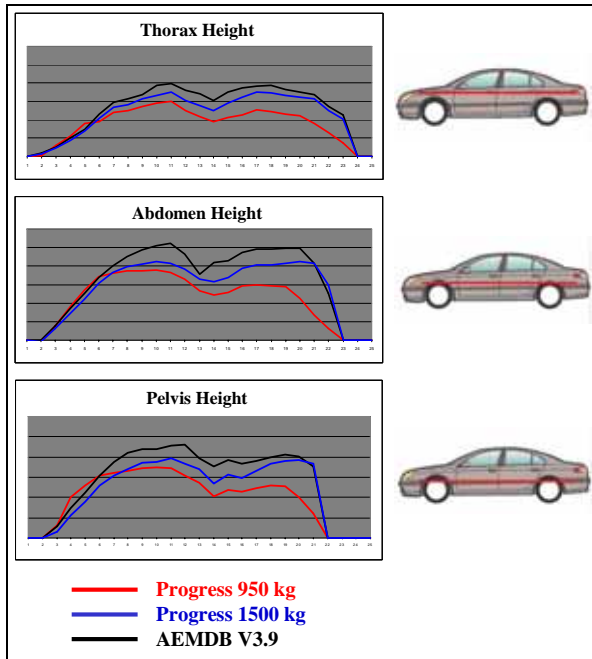


Figure 4. Comparison of the exterior intrusion profile measured at different heights for the three different barriers.

With the use of AE-MDB, there are two steps on the way of a more severe procedure. The weight of the trolley causes a first increase of the exterior intrusions (see the blue curve compared to the red one in Figure 4).

The new deformable face, much stiffer than the Progress one, creates a second increase in the exterior intrusions. In overall, intrusions are at least 40% higher on V3.9 barrier than on the current ECE 95.

Looking at B-Pillar intrusions, we find the same type of conclusions (see Figure 5).

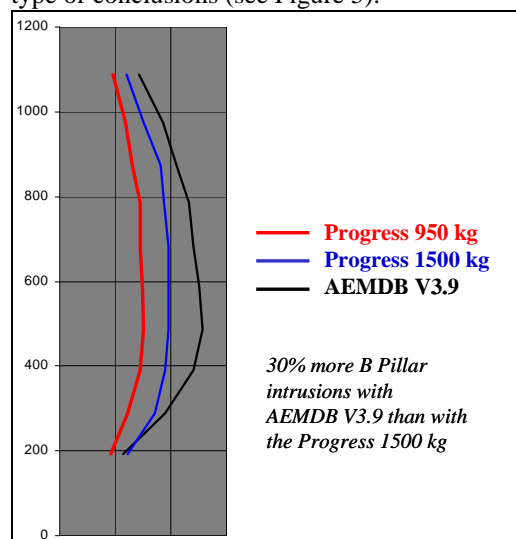
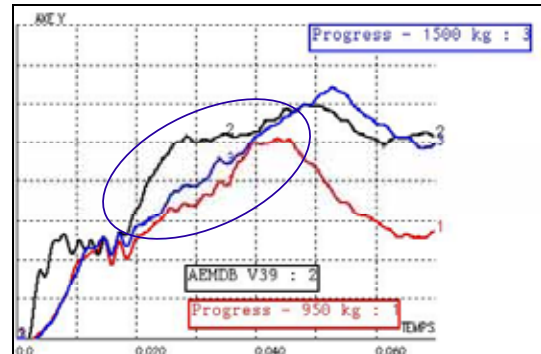
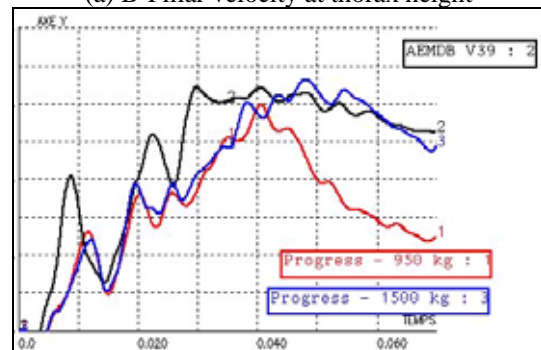


Figure 5. Comparison of the B-Pillar intrusion profile for the three different barriers.

There are 30% more B-Pillar intrusions with AE-MDB V3.9 than with the Progress 1500 kg. As they have a direct impact on biomechanical criteria, door and B-Pillar velocities were also compared between the different calculations. Figure 6 presents door velocity at abdomen height and B-pillar velocity at thorax height.



(a) B-Pillar velocity at thorax height



(b) Door velocity at abdomen height

Figure 6. Comparison of the velocity measured at different heights for the three different barriers.

The first slope of the velocity curves is far much greater in AE-MDB V3.9 than in Progress-1500 kg or 950 kg. This phenomenon is a consequence of the higher stiffness of the deformable face which introduces a higher initial velocity on the vehicle. Dynamic displacements are therefore higher. This is related to what we have seen above on the intrusions (greater intrusion with AE-MDB V3.9 than with Progress – 1500 kg).

Comparing both calculations with Progress 950 kg and 1500 kg, we can see that the initial slope is identical. The impact of the increase of the trolley weight is seen on the maximal level of velocity. This higher level will have a direct impact on biomechanical criteria.

As a conclusion, the higher severity of the new AE-MDB side impact procedure is not only linked to the increase in the trolley weight. Indeed, the stiffness of the deformable face in comparison to ECE 95 leads to higher initial dynamic displacements and intrusions. The increased trolley weight leads to higher levels in maximal velocities.

Therefore, coupling both phenomena (increased trolley weight and higher barrier stiffness) leads to more severe test procedure with higher biomechanical criteria and intrusions.

COMPARISON OF THE TWO PROCEDURES THANKS TO FULL-SCALE TESTS

In order to have a better knowledge of the new AE-MDB procedure, PSA Peugeot Citroën performed full-scale testing of vehicles of different sizes against AE-MDB V3.9: Small Family Car, Large Family Car and MPV.

The result of each car in the AE-MDB V3.9 test (1500 kg – 50 km/h) has been compared to the result of the same car in the current ECE 95 Progress test (950 kg – 50 km/h).

Structural behaviours (door and B-Pillar intrusions and velocities) have been compared as well as biomechanical criteria on the driver.

Tests are conducted with EuroSID 2 dummies and the same seat position is always used. Since current ECE 95 has no rear dummy, the rear area is not analysed in this section but will be studied in a specific chapter.

Small Family Car

On the small family car test, the B-Pillar was much more loaded with AE-MDB V3.9 than with current ECE 95. A rupture occurred on the lower part of the B-Pillar on the AE-MDB test whereas the B-Pillar was intact in the ECE95 test (see Figure 7 and Figure 8).



Figure 7. B-Pillar structural deformation for the Progress 950 kg test.

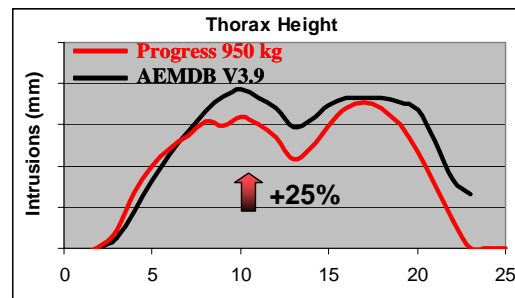


(b) AE-MDB V3.9 Test

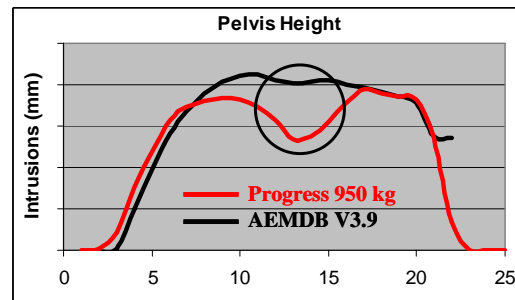
Figure 8. B-Pillar structural deformation for the AE-MDB V3.9 test.

On the intrusion graphs (see Figure 9 and Figure 10), we clearly see this rupture of the B-Pillar. (+126% intrusions in the area).

Elsewhere, intrusions are approximately 25% higher with AE-MDB V3.9 than with Progress barrier.



(a) Intrusion profile –Thorax height



(b) Intrusion profile –Pelvis height

Figure 9. Small family car - Comparison of the intrusion profile measured at different heights for the two different barriers (Progress 950 kg and AE-MDB V3.9) (a) Thorax height and (b) Pelvis height.

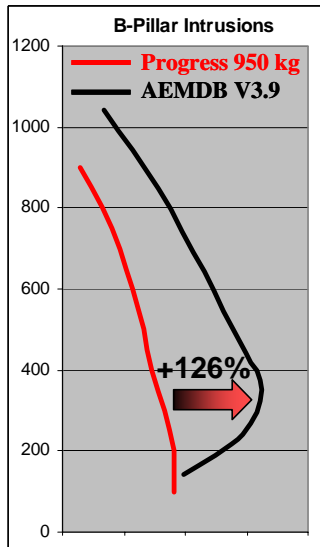
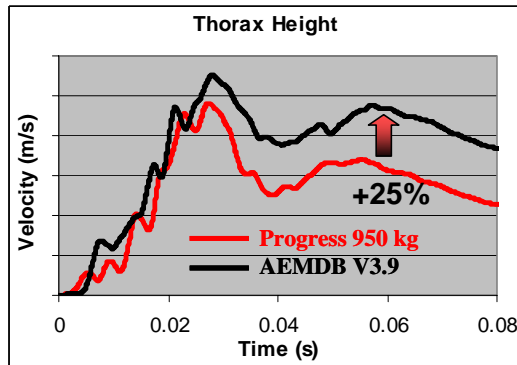
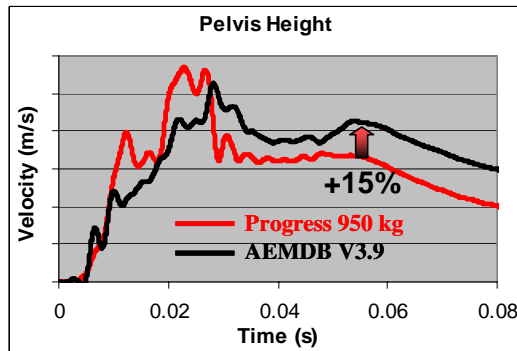


Figure 10 . Small family car - Comparison of the B-Pillar deformation profile for the two different barriers (Progress 950 kg and AE-MDB V3.9).

Doors velocities are also heightened up to 25% at their maximal level with the use of barrier AE-MDB V3.9 in place of Progress barrier at 950 kg (see Figure 11).



(a) Door velocity –Thorax height



(b) Door velocity – Pelvis height

Figure 11. Small family car - Comparison of the door velocity measured at different heights for the two different barriers (Progress 950 kg and AE-MDB V3.9) (a) Thorax height and (b) Pelvis height.

This increase in door velocities will lead to worse biomechanical criteria. This is shown in Figure 12 which represents biomechanical criteria versus EEVC regulatory limits and in Figure 13 where biomechanical criteria are scaled to the Euro NCAP 4 points limits.

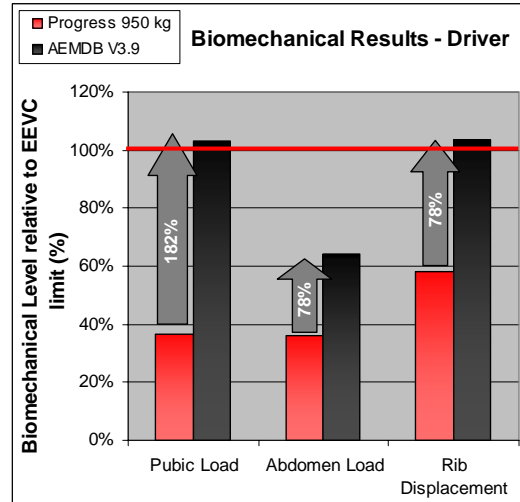


Figure 12. Small family car - Comparison of the driver biomechanical results for the two different barriers (Progress 950 kg and AE-MDB V3.9) with respect to EEVC limits.

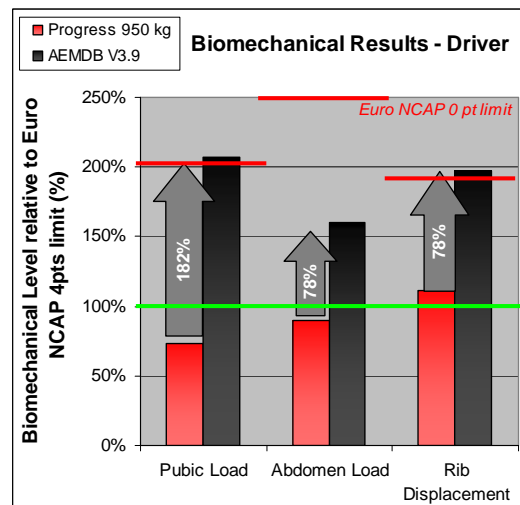


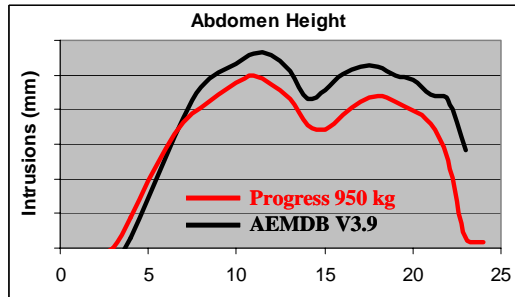
Figure 13. Small family car - Comparison of the driver biomechanical results for the two different barriers (Progress 950 kg and AE-MDB V3.9) with respect to Euro NCAP limits.

Rib deflexion and pelvis load go over the EEVC regulatory limit. Pelvis load may be a consequence of the rupture of the base of the B-Pillar seen in the AE-MDB test.

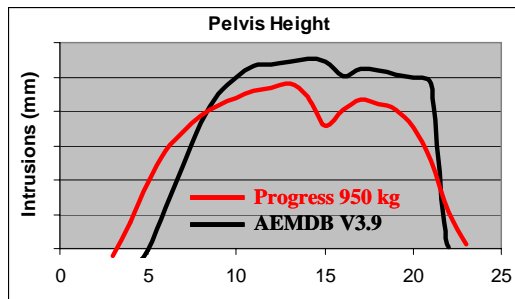
Rib deflexion is the consequence of a bottoming out of the thorax airbag caused by the increase of dynamic door displacement.

Large Family Car

On this vehicle family, conclusions are equivalent to the ones derived on the small family car. Doors intrusions (see Figure 14) are heighten up from 20% with the AE-MDB V3.9 test and B-Pillar intrusions by 15% (see Figure 15).



(a) Intrusion profile - Abdomen height



(b) Intrusion profile - Pelvis height

Figure 14. Large family car - Comparison of the intrusion profile measured at different heights for the two different barriers (Progress 950 kg and AE-MDB V3.9) (a) Thorax height and (b) Pelvis height.

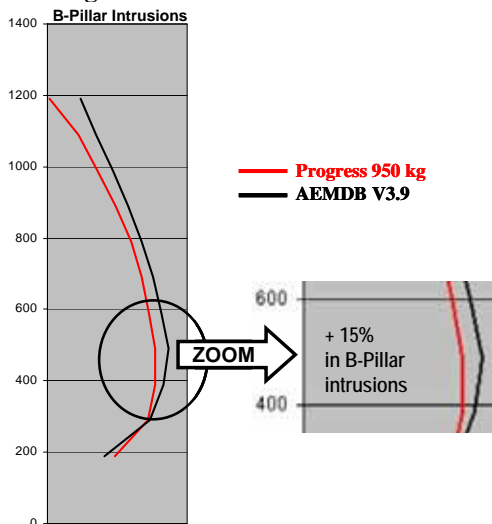
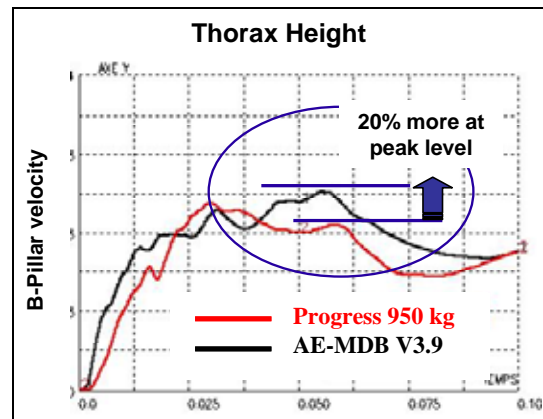
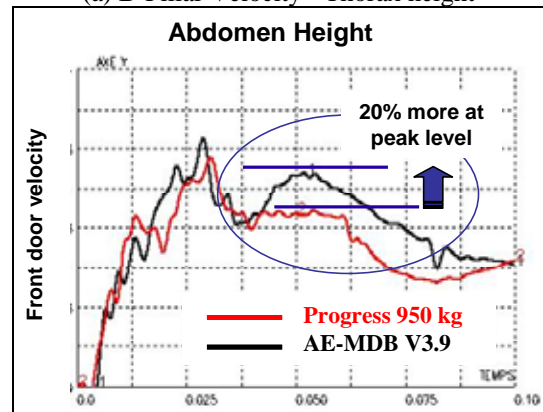


Figure 15. Large family car - Comparison of the B-Pillar deformation profile for the two different barriers (Progress 950 kg and AE-MDB V3.9).

Door and B-Pillar velocities are about 20% higher with AE-MDB V3.9 (average of 1.5 m/s more at peak level) (see Figure 16).



(a) B-Pillar Velocity - Thorax height



(b) Front Door velocity - Abdomen height

Figure 16. Large family car - Comparison of the door velocity measured at different heights for the two different barriers (Progress 950 kg and AE-MDB V3.9) (a) Thorax height and (b) Abdomen height.

This increase in intrusion and velocity are shown in Figure 17 and 18 which present biomechanical criteria versus EEVC regulatory limits and versus Euro NCAP 4 points limits.

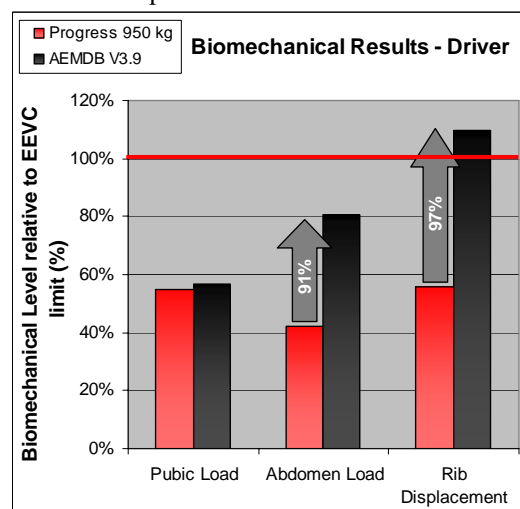


Figure 17. Large family car - Comparison of the driver biomechanical results for the two different barriers (Progress 950 kg and AE-MDB V3.9) with respect to EEVC limits.

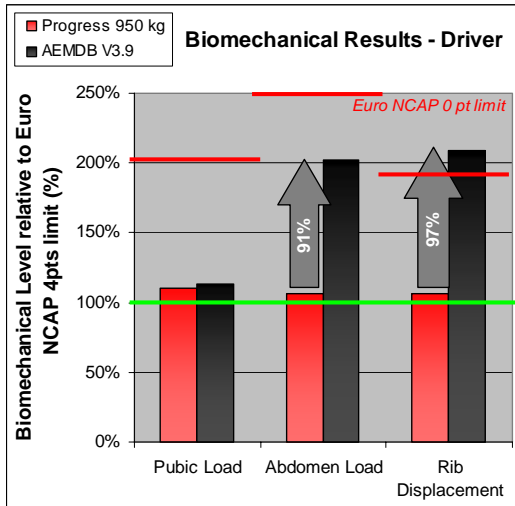
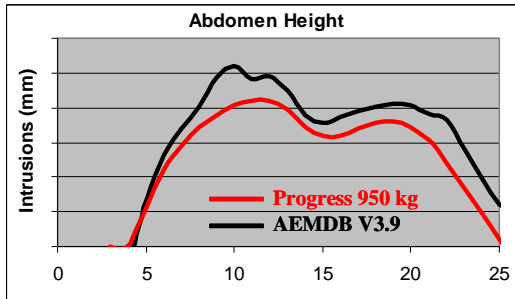


Figure 18. Large family car - Comparison of the driver biomechanical results for the two different barriers (Progress 950 kg and AE-MDB V3.9) with respect to Euro NCAP limits.

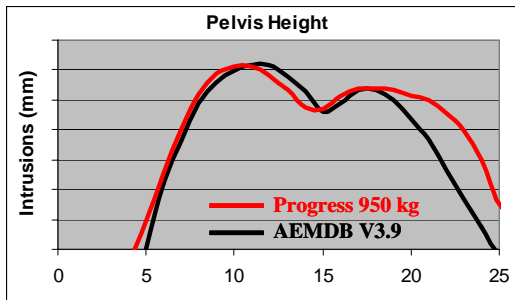
Biomechanical criteria that were all under the 4 points Euro NCAP limit in the Progress 950 kg test increased up to 100% more with the use of AE-MDB V3.9. We can even note that rib displacement would pass over the regulatory limit.

MPV

Again, doors and B-Pillar intrusions are heighten up from 20% with the AE-MDB V3.9 test (see Figure 19 and Figure 20).



(a) Intrusion profile - Abdomen height



(b) Intrusion profile - Pelvis height

Figure 19. MPV - Comparison of the intrusion profile measured at different heights for the two different barriers (Progress 950 kg and AE-MDB V3.9) (a) Thorax height, (b) Pelvis height.

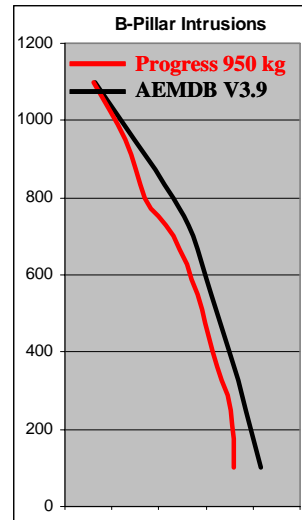
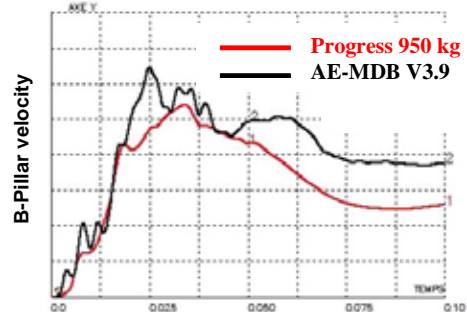


Figure 20. MPV - Comparison of the B-Pillar deformation profile for the two different barriers (Progress 950 kg and AE-MDB V3.9).

Velocities, again, are in this case higher with AE-MDB V3.9 than with Progress. The initial slope is clearly steeper (as a result of the increased barrier stiffness), causing the dynamic displacement to be greater. This will have an effect on the thorax airbag that will have less space to absorb the energy at the beginning of the crash (risk of bottoming out) (see Figure 21).

Thorax Height



(a) B Pillar Velocity - Thorax Height

Abdomen Height



(b) Door Velocity - Abdomen Height

Figure 21. MPV - Comparison of the door velocity measured at different heights for the two different barriers (Progress 950 kg and AE-MDB V3.9) (a) Thorax height and (b) Abdomen height.

As usual, the consequences of the extra severity in intrusion and velocity will be shown in the biomechanical results, see Figure 22 and 23 which represent biomechanical criteria versus EEVC regulatory limits and Euro NCAP 4 points limits.

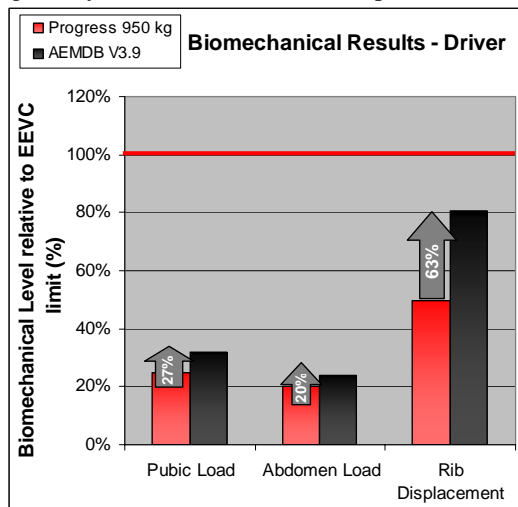


Figure 22. MPV - Comparison of the driver biomechanical results for the two different barriers (Progress 950 kg and AE-MDB V3.9) with respect to EEVC limits.

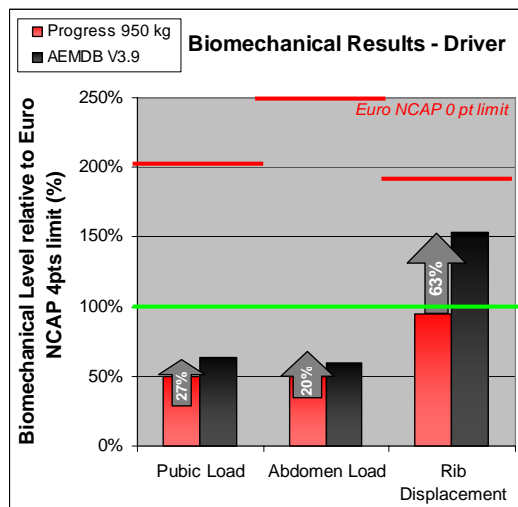


Figure 23. MPV - Comparison of the driver biomechanical results for the two different barriers (Progress 950 kg and AE-MDB V3.9) with respect to Euro NCAP limits.

All the biomechanical criteria are increased with the use of AE-MDB V3.9. Rib deflections are heightened up by 63% as a result of a higher dynamic displacement and an increased deformation of the seat.

Biomechanical criteria are not as much increased on this vehicle size than on the other tested (small family vehicle and large family vehicle). MPV's are quite favoured by the height of the seat. The dummy being seated higher is less affected by the structural behaviour.

Driver protection: Conclusion

The same conclusions can be derived from the different sizes of vehicles by comparing ECE 95 side impact procedure (Progress barrier 950 kg) and AE-MDB procedure. The introduction of the AE-MDB V3.9 barrier always leads to higher door and B-Pillar intrusions, an increase by 25% as an average. On some vehicles, the more severe deformations have even generated the loss of some structural parts. (Rupture of the B-Pillar base for example, which was unseen on the ECE 95 test) Door and B-Pillar velocities are hence also penalized by 30%. Initial dynamic displacements are higher (as a result of the stiffer body barrier) and lead to thorax airbags with less space to deploy and to absorb energy. Maximal velocities are heightened up causing the injury risk on dummy to be higher in case of a bottoming out for example.

Therefore, in all cases, biomechanical criteria could reach up to 125% more in the worst cases. On some vehicles, some biomechanical criteria even go over EEVC regulatory limit.

REAR OCCUPANT PROTECTION

The introduction of AE-MDB barrier, with its higher width and its impact point located rearwards, enable to introduce an assessment of the rear passenger protection in side impact. The Progress barrier, currently used in ECE 95, is too narrow and centred on R-Point (in comparison to R+250 mm for AE-MDB barrier), and therefore does not impact the vehicle in the area of the rear occupant. Yet, a good discrimination of the rear passenger protection offered by the different vehicles was not possible with the Progress barrier.

This part of the study presents the assessment of the level of protection of the second row for the different cars tested and presented previously (Small Family Car, Large Family Car, MPV). We first studied the structural behaviour of the rear area in front of the dummy. Then, in a second part, we processed dummy readings.

As we could not compare the level of protection of this second row in the AE-MDB test to the one obtained in the Progress test (no passenger), we have plotted, in the three figures below (Figure 24 to 26), the velocity of the rear door compared to the velocity of the front door. This will enable us to have a point of comparison for rear door velocities.

Only the charts of the velocity at thorax height are shown hereafter. The graphs measured on the other location would show the same trends.

Velocities of the three different sizes of vehicle (small family car, large family car and MPV) are plotted in figure 24 to 26.

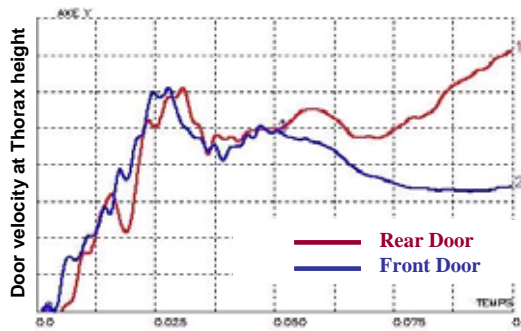


Figure 24. Small Family Car – Comparison of the door velocity measured on the front and on the rear door at the thorax height on the AE-MDB V3.9 test.



Figure 25. Large Family Car – Comparison of the door velocity measured on the front and on the rear door at the thorax height on the AE-MDB V3.9 test.

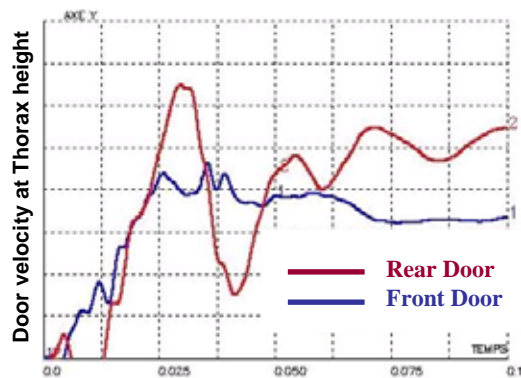


Figure 26. MPV – Comparison of the door velocity measured on the front and on the rear door at the thorax height on the AE-MDB V3.9 test.

For each car, we can see that rear door velocity is higher than front door velocity. Rear door velocities have higher initial peak values and have very often higher maximum level. We can also see the effect of the rotation of the car, rear door velocities “finishing” at a very high level (much bigger than the front door) at time 100 ms and after.

For example, on the MPV graph, there is at least 30% more velocity 50 ms after impact and the

higher initial peak value will lead to 25% more dynamic displacement.

Thus, we can clearly see that rear door structural behaviour is not at the same level as the front door. The current level of protection offered on rear passengers is therefore not at the level as the one offered to the front driver.

Figure 27 presents the biomechanical criteria of the rear passenger with respect to 4 points Euro NCAP limit.

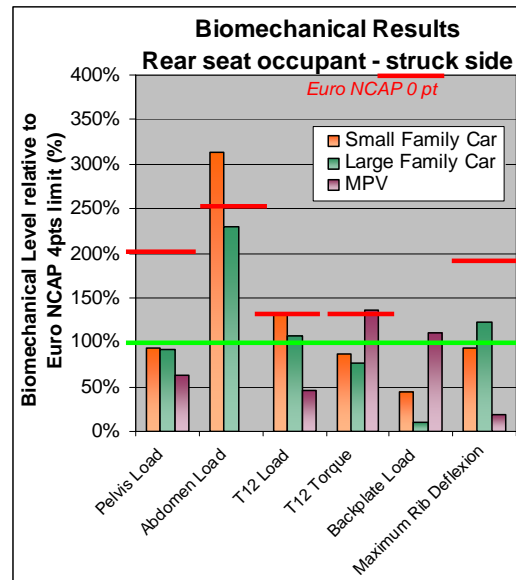


Figure 27. Comparison of the driver biomechanical results measured on AE-MDB V3.9 for the three different car size with respect to Euro NCAP limits.

From figure 27, we can conclude that all vehicles are far beyond the 4 points Euro NCAP limits. Therefore, in order to reach the same level of protection for the back and the front, these vehicles should be loaded on the rear as well as on the front and should be equipped with performing restraint devices and should reinforce their structural dimensioning.

DISCUSSION

The first major point in analysing the AE-MDB V3.9 side impact procedure in comparison to ECE 95 is its better representativeness of the average European vehicle. Its design itself is done by comparing it to car-to-car tests. Thus, validation tests, conducted by the Aprosys project and by ACEA, have shown that deformation, loading patterns and biomechanical criteria were representative of car-to-car tests (in between a Freelander and a Golf V).

Numerical studies carried out by PSA Peugeot Citroën showed that the AE-MDB V3.9 side impact test procedure show a higher severity than the ECE 95 procedure thanks to two major evolutions:

- an increased trolley weight (1500 kg instead of 950 kg)
- a stiffer body barrier with use of the AE-MDB V3.9 instead of the Progress.

Thanks to the virtual testing, we have seen that the coupling of both phenomena (increased trolley weight and stiffer body barrier) leads to worse biomechanical criteria and higher intrusions. The increased trolley weight has an effect on maximal door and B-Pillar velocities, whereas the barrier stiffness itself has an effect on the intrusions and the initial dynamic displacements. In overall, the increased severity of the new AE-MDB side impact procedure compared to ECE 95 is about 30% more.

Full-scale testing, done on different PSA Peugeot Citroën vehicles of different sizes, has shown deterioration in the structural behaviour by about an average of 25%. (Some non-linear phenomena have even appeared with the use of the AE-MDB V3.9 barrier such as complete loss and rupture of structural parts that were not seen with the Progress barrier used in the ECE 95 procedure). Intrusions and velocities are higher, as well as biomechanical criteria.

The increased severity seen with AE-MDB side impact procedure will have a direct influence on the conception of vehicles.

In order to keep the same protection level as the one offered in the current ECE 95 on in the consumer tests, the structural behaviour will have to be the same as the one seen today with the Progress barrier. Therefore B-Pillars will have to be stiffer, and doors reinforcements bigger. Structural basement of the car should also be able to support bigger loads coming out from doors and B-Pillar. These structural improvements will enable future vehicles to show lower intrusions and velocities despite the more severe barrier loading. New load paths could also be studied by trying to transmit a higher proportion of energy through the seat or the console.

Introducing rear passenger protection in the side impact test procedure will also lead to a general structural reinforcement and especially the rear area. Nowadays, vehicles have usually no structural door reinforcement in the rear door. But these will become essential in order to control structural rear velocities and thus rear biomechanical criteria. In order to deal with this new side impact procedure, each vehicle will have to add an average of 15 kg structural reinforcements to its weight, (in

the structural baseline, with door reinforcements, and with new load paths through the seats for example).

Restraints devices will also have to be more performing. Especially on the rear area that usually hasn't, on nowadays vehicles, any specific devices for the improvement of side impact protection. Rear side impact airbags, absorbing energy foams in the rear panel, and seat-belt pretension will have to appear on the future vehicles.

Therefore, taking into account AE-MDB side impact test procedure will lead to a better equipped compartment area as well as a reinforced structural behaviour.

CONCLUSIONS

This new AE-MDB side impact procedure is more representative of the last generation vehicles. Its severity is clearly in between a crash against a Freelander and a crash against a Golf V.

Its integration in consumerism or regulatory procedure will lead to a global reinforcement of the structural area and a better level of equipment for future vehicles. This will have a direct consequence on the improvement of security in side impact for car users for front occupants as well as for rear occupants.

ACKNOWLEDGMENTS

The authors wish to thank all the labs, car manufacturers (ACEA) and research teams that where involved in this study.

REFERENCES

- [1] European_Council, regulation ECE 95
- [2] A.K. Roberts & M.R. Van Ratingen on behalf of EEVC WG13 "Progress on the development of the advanced European mobile deformable barrier face (AEMDB)" in 18th ESV Conference Nagoya 2003
- [3] Yonezawa, H., T. Haragae, and Y. Ezaka "Japanese research activity on future side impact test procedures" in 17th ESV conference 2001. Amsterdam

APPENDICES

Appendix 1

Figure 28 presents the response of the two versions of barrier (AE-MDB V2 and AE-MDB V3.9) in the corridor created from the frontal test of cars to Load Cell (rigid) Wall and the theoretical corridor that has been derived from the theoretical characteristics of the V2 barrier face.

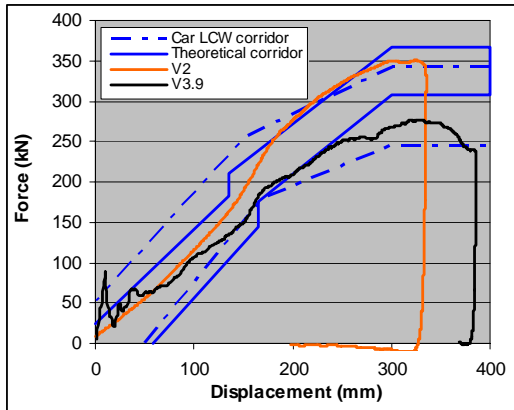


Figure 28. AE-MDB V2 and V3.9 response compared with the two corridor proposed to define AE-MDB

We can notice that version V3.9 of AE-MDB barrier is in the corridor only in the first 200 mm of displacement. But being out of the corridor after 200 mm of crush is not a problem since biomechanical criteria always occur before 200 mm of barrier deformation.

ASSESSMENT OF OCCUPANT PROTECTION SYSTEMS IN VEHICLE-TO-POLE LATERAL IMPACT USING ES-2 AND WORLDSID

Thomas Belcher, Craig Newland

Australian Government Department of Transport and Regional Services

Paper No. 07-0255

ABSTRACT

A series of vehicle-to-pole lateral impact tests were conducted using ES-2 and WorldSID dummies. Pure lateral (90°) and oblique (75°) impacts were included in the test series and the level of protection offered by the head protecting side airbag was assessed under each condition.

The head injury risks predicted by the ES-2 and WorldSID dummies under the same oblique pole test conditions were dramatically different, with the ES-2 indicating a low risk of head injury and the WorldSID indicating a very high risk of head injury. Sled tests were used to investigate the kinematics of the ES-2 shoulder, the consequent influence of shoulder load on head / neck kinematics, and the ability of this dummy to discriminate the level of head protection offered by head protecting side airbags. The head, neck, and shoulder kinematics and peak shoulder loads of the ES-2 were found to be highly sensitive to the direction of loading to the shoulder resulting from each pole impact angle.

INTRODUCTION

The EuroSID 2 (ES-2) dummy was originally developed for mobile deformable barrier side impact testing, and is the current regulatory dummy specified in UNECE R95 (Protection of Occupants in the Event of a Lateral Collision). The WorldSID dummy was developed as part of a collaborative project to develop a world harmonized side impact dummy with superior biofidelity to earlier generations of side impact dummies. Like all anthropomorphic crash test devices, these dummies are essentially an assembly of mechanical components and instruments, the purpose of which is to simulate a human biomechanical response and measure injury risks.

The ES-2 shoulder assembly (see Figure 1) consists of an arm clavicle mounted between two metal plates, and an elastic cord which is used to hold the shoulder in position. This design allows transverse adduction of the shoulder, but does not allow significant other movements of the shoulder. A tri-axial load cell is used to measure shoulder loads. The WorldSID shoulder consists of a mounting bracket and a shoulder rib. The shoulder bracket allows some transverse adduction of the shoulder, and the shoulder rib permits medial deflection of

the upper arm / shoulder. A tri-axial load cell is used to measure shoulder loads, and an IRTRACC (see Figure 3) is used to measure shoulder rib deflection.

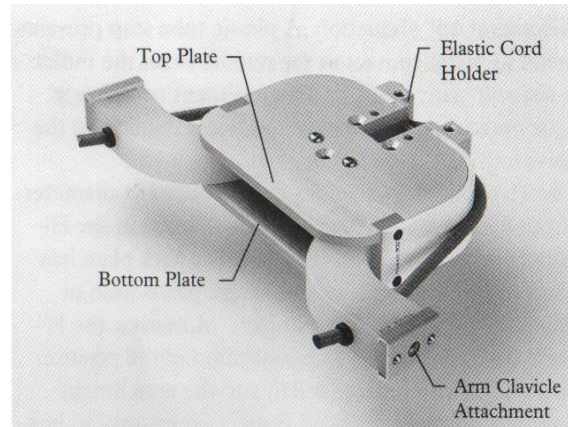


Figure 1. ES-2 shoulder assembly (note: arms are attached to each clavicle attachment).

The ES-2 has three rectangular thorax ribs (see Figure 2). These ribs are mounted to a spring slide and hydraulic damper assembly, and are capable of purely lateral deflection from one side only. ES-2 rib deflections are measured by linear potentiometers. The WorldSID has three circular thorax ribs mounted either side of a central spine box (see Figure 2 and Figure 3). These ribs are capable of deflection in all directions, and from both sides. An IRTRACC is used to measure the lateral component of rib deflection. It is not practical to package sufficient instrumentation to simultaneously measure deflections on each rib on both sides of the dummy.



Figure 2. ES-2 (left) and WorldSID (right) shoulder, thorax, and abdomen design.

The ES-2 abdomen (see Figure 2) consists of a load cell element. Load cells are used to measure front, middle, and rear abdomen loads. In contrast, the WorldSID has two circular abdomen ribs mounted either side of its central spine box. An ITRACC is also used to measure the lateral component of abdomen rib deflection.

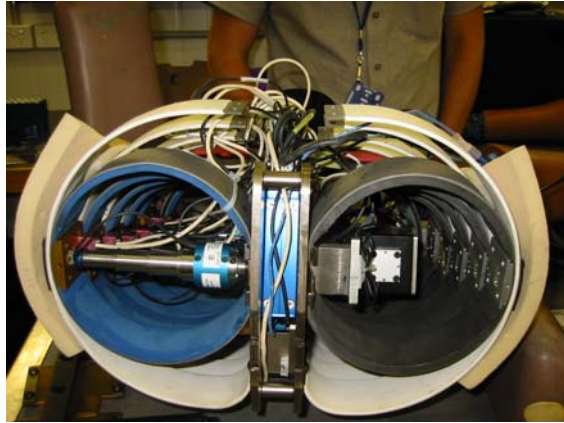


Figure 3. WorldSID thorax rib assembly (including ITRACC and rib accelerometer instrumentation).

The suitability of the ES-2 and WorldSID dummies for lateral impact testing is therefore determined by the capacity of each mechanical component / sensor to measure the types of impact loadings that occur in lateral impact. It is also determined by the capacity of each dummy to simulate a human biomechanical response to side impact conditions.

In this study, results obtained from a series of vehicle-to-pole side impact tests, are used to analyse the crash responses of ES-2 and WorldSID. Results obtained from a series of pole sled tests are then used to further investigate the kinematics of the ES-2 shoulder, neck, and head.

METHOD

Vehicle Pole Test Series

A series of 3 full scale vehicle-to-pole side impact tests were conducted using ES-2 and WorldSID dummies (see Table 1). The vehicle model chosen for this series of tests was a 2004 model, right hand drive, 5 door mid-sized SUV, with curtain and seat mounted thorax (front row) side airbags. This vehicle model was popular in the Australian market, and was used for each test in this series.

Table 1 summarises test conditions for each full scale vehicle pole side impact test. A perpendicular pole test was conducted using an ES-2 dummy situated in the drivers seating position. Two oblique pole tests were also conducted; one with an ES-2 driver's side dummy, and the other with a

WorldSID dummy in each front row seating position. WorldSID dummy sensor data is therefore available for both the struck side and non-struck side occupant. Interactions occurred between the two WorldSID dummies; however, this paper will focus on struck side injuries. It is important to recognise that results show dummy interaction responses to be separate events to struck side injuries. Therefore the presence of a front passenger dummy does not affect the assessment of struck side injuries.

**Table 1.
Test Matrix
(Vehicle Pole Test Series)**

Impact Angle (Degrees)	Impact Speed (km/h)	Driver Dummy	Front Passenger Dummy	Side Airbags
90	28.8	ES-2	-	Thorax Curtain
75	32.2	ES-2	-	Thorax * Curtain
75	32.0	WS	WS	Thorax * Curtain

* Airbag failed to deploy correctly / deployed inside the drivers seat

The seatback angle was set to achieve a manufacturer specified torso angle of 21° and the seat was locked in the mid track seating position. A 3-D H-point machine was used in accordance with the requirements of EuroNCAP pole side impact testing protocol (version 4.1) [1] to determine the H-point of the driver's seat. For the tests conducted using an ES-2 dummy, a FARO arm was used to match, as closely as possible, the dummy with the seating reference point determined with the 3-D H-point machine. A FARO arm was also used to measure and match the location of the head centre of gravity for each ES-2 test. The ES-2 dummy has a more upright seating posture than the WorldSID. It is therefore not possible to match both the H-point and head centre of gravity of each dummy. The WorldSID dummy was therefore positioned using the same seating track position and seat back angle, and a FARO arm used to accurately match the dummy head centre of gravity location (x-coordinate) to those recorded for the previous ES-2 tests. This ensured that the pole was aimed at the same location on the vehicle for each oblique pole test.

Each pole side impact test was conducted with either a perpendicular (90°) or oblique (75°) angle between the direction of travel and the vehicle longitudinal centreline / axis (see Figure 4 and Figure 5). For each test, a laser was used to align the pole with the dummy head centre of gravity, and a carrier sled was used to impact the vehicle with the pole. The pole used was in accordance

with the specifications of EuroNCAP pole side impact testing protocol (version 4.1) [1].



Figure 4. Overhead view of 90 degree (perpendicular) pole side impact test.



Figure 5. Overhead view of 75 degree (oblique) pole side impact test.

The perpendicular pole test was conducted with a targeted impact speed of 29 km/h. For the oblique pole tests, the targeted impact speed was 32 km/h. In all cases, the actual impact speed was within ± 0.2 km/h of the targeted impact speed. For each full scale vehicle test, the actual impact alignment was within 4 mm of the intended impact alignment.

Pole Sled Test Series

A series of pole sled tests were conducted to further investigate the biomechanical response (i.e. head, neck, shoulder) of the ES-2 dummy (see Table 2). In this series of tests, a UNECE R16 hard seat was mounted to a crash sled, and a head curtain airbag (from one of the earlier full scale vehicle tests) was pre-inflated to a constant regulated pressure (approx 45 kPa) and secured against the pole by a fabricated test fixture (see Figure 6 and Figure 7). A stepped pole fixture was used in one of the tests to simulate shoulder deflection for an ES-2 dummy (see Figure 8). The stepped portion of the pole was positioned

to interact with the dummy head, but not the dummy shoulder.

The curtain airbag was able to be moved relative to the pole, using the fabricated test fixture. This made it possible to simulate different head impact locations with the curtain airbag. Four head impact locations were tested. Three of these locations were chosen to match the head to airbag impact locations for each full scale vehicle test. The remaining head impact location was chosen to approximate an estimated WorldSID head impact location for a perpendicular pole test.

**Table 2.
Test Matrix
(Pole Sled Test Series)**

Dummy Angle (Degrees)	Impact Speed (km/h)	Pole Step (mm)	Head / Airbag Impact Location	Right Arm Angle (Degrees)
90	22	0	ES-2 / 90	0
90	22	0	WS / 90	0
75	22	0	WS / 75	40
75	22	0	ES-2 / 75	40
75	22	50	ES-2 / 75	40

Each pole sled test was conducted with the ES-2 dummy midsagittal plane oriented at either a perpendicular (90°) or oblique (75°) angle to the direction of motion. Foam block padding was used to ensure the correct pre-impact orientation of the dummy. For each test, the centre of the pole was aligned with the dummy head centre of gravity.

The right arm was set to a 0° (horizontal) or 40° angle depending on the dummy / pole impact angle being simulated. For the perpendicular tests, the dummy arm was set to a horizontal position prior to impact; this was done to simulate the position of the arm following successful deployment of the thorax airbag. For the oblique pole sled tests the dummy arm was lowered by 40°; this was done to simulate the lower arm positions observed, when the thorax airbag fails to deploy successfully.

Each pole sled test was conducted with a 22 km/h impact speed. This impact speed was selected following an initial investigation of dummy head acceleration. This initial investigation involved the conduct of some experimental tests, the purpose of which was to determine a set of test conditions (including test speed) which would give marginal head contact with the pole through the airbag. This enabled further investigation of the effect of pole test variables on ES-2 head, neck, and shoulder responses.



Figure 6. Onboard view of pole sled test (at maximum head acceleration).

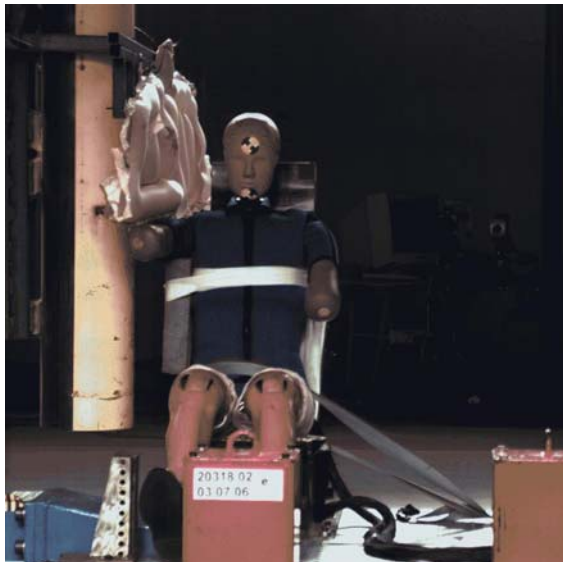


Figure 7. Front view of pole sled test (approx. 10-15 ms prior to impact).

A 70 mm foam block was used to improve the simulation of dummy thorax interaction with the pole. A webbing strap located around the pelvis and anchored to the sled, was used in each test to restrain the pelvis and upper legs of the dummy. A metal fixture was used to limit / restrain the motion of the lower legs (see Figure 7).



Figure 8. Stepped pole test fixture.

Data Acquisition

All dummy and vehicle sensor channel data was collected at a 20 kHz sampling frequency. All data presented in this paper is in accordance with the filtering and sign conventions specified by SAE J211-1 (December 2003) [2].

RESULTS

Vehicle Pole Test Series

Table 3 shows struck side 3 ms head acceleration and HIC 36 results for each vehicle-to-pole side impact test. The ES-2 dummy head avoided hard contact with the pole for each pole impact condition. In contrast, the WorldSID head was observed to bottom out the curtain airbag, making hard contact with the pole. Consequently, for oblique pole impact, WorldSID indicated a higher head injury risk (i.e. HIC 36) than ES-2. Figure 9 shows resultant head acceleration for each test. Two separate head acceleration spikes were recorded for the oblique pole test conducted using the WorldSID. The first of these acceleration spikes was co-incident with the dummy head-to-pole collision; the second was co-incident with a collision of the driver and front passenger dummy heads (not discussed in this paper).

**Table 3.
Head Acceleration / HIC 36**

Impact Angle (Degrees)	Impact Speed (km/h)	Driver Dummy	3 ms Head Acc. (g)	HIC 36
90	28.8	ES-2	60.89	352.7
75	32.2	ES-2	80.43	809.1
75	32.0	WS	65.92	2941.6

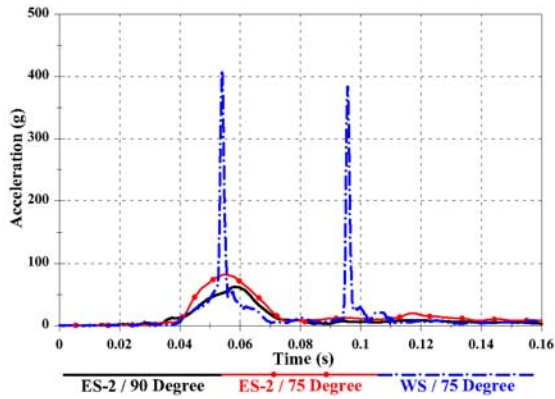


Figure 9. Resultant head acceleration.

Figure 10 shows longitudinal (x-axis in dummy coordinate system) head acceleration for each vehicle-to-pole side impact test. For the ES-2 dummy, oblique pole impact produced an earlier and larger longitudinal head acceleration response, than perpendicular impact. This increase in ES-2 longitudinal head acceleration is due to the longitudinal component of impact velocity; it is also a product of the longitudinal components of shoulder load, upper spine acceleration, and upper neck load. The WorldSID longitudinal head acceleration response shows the occurrence of a dummy head-to-pole collision ($t \approx 54$ ms). However, in the period immediately following impact and preceding this head collision (i.e. between $t = 0$ and $t \approx 51$ ms), WorldSID longitudinal head acceleration was substantially lower than that of ES-2.

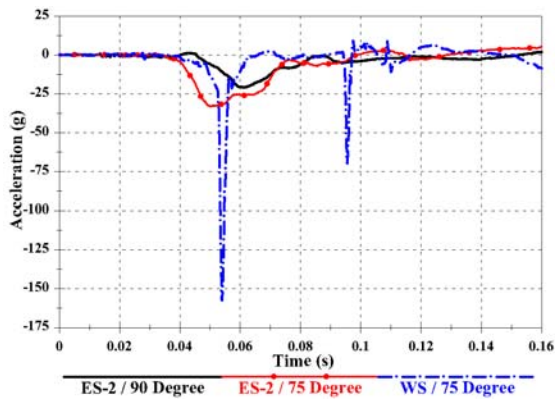


Figure 10. Longitudinal head acceleration (A_x).

Figure 11 shows lateral (y-axis in dummy coordinate system) head acceleration for each vehicle-to-pole side impact test. For the ES-2 dummy, oblique impact also produced more lateral head acceleration than perpendicular impact. This increase is likely to have been caused by a combination of factors, including a small increase in the lateral component of vehicle impact velocity, and a substantially larger lateral shoulder load (see Figure 13). The lateral head acceleration recorded

during the oblique WorldSID test was initially similar to that recorded during the perpendicular ES-2 test (i.e. up until the occurrence of the head-to-pole collision). This suggests that the ES-2 dummy head came very close to colliding with the pole for each pole impact condition. For the oblique pole test conducted using ES-2, there was just enough initial head acceleration to prevent hard impact from occurring between the head and pole through the airbag.

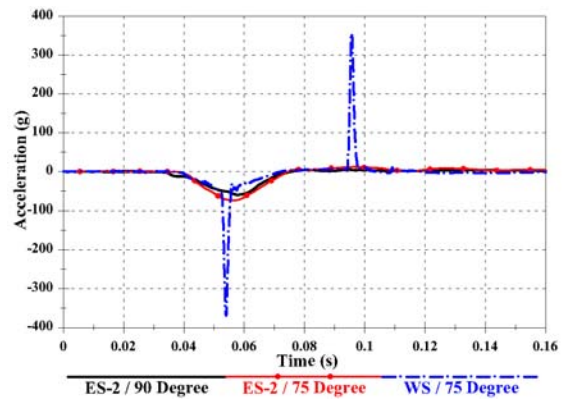


Figure 11. Lateral head acceleration (A_y).

Figure 12 shows struck side longitudinal shoulder load for each vehicle-to-pole side impact test. For the ES-2 dummy, oblique pole impact produced substantially more longitudinal shoulder load than perpendicular impact. This relatively large longitudinal shoulder load acts in an anterior direction (i.e. pushes shoulder back relative to chest), and is a result of the longitudinal component of oblique pole test impact velocity. Under these conditions, the relative stiffness of the ES-2 shoulder is likely to prevent any substantial relative transverse lateral, longitudinal, or vertical motion between the shoulder and upper spine, as the shoulder is pushed onto its limit stops. For the oblique pole test condition, WorldSID recorded substantially less longitudinal shoulder load than ES-2.

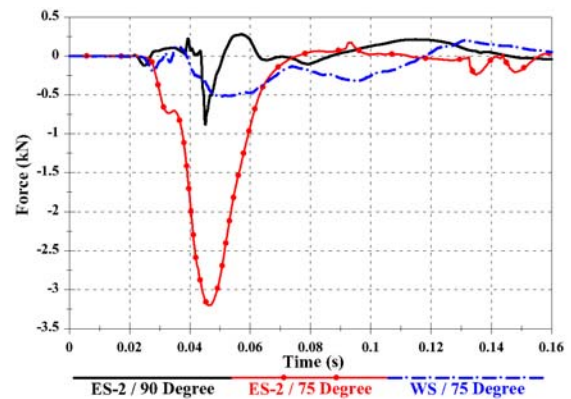


Figure 12. Longitudinal shoulder force (F_x).

Figure 13 shows lateral shoulder load for each vehicle-to-pole side impact test. For the ES-2 dummy, oblique pole impact produced substantially more lateral shoulder load than perpendicular impact. For this dummy and oblique pole impact condition, a large longitudinal shoulder load coincided with a large lateral shoulder load. Under these conditions, there is a direct lateral load / energy transfer path from the ES-2 shoulder to the upper spine and neck. In oblique impact, the WorldSID struck side shoulder rib deflected 51.5 mm. The WorldSID shoulder rib therefore stored / absorbed energy during impact. As a result, under oblique impact conditions, WorldSID recorded a smaller peak lateral shoulder load than ES-2.

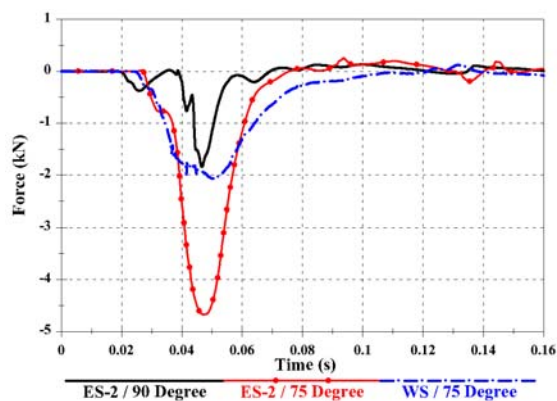


Figure 13. Lateral shoulder force (F_y).

Figure 14 shows vertical shoulder load for each vehicle-to-pole side impact test. For the ES-2 dummy, oblique pole impact produced substantially more vertical shoulder load than perpendicular impact. For both impact conditions, the ES-2 shoulder was initially pushed upwards (negative load) by the intruding door at the window line. In the case of perpendicular impact, successful thorax airbag deployment caused the ES-2 shoulder and arm to rise above the intruding door, and the vertical shoulder load to change from negative (upward acting) to positive (downward acting). For the oblique pole test condition, WorldSID recorded substantially less vertical shoulder load than ES-2.

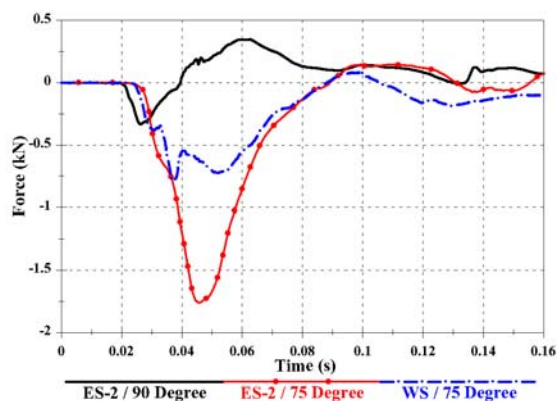


Figure 14. Vertical shoulder force (F_z).

During the perpendicular pole test, the ES-2 arm and shoulder were able to move both forward and inboard (see Figure 15). This movement of the shoulder / arm was assisted by the successful deployment of the thorax airbag. In contrast, during the ES-2 oblique pole test, the thorax airbag failed to deploy correctly, the arm was jammed between the intruding pole and the thorax, and the shoulder was unable to move substantially forward or inboard relative to the upper spine (see Figure 16). In oblique impact, the WorldSID shoulder was deflected inwards and the arm was jammed between the intruding pole and the thorax (see Figure 17). This medial shoulder deflection reduces the distance between the intruding pole and the base of the neck. This increases the likelihood of dummy head-to-pole hard contact through the airbag.



Figure 15. ES-2 arm and shoulder position approximately 75 ms after time-zero (perpendicular impact condition).

Figure 18 and Figure 19 show the longitudinal and lateral components of upper spine acceleration for each vehicle-to-pole side impact test. For each dummy and pole impact condition, there is a correlation between the corresponding components of shoulder load and upper spine acceleration (see Figure 12 and Figure 13). All else being equal, higher shoulder loads will increase acceleration of the upper spine, head, and thorax. For the ES-2 dummy, oblique impact produced higher peak longitudinal and lateral upper spine accelerations than perpendicular impact. For oblique impact, WorldSID longitudinal and lateral upper spine accelerations peaked at lower levels than ES-2 (note: the WorldSID upper spine acceleration response includes interaction with front passenger occupant at $t \approx 95$ ms). Also notable is the later occurrence (approx. 10 ms) of WorldSID peak

inboard and backward upper spine accelerations compared with ES-2.



Figure 16. ES-2 arm and shoulder position approximately 75 ms after time-zero (oblique impact condition).



Figure 17. WorldSID arm and shoulder position approximately 75 ms after time-zero (oblique impact condition).

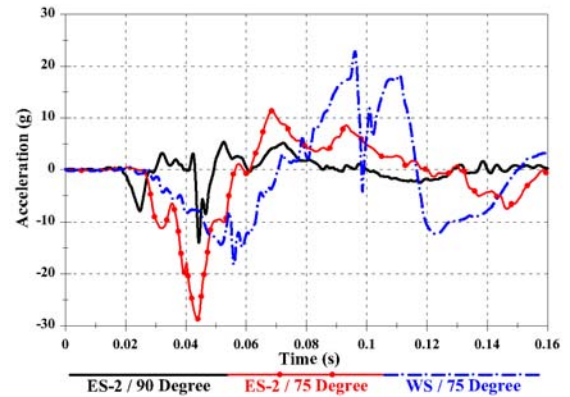


Figure 18. Longitudinal upper spine acceleration (Ax).

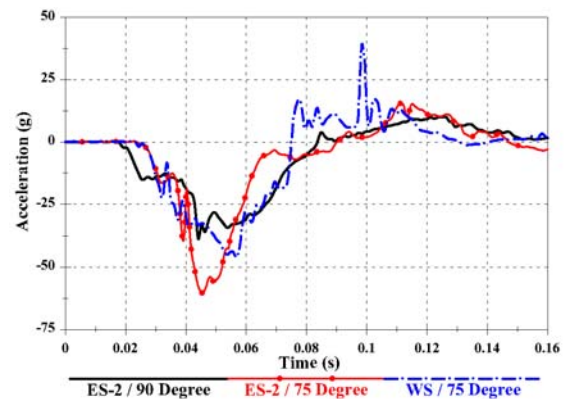


Figure 19. Lateral upper spine acceleration (Ay).

Figure 20 shows longitudinal upper neck load for each vehicle-to-pole side impact test. For the ES-2 dummy, oblique pole impact produced substantially more longitudinal upper neck load than perpendicular impact. In oblique impact, ES-2 longitudinal upper neck load is predominantly negative. This indicates forward movement of the head relative to the chest. It is also noteworthy that peak (negative polarity) longitudinal upper neck load occurred at approximately the same time as peak (negative polarity) longitudinal shoulder load (see Figure 12). This suggests that the ES-2 dummy head is pulled / accelerated rearward of the pole by load transferred through the shoulder and upper neck. For the oblique pole impact condition, WorldSID longitudinal head acceleration rapidly changed from negative to positive. This polarity change was coincident with dummy hard head contact with the pole, and indicates rearward movement of the head relative to the chest (i.e. pole pushed dummy head back relative to chest).

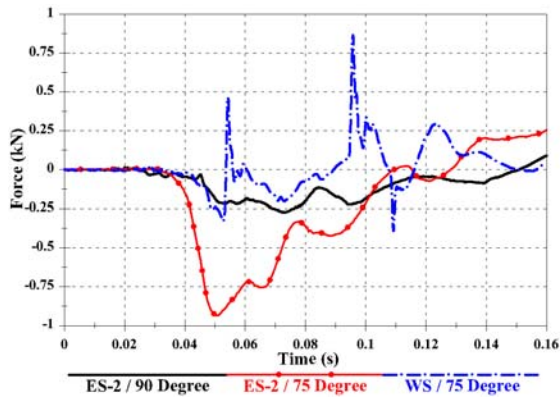


Figure 20. Longitudinal upper neck force (F_x).

Figure 21 shows lateral upper neck load for each vehicle-to-pole side impact test. For the perpendicular pole test, ES-2 lateral upper neck load is predominantly positive. This means the head moves leftward (inboard) relative to the chest. For the oblique impact condition, the ES-2 lateral upper neck load is initially negative (i.e. head moves right relative to chest). This negative lateral upper neck load pulls the upper neck towards the pole, and an equal and opposite (i.e. positive) resistive load pulls the head away from the pole. For the ES-2 dummy and oblique impact condition, peak (negative polarity) lateral upper neck load occurred at approximately the same time as peak (negative polarity) lateral shoulder load (see Figure 13). This suggests that the ES-2 dummy head is pulled / accelerated away (inboard) from the pole by relatively large (negative polarity) lateral upper neck and shoulder loads. For the oblique pole impact condition, WorldSID lateral upper neck load was also initially negative. However, the peak magnitude and the duration of negative lateral upper neck load were considerably less for the WorldSID. For this dummy, lateral upper neck load changed polarity immediately prior to hard head-to-pole contact. Therefore, in contrast to ES-2, the WorldSID head was pushed inboard relative to the chest, during head interaction with the curtain airbag / pole.

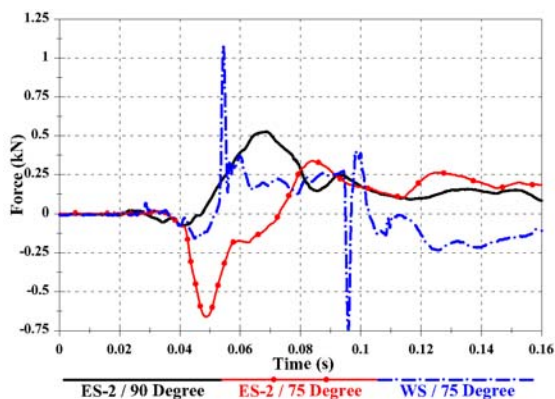


Figure 21. Lateral upper neck force (F_y).

Figures 22 to 24 show upper, middle, and lower thorax rib deflection for each vehicle-to-pole side impact test. For the ES-2 dummy, perpendicular impact produced more upper and middle rib deflection, than oblique impact. This is despite the fact that the thorax airbag failed to deploy successfully during oblique impact. For the oblique impact condition, the location of maximum rib deflection (i.e. upper, middle, or lower rib) varied depending on the dummy used. WorldSID predicted greatest injury risk (i.e. highest rib deflection) at the upper thorax, while ES-2 predicted greatest injury risk at the lower thorax. This is likely to be attributable to a range of factors, including differences in the seating posture, and biomechanical response of each dummy. The capacity of each dummy to detect oblique (i.e. not purely lateral) rib loads may also be a factor. It should be noted that the ES-2 rib is only capable of lateral rib deflection, and the WorldSID is only capable of measuring the lateral component of rib deflection. Furthermore, under oblique impact, friction in each dummy's linear rib deflection sensor could potentially provide resistance to rib deflection. As a result, it is possible that either dummy could have failed to detect some oblique rib loading.

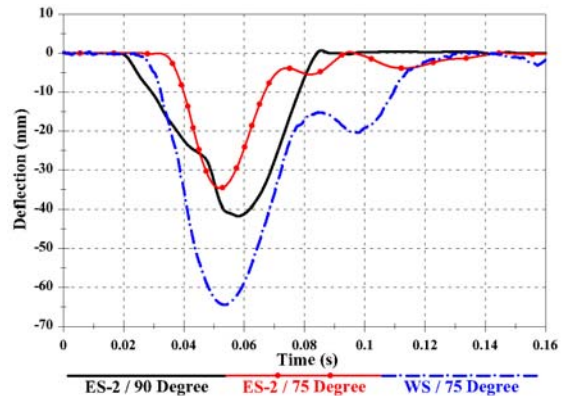


Figure 22. Upper thorax rib deflection.

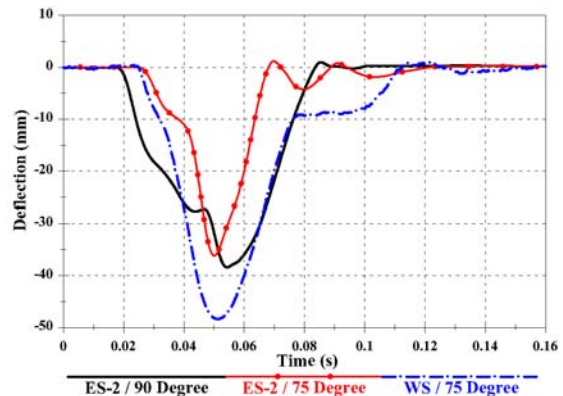


Figure 23. Middle thorax rib deflection.

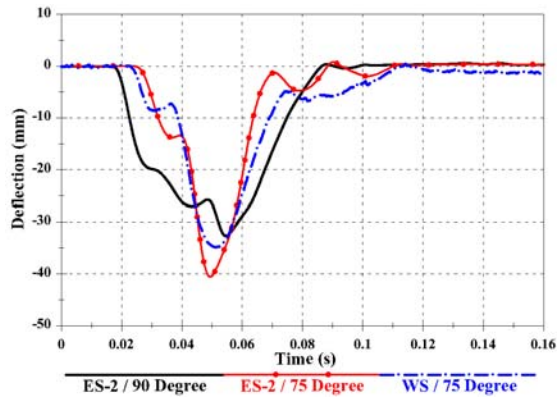


Figure 24. Lower thorax rib deflection.

Pole Sled Test Series

Table 4 includes dummy head, neck, shoulder, and upper spine results for each pole sled test. Each test was conducted with an ES-2 dummy at a 22 km/h impact speed. This impact speed was selected to achieve marginal head contact with the pole. A 40° arm angle was used for oblique impact, and a 0° (horizontal) arm angle was used for perpendicular impact. The test variables investigated were pole impact angle, head impact location, and shoulder deflection (simulated by a stepped pole). The purpose of these tests was to investigate the relative influence of each test variable on dummy head, neck, and shoulder response.

Oblique and perpendicular pole impact conditions were simulated by altering the dummy orientation relative to the seat and pole. Results show dummy impact angle (i.e. pole impact angle) to have a greater effect on shoulder load, upper neck load, and upper spine acceleration, than any other test variable. Similar to results obtained from the full scale vehicle-to-pole tests, peak longitudinal and lateral components of shoulder load and upper spine acceleration were all greatest for the oblique impact condition. Other similarities between these

results and those obtained from the full scale vehicle tests include, increased HIC 36 for oblique impact, and reversal of peak upper neck load polarities for each impact angle. In this series of tests, peak longitudinal / lateral upper neck loads were negative for oblique impact, and positive for perpendicular impact.

Head impact location was controlled by moving the head curtain airbag relative to the pole. Four head impact locations were tested. These were chosen to match ES-2 and WorldSID head-to-airbag impact locations from full scale vehicle-to-pole oblique and perpendicular impact tests. Of all the test variables investigated, head-to-airbag impact location had by far the least effect on dummy head, neck, shoulder, and upper spine results.

The ES-2 shoulder design does not allow pure lateral deflection of the shoulder relative to the upper spine. In contrast, the WorldSID shoulder is able to deflect inwards, thereby reducing the lateral distance between the point of the shoulder / pole and the side of the head. In this series of tests, pure lateral deflection of the ES-2 shoulder was simulated by conducting a pole sled test with a stepped pole fixture. This stepped pole was used to reduce the lateral distance between the pole and the head, during shoulder interaction with the pole. The simulated shoulder deflection condition (test 5) produced a substantially greater HIC 36 than any other test condition. Therefore, of the test variables investigated, shoulder rib deflection / design appears to have the greatest influence on 3 ms head acceleration and HIC 36 results. This relationship between shoulder rib deflection and 3 ms head acceleration / HIC 36 could be further substantiated by conducting similar pole sled tests using a WorldSID. This work is part of further planned research.

Table 4. Pole Sled Test Results

Test	Dummy Angle (Degrees)	Pole Step (mm)	Head / Airbag Impact Location	Right Arm Angle (Degrees)	3 ms Head Acc. (g)	HIC 36	Peak Upper Neck Load X (kN)	Peak Upper Neck Load Y (kN)	Peak Upper Spine Acc. X (g)	Peak Upper Spine Acc. Y (g)	Peak Shoulder Load X (kN)	Peak Shoulder Load Y (kN)
1	90	0	ES-2 /	0	40.2	155	0.13	0.42	17.7	-30.8	-2.00	-2.88
2	90	0	WS / 90	0	40.4	153	0.13	0.46	17.0	-29.1	-1.97	-2.77
3	75	0	WS / 75	40	43.0	218	-0.38	-0.58	-16.7	-50.3	-3.43	-3.70
4	75	0	ES-2 /	40	46.5	242	-0.44	-0.72	-16.8	-52.4	-3.92	-4.46
5	75	50	ES-2 /	40	56.9	1009	-0.52	-0.66	-18.6	-50.7	-3.86	-4.56

CONCLUSION

Under oblique vehicle-to-pole lateral impact test conditions using the same vehicle model, ES-2 and WorldSID dummies predicted very different levels of head injury protection provided by a head protecting curtain airbag. The test data suggest that these differences are a result of the design and mechanical response of the shoulders of the ES-2 and WorldSID dummies.

Perpendicular and oblique vehicle-to-pole lateral impact tests using ES-2 show a significant difference in shoulder behaviour between these test conditions. Dummy to pole sled tests confirmed the influence of ES-2 shoulder behaviour on head kinematics and consequently on the ability of this dummy to discriminate the level of head protection offered by head protecting side airbags. The head, neck, and shoulder kinematics and peak shoulder loads of the ES-2 were found to be highly sensitive to the direction of loading to the shoulder resulting from each pole impact angle.

These results suggest that ES-2 may not be an appropriate test tool for evaluation of side impact head protection systems in vehicle-to-pole lateral impact tests.

REFERENCES

- [1] European New Car Assessment Programme (EuroNCAP) Pole Side Impact Testing Protocol (Version 4.1), EuroNCAP (www.euroncap.com), March, 2004.
- [2] SAE J211-1, SAE International, December, 2003.

ACKNOWLEDGEMENTS

The authors gratefully acknowledge the contribution of the Australasian New Car Assessment Program (ANCAP) in making available the results of a perpendicular vehicle-to-pole test with an ES-2 dummy.

The authors would also like to acknowledge the generosity of Transport Canada in providing the two WorldSID dummies used in this research.

A STUDY ON INVISIBLE KNEE AIRBAG CUSHION FOLDING DESIGN USING DOE (DESIGN OF EXPERIMENTAL) METHOD

Soongu Hong
Hunhee Jung
Byungryong Cho
Ikwhan Kim
Hyundai MOBIS
Korea
Paper Number 07-0274

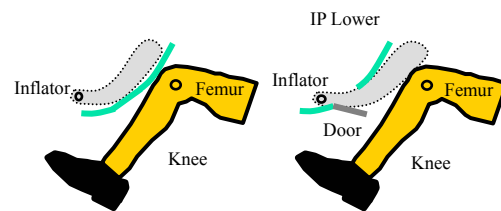
ABSTRACT

Recently, the application and development of knee airbag module into the vehicle are increasing to achieve a good rating during EuroNCAP and IIHS test. Also, EuroNCAP and IIHS press the automotive company to equip knee airbag module to improve occupant knee injury and give some benefit regarding knee airbag equipped vehicles at barrier test.⁽¹⁾ Therefore, the invisible knee airbag module has been independently developed through design, simulation, static deployment test and knee impact test. But it was very difficult to position the knee cushion in case of short space between IP lower panel and knee surface. To overcome this problem and optimize knee airbag cushion shape, DOE (Design Of Experimental) method has been applied on knee airbag cushion folding methodology and cushion inner shape using by blow test. But it was presented just knee airbag folding DOE in this paper and verification test results are presented. A good relationship between DOE result and previous study (=trial & error method) for knee airbag folding process has been found in this study.

INTRODUCTION

The majority of occupant injuries are caused by frontal crashes and the distribution of seriously injured occupants in frontal crashes is 69% in Europe. Also, in previous research, 17% of distribution lies in side crashes, 9% in rollover and 3% in rear crashes⁽²⁾. The knee is one of the more frequently injured parts of the lower limbs with femur and patella fractures that represent 34% of lower limb injuries in a UK research report.^(2,3) Mark R. Socher et al⁽⁴⁾ studied the injury pattern of knee, thigh and hip in frontal crashes and the results show that hip injuries tend be more debilitating than knee and thigh injuries. Hip injuries occurred more frequently to drivers than to passengers, to heavier and taller occupants than lighter, smaller occupants, to males than to females

and to unbelted occupants than to belted occupants. Some companies also presented papers for knee airbag development. Raj S. Roychoudhury, James K. Conlee et al⁽⁵⁾ developed a blow molded active plastic kneebolster using TPO (Thermoplastic Poly Olefin) material and Jeff Jenkins, Stephen Ridella, and Suk Jae Ham⁽⁶⁾ predicted the injury after inflatable knee bolster has been applied in offset deformable barrier crashes using MADYMO simulation. Patrick Borde⁽²⁾ predicted the occupant injury with an applied pyrotechnic knee bolster using MADYMO and Trevor Ashline and Henry Bock⁽⁷⁾ obtained good results in frontal and rear crash using an IRL Tub (aircraft) knee airbag. The world's first knee airbag is equipped in a Kia Sportage on the driver side only and the number of dual knee airbag equipped vehicles are increasing gradually in the marketplace. Generally, the knee airbag can be categorized by IKB (Inflatable Knee Bolster) type and KAB (Knee AirBag) type. The IKB type deploys the knee airbag cushion within the IP Lower (Instrument Panel Lower) and indirectly restrains the occupant's knees using the IP lower panel. The KAB restrains the occupant's knees using the knee airbag cushion directly. In addition, the KAB module can be divided by visible and invisible type. The visible type KAB has a separate airbag door and IP lower part. The invisible type KAB, such as on the driver side, is integrated with airbag door and IP lower part, and the tear seam or outline of the KAB door can not be seen.



(1) IKB (Inflatable KneeBolster) (2) KAB (Knee AirBag)

Figure 1. Comparison between IKB and KAB

type knee airbag

For example, the IKB type is equipped in the BMW 745i and Chrysler Pacifica and the KAB type is equipped in Lexus LS430, Audi A8, MY06 Chrysler PT Cruiser and MY06 Dodge Caliber (Figure.1). The invisible KAB type for driver and passenger seating positions was chosen to be developed in this study and the knee airbag module was named DKAB.

INVISIBLE KNEE AIRBAG MODULE

Driver Knee Airbag Module

The visible knee airbag on the driver side may have some appearance issues. Visible knee airbag assembly variation may lead to gap issues between the IP lower LH (Left Hand, driver side of Left Hand drive vehicle) panel and the knee airbag module.

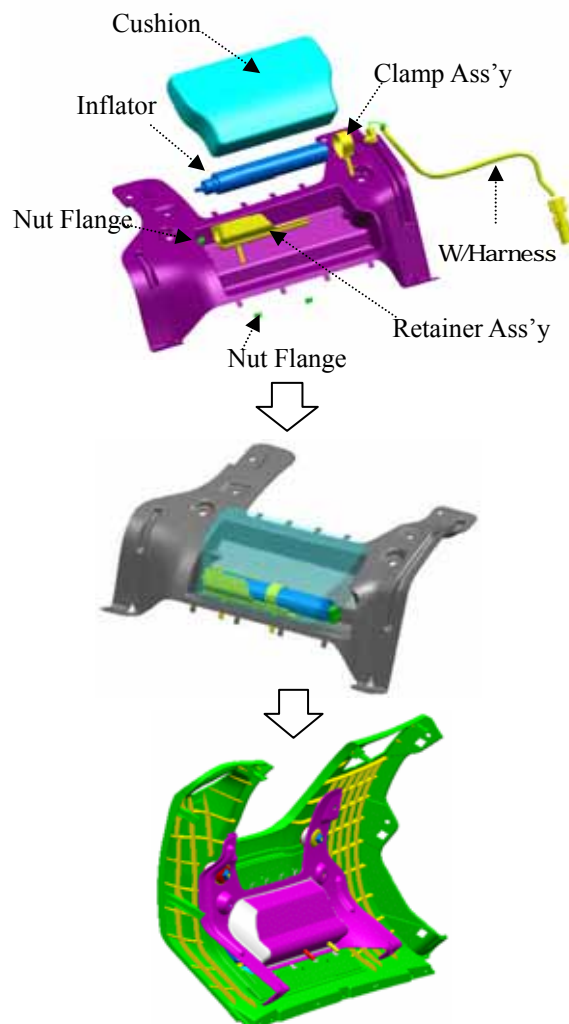


Figure 2. Assembly drawing of DKAB module

To overcome this problem and achieve wide design flexibility, an invisible type of knee airbag has been designed. Also, a knee bolster integrated housing has been designed to absorb the kinetic energy of the dummy's knees after the knee airbag cushion is

compressed (Figure.3). It shares the same mounting point as the conventional knee bolster to avoid increasing number of job processes. The IP lower LH panel has been designed to be equipped in final assembly line with the same job process. Also, it is required to provide a mounting method for the IP lower LH panel (=KAB door) which is not detached during knee airbag deployment. To accomplish this, the IP lower LH panel and KAB housing have been attached by using two screw bolts in this project as shown in Figure.4.

The knee airbag door has been designed by the same methodology as for the invisible PAB (Passenger AirBag) module. Therefore, it is required to develop a laser scoring methodology according to door size to meet deployment performance.

Passenger Knee Airbag Module

The coverage zone study of passenger knee airbag cushion is required to avoid the contact between the PAB cushion and the PKAB cushion. The PKAB cushion was harmonized with the driver side one in this study.

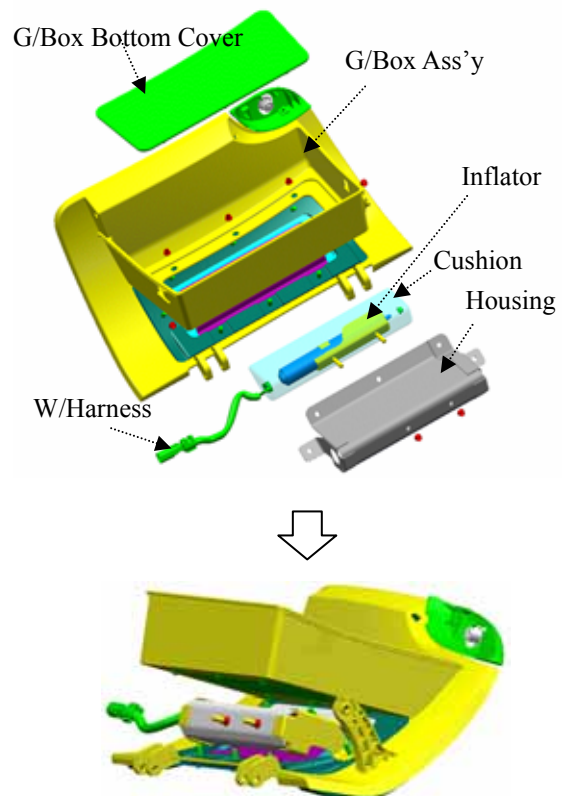


Figure 3. Assembly drawing of PKAB module

Also, the PKAB housing has been designed to be integrated into the glove box using six nuts and the glove box bottom cover has been designed to be a separate piece type in order to assemble the KAB module into the glove box easily (Figure.3) A

package study to obtain a sufficient space of glove box was not conducted in this study.

The glove box housing and PKAB door were connected by using frequency welding. The prototype sample is shown in Figure 4. The inflator, diffuser and cushion assembly were harmonized with the ones used on the driver side.



Figure 4. Proto sample of KAB module

Coverage Zone Study

A package layout study has been conducted to establish the knee airbag mounting location and the cushion coverage zones using hybrid III 5thile, 50thile and 95thile package dummies. The knee impact zone to be restrained with a knee airbag cushion has been calculated assuming that the unbelted dummy is in free flight during frontal impacts and assuming that the cushion width is established for the dummy trajectory in a 30 degree angle barrier test (Figure 5. and 6.)

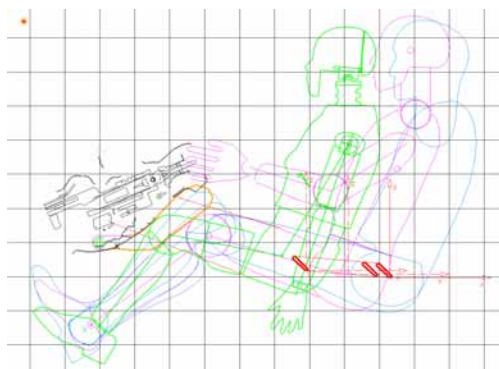


Figure 5. Coverage zone study result for the knee airbag (Side view profile)

As a result, the driver knee airbag cushion volume was found to be 17 liters and the passenger knee air bag cushion volume was found to be 19 liters.

Knee Airbag Cushion

The knee airbag cushion was made from Nylon 66, 420 Denier 49x49 weave silicon coated material. Four tethers with integral vent holes have been provided within the knee airbag cushion to control

the volume as shown Figure 7. Also a diffuser to control inflator gas flow has been provided in the knee airbag cushion.

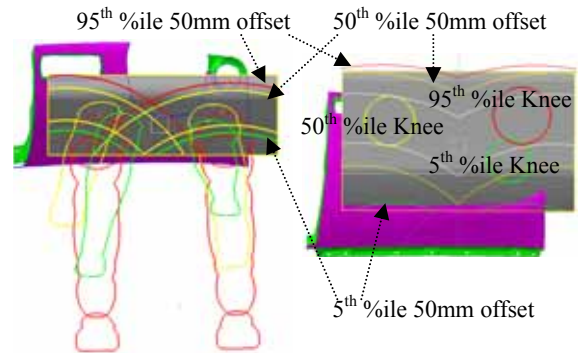


Figure 6. Coverage zone study result for knee airbag cushion (Front view profile)

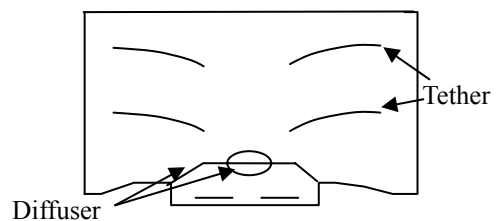


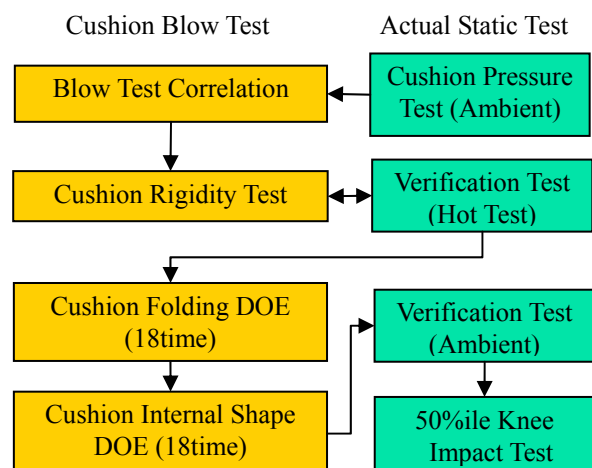
Figure 7. Knee airbag cushion drawing

INVISIBLE KAB CUSHION SHAPE DESIGN PROCESS USING DOE

As shown Table 1. , the invisible KAB cushion design process has been presented using by DOE method. The blow tests were conducted to reduce actual test number and the cushion pressure test was conducted to correlate between blow and actual test.

Table 1.

Invisible KAB shape design process using DOE



And cushion rigidity tests were conducted to evaluate cushion rigidity before the cushion DOE application. And then, cushion folding and internal shape DOE

tests were conducted using by blow test equipment. Finally, verification test and knee impact test were conducted to verify the optimized KAB cushion folding and shape using actual test.

KAB Cushion Pressure and Blow Test Correlation

A pressure tap has been attached on KAB cushion center to measure the actual and blow test cushion pressure during deployment as shown Figure 8. And the comparison result of cushion pressure has been shown at Figure 9.

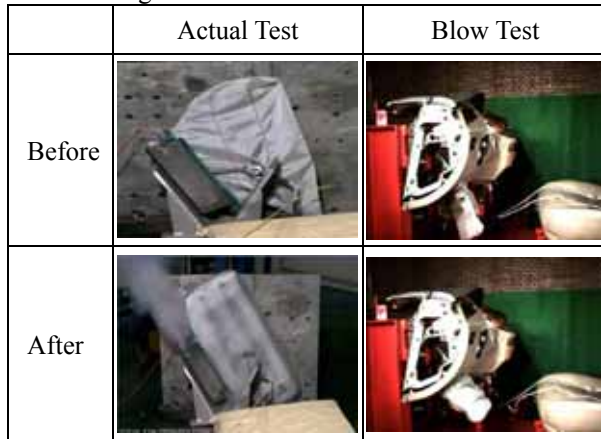


Figure 8. Comparison result of actual and blow test set up condition

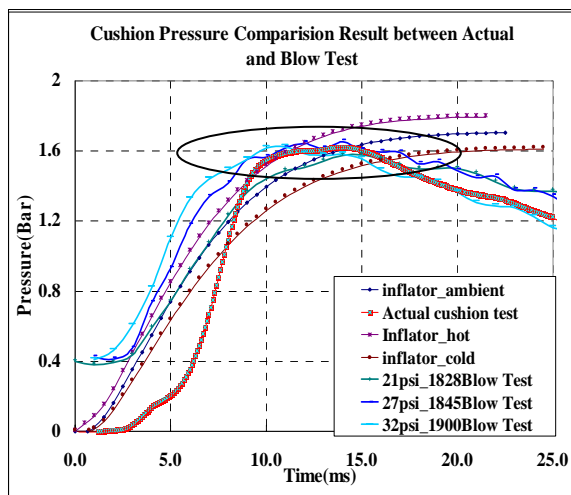


Figure 9. A cushion pressure comparison result of actual and blow test

As the comparison results, a peak cushion pressure was similar with actual one, but the initial slope has some difference. Actually, hot and cold test were reproduced using blow test, but the limitation of cushion sealing in gas exit area has been found.

Blow Test Set-Up

A Hybrid III 50th percentile dummy has been set up at the middle of lowest seating position with seat, instrument panel and KAB module. A SureFire inflation system (250V, 50Hz) of Microsys technologies which has been installed at Kolon Inc.

was used for the cushion blow test to tune the cushion shape and develop the folding methodologies as shown in Figure 10.



Figure 10. A cushion rigidity test set up condition

The initial tank pressure of SureFire inflation system was 2.3 psi [=15.8KN/m²] and internal cushion pressure of knee airbag was 1.6bar [=160KN/m²].

Cushion Rigidity Test and Results

Originally, some cushions which has been sewn tether, diffuser, vent hole and side panel were conducted using blow test, but all cushions were torn at sewn areas. Therefore, cushion rigidity test was conducted regarding to with and w/o tether and diffuser shapes as shown at Table 2. And the test result has been shown at Figure 11.

Table 2.

Cushion rigidity test matrix and result

Test No	Tether	Diffuser	Test result
1	Yes	Yes	OK
2	Yes	No	Non-OK
3	No	Yes	Non-OK
4	No	No	Non-OK

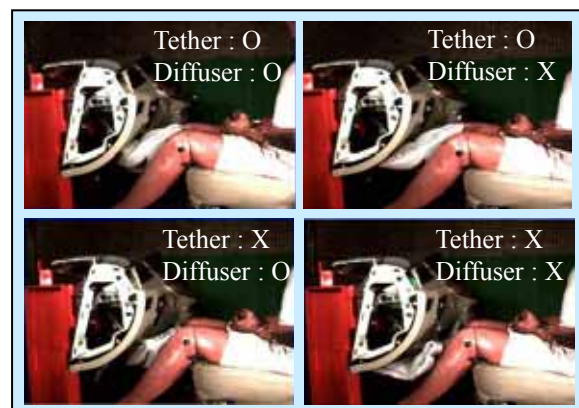


Figure 11. Cushion rigidity test results

As the results, DOE has been conducted using four tether and diffuser cushion, test number 1.

Shape and Folding Optimization Concept and Object Function

The knee airbag shape can be divided to airbag folding method and inner cushion shape. At first, KAB folding DOE has been conducted and then,

inner cushion shape DOE was performed. The TEMA software has been used to measure KAB side view contour at each 5ms or 10ms of static deployment test and blow test. And the center points of measured KAB contour area were obtained at each time and then, the trajectory has been obtained through the center point's connection. And KAB deployment slopes were obtained from regression analysis as shown at Figure 12. And it was used for the object function (=magnitude of KAB deployment slope) of KAB shape optimization. The example of real blow test has been shown at Figure 13.

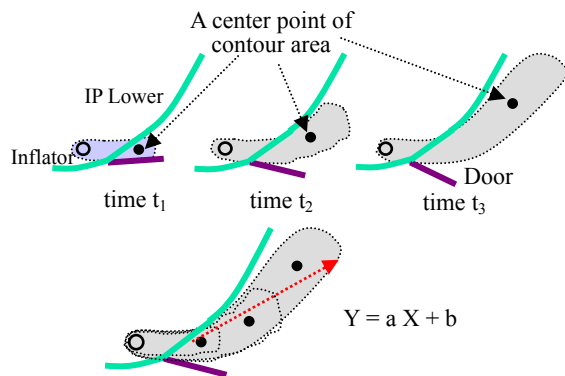


Figure 12. Shape and Folding optimization concept and object function

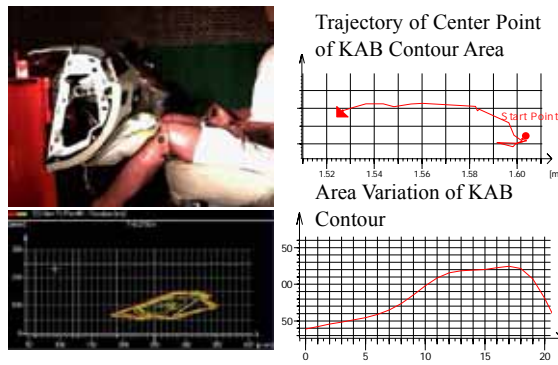


Figure 13. Example which was induced the object function from motion analysis.

DOE Application of KAB Cushion Folding

Basically, airbag folding can be divided to folding

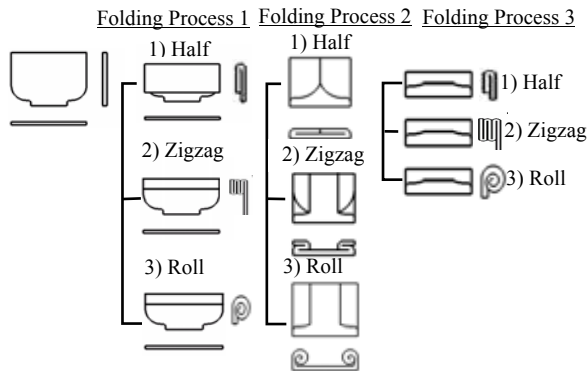


Figure 14. DOE range of KAB folding method

method and process. The airbag folding method could be divided by flattening, half, tuck, roll and accordion (=zigzag) folding. And KAB folding process has been categorized three phases in this study as shown Figure 14.

L_9 matrix of Taguchi method has been used and folding types were applied for DOE factor. And folding processes were applied for DOE level as shown at Table 3.

Table 3.
Folding DOE Matrix, Factor and Level
Level: Folding Process

	Process 1	Process 2	Process 3
Factor: Folding Type			
Half			
Roll			
Zigzag			

Taguchi Matrix: L_9

Otherwise, the distance between IP lower and knee surface was applied for the noise factor. Because KAB folding types are effect to KAB deployment shapes according to that distance. (55mm, 75mm)

DOE Results of KAB Cushion Folding

Eighteen blow tests were conducted at 75mm and 50mm gap (=distance between IP lower and knee surface) using KAB cushion which has chosen at rigidity test. The eighteen test results of trajectory of center point of KAB contour area had been shown at Figure 15.

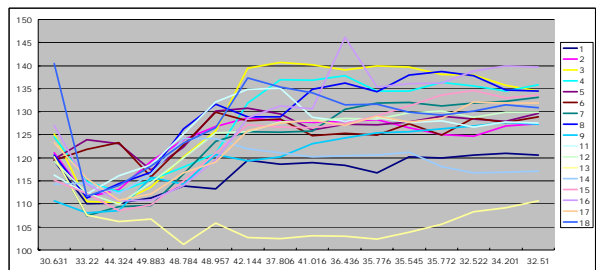


Figure 15. Trajectory results of center point of KAB contour area during deployment

The values of object function (=Deployment Slope)

Table 4.

KAB Folding DOE Result of Blow Test (Slope)

Level: Folding Process →

	P 1	P 2	P 3	N1=75mm	N2=55mm
Factor: Folding Type ←					
1	Half	Half	Half	0.6038	0.7033
2	Half	Roll	Roll	1.7592	1.5722
3	Half	Zigzag	Zigzag	0.5499	0.5196
4	Roll	Half	Roll	1.6476	1.6047
5	Roll	Roll	Zigzag	1.3558	Data Loss
6	Roll	Zigzag	Half	0.8068	1.215
7	Zigzag	Half	Zigzag	-0.155	0.1389
8	Zigzag	Roll	Half	1.7698	1.9863
9	Zigzag	Zigzag	Roll	1.2546	0.653

N1, N2: distance between IP lower and knee surface
P1, 2, 3: Folding Process 1, 2, 3

are obtained from regression analysis of trajectory results as shown at Figure 15. and applied the weighting factor to consider KAB top view shapes, Good → +1, OK → 0, Bad → -1 and the values of object function are summarized at table 4., 5. and Figure 16. The Data loss was assumed to 1.3 as shown at Table 4. The compensated slope has been summarized at Table 6.

Table 5.
KAB Folding DOE Result _Top View Shape

Level: Folding Process →

Factor: Folding Type ↓	Level: Folding Process →			N1=75mm	N1=55mm
	P 1	P 2	P 3		
1	Half	Half	Half	OK	OK
2	Half	Roll	Roll	Good	Good
3	Half	Zigzag	Zigzag	OK	Good
4	Roll	Half	Roll	Bad	Bad
5	Roll	Roll	Zigzag	Good	Bad
6	Roll	Zigzag	Half	Good	OK
7	Zigzag	Half	Zigzag	OK	Bad
8	Zigzag	Roll	Half	Bad	Bad
9	Zigzag	Zigzag	Roll	Bad	Good

N1, 2: distance between IP lower and knee surface
P1, 2, 3: Folding Process 1, 2, 3

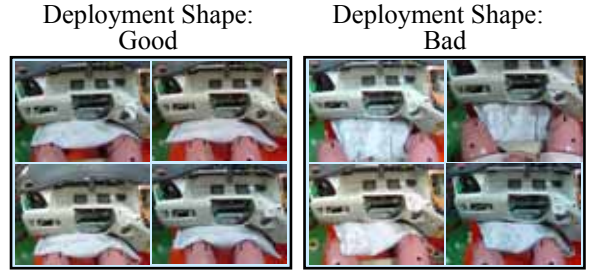


Figure 16. KAB Blow Test Results of Deployment Shape _Top View

Table 6.
KAB Folding DOE Result _Compensated

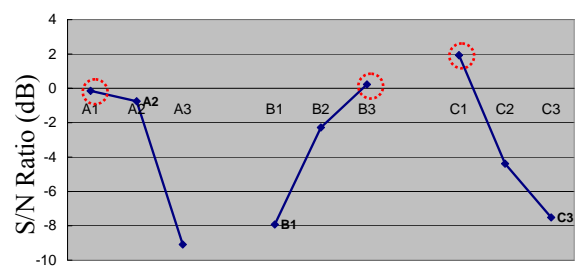
Level: Folding Process →

Factor: Folding Type ↓	Level: Folding Process →			N1=75mm	N2=55mm
	P 1	P 2	P 3		
1	Half	Half	Half	0.6038	1.733
2	Half	Roll	Roll	1.7592	0.5722
3	Half	Zigzag	Zigzag	1.5499	1.5196
4	Roll	Half	Roll	1.6476	0.6047
5	Roll	Roll	Zigzag	0.3558	1.3
6	Roll	Zigzag	Half	1.8068	2.215
7	Zigzag	Half	Zigzag	0.1	0.1
8	Zigzag	Roll	Half	1.7698	0.9863
9	Zigzag	Zigzag	Roll	0.2546	1.653

N1, N2: distance between IP lower and knee surface
P1, 2, 3: Folding Process 1, 2, 3

S/N ratio of KAB folding DOE had been calculated and the main effect plot has been shown at Figure 16. As the result, it was found that the third folding process was largely effect on KAB deployment shape. And it was found that the best level of KAB folding process compose of P1 → half, P2 → zigzag (=accordion), P3 → half folding. The best level has been indicated to

a red dot line at Figure 17.



A, B, C: Folding Process, A P1, B P2, C P3
1, 2, 3: Folding Type, 1: Half, 2: Roll, 3: Zigzag

Figure 17. Main Effect Analysis of KAB Folding

VERIFICATION

The static deployment tests of DKAB and PKAB module were conducted to verify the best level of DOE result. It was found to be a good deployment without any jamming between knees as shown at Figure 18. But it was found to be torn the tether at cushion inner. Otherwise, the gain between actual and blow test has not been calculated, because the actual test could not be set up with the same camera viewing and zooming of blow test.

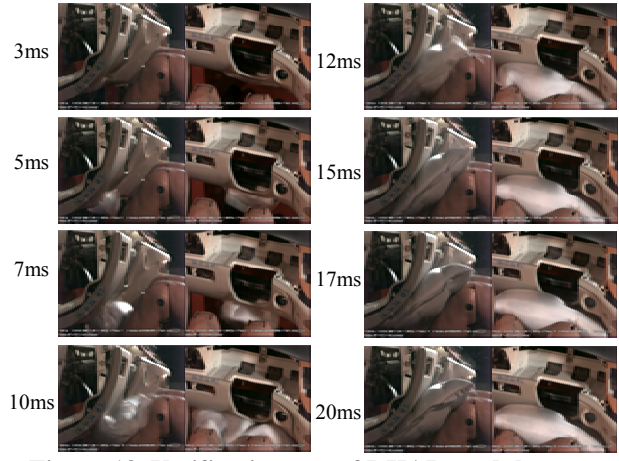


Figure 18. Verification test of DKAB module

In previous study (13), KAB folding process has been developed using trial and error method as shown at Figure 19. And DOE result of KAB folding process has been compared with the one.

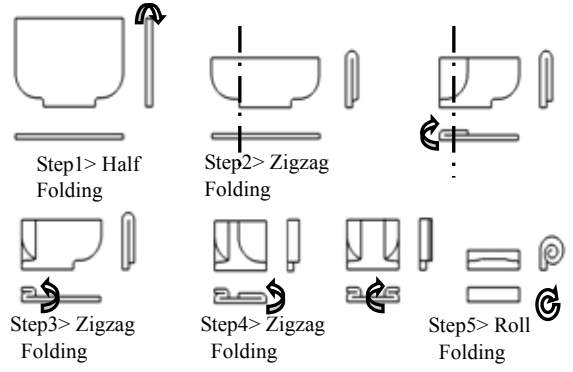


Figure 19. Folding process of KAB cushion

As the results, it was found to be same process with the one except folding process 3 and the result was summarized at Figure 20.

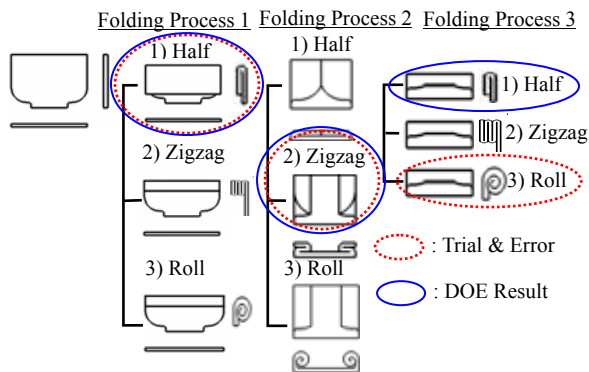


Figure 20. Comparison result between DOE result and previous study

CONCLUSION

The invisible knee airbag module has been developed independently and evaluated through design, simulation and test. Generally, airbag folding process has been developed using by trail & error method in the past. But, the knee airbag folding methodology has been developed using by DOE technique in this paper and conclusion remarks are as follows:

1. It was found the DOE application result for knee airbag folding process was same with the ones in previous approach (trial & error method) except third folding process. And it was found the final folding process (third folding process) was a main effect.
2. It could be used widely the DOE technique on shape study and folding process development of other airbag (DAB, PAB, SAB, etc) using proposed optimization concept in this paper.
3. It will be conducted the further study for knee airbag inner shape design using DOE technique continuously.

REFERENCE

- [1] "Sled Test Procedure for assessing Knee Impact Area", European New Car Assessment Program Version 1.0a, 2004
- [2] Patrick Borde, "Pyrotechnic Kneebolster Development and Its Contribution to Car Drivers Safety", SAE2001-01-1049.
- [3] Lisa Shoaf Ore and C. Brian Tanner et al, "Accident Investigation and Impairment Study of Lower Extremity Injury", SAE930096.
- [4] Mark R. Sochor, Daniel D Faust and Stewart C. Wang et al, "Knee, Thigh and Hip Injury Patterns for Drivers and Right Front Passengers in Frontal

Impacts", SAE2003-01-0164.

[5] Raj S. Roychoudhury, James K. Conlee et al, "Blow-Molded Plastic Active Knee Bolster", SAE2004-01-0844.

[6] Jeff Jenkins, Stephen Ridella and Suk Jae Ham, "Development of an Inflatable Kneebolster by using MADYMO and DOE", 9th International MADYMO Users Conference, 2002.

[7] Trevor Ashline and Henry Bock, "Investigating the Effects of Anchor Pretensioners, Kneebolster Airbag and Seat Belt Changes In an IRL Tub", SAE 2004-01-3563.

[8] James K. Conlee, "Passenger Side Airbag System for Open Interior Architecture", SAE970721.

[9] Donald F. Huelke, "Anatomy of the Lower Extremity-An Overview", SAE861921.

[10] Posz & Bethards, "Knee Protection Airbag Device", Patent No : 20040164527a1.

[11] MADYMO User's Manual ver.6.1, TNO, 2003.

[12] S.G.Hong et al, "Design Considerations of Invisible Knee Airbag Module Development", 6th Korea MADYMO Users Conference, 2005

[13] S.G.Hong et al, "Invisible Knee Airbag Module Development", SAE2007-01-0347

DEFINITIONS, ACRONYMS,

ABBREVIATIONS

Euro NCAP : Europe New Car Assessment Program

IIHS : Insurance Institute for Highway Safety

MADYMO : MATHmatical DYnamic MODelling

DAB : Driver AirBag

PAB : Passenger AirBag

DKAB : Driver Knee AirBag

PKAB : Passenger Knee AirBag

SAB : Side AirBag

DEVELOPMENT AND EVALUATION OF THE SIDE IMPACT TEST PROCEDURE PROPOSED BY IHRA

Ton Versmissen, Margriet van Schijndel

TNO Integrated Safety

The Netherlands

Mervyn Edwards

TRL

United Kingdom

Tobias Langner

BASf

Germany

On behalf of APROSYS SP1.1 consortium

Paper Number 07-0310

ABSTRACT

At the 2005 ESV conference, the International Harmonisation of Research Activities (IHRA) side impact working group proposed a 4 part draft test procedure, to form the basis of harmonisation of regulation world-wide and to help advances in car occupant protection. This paper presents the work performed by a European Commission 6th framework project, called APROSYS, on further development and evaluation of the proposed procedure from a European perspective.

The 4 parts of the proposed procedure are:

- A Mobile Deformable Barrier test.
- An oblique Pole side impact test
- Interior headform tests
- Side Out of Position (OOP) tests

Full scale test and modelling work to develop the Advanced European Mobile Deformable Barrier (AE-MDB) further is described, resulting in a recommendation to revise the barrier face to include a bumper beam element.

An evaluation of oblique and perpendicular pole tests was made from tests and numerical simulations using ES-2 and WorldSID 50th percentile dummies. It was concluded that an oblique pole test is feasible but that a perpendicular test would be preferable for Europe. The interior headform test protocol was evaluated to assess its repeatability and reproducibility and to solve issues such as the head impact angle and limitation zones. Recommendations for updates to the test protocol are made.

Out-of-position (OOP) tests applicable for the European situation were performed, which included additional tests with Child Restraint Systems (CRS) which use is mandatory in Europe. It was concluded that the proposed IHRA OOP tests do cover the worst case situations, but the current test protocol is not ready for regulatory use.

INTRODUCTION

In Europe, the order of 10,000 car occupants die in side impact crashes annually. At the 2005 ESV conference, the International Harmonisation of Research Activities (IHRA) side impact working group proposed a 4 part draft test procedure, to form the basis of harmonisation of regulation world-wide and to help advances in car occupant protection [11]. The European 6th Framework Programme Integrated Project (IP) on Advanced Protection Systems (APROSYS) focuses on developments in the field of passive and adaptive vehicle safety. The aim of Sub-Project 1 (SP1), titled 'Car Accidents', is to reduce the number of car occupant fatalities and serious injuries in Europe through the development of test and evaluation procedures that once implemented in regulation and / or consumer testing will improve car crashworthiness in side and frontal impacts.

Four tasks in SP1.1 evaluate the draft side impact test procedure proposed by IHRA. The tasks and associated type of tests investigated are:

1. Advanced protection in multi-vehicle lateral crashes – Mobile Deformable Barrier test
2. Protection in single vehicle crashes involving narrow objects – Oblique Pole test
3. Interior head protection in lateral impact - Interior headform test proposed by EEVC WG13
4. Occupant injury risk from deploying (side) airbags – Out of Position (OOP) tests

This paper details the research performed in these tasks, during the first 36 month period of the programme.

AE-MDB DEVELOPMENTS

Objectives

This section details the research of task ‘Advanced protection in multi-vehicle lateral crashes’.

To represent better the world-wide car fleet IHRA proposed two tests with different Mobile Deformable Barriers (MDB):

- An MDB to represent Light Trucks and Vans (LTVs) type vehicles in the USA developed by the Insurance Institute for Highway Safety (IIHS) referred to as the IIHS-MDB [2].
- An MDB to represent the European passenger car fleet referred to as the Advanced European MDB (AE-MDB) developed by the European Enhanced Vehicle safety Committee (EEVC) side impact working group (WG13) [3].

Based on the strategy that APROSYS should focus on European problems the objectives of this task were:

- Complete the development of the AE-MDB.
- Perform an initial evaluation of the test procedure with the AE-MDB from the European perspective.

Background Information

History - The development of the new EU-barrier was started by EEVC WG13 in 2001 in support of European Governmental contributions to IHRA. The new barrier was called Advanced European Mobile Deformable barrier (AE-MDB) to differentiate it from the Regulation 95 barrier. The first test results using the AE-MDB were presented at the ESV 2003 [4]

The AE-MDB V2 specification, as defined by EEVC WG13, was presented at the 2005 ESV conference [4].

However, various members of WG13 identified major concerns with AE-MDB V2. The main concern was that in tests with this barrier face the resulting vehicle deformation (low b-pillar deformation / high door intrusions) did not compare well with that seen in baseline car to car tests. To resolve this concern, further barrier development was required which was performed in APROSYS.

AE-MDB geometry - The plan view of the new AE-MDB face design was derived taking into account two main considerations and objectives:

- The AE-MDB should reproduce, in a purely perpendicular impact with a stationary target vehicle, the loading pattern to front and rear occupants seen in a moving-car-to-moving-car side impact configuration.

- The AE-MDB face should not allow simultaneous loading of the A and C pillars, which could prevent realistic loading of the passenger compartment.

Based on this, and analysis of the dimensions of modern vehicles, the AE-MDB face (see Figure 1) was designed. It has a front face which is 1100mm wide and an overall width of 1700mm and a centre section of 500mm wide (corresponding to the width of the standard load cell wall) with edges chamfered at 45°.

Figure 1. AE-MDB dimensions.

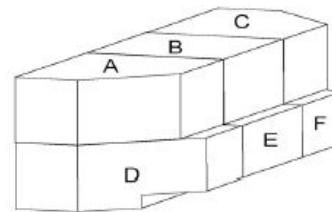
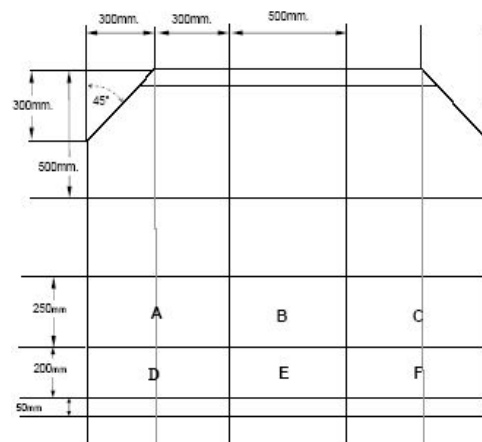


Figure 1 Isometric view of AE-MDB



AE-MDB V3 specifications – As mentioned previously, the resulting vehicle deformation in tests with the AE-MDB V2 did not compare well with that seen in baseline car to car tests. The reason for this was found to be that the AE-MDB V2 barrier block to block stiffness distribution did not adequately represent the frontal stiffness distribution of a car. The block stiffnesses for AE-MDB V2 were determined by WG13 from car crash tests into a rigid Load Cell Wall (LCW). The following remarks were made about the rigid LCW results of WG13:

- Concern was raised that the rigid LCW test may not show the effect of stiff lateral connections, such as bumper crossbeams, because they may not be strained in this test. This could result in the

specification of a barrier face with an unrepresentative weak middle block (E).

- Offset deformable tests and compatibility appear to direct vehicle design toward stronger lateral connections between energy absorbing structures.

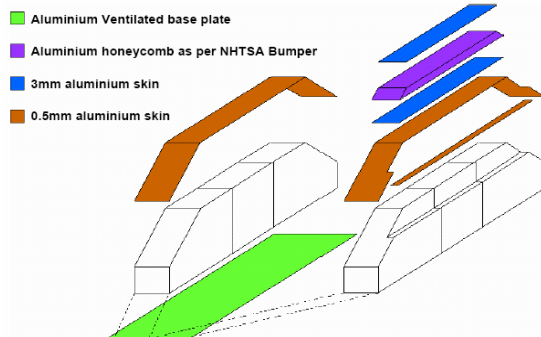
In light of the available test and simulation results the members of EEVC WG13 discussed a series of modifications to the barrier face. It was decided by APROSYS to evaluate the following two barrier versions, both of which have a bumper beam element in contrast to the V2 face which does not.

Version 3.1 A barrier with block stiffness identical to the V2 barrier but with a bumper beam element to spread the load in lateral direction. The original depth of the lower row of blocks was reduced by 60 mm and replaced by the bumper beam element. The depth reduction was realised by removing the soft front of the blocks to obtain a stable connection of the beam element.

Version 3.9 A barrier with a reduced stiffness of the lower blocks. The two outer blocks have a design stiffness of 55% of the original V2 outer blocks and the middle block a design stiffness of 60% of the V2 outer blocks. The bumper element was identical to the V3.1 element.

Figure 2 shows the bumper element design, used on V3.1 and V3.9, which was based on the FMVSS-214 specifications.

Figure 2. AE-MDB bumper beam specifications



Test and simulation activities

Full-Scale Test Program

An extensive test program (see Table 1) with LCW barrier calibration tests, AE-MDB V3.1 and V3.9 to car tests and car to car tests was used to evaluate the AE-MDB V3 barriers. The main aim of the test program was to determine which barrier version best represented the baseline car to car tests. The Fiesta

and Golf barrier tests were performed to provide a comparison between the two versions of barrier and the baseline tests. For all car to car and AE-MDB tests within the program the ES-2 dummy was positioned on the struck side in both the driver and rear seat passenger seating positions. The configuration of the AE-MDB test is presented in Figure 3 and the car to car in Figure 4.

Figure 3. AE-MDB test set-up, trolley mass 1500 kg.

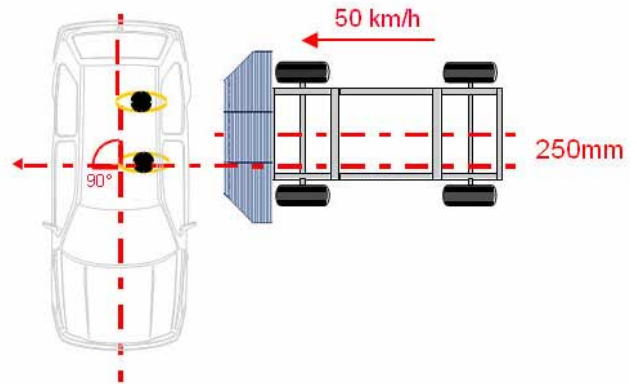


Figure 4. Car to car test set-up.

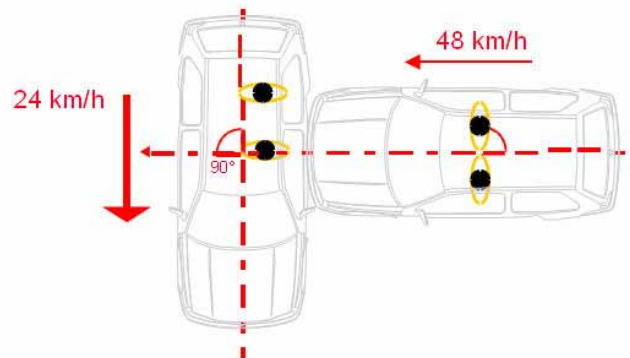


Table 1.

**AE-MDB evaluation test matrix
“Green” APROSYS / “Blue” additional tests**

Target Cars	Bullet cars/barriers			
	V3.1	V3.9	Baseline tests	
			Golf	Frelander
LCW calibration				
Ford Fiesta				
VW Golf				
Toyota Prius	*	*		
Volvo S80				
Robustness – sill				
Robustness - pole				

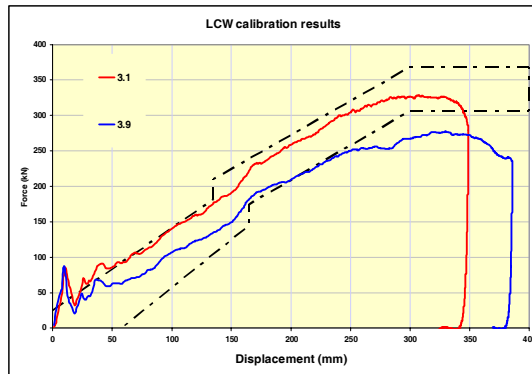
* performed without firing ANY airbag

For a barrier to be accepted into future regulation the design must be robust and repeatable. At the 1998 ESV, WG13 presented a series of test methods to assess the performance and integrity of side impact barrier faces[6]. Two of the tests proposed by WG13

were performed with both versions of the barrier. The rigid sill loading test and the offset pole test were chosen as they are considered to be the most discriminating of the tests.

LCW test results - The aim of these tests was to compare the force deflection characteristics of the V3 barriers with the V2 design corridors. The results (see Figure 5) show that both barriers are within the AE-MDB V2 design corridors for the first 200 mm of barrier deformation. For deformations larger than 200 mm the force of V3.9 is below the V2 design corridor. However, it should be noted that in all AE-MDB V3.9 tests the average maximum crush of the barrier was less than 200mm and the maximum dummy injury values were reached prior to maximum barrier deformation.

Figure 5. LCW test results AE-MDB 3.1 and 3.9 Total barrier force



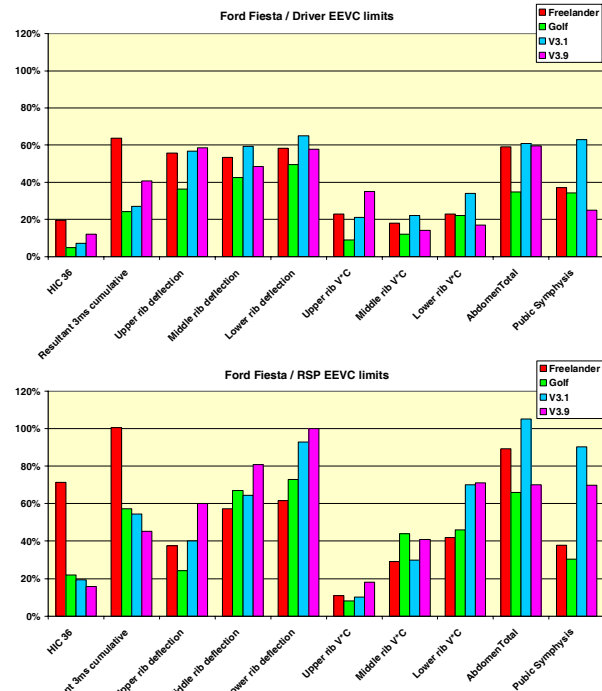
Car to car and AE-MDB test results - The dummy responses of AE-MDB and car to car tests for each dummy are shown in Figure 6 to Figure 9. The results have been expressed as a percentage of the EEVC critical limits where possible. The limits used are described in Table 2.

Table 2. EEVC critical limits ES-2 dummy

Dummy results		EEVC limit
HIC 36		1000
Resultant 3ms cumulative	g	88
Rib deflection	mm	42
Rib V°C	m/s	1
Abdomen Total	kN	2.5
Pubic Symphysis	kN	6

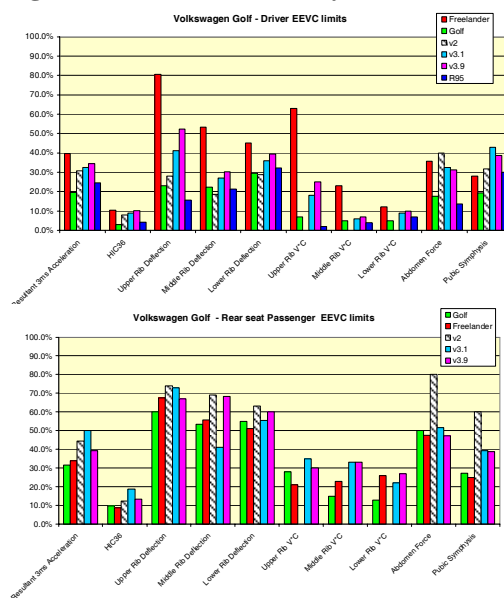
The responses from the Fiesta tests are shown in Figure 6. Examining the driver results shows that the EEVC limits were not exceeded in any test. Results of the Freelander tests were generally similar to those of both barrier impacts; in most cases the Golf test provided the lowest response. Comparison of the barrier test results indicates a difference of no more than 17% for all of the dummy body regions apart from the pubic symphysis force, where there was a difference of 38%.

Figure 6. Ford Fiesta dummy results – driver (top) and rear seated passenger (bottom).



The responses from the Golf tests are shown in Figure 7. None of the driver results exceeded the EEVC limit. Additional results from an AE-MDB V2 test and a EuroNCAP test using the ECE Regulation 95 (R95) barrier have been included. The largest difference between the V3.1 and V3.9 results was only 11%. Both graphs show that the driver and passenger dummy results for the V3.1 and V3.9 are generally more in line with the baseline tests than the results from the V2. For the rear seated passenger, all

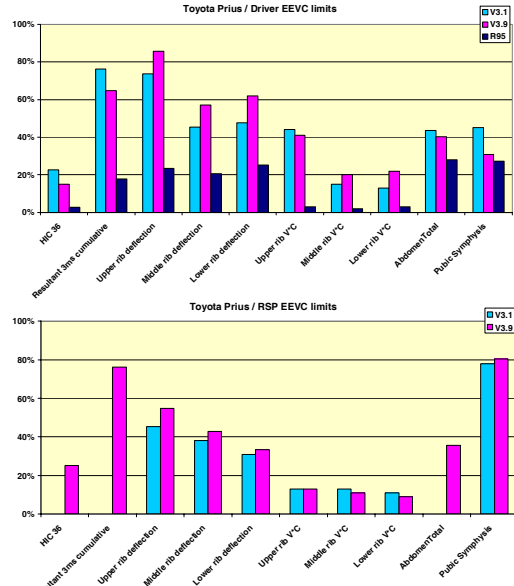
Figure 7. VW Golf V dummy results



results show very similar trends.

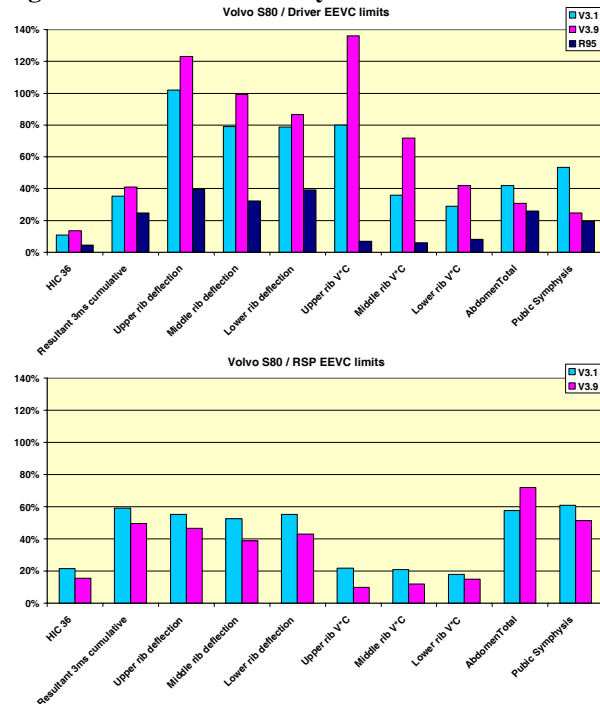
Figure 8 shows the Prius results. No baseline test is available for Prius, therefore R95 results are presented in Figure 8 only as reference. Indeed the homologation results were obtained with side and curtain shield airbags, whereas no airbag was fired in AE-MDB tests. None of the results exceeded the EEVC limits.

Figure 8. Toyota Prius dummy results



The responses from the S80 tests are shown in Figure 9. No baseline test data was available so only the V3.1, V3.9 and R95 barriers can be compared.

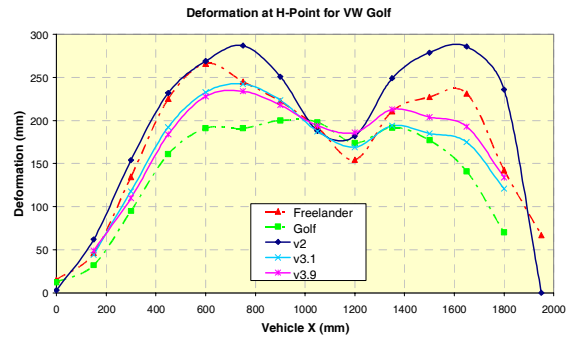
Figure 9. Volvo S80 dummy results.



For the driver, three of the EEVC limits were exceeded.

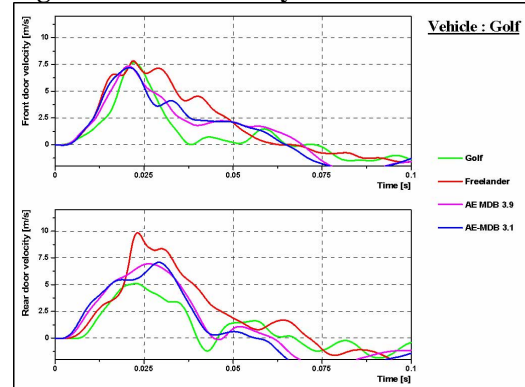
The V3.9 barrier was generally more severe than the V3.1 with the largest difference being 56% of the limit. For the rear seat passenger there were no significant differences between the barriers. Before and after each test the profile of each target vehicle was measured to highlight the post test deformation profile left by each bullet. The deformation profiles of the Golf are typical of the vehicles tested. Further information can be found in the APROSYS deliverable [3]. The horizontal profiles for the Golf were taken at three levels, the door line, H-point height and rocker flange height. At the H-point height, see Figure 10, a similar trend as described for the Fiesta, can be seen.

Figure 10. Deformation at H-point level - VW Golf



For each impact the velocity of the driver and passenger door intrusion was measured from the inner door skin. The transducers were placed as close as possible to the dummies to gain the best indication of the loading received. The plots for the Golf are provided in Figure 10. All other results are available in the APROSYS deliverable [3]. For the driver the Golf, V3.1 and V3.9 had similar peak values which were almost 4m/s below that of the Frelander. For the rear door the difference was much less, but the velocities were higher than those of the front door.

Figure 11. Door velocity VW Golf



There was very little difference in the associated door velocities of all tests using the two barriers, all of the data recorded in the program suggests both barriers induce similar door velocities.

Robustness test results – Both barriers V3.1 and V3.9 showed stability problems in the sill robustness tests, failing in bending and shear as shown in Figure 12.

Figure 12. Barrier failure in sill robustness test



Investigations are ongoing to improve the barriers on this subject. Also the severity of the sill test is under discussion as the vertical forces are likely to be significantly higher than in a full scale test where the barrier would override the vehicle sill. No barrier robustness problems were observed during the full scale tests.

The performances of V3.9 and v3.1 were very similar in the offset pole test. In both tests the side of the barrier came detached from the ventilation frame but no major stability problems were seen.

Simulation Program

Based on the slightly better results of the V3.9 barrier it was decided that further development of the AE-MDB design should be continued based on the V3.9 barrier. The main issues of the modelling program were:

Barrier stiffness The V3.9 barrier was not designed to meet the EEVC WG13 defined global force corridors but it was a requirement of the partners during the project. The LCW test showed that the current barrier is below this corridor after a displacement of about 200 mm.

Bumper beam element In the rigid sill robustness test the bumper beam element detaches from the main body of the barrier and rotates in the first 6 ms of the impact, indicating a possible stability problem. The current bumper beam specification is based on the FMVSS-214 barrier beam element geometry and stiffness. As a result of this it is 200 mm high.

Modelling runs were performed to investigate the following changes to the V3.9 barrier:

- Stiffness

- Modifying the stiffness of the barrier blocks so that it met the WG13 defined global force deflection corridors.
- Bumper beam element stability
 - Splitting it into two sections along its length
 - Reducing its height from 200 mm to 100 mm

The results of the simulations showed:

Changing the barrier stiffness profile to enable it to comply with the EEVC WG13 global stiffness corridors made no / little difference to the performance of the ES-2 dummy or car. This was because the barrier did not deform as far back as the point where the stiffness changes were made when impacting the car, thus the stiffness changes were effectively not seen.

For the bumper beam refinements, the simulations showed a small reduction in the dummy pelvic injury criterion and a small difference in the car deformation at the lower levels.

Conclusions

- Both V3 barriers give more comparable dummy injury values and final deformation measures to the baseline Golf and Freelander tests than the V2 barrier does. Note both V3 barriers have a bumper beam element whereas the V2 does not.
- The dummy injury values for both V3 barriers are higher than for the regulation R95 barrier
- The differences in the cars' performances for the V3.1 and V3.9 barrier tests were slight for the dummy injury values, door velocities and deformations. However, the driver dummy pubic symphysis values for the V3.9 barrier compared better to the baseline test values than the V3.1 barrier.
- In the sill robustness tests both V3.1 and V3.9 barrier failed in shear / bending showing barrier stability problems. In the pole robustness tests no stability problems were seen with V3.1 or V3.9.
- Refining the AE-MDB V3.9 stiffness profile to enable it to comply with the EEVC WG13 global stiffness corridors made no / little difference to the performance of the ES-2 dummy or car. This was because the barrier did not deform as far back as the point where the stiffness changes were made when impacting the car, thus the stiffness changes were effectively not seen. For the bumper beam refinements, the simulations show a small reduction in the dummy pelvic injury criterion and a small difference in the car deformation at the lower levels.

CAR TO POLE

Objectives

The evaluation of the IHRA car to pole test protocol was carried out using full scale tests and numerical simulations. The main objectives of the full scale test program were:

- To carry out an assessment of practicality and repeatability of the car to pole test proposed by IHRA, which is based on NPRM-214 [7]
- To check the feasibility of using the ES-2 dummy or the WorldSID dummy in the proposed test procedure.
- To investigate the effect of impact location variation.

Main objective of the simulation study was:

- To investigate the influence of test parameters such as impact angle, velocity, pole impact position and diameter on the injury levels for several body regions.

Work Programme

Within APROSYS four car to pole full scale tests were carried out. To broaden the protocol assessment, results from four other tests performed outside APROSYS were also used. The complete test matrix is presented in Table 3.

Table 3.
Car to pole (above) and car to car test matrix including input test parameters

Subaru Legacy	Test S1	Test S2	Test S3	Test S4
• angle/speed	75° / 32 km/h	90° / 32 km/h	75° / 32 km/h	90° / 29 km/h
• impact location	NPRM-214	Euro NCAP	NPRM-214	Euro NCAP
• dummy	WorldSID 50%	WorldSID 50%	ES-2	ES-2
• project	APROSYS	APROSYS	-	-
Toyota Avensis	Test T1	Test T2	Test T3	Test T4
• angle/speed	75° / 32 km/h	75° / 32 km/h	75° / 32 km/h	90° / 29 km/h
• impact location	NPRM-214	NPRM 214	Euro NCAP	Euro NCAP
• dummy	ES-2	ES-2	ES-2	ES-2
• project	APROSYS	APROSYS/DOTARS	APROSYS	Euro NCAP

Subaru Legacy	Test S1	Test S2	Test S3	Test S4
• Test ID	045106JI	03GQ	PB3TRZP	E4B2RZP
• Laboratory	IDIADA	TRL	Subaru	Subaru
• Dummy	WorldSID	WorldSID	ES-2	ES-2
• Test mass	1725 kg	1730 kg	1789 kg	1681 kg
• Test angle	75°	90°	75°	90°
• Test velocity	31.8 km/h	31.7 km/h	31.5 km/h	29.0 km/h
• Impact accuracy	4 mm fore	8 mm aft	2 mm/°	6 mm/°
Toyota Avensis	Test T1	Test T2	Test T3	Test T4
• Test ID	FD44703	FD51701	14497	04NQ
• Laboratory	TNO	TNO	Fiat	TRL
• Dummy	ES-2	ES-2	ES-2	ES-2
• Test mass	1500 kg	1505 kg	1501 kg	1506 kg
• Test angle	75°	75°	75°	90°
• Test velocity	32.4 km/h	31.9 km/h	32.5 km/h	29 km/h
• Impact accuracy	4 mm fore	7 mm fore	7 mm fore	14 mm aft

The influence of test parameters such as impact angle, velocity, pole impact position and pole diameter on the injury levels for head and other body regions was investigated. APROSYS performed simulations using a Generic Car FE Model of a mid-sized vehicle developed by another APROSYS sub-project. This model was equipped with thorax and curtain airbags. In addition to the APROSYS work

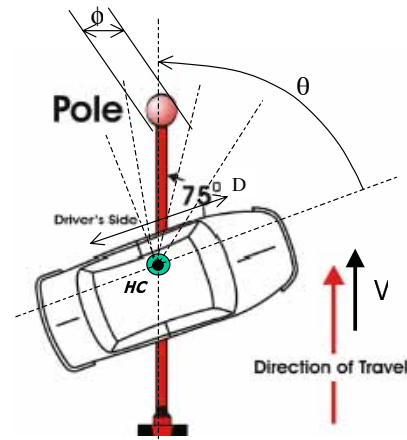
similar simulations were carried out by Subaru, using a FE model of the Legacy.

The specifications for the APROSYS numerical study are presented in Table 4 and Figure 13.

Table 4.
Specifications APROSYS / SUBARU numerical study

Parameter	
Vehicle model	▪ ‘Generic’ model of a 4-doors passenger car ▪ Subaru Legacy
Impact angles θ [°]	90 (FMVSS-201) / 82.5 / 75 (NPRM-214)
Test velocities V [km/h]	29 (FMVSS-201) / 32 (NPRM-214) / 36
Impact point	-100, 0 and 100 mm shifted from specified, along vehicle for-aft axis
Pole diameters Φ [mm]	254 (NPRM-214) / 350 (ISO)
Dummy	ES-2 model

Figure 13. NPRM 214 test set up, including parameters numerical studies

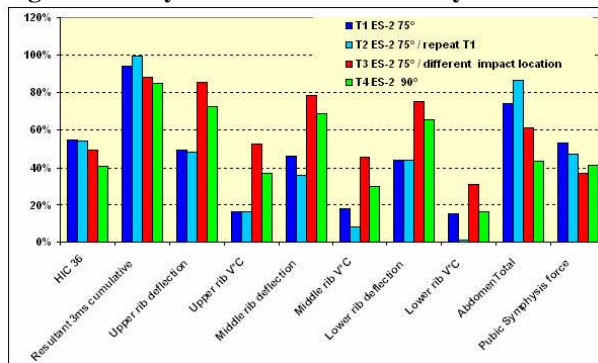


Results

The main dummy results of the full scale tests with the Toyota Avensis are shown in Figure 14. Unfortunately, the high speed video recordings of the four Legacy tests show such large differences in airbag timing and airbag behaviour that they could not be used to compare the test methods. The dummy injury values are expressed relative to the ECE R95 limits for the ES2 dummy, see Table 2. The following observations were made:

- The repeatability of the test with the ES-2 dummy was good (compare T1 with T2). The changes in dummy injury criteria values did not exceed 15% of the performance limit.

Figure 14. Toyota Avensis main dummy results.



- Changing the impact location in the oblique test from NPRM to EuroNCAP (effectively moving the impact point on the car rearwards) results in a large increase in the rib injury criteria and a slight decrease in the other body region injury criteria (compare T1/T2 with T3).
- The proposed test configuration (NPRM-214) results in significantly lower injury criteria values for the ribs but higher values for other body regions, especially the abdomen, compared to the EuroNCAP configuration (compare T1/T2 with T4). The observation that these injury value changes are similar to those seen for the change in impact location indicates that the major influencing factor on test severity, when changing the impact angle, is likely to be the change in impact location.

Further detail can be found in the APROSYS deliverable AP-SP11-0086 [8].

Discussion and Conclusions

- Two similar oblique tests (IHRA specifications) with the Toyota Avensis showed good repeatability.
- The Toyota Avensis tests and Subaru simulation work showed that the dummy injury values found in the proposed oblique test are approximately the same as those found in a perpendicular test with the initial impact point moved 100 mm forward.
- An oblique test needs a modification of the currently used test equipment and is more complex to perform. Also the currently available dummies, ES-2 and WorldSID, are nowadays more accurate in a perpendicular loading situation. Design changes for the WorldSID dummy are ongoing to improve the behaviour for oblique loading conditions.
- Since other programs to evaluate the pole test procedure proposed by IHRA are still ongoing, worldwide harmonisation must be a leading priority in future decisions about its specification.

INTERIOR HEADFORM TESTS

Introduction

Accident analyses have shown that in real world crashes serious head contacts occur with the interior structure of cars. These are only very rarely observed in ECE R95 type side impact tests. One reason for this is that real world accidents occur in various impact configurations, which cannot be represented in only one test set-up. To overcome this deficiency in type approval evaluations, EEVC WG13 was tasked by the EEVC Steering Committee to develop an interior headform test procedure for Europe. The ongoing development of the EEVC WG13 interior headform test procedure has been reported at previous ESV conferences [12]. A test procedure for head contacts in the interior of cars already exists in the USA (FMVSS 201).

Objectives

The overall aim of APROSYS task “Improved Interior Head Protection in Lateral Impacts” was to evaluate the latest test protocol version 103r. This draft protocol is available on the EEVC home page: www.eevc.org. The main objectives of this work were:

- to evaluate the repeatability and reproducibility of the WG13 test procedure.
- to evaluate the WG13 target limitation zone procedure for rear seat occupants.

Repeatability / Reproducibility

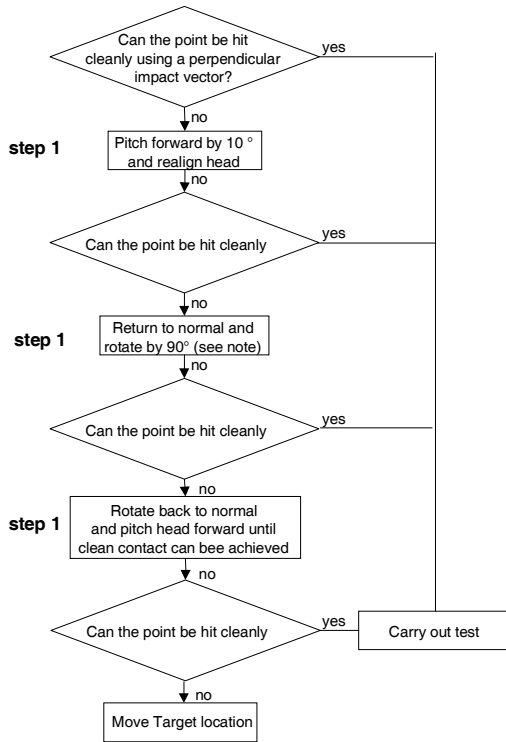
One of the major factors to affect reproducibility is head alignment, i.e. the effects of different head alignments at same targets when tested within different laboratories. The head alignment procedure is described in the flow chart in Figure 15.

The results of the work programme to investigate the affect of head alignment on reproducibility for two cars are described below. The test houses involved were IDIADA, TRL, Fiat and BAST.

Fiat Stilo

Fiat selected the worst case targets and provided IDIADA with the 3D measurement data to mark the car. The test institutes performed the head alignment completely independently from each other for exactly the same targets by following the flowchart for the FMH alignment. The results of head alignments from Fiat and IDIADA were compared to identify if the testing protocol and flowchart were clearly defined.

Figure 15. Head alignment flow-chart



Direction of 90° roll in step 2:

Target area	Left hand side of the vehicle	Right hand side of the vehicle
A post target points	90° clockwise	90° anticlockwise
Roof rail target points	90° clockwise	90° anticlockwise
B post target points	90° anticlockwise	90° clockwise

Finally, IDIADA and Fiat tested the car according to their own head alignment to get information on the differences of HIC results on identical targets with their own head alignments.

The following aspects were of interest:

- if same head alignments were chosen by two different test houses following the test procedure.
- the deviation of HIC values obtained by different test houses, testing identical targets using their own head alignments.

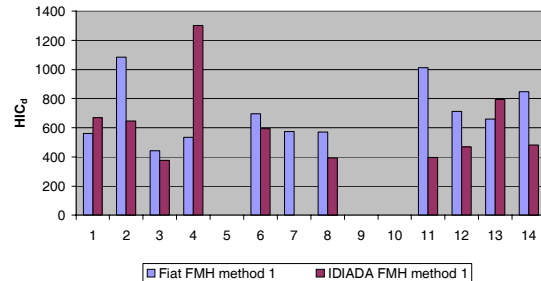
In an optimal situation the results should have been identical. The head alignment results are shown in the following table.

Table 5. Comparison of head alignment at IDIADA and Fiat.

Target	Horizontal angle [°]		diff. [°]	Vertical angle [°]		diff. [°]	last step in flowchart	
	IDIADA	Fiat		IDIADA	Fiat		IDIADA	Fiat
1	281	270	11	16	0	16	1	1
2	268	270	-2	10	9	1	1	1
3	259	270	-11	-10	0	-10	2	1
4	252	270	-18	-20	7	-27	4	3
5								
6	283	270	13	-11	-11	0	1	3
7	264	270	-6	-7	-40	33	4	1
8	270	270	0	-45	-39	-6	2	1
9								
10								
11	291	270	21	48	32	16	1	1
12	283	325	-42	-1	0	-1	3	4
13	283	270	13	-10	-12	2	4	4
14	286	270	16	-14	-4	-10	1	1
	average deviation		14	average deviation		11		

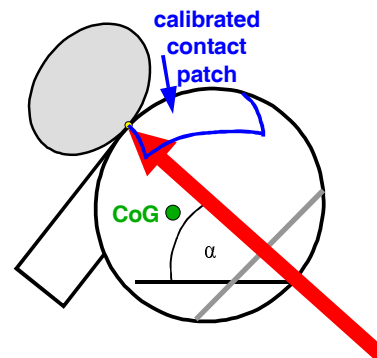
It was of interest how much influence this deviation of impact angles had on the HIC results. Figure 16 shows the obvious differences in HIC.

Figure 16. Comparison of FMH tests at Fiat and IDIADA according to method 1



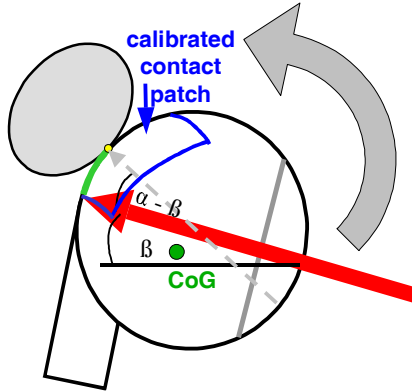
It was found by analysing pictures and videos that different contacts in the contact patch were chosen at both test houses. This might influence the test results significantly. To minimise rotation of FMH, it always should be the aim to keep the lever between contact point and FMH's centre of gravity as small as possible. Therefore it is suggested to select the most downward point on the contact patch, which can contact the target as first contact point. If head alignment is perpendicular to the surface of the target, it must always be the same target point in the lowest part of the contact patch as shown in Figure 17.

Figure 17. Contact point in contact patch for perpendicular impact



Perpendicular to the surface of the interior does not always result in realistic impact directions. Therefore impact angles are limited for horizontal and vertical alignment. For some targets, angle limitation leads to non perpendicular impacts. Nevertheless, the contact point should be as much downwards as possible and has to be the first contact point during the impact. A vertical limitation to an angle β would result in an upwards movement of the contact point in the contact patch as shown in Figure 18.

Figure 18. Contact point in contact patch for non perpendicular impact



To achieve reproducible results, it is recommended that the procedure is revised to include a definition of the contact point in the contact patch as above.

VW Golf

It was of interest, if identical head alignments would be chosen by two different test houses which are well trained in the use of the procedure, TRL and BAST. BAST selected worst case targets and provided TRL with the 3D measurement data to mark the car. Both test institutes performed the head alignment completely independently from each other for exactly the same targets by following the flowchart as in Figure 15.

The results of the head alignments from TRL and BAST, shown in

Table 6, were compared. The variation in angle definition and choice of the alignment step in the flow chart are quite similar between the two test houses for identical targets. An average deviation of 3° for horizontal and 4° for vertical angles is very low. The low variation in head alignment is probably the result of a high training level. TRL and BAST have been involved in the development of the test procedure and therefore might have a similar understanding / interpretation.

Table 6. Head alignment results

Target	Horizontal angle [°]		diff. [°]	Vertical angle [°]		diff. [°]	last step in flowchart	
	BAST	TRL		BAST	TRL		BAST	TRL
AP2	77	80	-3	35	29	6	0	0
AP1	88	85	3	46	45	1	0	0
SR1	87	89	-2	50	58	-8	1	0
SR2	89	90	-1	53	59	-6	0	0
BP1	85	85	0	25	25	0	3	3
BP2	90	90	0	0	15	-15	0	0
BP3	-	-	-	-	-	-	-	-
BP4	101	100	1	15	15	0	2	2
BP5	96	90	6	36	39	-3	3	2
BP6	39	30	9	12	10	2	2	1
SR3	87	89	-2	48	50	-2	1	1
CP2	119	111	8	20	23	-3	2	2
average deviation			3	average deviation		4		

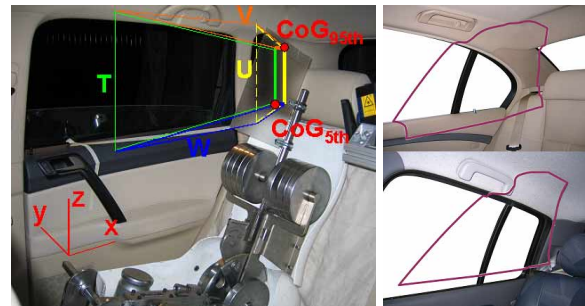
To achieve reproducible results it will be necessary to improve the head alignment definition, in particular the contact point in the contact patch.

Limitation Zones for Rear Seat Occupants

To be in line with the AE-MDB test procedure the WG 13 interior headform test procedure was extended for rear seat positions. Technical University Graz (TUG) compared the defined head contact zone defined by the WG13 procedure with head contact points from accident data.

TUG and BAST chose 10 cars and defined the contact zones according to the WG13 protocol. A funnel created by four planes, (see figure below) projects an area in which targets can be selected for interior headform testing. The planes start from the head's centre of gravity of a large male and a small female. These planes are V 60° upwards, W 20° downwards, T and U 45° sideways.

Figure 19. Example of limitation zone according to WG13 test procedure



It was found that the currently proposed limitation zone for rear seating positions does not include important areas identified in real world accidents. TUG gave recommendations to optimise these limitation zones to be closer to real world data: Plane

V must be more upwards to include roll over. Plane T must be more forward to include the grab handle and the B-pillar. Plane W must be more downwards to include the upper door panel, especially for non struck side head contacts. Plane U is sufficient, but targets behind the rear headrests must be excluded.

Conclusions

The Interior Headform tests in the different laboratories showed that the results of the tests following the draft EEVC WG13 protocol are very sensitive to the head alignment (impact vector deviation and the contact point position in the contact patch). A procedure to position the contact point in the contact patch to minimize head rotation and help reproducibility has been defined. Concerning the head contact limitation zone for rear seat occupants, a small change in the definition procedure is recommended to give a more realistic testing zone. Progress with respect to protocol clarification, point selection and testing the rear seat occupant zone has been made. However, further work on the head alignment procedure and angle limitations is still needed to ensure a reproducible and robust test.

SIDE OUT OF POSITION TESTS

Objective

The main objective of APROSYS task “Evaluation of occupant injury risk for deploying side airbags” was to evaluate the need and appropriateness of the IHRA proposed Side Out of Position (S-OOP) test procedure for application in Europe [9]. This test was proposed to minimise the potential negative effects of side airbag systems.

The test procedures include tests for seat-mounted airbags, door/quarter panel-mounted and roof-rail mounted airbags using 3-year old, 6-year old Hybrid-III and small female SID-IIs dummies. The test procedure has been accepted as part of IHRA harmonized test procedures in order to encourage car manufacturers and suppliers to take measures that minimise the potential negative side effects of side airbags.

Two activities were undertaken, firstly a review of the protocol for application in Europe and secondly a test programme to investigate issues such as repeatability and reproducibility.

Review of IHRA Protocol for Europe

A review of the procedure was performed to answer the following questions:

- Are the proposed dummies representative for the European situation?
- Are the proposed injury levels representative for the European situation?
- Which test configurations, dummy type / dummy positions, should be tested?
- Are there any technical and/or practical problems to carry out the proposed tests?

The review of the IHRA proposal showed clear differences between the US and EU situation, particularly related to assumptions of belt use and child restraint use.

It was proposed to limit the number of different scenarios to be tested in a potential EU side OOP proposal to the ones considered relevant for the EU. In the IHRA proposal, combinations of airbags can be fired. When both side and curtain airbags are fired, the dummy could be moving out of the way of the other deploying airbag as a result of the other airbag, thereby potentially lowering the total dummy loading. Therefore it was decided that in the current research, the airbag modules should only be tested on their own, e.g. combinations of airbags would not be tested.

European Regulations. In Europe, the usage of seat belts is mandatory, as well as the use of child restraint systems (CRS) for the transport of children in cars. These regulations have an effect on the OOP risk in Europe. Hence it was decided that in the current research only belted dummies would be tested and additional tests with CRS would be added to the program.

Accident Statistics. From the over 40.000 car occupants cumulatively documented till June 2004 in the available databases no deaths or serious injuries have been recorded worldwide from side airbags. In Europe only eight side airbag induced injuries were found, all but one being rated as minor injuries (\leq AIS1). Therefore it was concluded that currently, these kind of injuries are very rare.

Test Programme

Based on the IHRA protocol and the review results of the partners a test program was defined that covers the following:

- Side OOP tests following the IHRA-TWG proposal, for those scenarios relevant for Europe.
- Side OOP tests including CRS systems, additional to the IHRA-TWG proposal.

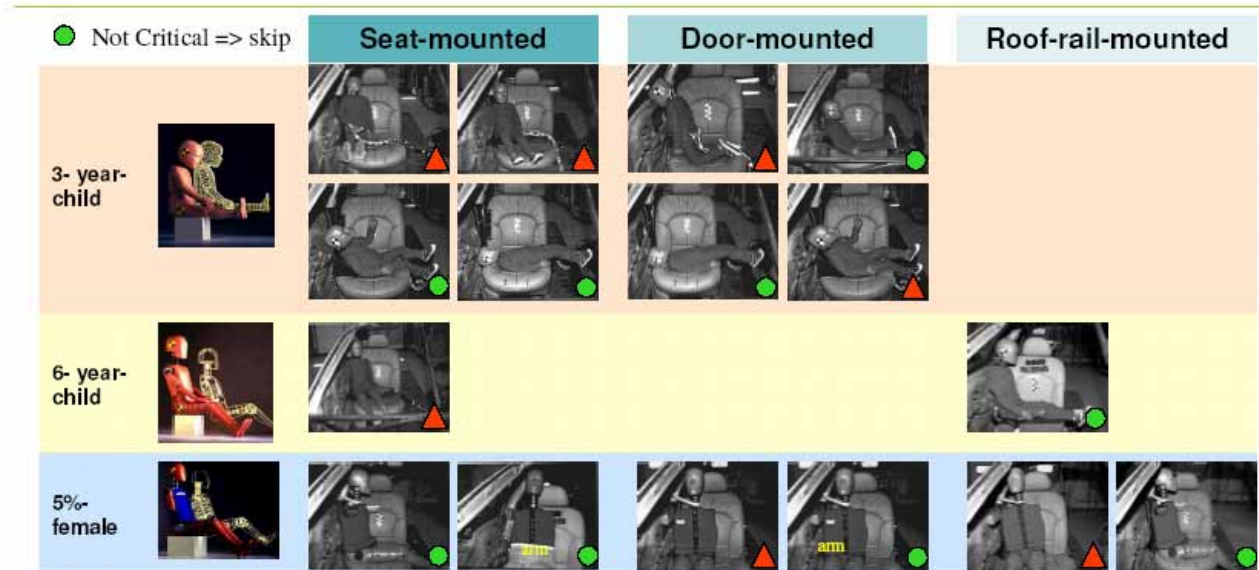
Attention was paid towards repeatability and reproducibility, particularly focussed on the dummy positioning procedures.

Although door mounted airbags have tended to be replaced by seat mounted airbags, door mounted Therefore seat mounted side airbags, door mounted **Figure 20. Investigation of Side OOP scenarios.**

3yo	Head/thorax	Rearward		1	1
6yo	Thorax	Forward	2		
6yo	Head/thorax	Forward		1	
SID	Curtain	Forward	2	2	2

In total three different vehicles models were used because it was not the purpose of this study to assess

▲ Maybe critical => investigate



airbags might become more important again because of the increasing number of MPV/SUV type of cars. side airbags, head thorax bags and curtain airbags were included in the study. Because of the poor availability of vehicles equipped with door mounted airbags, the part of the work on door mounted airbags was covered by a short literature survey.

The selected positions, dummies and airbags tested are summarized in Figure 20. **Error! Reference source not found.** All critical scenarios, marked with ▲, were tested in the program, except the scenarios with door mounted airbags. The rearward positions of the dummy are not a realistic seating position in Europe but were chosen as a potential test to measure the airbag aggressiveness.

The complete IHRA protocol test matrix is presented in Table 7.

Table 7.
Test matrix IHRA protocol.

Dum	Airbag	Test	Laboratory			
			A	B	C	D
3yo	Thorax	Forward	2	2		
3yo	Thorax	Rearward	2		2	2
3yo	Head/thorax	Forward			1	

individual airbags or vehicles. One model was chosen as typical example of cars having a seat integrated

thorax bag in combinations with a curtain airbag system. Two models were chosen as typical examples of cars equipped with head-thorax bags.

Additionally, tests with child restraint systems were carried with group 2/3 child restraint systems, since these groups were assumed to give the largest chance of interaction between a side airbag and a child and/or CRS. Different qualities of CRS were used, with and without backrest for group 2 and group 3 respectively. Tests were performed with 3-yo and 6-yo Hybrid-III dummies in forward facing positions to be able to compare with the forward facing IHRA positions. Both seat mounted thorax airbags and seat mounted head thorax bags were included. The CRS was initially mounted according its manual; the dummy was then positioned following as close as possible to the TWG protocol for forward facing positions, aiming at the largest possible interaction between dummy, CRS and airbag. The complete matrix, including repeatability tests, is presented in Table 8.

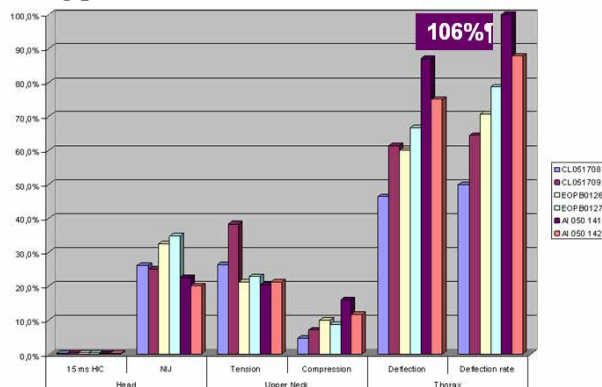
Table 8.
Test matrix with dummies in CRS.

Dum	Airbag	CRS	Laboratory		
			A	B	D
3yo	Thorax	High end		2	
3yo	Thorax	Simple		2	
6yo	Thorax	High end	2		
6yo	Head/thorax	High end			1
6yo	Thorax	High end	1		
6yo	Thorax	Simple	2		

All dummy test results are available in the APROSYS deliverable [10].

From the test results of the seat integrated thorax bags, it is concluded that most probably the airbags have been designed following the TWG proposal. The injury reference values found were all well below the reference values, except for the thorax deflection rate in one rearward facing test, see Figure 21. (The dummy injury values are expressed as a percentage of the reference values of the IHRA protocol.). The figure presents the results of 6 identical test carried out in 3 laboratories. Please not also that this is not a realistic seating position in Europe.

Figure 21. Test results 3yo dummy in rearward facing position.



From the test results in one laboratory it was concluded that the repeatability was reasonable, whereas, by comparing results from various laboratories, the reproducibility was poor. This was mainly caused by a different interpretation of the TWG protocol. Generally, the injury risk for the 6-year-old dummy seems to be less than for the 3-year-old dummy.

Concerning the CRS tests with seat mounted airbags the following remarks can be made:

- Using a CRS with a backrest decreases the risk of interaction between dummy and airbag during airbag deployment. No serious airbag – dummy or CRS

interaction was observed in these seat mounted thorax airbag tests.

- No significant differences were found between different types of CRS, although with a simple booster (without horns) it is easier to come closer to the airbag, in the potential zone of danger.
- Generally it was concluded that the TWG proposal for forward facing 3 and 6 year old dummies covers the worst case situation that could occur when seated in a CRS.
- From the TWG proposal, the rearward facing 3 year old dummy is facing the most severe loading.

The tests with the combined head/thorax airbags showed that this airbag design seems to include a risk in CRS- out-of-position conditions (sleeping child), however, this risk is likely to be covered by the TWG tests (forward facing on booster seat, not checked in this project). A general note is that CRS positioning on the rear bench should be preferred over the front passenger seat.

In the tests with the curtain bags large differences are observed, particularly between the Nij values, with one test exceeding the limits. This is related to the different airbag – dummy interaction observed. In 50% of the tests, the airbag was deployed between the dummy and the window, whereas in the other 50%, the dummy was in between the airbag and the window. Differences in the dummy positioning and seat adjustment contribute to differences in the airbag – dummy interaction. The positioning protocol of the SID-II's for this position needs further refinement for potential use in regulatory testing.

Conclusions

The following conclusions were drawn:

- No relevant accident data was found regarding injuries induced by side airbags.
- Out of the IHRA/TWG protocol, test scenarios relevant for Europe were identified
- Different side OOP tests were performed in four different laboratories over Europe, resulting in a reasonable repeatability within laboratories but poor reproducibility between different laboratories. The current test protocol is not clear enough to be used in a European regulatory environment at this stage.

SUMMARY OF CONCLUSIONS

The 4 parts of the draft IHRA proposal have been evaluated and additional development activities have been carried out.

- The AE-MDB work showed that both V3 barriers gave more comparable dummy injury values and car

deformation measures to the baseline car to car tests than the V2 barrier. Please note that the major difference between the V3 barriers and V2 barrier is the addition of a bumper beam element. For one car, the results of V3.9 were slightly more comparable with the baseline test than V3.1. Tests with the AE-MDB V3, which has a trolley mass of 1500 kg, were found to be more severe than the current regulation ECE R95, which has a trolley mass of 950 kg. Both V3.1 and 3.9 exhibited stability problems in sill robustness tests. However, the severity of this test is under discussion as it may be unrealistically high. Further work, based on the modeling work in the project, is needed to finalize the barrier design and to solve, if needed, the stability problem.

- Car to pole full-scale tests and numerical studies showed that the severity of a car to pole test has a stronger relation to the impact location than to the impact angle. Therefore, based on practicality of the test and the better performance of the current side impact dummies with perpendicular loading, a perpendicular car to pole test with the impact location positioned ahead of the head centre of gravity would be preferable for Europe. However, an oblique test could be acceptable if other reasons, such as international harmonization, demand it.

- The Interior Headform tests in the different laboratories showed that the results of the tests following the draft EEVC WG13 protocol are very sensitive to the head alignment (impact vector deviation and the contact point position in the contact patch). A procedure to position the contact point in the contact patch to minimize head rotation and help reproducibility has been defined. Concerning the head contact limitation zone for rear seat occupants, a small change in the definition procedure is recommended to give a more realistic testing zone. Progress with respect to protocol clarification, point selection and testing the rear seat occupant zone has been made. However, further work on the head alignment procedure and angle limitations is still needed to ensure a reproducible and robust test.

- Current accident statistics show no need for a Side Out of Position regulation in Europe. If future accident studies show a need for an OOP regulation only a limited number of scenarios of the IHRA draft protocol will be needed in Europe to cover the situation with belted occupants and children in child restraint systems. Then an update of the IHRA protocol will be required to make the protocol suitable for European regulatory testing, especially with respect to the seat and dummy positioning. Special attention for the risks of OOP injuries will be needed if door mounted airbags are re-introduced in the car fleet.

The current APROSYS SP1.1 consortium members are:

- BAST, Germany
- Cellbond Composites Ltd, United Kingdom
- CRF Italy
- Fiat Italy
- IDIADA, Spain
- INSIA, Spain
- Takata Petri, Germany
- Technical University Graz, Austria
- TNO, the Netherlands
- TRL, United Kingdom
- Toyota motor Europe NV/SA, Belgium
- Volkswagen, Germany

ACKNOWLEDGEMENTS

The consortium is grateful for the financial sponsorship of:

- European Commission DG-TREN
- Cellbond Composites Ltd, United Kingdom
- Takata Petri, Germany
- TNO, the Netherlands
- Toyota motor Europe NV/SA, Belgium
- Volkswagen, Germany
- UK Department of Transport,

Special thanks for:

- Subaru, test vehicles and numerical simulations
- DC, test and simulation results
- Ford, test vehicles
- Volvo, test vehicles

REFERENCES

- [1] APROSYS SP1 Deliverable D1.1.1A, AP-SP11-0001 "Status review IHRA test procedures" Available from www.aprosys.com sp1 "car accidents".
- [2] IIHS side impact test protocol available from www.iihs.org.
- [3] APROSYS SP1 Deliverable D1.1.1B, AP-SP11-0083 "Protection in multi vehicle lateral crashes" Available from www.aprosys.com sp1 "car accidents".
- [4] 2003 ESV paper, Progress on the development of the advanced European mobile deformable barrier face (AE-MDB), Ratingen M. van, Roberts A.K. papernumber 03-0126.
- [5] 2005 ESV paper, The Development of an Advanced European Mobile Deformable Barrier Face (AE-MDB), Ellway J, 2005, paper number 05-0239
- [6] 1998 Test Methods for Evaluating and Comparing the Performance of Side Impact Barrier Faces de Coo, P. Roberts, A. Seeck, A. Cesari, D. paper number 98-S8-O-02

[7]http://www.nhtsa.dot.gov/cars/rules/rulings/sideimpact/index.html#TABLE_of_Content

[8] APROSYS SP 1 Deliverable D1.1.2.A, AP-SP11-0086 “An Evaluation of the Side Impact Pole Test Procedure” Available from www.aprosys.com sp1 “car accidents”.

[9] Recommended Procedures for evaluation occupant injury risk from deploying side airbags Adrian K. Lund (IIHS), available from www.iihs.org.

[10] APROSYS SP 1 Deliverable 1.1.4, AP-SP11-0115, “Recommendation on feasibility of side OOP test procedure for Europe”. Procedure” Available from www.aprosys.com sp1 “car accidents”.

[11]ESV 2005 IHRA status report, Craig Newland on behalf of the IHRA Side Impact Working Group (conference paper 05-0460)

[12] 2005 ESV paper, EEVC Research in the Field of Developing a European Interior Headform Test Procedure, Langner T, 2005, paper number 05-0158

A REVIEW OF THE EUROPEAN 40% OFFSET FRONTAL IMPACT TEST CONFIGURATION

Richard Cuerden

Rebecca Cookson

Phillip Massie

Mervyn Edwards

TRL Limited (Transport Research Laboratory)

United Kingdom

Paper Number 07-0318

ABSTRACT

Frontal impacts are the most frequent crash type and account for the majority of Killed and Seriously Injured (KSI) car occupant casualties in Europe. This study reviews the performance of modern cars (registered in 1996 or later) in frontal impacts, which are most associated with KSI casualties. Comparison is made with the 40% offset legislative (UNECE R94) and consumer (EuroNCAP) tests. The aim of the study is to evaluate how well the 40% offset configuration and the associated vehicle loading and intrusion factors represents the real life injury experience sustained in frontal impacts.

Co-operative Crash Injury Study (CCIS) data collected from June 1998 has been used. There were 806 KSI seat belted casualties who experienced frontal impacts and were occupants of cars registered in 1996 or later. The majority of these victims were drivers. The study then analyses 435 drivers who had impacts that involved direct contact to the front right corner of the car. The nature of the vehicle loading in terms of structural features is considered and compared with the injury outcome and the associated mechanisms. Car to car impacts are the most common, although larger goods and passenger vehicles are prominent among crash partners in fatal crashes. About 80% of the fatalities are encompassed by the EuroNCAP frontal test speed rising to 95% of the seriously injured survivors.

More than half of the KSI car occupants sustain their injuries in impacts with more than 40% overlap and a significant proportion of these crashes involve direct loading to both longitudinals. Thoracic injuries caused by seat belt loading and lower extremity injuries caused by facia and footwell contact are the main body regions injured. Approximately 80% of the MAIS=2 and 50% of the MAIS 3+ injury is sustained by survivors with little or no intrusion to the compartment (<10cm).

INTRODUCTION

Over the past ten years frontal impact crashworthiness has significantly improved with the advancement of car structures and restraint systems. The European frontal impact directive (UNECE R94) and EuroNCAP tests continue to promote the enhancement of crash energy management structures, aimed at reducing the amount of loading occupants experience.

The EuroNCAP frontal impact test is based on the European legislation, but is conducted at a higher impact speed. The car strikes a 40% offset deformable barrier head-on at 64kph. The 40% offset is a percentage measure of the car's width. The test requirements have resulted in an increase in compartment strength and, as a consequence, intrusion is less common in real-life frontal impacts (Edwards, 2007). Over the same period, developments in airbag and seat belt restraint system technologies have reduced the likelihood of head contacts with the interior of the vehicle during a frontal impact (Cuerden, 2001). Correctly restrained occupants' head and facial injuries have been significantly mitigated. However, frontal impacts are still the most frequent crash type and account for the majority of Killed and Seriously Injured (KSI) car occupant casualties in Europe.

This paper outlines the characteristics of relatively modern cars (registered in 1996 or later) in frontal impacts, which are most associated with KSI casualties. Comparison is made with the 40% offset legislative and consumer tests.

The data source is the UK's Co-operative Crash Injury Study (CCIS), which is one of Europe's largest car occupant injury causation studies (www.ukccis.org). The programme of research started in 1983 and continues to investigate real-life car accidents. Multi-disciplinary teams examine crashed vehicles and correlate their findings with the injuries the victims suffered to determine how car occupants are injured. The objective of the study is to improve car crash performance by continuing to develop a scientific knowledge base, which is used to identify the future priorities for vehicle safety design as changes take place.

The study carefully selects accidents to be representative of injury car crashes that occur in the UK and is a good data source to undertake an in-depth review of the characteristics of frontal crashes that result in KSI car occupant casualties.

METHOD

Co-operative Crash Injury Study

The Co-operative Crash Injury Study investigates and interprets real-world car occupant injury crashes retrospectively. Police reported injury road traffic crashes from defined geographical areas of England are reviewed to establish if they meet the CCIS sample criteria. The basic selection criteria used for the accidents presented in this analysis were:

- The accident must have occurred within the investigating teams geographical area
- The vehicle must be a car or car derivative
- The vehicle must have been less than 7 years old at the time of the accident
- The vehicle must have at least one occupant who is injured (according to the police)
- The vehicle must have been towed from the scene of the accident.

The CCIS case or accident injury severity is based on the most severe injury to an occupant of a car less than 7 years old and therefore may be lower than the police reported accident severity. Accidents were investigated according to a stratified sampling procedure, which favoured cars that met the age criteria and contained a fatal or seriously injured occupant as defined by the British Government definitions of fatal, serious and slight. Where possible all crashes that met the criteria and involved a CCIS classified fatal or seriously injured occupant were investigated. Random selections of accidents involving slight injury were also investigated, up to a target maximum.

Vehicle examinations were undertaken at recovery garages several days after the collision. An extensive investigation of the cars' residual damage and structural loading along with detailed descriptions of the restraint system characteristics and any occupant contact evidence was recorded using the CCIS data collection protocols. This process allows the nature and severity of the impact(s) and/ or rollover damage to be precisely documented so different crash types can be compared.

Car occupant injury information was collected from hospital records, coroners' reports and

questionnaires sent to survivors. The casualties' injuries were coded using the Abbreviated Injury Scale (AIS, AAAM 1990 Revision). AIS is a threat-to-life scale and every injury is assigned a score, ranging from 1 (minor, e.g. bruise) to 6 (currently untreatable). The Maximum AIS injury a casualty sustains is termed MAIS. The scale is not linear; for example, an AIS 4 is much more severe than two AIS scores of 2.

Table 1.
AIS Score Categories

AIS Score	Description
0	No Injury
1	Minor
2	Moderate
3	Serious
4	Severe
5	Critical
6	Maximum
9	Unknown

The casualties' characteristics (age, gender, seat belt use) and injury information were correlated with the vehicle investigation evidence. This methodology allows the causes and mechanisms of the injuries to be documented.

The crash severity parameter used for this study is the car's change of velocity (Delta-V).

Accidents investigated between June 1998 and March 2006 are included in the analysis (CCIS Phases 6, 7 and 8 – to data release 8a).

Car Occupant Casualties in Great Britain

In the UK, STATS19 accident forms are completed for all injury road traffic crashes. The information recorded captures the details of all road users, but compared to in-depth studies such as CCIS, provides only an overview of the event. However, the first point of contact on the vehicle is identified by the investigating police officer. This may not be the principal or most severe impact, but it is a good estimate as to the nature and respective importance of the different crash types.

Five years of STATS19 data were analysed (1999 to 2003) and car occupant casualties selected. On average in this period there were 1,723 fatalities and 19,106 KSI car occupant casualties per year. The front was described as the first point of impact on the car for 50% (853 occupants) of the killed and 58% (11,041) of the KSI casualties, emphasising the relative importance of this crash type.

In Great Britain in 2004 (RCGB 2004) there were 11,885 under 16 year olds and 167,797 people aged 16 years or older reported as injured car occupant casualties. Proportionally, there are far more under 16 year olds seated in the rear of the car (Figure 1). Rear passengers represent a little over 10% of all car occupant casualties.

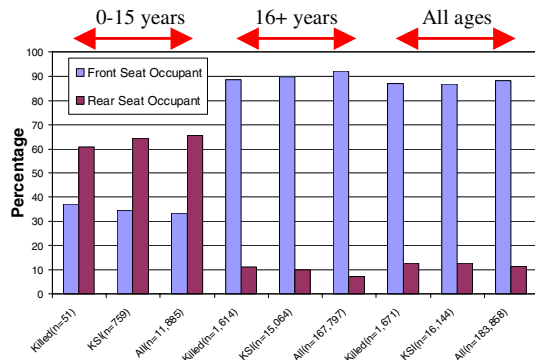


Figure 1. Car Occupant Casualties by Seating Position (RCGB 2004)

The casualties' seat belt use is not recorded in STATS19 and so CCIS was analysed to estimate the relative usage rates by seating position and gender. Figure 2 shows that drivers are most likely to be belted, followed by Front and Rear Seat Passengers (FSP and RSP). Females in all seating positions used their seat belts more frequently. Seat belt use decreased with increasing occupant injury severity. Figure 2 shows that 29% of the male and 16% of the female drivers were unbelted and fatally injured. Approximately 70% of the male and 56% of the female RSPs were unbelted and fatally injured. Occupant age is also a significant factor when seat belt use is investigated.

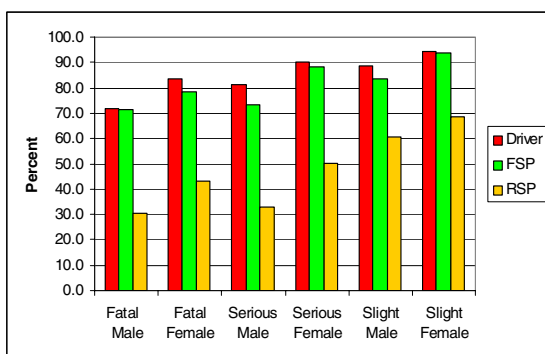


Figure 2. Seat belt use rate by Injury Severity, Gender and Seating Position

Car seat belts are very effective safety devices, reducing the risk of serious and fatal injury. It is often assumed that seat belt performance in crashes is the same for all seating positions, and yet there are good and obvious reasons why that is not the

case. The surrounding physical environment and the seat belt and airbag technologies differ between the seating positions. The driver, front and rear seat passenger populations are very different with respect to gender and age. These different occupant characteristics and seat belt use rates are observed by road-side surveys and recorded casualties (Figure 2). Only seat belted occupants were considered for this analysis and so a large percentage of rear seat passengers were excluded. Similarly, a significant number of male serious casualties and a proportion of the fatalities were excluded due to the seat belt criteria.

The CCIS database is far better at describing crash types with respect both to the chronological order of the impacts and to the extent of the measured damage compared with STATS19. Further, occupant characteristics such as seat belt use are routinely recorded unlike in STATS19. Finally, the use of AIS as a descriptor ensures a more precise definition of the injury severity compared with 'serious', which covers most injury outcome from minor fractures to death more than 30 days after the crash. However, the CCIS database is not fully representative of the national car occupant crash population and there are some limitations to this study.

CCIS Occupant Selection

There were 1,652 MAIS 2+ seat belted casualties who were occupants of cars registered in 1996 or later. The injury severity classifications used for this paper are grouped as:

- MAIS = 2, Moderate
- MAIS 3+, Serious, Survivors
- Killed

Approximately half of the selected casualties sustained MAIS 2 injury. All ages were included; some 12 children were secured on or by child restraints. To explore the relative importance of frontal impacts, occupants were differentiated by their crash type.

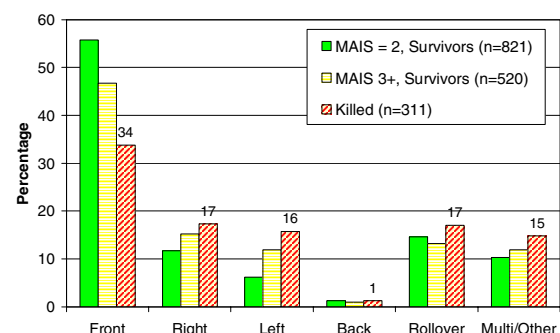


Figure 3. Crash Type by Injury Severity for Seat Belted MAIS 2+ Car Occupants

Figure 1 shows the relative importance of frontal impacts compared with the other main crash types and identifies the level of injury suffered respectively. The crash types were classified by the principal impact location on the car. If there were two or more significant impacts to different sides of the vehicle, each causing more than 10cm of crush, these vehicles are grouped as 'Multi/other' crash type. Any car that rolled over, with or without an impact, either before, after or during the roll, are classified as 'Rollover' crash type.

For all MAIS 2+ casualties frontal impacts represent nearly half of the crash types. As the injury severity increases other crash types become proportionally more common, but frontal crashes are still the most frequent. Eight hundred and six casualties who had experienced frontal impacts with no rollover or other significant impacts were selected.

Casualties with a MAIS 2 or greater were selected for this study to represent police reported KSI casualties. It is recognised that this is not an exact match. Approximately 38% of the CCIS casualties described by the police as serious were classified as MAIS 0 or 1. Approximately 9% of the CCIS casualties described by the police as slight were classified as MAIS 2+. Therefore in general the selection criteria bias the analysis to occupants who sustained specific and more severe injury than that suffered by the average 'serious' car occupant casualty population in Great Britain. Nonetheless, for the ease of analysis, the MAIS 2+ category provides a useful estimate. Some serious injury is not directly related to impact trauma, such as shock, and this research excludes non-injury based outcomes and concentrates on the identification of specific and severe injuries that are sustained by car occupants in modern vehicles as a result of frontal impacts.

RESULTS

Table 2 shows the injury severity by seating positions for the 806 selected casualties who experienced a frontal impact. Approximately 70% of the occupants were drivers. Males accounted for roughly 62%, 25% and 35% of the drivers, FSPs and RSPs respectively. Tables 3 to 5 indicate that the distribution of casualty age is different with respect to seating position; generally FSPs were older and RSPs younger than the drivers. When the crash severity (Delta-V) is known, drivers are typically found to experience higher values for the same injury level compared with passengers.

Table 2.
Occupants by Position and Injury Group

Seating Position	Injury Group			Total
	MAIS=2	MAIS 3+	Killed	
Driver	310	183	74	567
FSP	126	42	25	193
RSP	22	18	6	46
Total	458	243	105	806

Table 3.
Summary of Driver Characteristics

	MAIS = 2 (n=310)	MAIS 3+ (n=183)	Killed (n=74)
Age 25%ile	31 years	26 years	31 years
Age 50%ile	45 years	42 years	49 years
Age 75%ile	57 years	56 years	65 years
% Male	59.4%	63.9%	68.9%
With known DV N=	156	114	36
DV 25%ile	29 kph	37 kph	47 kph
DV 50%ile	37 kph	45 kph	54 kph
DV 75%ile	44 kph	53 kph	65 kph
% hit a car	68.6 %	60.1 %	47.3 %
% hit larger vehicle	19.1%	27.3%	40.5%

Table 4.
Summary of Front Passenger Characteristics

	MAIS = 2 (n=126)	MAIS 3+ (n=42)	Killed (n=25)
Age 25%ile	30 years	20 years	29 years
Age 50%ile	44 years	52 years	56 years
Age 75%ile	63 years	65 years	74 years
% Male	22.2 %	28.6 %	36.0 %
With known DV N=	65	23	16
DV 25%ile	24 kph	30 kph	30 kph
DV 50%ile	33 kph	39 kph	37 kph
DV 75%ile	44 kph	48 kph	49 kph
% hit a car	71.8 %	66.7 %	48.0 %
% hit larger vehicle	12.9 %	26.2 %	36.0 %

With respect to the object hit there is some variation, but it was most commonly found to be another car or a larger vehicle. The small RSP sample is due both to the low occupancy rates for this seating position and the low seat belt use rates.

Table 5.
Summary of Rear Passenger Characteristics

	MAIS = 2 (n=22)	MAIS 3+ (n=18)	Killed (n=6)
25%ile	11 years	13 years	-
Age 50%ile	17 years	17 years	31 years
75%ile	53 years	23 years	-
% Male	27.3 %	38.9 %	50.0 %
With known DV N=	14	12	3
25%ile	24 kph	30 kph	-
DV 50%ile	31 kph	42 kph	58 kph
75%ile	48 kph	49 kph	-
% hit a car	59.1 %	61.1 %	50.0 %
% hit larger vehicle	9.1 %	11.1 %	50.0 %

The 806 casualties' frontal impacts are summarised in Figures 4 to 8 with respect to the loading and severity of damage to the car's structure. Although each crash is individual, the following representation of the data attempts to group and compare the similarities found in each scenario. Figure 4 shows that the majority of frontal impact MAIS 2+ casualties were in collisions with other cars. Crashes with heavier vehicles (HGVs - including large passenger service vehicles) were far less common, but accounted for some 30% of the fatalities. It is worth noting the small number of crashes that occurred with roadside objects (narrow and wide).

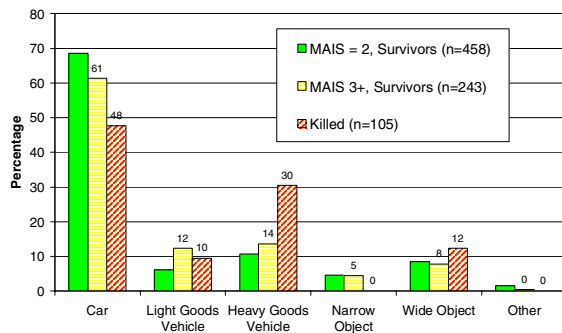


Figure 4. Object Hit by Car Occupant Injury Severity

The crash severity parameter used for this study is Delta-V (DV) or the Change of Velocity measured in kph. This is calculated based on the amount of residual crush the impact partners experienced. It is not always possible to determine a Delta-V for a variety of reasons associated with the manner in which the vehicle was loaded and the characteristics of the impact partner. However, of the 806 MAIS 2+ occupants, 438 (54%) had a Delta-V and are shown in Figure 5. Differentiating between the different injury severity groups and

considering the 80th percentile, we find that the Delta-Vs for MAIS=2, MAIS 3+ (Survived) and Killed were 47kph, 54kph and 64kph respectively. Note that, when Delta-V is known there is a bias towards more survivable crashes with other cars; it is often not possible to calculate a crash severity measure for massive impacts and/or impacts with larger vehicles where the stiff structures have been over-run.

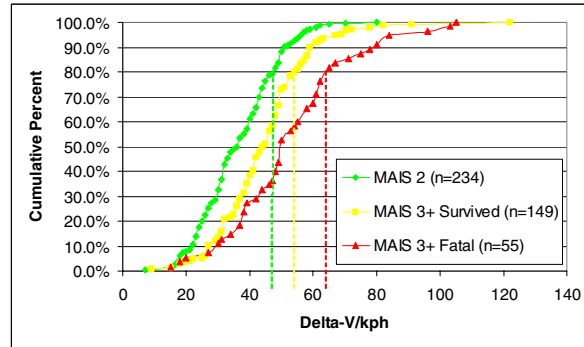


Figure 5. Distribution of Delta-V by Injury Severity

Figures 6 and 7 describe the frontal impact characteristics in more detail. CCIS uses the Collision Deformation Classification (CDC) to describe the damage cars sustain. Two variables within the code are used in this study, the Principal Direction of Force (PDF) of the impact and the specific location of the direct contact damage on the car (Figure 7 details the key for the coding letters).

Approximately 75% of the occupants experienced a PDF that was head-on ($0^{\circ} \pm 15^{\circ}$) (Figure 6).

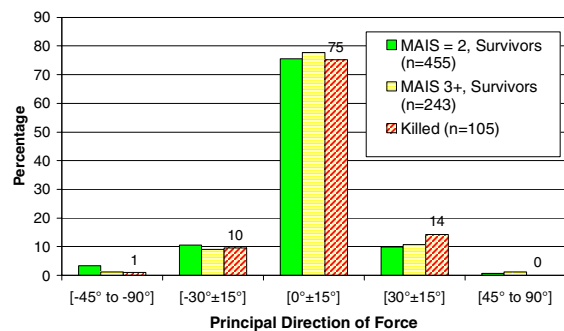


Figure 6. PDF by Car Occupant Injury Severity

Figure 8 is based on all PDFs. The most common loading location for MAIS 2+ casualties involved more than 66% direct contact (code D - 66-100% of car's width). However, it is not possible to compare this directly with the 40% offset configuration used in legislative and consumer tests, as not all the impacts will have involved loading to a front corner of the vehicle. In addition, the position and percentage overlap of the direct

loading with respect to the side the occupant is seated can be an important factor, in terms of the amount of intrusion and/or rotational accelerations experienced. In Figures 4 to 8 all seating positions have been considered and consequently there is a bias towards drivers.

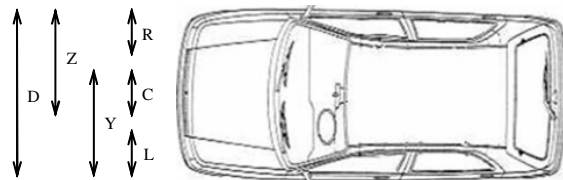


Figure 7. CDC Part Code, Direct Damage Location

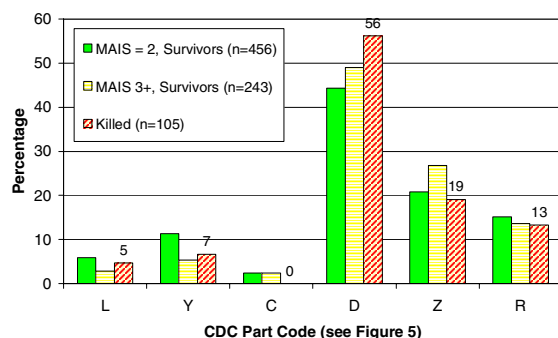


Figure 8. Direct Damage Location by Car Occupant Injury Severity

Body Regions Injured

The occupants were divided by seating position and the relative rate of injury to their different body regions by severity is given in Figures 9 to 11, for drivers, front and rear seat passengers. The percentage plotted for each body region is calculated as the proportion of occupants with an injury to a body region of the same AIS level as their injury grouping. For example, there were 310 drivers classified as MAIS = 2, some 115 of these drivers had an AIS 2 thorax injury or 37% (115/310). The AIS 3, 4, 5 and 6 injuries are all grouped as AIS 3+.

The relative frequency of injury to the body regions varies with respect to the seating position; this is related both to the different occupant characteristics in terms of age and gender associated with each seating position; and the different protection afforded to each seating position in terms of seat belt and airbag technologies. It is often assumed that seat belt performance in crashes is the same for all seating positions, and yet there are good and obvious reasons why that is not the case. In the front of a car, the instrument panel or fascia is contacted by the knees in most front impacts where the velocity change exceeds 30kph. Airbags are now standard

features for front impact protection and supplement the seat belt performance. This means that in higher energy front crashes a substantial proportion of an occupant's energy is transferred through these knee and airbag contacts, reducing seat belt loads. The kinematics of the restrained rear seat occupant are different as there are no equivalent limiting knee or airbag contacts. The backs of the front seats are much more compliant and deformable; hence the rear seat belts have to manage proportionally more of the crash energy. It is therefore a more challenging condition from the point of view of rear seat restraint design. A particular concern is the potential for rear seat occupants to submarine under the lap portion of the seat belt webbing, causing the abdomen to be loaded.

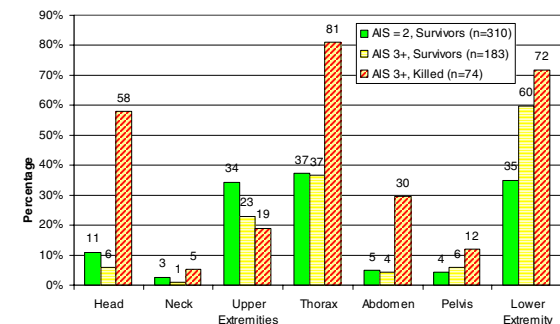


Figure 9. Injury Regions for Drivers

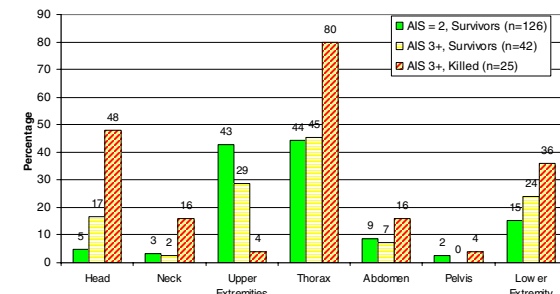


Figure 10. Injury Regions for Front Seat Passengers

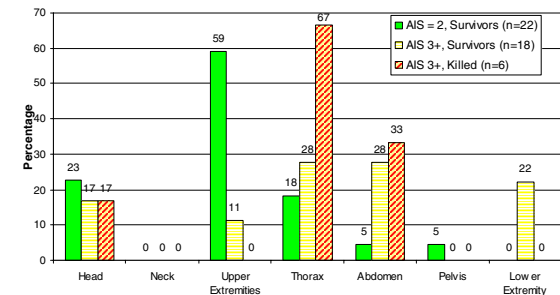


Figure 11. Injury Regions for All Rear Seat Passengers

For MAIS = 2 and MAIS 3+ survivors, abdomen injury was relatively uncommon for drivers and front passengers. However, 28% of the MAIS 3+

rear passengers sustained an AIS 3 or greater abdomen injury. The sample size is small and more detailed investigation is required to fully understand the mechanism that resulted in these injuries and to determine if more modern seat belt designs would have mitigated them or reduced their severity.

For MAIS = 2 casualties, the most commonly injured body regions at AIS = 2, for drivers were the thorax (37%), lower (35%) and upper (34%) extremities. For FSPs the order changed and the rate of injury observed was different with injuries to the thorax (44%), upper (43%) and lower (15%) extremities. The largest difference was observed for the RSP, with the upper extremities (59%), the head (23%) and the thorax (18%) being most commonly injured.

For MAIS 3+ survivor casualties, the most commonly AIS 3+ injured body regions, for drivers were the lower extremities (60%), the thorax (37%) and the upper extremities (23%). For FSPs the order changed and the rate of injury observed was different with injuries to the thorax (45%), upper (29%) and lower (24%) extremities. The largest difference was observed for the RSPs, with the thorax (28%), the abdomen (28%), the lower extremity (22%) and the head (17%) being most commonly injured.

For those casualties who were killed, the most common body regions injured at AIS 3+ were the thorax and head for the drivers and FSPs and the thorax and abdomen for RSPs.

For those drivers and front passengers who sustained a thorax injury, the nature of the injury is further outlined in Table 6. Specifically, injuries were evaluated as to be either, Skeletal, Internal or a combination of the two. The most common injury type was skeletal only (28%), followed by skeletal and internal (14%) and internal only (4%).

Table 6.
Nature of Drivers' and Front Seat Passengers' Thorax Injuries

Thorax Injury	MAIS = 2	MAIS 3+	Killed	Total
AIS 0	145	83	11	239
AIS 1	116	45	4	165
Skeletal only	175	27	11	213
Internal only	0	22	12	34
Skeletal and Internal	0	48	61	109
Total	436	225	99	760

Detailed Evaluation of the Cars' Front Loading and Overlap for Drivers

The direct impact loading to the front structural components of the cars was evaluated with respect to the drivers' injury outcome. Each car's front structure was simplified to comprise an offside (right or UK driver's side) longitudinal, a nearside longitudinal and an engine. The CCIS vehicle investigators record if these components were directly loaded in the crash and outline the extent of the crush and/or bending. For this paper, a simple matrix has been established to outline which combinations of structural loading most commonly occur for the injured drivers (MAIS 2+).



Figure 12. View of offside (right) longitudinal and engine compartment.

Table 7.
Directly loaded longitudinals and/or engine related to occupant injury severity

	MAIS = 2 (n=310)	MAIS 3+ (n=183)	Killed (n=74)	Total (n=567)
None loaded	10.32%	7.65%	5.41%	8.82%
Offside only	8.71%	6.01%	8.11%	7.76%
Nearside only	4.19%	1.09%	0.00%	2.65%
Offside and Nearside	5.48%	3.28%	2.70%	4.41%
Engine only	8.39%	5.46%	9.46%	7.58%
Offside and Engine	26.45%	37.16%	40.54%	31.75%
Nearside and Engine	11.29%	8.20%	2.70%	9.17%
All	24.52%	31.15%	29.73%	27.34%
One or more unknown	0.65%	0.00%	1.35%	0.53%
Total	100%	100%	100%	100%

Table 7 highlights that the offside longitudinal and the engine are the areas which are directly loaded together most commonly. The second most common configuration involves the offside and nearside longitudinals and the engine (All) being

directly loaded. Some 31% of the drivers experienced loading to the offside and nearside longitudinals only or to 'All' three components. It is interesting to note that for the more seriously injured or killed drivers, the relative frequency of loading to the offside and engine or all three components increases.

To establish a more direct comparison with the current frontal impact legislation, cars were selected which had experienced direct contact to the front right corner or experienced 80% offset loading or greater. This yielded a sub-sample of 435 drivers, or 77% of all the drivers who met the original sample selection criteria. The selected drivers are summarised in Table 8. The broad characteristics of the sub-sample of 435 drivers were found to be very similar to those of the 567 drivers included in the early findings.

As with the original selection of drivers (567), significant differences were observed between the three injury groups; the sub-sample of drivers ages and Delta-Vs were found to increase ($p < 0.05$) with the increasing injury severity.

Table 8.
Summary of Driver Characteristics with Right Front Corner Direct Contact Damage

	MAIS = 2 (n=225)	MAIS 3+ (n=146)	Killed (n=64)
25%ile	31 years	27 years	32 years
Age 50%ile	44 years	42 years	50 years
75%ile	57 years	56 years	68 years
% Male	60.9%	64.4%	70.3%
With known DV N=	119	94	33
25%ile	30 kph	38 kph	47 kph
DV 50%ile	40 kph	46 kph	55 kph
75%ile	45 kph	53 kph	66 kph
% hit a car	76%	65.8%	51.6%
% hit larger vehicle	17.8%	26.7%	40.6%

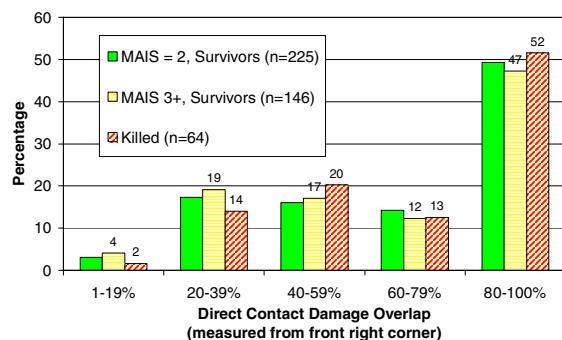


Figure 13. Percent Overlap by Driver Injury Severity

Figure 13 shows the distribution of injury severity by the percentage overlap; the injury severity is reasonably consistent within each of the offset groups, with similar proportions of MAIS =2 and MAIS 3+. Only about 36% of the killed and 40% of the MAIS 3+ survivors had an impact that was less than 60% offset.

The accuracy of the percentage overlap measured in the field is important to consider. Experienced examiners record the damage they find as accurately as practical, but it is possible for some small measurement errors to occur. A greater concern is the potential for retrospective studies to overestimate the amount of direct contact damage for cars that have rotated during the impact due to their angular momentum. When a car collides an extra degree of deformation may take place compared to the initial contact area due to rotation. This additional damage is sometimes difficult to differentiate from that caused at the initial point of contact.

This potential overestimation may affect the results of the degree of overlap shown in Figure 11 and underestimate the number of cars that are involved in impacts below 60% overlap. However, it is still believed that the most frequent type of impact has a greater overlap than the 40% used in either of the tests.

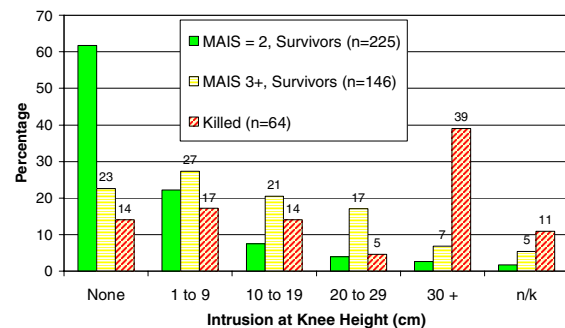


Figure 14. Facia Intrusion by Driver Injury Severity

Figure 14 shows the amount of intrusion rearwards into the compartment space at the driver's facia knee height level. Intrusion of the facia top and foot well were also considered and similar results to those shown in Figure 14 were observed. The percentage of MAIS 3+ survivors who experienced less than 10cm of intrusion at the facia top, facia knee height and foot well were 48%, 50% and 46% respectively. The percentage of killed drivers who experienced less than 10cm of intrusion at the facia top, facia knee height and foot well were 27%, 31% and 22% respectively. Significant intrusion is therefore much more common for killed drivers

than for MAIS 3+ survivors, approximately half of whom experienced less than 10cm.

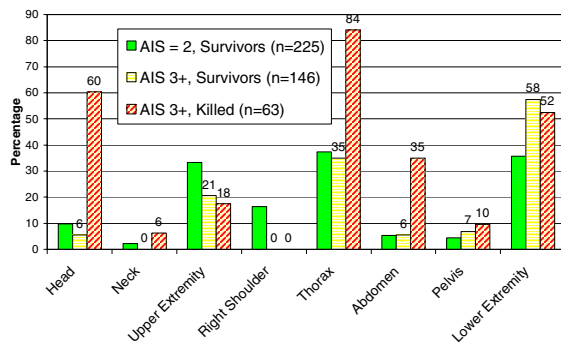


Figure 15. Rate of Driver Body Region Injury

Figure 15 shows the distribution of AIS=2 injuries by body region for the MAIS=2 group and the distribution of AIS 3+ injuries for the other two groups. One MAIS=2 driver who died was excluded from Figure 13; no Delta-V was known for this victim. AIS 3+ head and thoracic injuries are sustained much more frequently by the MAIS 3+ killed compared to the survivors. Thigh and leg injuries (lower extremities) are the most frequent AIS 3+ scores for the MAIS 3+ survivors. For the MAIS=2 drivers only, the rate of AIS 2 right shoulder injury was noted, with 16% of the casualties sustaining clavicle fractures or dislocations from seat belt webbing loading.

CONCLUSIONS

Significant numbers of fatal and rear seat passengers are excluded from this analysis due to low seat belt use rates.

The different occupant characteristics with respect to seating position are emphasised, and indicate that different dummies may potentially be required in each seat to best represent the real-world frontal impact injury population in future tests.

Frontal impacts remain the most significant crash type accounting for the majority of MAIS 2+ and MAIS 3+ car occupant casualties. Car to car impacts are the most common, although larger goods and passenger vehicles are prominent crash partners in fatal collisions.

About 80% of the fatalities (drivers and passengers) are encompassed at the EuroNCAP frontal test speed (64 kph) rising to 95% of MAIS 3+ seriously injured survivors.

Drivers, FSPs and RSPs were found to sustain injury to similar body regions, but the relative rates were different. Thorax, lower and upper extremity

injuries were identified as frequently injured body regions for front occupants.

A detailed evaluation of the cars' front structural loading found that for all 567 MAIS 2+ drivers, the offside and nearside longitudinals were both directly contacted in approximately one third of cases (31%); and the engine was also loaded in the most of these crashes (27%). A further third of the MAIS 2+ drivers were in cars with direct contact to the offside longitudinal and engine (32%).

Evaluating the amount of car frontal direct contact damage by the percentage overlap recorded by the crash investigators, found similar results to those reported from the investigation of the structural component loading. More than half of the MAIS 2+ car drivers sustain their injuries in frontal impacts with more than 40% overlap. However, further analysis of the data would be required to determine the specific nature of these crashes in order to understand their significance with respect to current test configurations.

Compartment intrusion of ≥ 10 cm is common for frontal crashes resulting in driver death, but over 80% of moderate injury (MAIS =2) and approximately 50% of serious injury (MAIS 3+) is sustained with little or no intrusion to the compartment (<10cm). Approximately a third of driver fatalities also occur in the absence of major intrusion.

For drivers, the head, thorax, abdomen and lower extremities are the main body regions injured in fatal crashes. This reduces to the lower extremities and thorax for survivors of very serious (MAIS 3+) crashes with the upper extremity particularly noteworthy among moderately injured (MAIS =2) survivors of less serious crashes. A significant proportion of the upper extremity injury was fractures or dislocations of the right clavicle from seat belt loading

Larger vehicles form a greater proportion of the collision partners for the killed compared to the survivors and are likely to be directly associated with the higher injury rates for the head, thorax and abdomen body regions

ACKNOWLEDGEMENTS

This paper uses accident data from the United Kingdom's Co-operative Crash Injury Study (CCIS) collected during the period 1998 to 2006 (Phases 6 and 7).

Currently CCIS is managed by the Transport Research Laboratory (TRL Limited), on behalf of the United Kingdom's Department for Transport (DfT) (Transport Technology and Standards Division) who fund the project along with Autoliv, Ford Motor Company, Nissan Motor Company and Toyota Motor Europe. Previous sponsors include Daimler Chrysler, LAB, Rover Group Ltd, Visteon, Volvo Car Corporation, Daewoo Motor Company Ltd and Honda R&D Europe (UK) Ltd.

Data was collected by teams from the Birmingham Automotive Safety Centre of the University of Birmingham; the Vehicle Safety Research Centre at Loughborough University; TRL Limited and the Vehicle & Operator Services Agency (VOSA) of the DfT

Further information on CCIS can be found at <http://www.ukccis.org>

8. AAAM (1990). "The Abbreviated Injury Scale. 1990 Revision." Des Plaines, Illinois 60018, U.S.A: Association for the Advancement of Automotive Medicine (AAA).

© Copyright TRL Limited 2007.

REFERENCES

1. Road Casualties Great Britain: 2005, DfT National Statistics, see <http://www.dft.gov.uk>
2. Edwards M et al. (2003). 'Development of Test procedures and Performance Criteria to Improve Compatibility in Car Frontal Collisions', Paper No. 86, 18th ESV conference, Nagoya, 2003.
3. Edwards M et al. (2007). 'Current Status of the Full Width Deformable Barrier Test', Paper No. 88, 20th ESV conference, Lyon, 2007.
4. Cuerden R W, Hill J R, Kirk A, Mackay G M, 'The potential effectiveness of adaptive restraints'. Proceedings of the 2001 International IRCOBI Conference on the Biomechanics of Impact, Isle of Man, 10-12 October 2001
5. Hill J R, Mackay G M and Morris A P (1994), 'Chest and abdominal injuries caused by seat belt loading'. Accident Analysis and Prevention, 26 (1) 11-26.
6. www.euroncap.com
7. Mackay G M, Ashton S J, Galer M D and Thomas P D (1985). "The methodology of in-depth studies of car crashes in Britain." SAE technical paper number 850556: Society of Automotive Engineers Inc. (SAE), 400 Commonwealth Drive, Warrendale, Pennsylvania 15096, U.S.A. pp. 365 390.

CHEST AND ABDOMINAL INJURIES TO OCCUPANTS IN FAR SIDE CRASHES

Brian Fildes and Michael Fitzharris
 Monash University Accident Research Centre,
 Melbourne, Australia

Hampton Clay Gabler
 Virginia Tech, Blacksburg, VA

Kennerly Digges
 George Washington University, VA

Stu Smith
 GM Holden Innovation

Paper No. 07-0384

ABSTRACT

This paper describes an analysis of collisions and injuries to occupants involved in far side collisions.

INTRODUCTION

Side impacts are particularly severe collisions, especially when the vehicle is impacted with a pole or a tree. In the USA in 2004, it was claimed that 26% of fatal crashes involved a side impact and 31% of non-fatal crashes (Resource4accidents 2005; IIHS 2003)

Estimates of the proportion of side impacts deaths in Australia are similar (25% casualty crashes, 28% fatalities and more than 30% occupant Harm (Gibson et al 2001). While the majority of Harm occurs to occupants seated on the struck side of the vehicle in both the USA and Australia, 30% does occur to those seated on the far side, that is, the non-struck side of the vehicle (Gabler et al 2005).

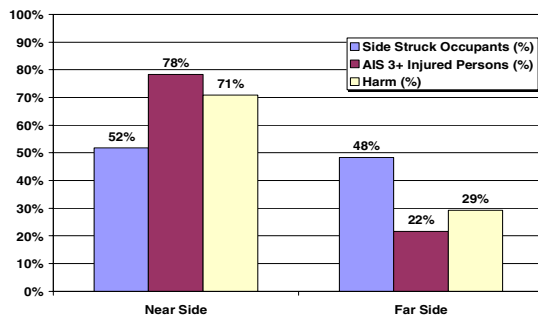


Figure 1: Near and far side injured occupants, AIS3+ injured occupants and occupant Harm (Gabler et al 2005).

Side impact vehicle regulations around the world quite rightly currently focus on near side collisions;

no provision is made for those seated opposite to the impacting source. Consequently, there are very few countermeasures available to improve far side occupant protection. Given that these occupants do experience a sizable amount of Harm in the collision, there is a real need to address this road safety problem urgently (Fildes et al 2005).

Definition

Far side occupants in a crash as explained earlier are those seated opposite to the crash as shown in Figure 2.

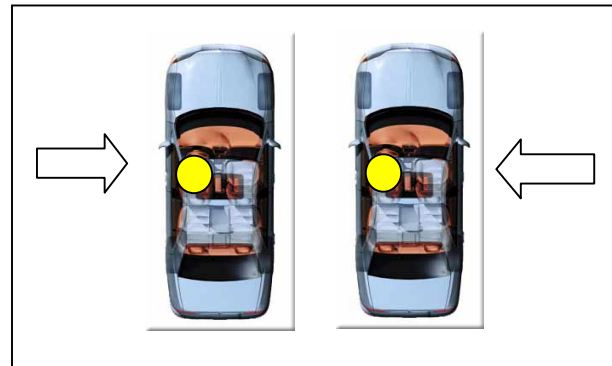
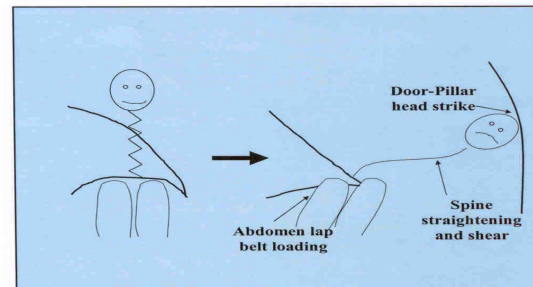


Figure 2: Position of occupants in a near side collision (on the Left) and a far side collision (Right) for a US driver.

They can be either the driver when struck on the passenger side of the vehicle or the passenger when struck on the driver's side. Near and far side definitions also apply to rear seated occupants in similar crash configurations.

Far Side Kinematics

The kinematics of occupants in far side crashes are noticeably different to those on the near or struck side (see Figure 3). Because their 3-point belt is not designed to restrain them laterally, they are thrown towards the impacting object on the struck side, some 100msec from the moment of impact (see



Fildes et al, 2002).

Figure 3 Far side occupant kinematics (Fildes et al 2002)

Study Objectives

This study set out to examine the extent of chest and abdominal injuries to occupants in far side crashes. These injuries are known to be life-threatening in side impact collisions generally and greater understanding of the Harm associated with these severe injuries will help identify opportunities for injury reduction countermeasures.

METHOD

Two in-depth databases were used in undertaking the analyses reported. In the USA, 10 years of NASS/CDS data were available for the model years 1995-2004. In Australia, 15 years of MIDS data were available for model years 1989 to 2003. Comparative analyses were undertaken using weighted data which revealed similar trends across both these databases (Fitzharris et al 2005a; 2005b, Gabler et al, 2005).

For both these databases, case selection criteria comprised the following:

- 3-Point Belt Restrained Occupants
- Front seat only
- 12 years and older occupants
- Occupant on Opposite Side of Impact
- Passenger Cars or LTV vehicles Only
- GAD = Left or Right Side
- No Rollovers

Analytical Approach

Even with such extensive databases, the number of far side cases available was rather small (106 cases in MIDS and 4570 cases in NASS/CDS) especially after slicing these data into various crosstabs. Thus, the analysis described here was essentially confined to a descriptive analysis of far side cases. For reasons of consistency, most analyses involved weighted data for both data sets.

Harm

Harm is a method of analysing crashes using frequency times the societal cost of injury as a measure of the extent of trauma. The measure used here was developed from early work in the USA by Malliaris and his colleagues during the 1980s but was extended in Australia in the early 1990s using a more reductionist approach to quantify the benefits of reducing the number of crashes or injuries (see MUARC 1992 for a more full description of the Harm approach).

In the use of the Harm method described here, Harm was expressed as a “relative” cost across all AIS and body region cells in the Harm matrix, based on the figures published in MUARC (1992).

RESULTS

Harm and AIS3+ Injuries

The first analysis undertaken here was to examine the incidence of AIS3+ injuries and Harm across all body regions for far side occupants, shown in Figure 4. Severe head injuries predominated both in terms of frequency and Harm for these far side cases. Interestingly, upper and lower extremity injuries were also quite frequent. Of particular note was that chest injuries were the fourth leading cause of Harm but the highest proportion of severe (AIS3+) injuries. This discrepancy can be explained by the low relative cost ascribed to extremity injuries in MUARC (1992). Nevertheless, severe injuries to the chest and abdomen are clearly both frequent and Harmful to occupants in far side crashes among these data.

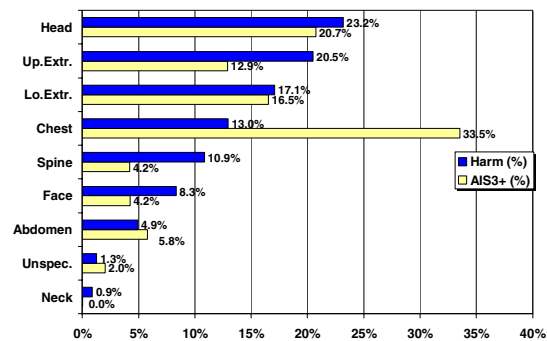


Figure 4: Harm and AIS3+ injuries for occupants in far side crashes (NASS/CDS 1995-2004)

Chest Injuries by Age

Figure 5 shows the breakdown of age across the chest injuries sustained by far side occupants in side impact collisions. While the proportion of severe chest injuries reduces as age increases among younger adults, this trend reverses for those age 70 years and older.

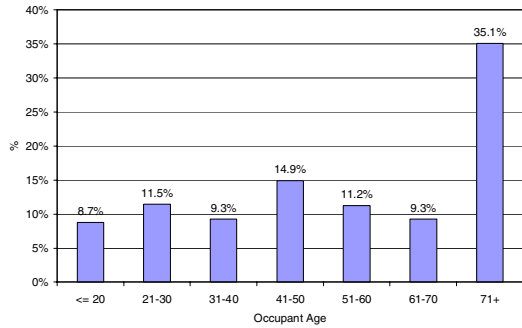


Figure 5: Distribution of occupant age for those sustaining a MAIS3+ chest injury (NASS/CDS 1993-2004)

Moreover, the pattern of injury varied across the type of crash (single vehicle vs. car-car collisions) as shown in Figure 6. Younger adults were more likely to be involved in collisions with fixed objects while older drivers were more likely to be involved in car-car collisions. Of particular note, older people were more likely to have sustained a severe chest injury than younger ones for both these collision types.

Differences between US and Australian finding here can be explained by differences in age of first licensing between these countries.

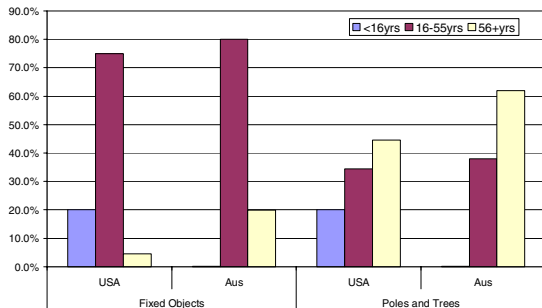


Figure 6: Distribution of occupant age by crash type (NASS/CDS and MIDS)

MAIS3+ Chest Injury Lesion

Figure 7 shows the distribution of AIS3+ chest injuries by anatomic structure in far side crashes. The rib cage and lung were most frequently severely injured, accounting for more than 80% of these AIS3+ injuries and a considerable proportion of chest Harm. Injuries to the internal organs (heart, aorta and veins) occurred in 6.9% of occupants injured in far side crashes.

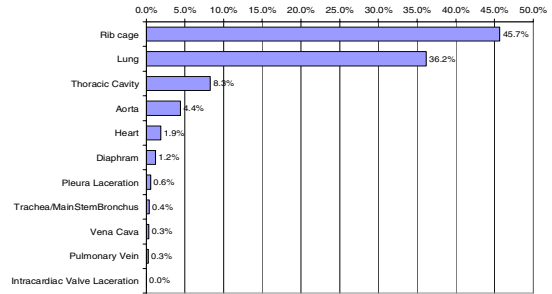


Figure 7: Distribution of AIS3+ Chest Injuries by Anatomic Structure (NASS/CDS 1995-2004)

MAIS3+ Chest Injury by Source

The sources of chest injuries are shown in Figure 8. Impact with the nearside interior, the seatbelt or buckle and the adjacent seat were ascribed to over two-thirds of the injuries, while other occupants (7.6%), the centre console (6.0) and near side door and associated components (5.4) were noteworthy sources of injuries for far side occupants.

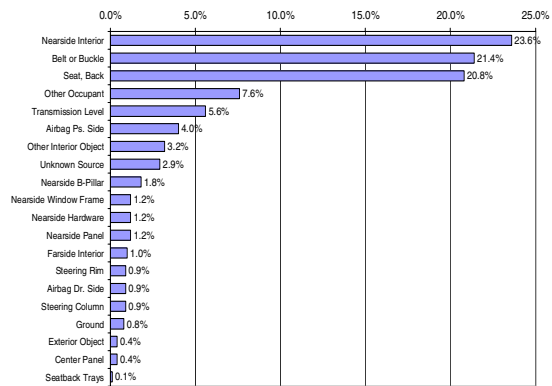


Figure 8: Source of AIS3+ chest injuries to far side occupants (NASS/CDS 1995-2004)

Abdominal Injuries

Figure 4 illustrated the extent of abdominal injuries to occupants in far side crashes. About 5% of the Harm in these crashes can be attributed to abdominal injuries which are also around 6% of the incidence of AIS3+ injuries. While these figures are less than the equivalent ones for chest injuries, they are, nevertheless, of a size to be concerned about, especially given the life-threatening nature and long-term consequence of these injuries.

Abdominal Injuries by Age

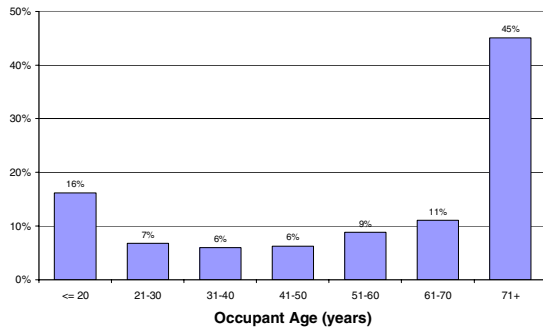


Figure 9: Distribution of occupant age for those sustaining an MAIS3+ abdominal injury (NASS/CDS 1993-2004)

The findings in Figure 9 show that the incidence of an abdominal injury is much higher for older occupants in far side crashes (they represented 45% of the population of those sustaining a serious abdominal injury). However, care should be taken in interpreting too much from this finding as there were only minimal numbers of abdominal injuries before weighting (124 AIS2+ injuries and 43 AIS3+ cases).

MAIS3+ Abdominal Injury lesions

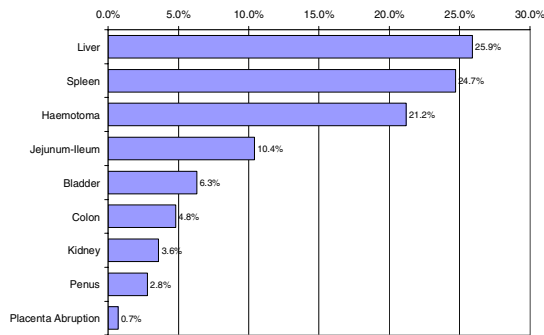


Figure 10: Distribution of AIS3+ abdominal injuries by Anatomical Structure (NASS/CDS 1995-2004)

Figure 10 shows the distribution of lesions in the abdominal area to occupants injured in far side crashes. The liver and spleen were particularly over-represented among these crash victims and to a lesser extent, kidney and colon. Haematoma including retroperitoneum haemorrhage also occurred in over 20% of the far side cases examined. These are particular nasty and severe injuries to these occupants with potential ongoing long-term consequences.

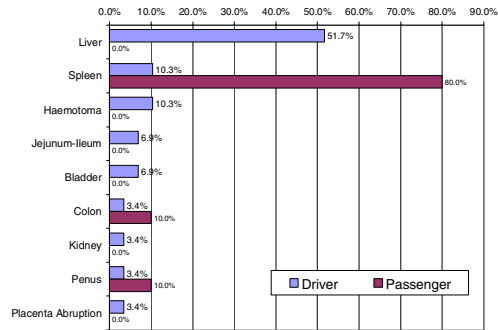


Figure 11 Distribution of AIS3+ abdominal injuries by Anatomical Structure by seating position (NASS/CDS 1995-2004)

In addition, as Figure 11 shows, the incident of lesion by seating position in a far side crash. While the number of cases here was small, it does suggest that liver injuries primarily occurred to drivers (seated on the LH side of the vehicle) and spleen injuries to front seat passengers seated on the RH side of the vehicle. These findings need to be taken with some care because of the small number of cases but do highlight an asymmetry in injury mechanism of potential importance for injury prevention.

MAIS3+ Abdominal Injury by Source

Figure 12 shows the sources of these severe abdominal injuries, where the predominant contact source was the seatbelt and buckle. This may help to explain why the liver, spleen and retroperitoneum haemorrhage were over-represented among these abdominal injuries. It might also help explain the liver and spleen asymmetry described above, too.

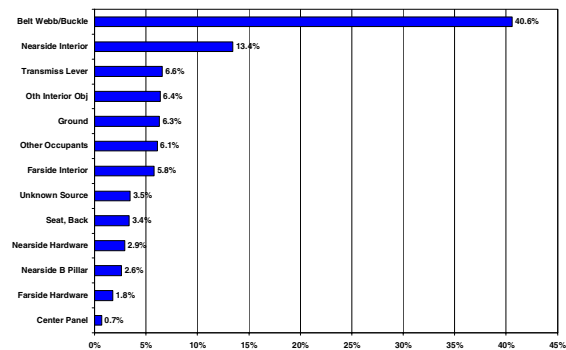


Figure 12: Source of AIS3+ abdominal injuries to far side occupants (NASS/CDS 1995-2004)

While the seatbelt and buckle assembly was the predominant cause of abdominal injury, again, other occupants featured quite highly in these far side abdominal injuries. This is difficult to explain

as supposedly all these occupants were wearing their seatbelts (a case selection criterion). This will be discussed in more detail later on.

Aorta Injuries

While aorta injuries were not specifically tested for in this far side research program, nevertheless, a number of observations were possible from the data analysis and from earlier findings.

- Aorta rupture was noted in 4.4% of occupant injuries from these far side crashes.
- Aorta injury tended to occur in low severity near- and far-side crashes.
- They were frequently occult injuries with no physiological cues.
- They frequently lead to a fatal outcome (it is estimated that 80-88% of occupants who suffer TRA die at scene of crash).
- When successfully identified and treated, there was usually complete recovery.

A previous study by Franklyn et al (2002) found that the risk of aortic injury was greater for near-side crashes than for far side crashes, and that given a near-side crash, the risk of aortic injury is greater when struck on the left rather than the right. They also found that the risk of aortic injuries is 1.4 times higher when the struck vehicle is an MPV / SUV, compared to that of another passenger car or a derivative.

DISCUSSION

These results have highlighted a number of potentially interesting findings.

First, head injury is clearly the most common injury type for occupants injured in a far side crash. Roughly one-quarter of all far side Harm involved a head injury, predominantly caused from contact with the struck side of the car or the intruding object (Gibson et al, 2001).

Chest and abdominal injury together, however, accounted for around 18% of the Harm but an alarming 40% of all AIS3+ injuries. These injuries were particularly evident among older occupants. Common lesions among chest injuries included the rib cage, lungs or the thoracic cavity, and often, these injuries were caused from contact with the nearside interior, the seat or seat back, the seatbelt or buckle, other occupants or the transmission lever.

This illustrates the ineffectiveness of the current restraint system to prevent injuries to far side

occupants in side impact collisions. As shown in Figure 3, the shoulder belt offers little restraint in this crash configuration to the chest, allowing the occupant and his or her chest to move freely out of the belt and contact a range of adjacent objects. The high incidence of seatbelt or buckle-related injuries is a matter of some concern as seatbelt is the primary means of restraint in vehicle crashes. Current designs clearly need further design improvement for far side crashes.

For severe abdominal injuries, common lesions included the liver and spleen and retroperitoneum haemorrhage or haematoma. Interestingly, the incidence of liver injuries was higher for the driver and the spleen, higher for the front passenger among US crashed vehicles. The seatbelt or buckle was seen to be the most common source of abdominal injury by far. Current generation buckles and tongues were designed primarily for frontal crashes over decades ago and from these results, suggest they are not optimised for far-side protection. Improvement to the restraint capabilities of the seatbelt in a far side crash would seem to be warranted from these findings, although some care needs to be taken with these findings given the small number of cases involved.

Older Occupants

Older occupants appeared to be over-represented in far side crashes. Those aged over 60 years sustained high numbers of chest and abdominal injuries, which is not too surprising from earlier research (Foret-Bruno et al, 1998; Zhou et al, 1996; Augenstein 2001; Kent et al 2005; Welsh; 2006). This can be explained from their frailty and especially brittle bony structures that fracture relatively easily (reference). Interestingly also, older drivers seem to be more involved in car-car intersection crashes than their younger counterparts who were more likely to be injured in a single-vehicle far side crashes with poles and trees. The over-involvement of older people in intersection crashes has also been reported elsewhere (Oxley et al 2006; Eberhard 2007) and confirms earlier reports that older people have difficulty judging when to turn in front of oncoming traffic (Andrea 2003).

Other occupants

Other occupants were seen to be a source of chest and abdominal injuries to occupants relatively frequently in these far side crashes (chest 7.6% and abdomen 10.2%). Given that the 2-occupant exposure rate in the front seat is around 20%

(Fildes et al, 2002), this suggests that occupant to occupant contacts are a major problem in side impacts when both front seats are occupied (up to 5 times the rate for this seating configuration).

It is not clear from these data however how the near side occupant can inflict damage to the far side occupant's abdomen as these occupants were all belted. It may be that the struck-side occupant is pushed into the far side occupant during the kinematic movement during the crash although generally, the far side occupant is still in contact with the seat through the lap belt. Alternately, the near side occupant's arms and legs seem to flail considerably in side impacts and they could play a role in these injuries. This warrants further investigation in helping determine ways of minimising these serious injuries.

Aorta

Aorta rupture was noted in 4.4% of occupant's chest injuries from these far side crashes. These are serious injuries that frequently lead to death. It is estimated that 80-88% of occupants who suffer TRA die at scene of crash. However, when successfully identified and treated, there was usually complete recovery (Digges and Augenstein 2006).

The injury mechanisms for these potentially fatal injuries are not well known for far side occupants. Digges and Augenstein (2006) argued that they commonly occur in low severity near-side crashes and are frequently occult, that is, there are no physiological cues.

They claimed that in nearside crashes, they tend to occur to front seat occupants, those sitting on the struck side of the vehicle and usually when their vehicle is struck by another vehicle, rather than a fixed object or pole. They propose that the thorax is impacted by a force component from the front; it experiences a severe vertical spinal stretching that causes the artery to stretch and fracture. Clearly, more research is needed to understand how these injuries occur to far side occupants.

COUNTERMEASURE OPPORTUNITIES

The results from this analysis highlight a number of possibilities for reducing injuries through improved vehicle design.

Restraint Systems

The obvious strategy for improving far side occupant protection is to better restrain the occupant in the seat. It was clear from these results

that a 3-point seatbelt alone is not sufficient for far side occupant protection. Across-belt configuration involving an additional belt on the inward side was proposed by Fildes et al (2003) as a possible measure to restrain the far side occupant, along with an additional side support on the seat. However, they argued that this configuration was not necessarily optimal as it had the potential to apply additional load to the occupant's neck.

Rouhana (2004) published an alternative 4-point belt configuration, which could also have the potential to provide improved restraint in a side impact. However, it is understood that this belt system has been primarily designed for frontal crashes and needs to be evaluated for improved protection for near and far side occupants in a side impact collision.

Physical Separation

A number of other opportunities exist for improved far side protection. A more scalloped seat, in conjunction with a pretensioned belt system might be an option, as well as side supports on the seat and even an internal seat-mounted airbag system (inflatable inboard torso side-support; Bostrom and Haland 2003). The efficacy of these systems, though, is still to be firmly established.

Test and Injury Criteria

Importantly, though, it is fundamental that injury criteria and test methods need to be determined to provide governments and auto manufacturers with the necessary tools to develop new and innovative in-vehicle solutions to protect far side occupants in these crashes.

Older Occupants

It is unlikely that any generic in-vehicle solution will suit all occupants. Older people are more frail and suspect to a poor outcome, especially in a side impact collision (Augenstein 2001). Thus, the best solution for them (and indeed for all vehicle occupants) is to prevent the crash from happening in the first place. The evidence collected here showed that older people were more likely to be severely injured in an intersection crash. Road design and traffic management solutions are desperately required here to address this problem.

CONCLUSIONS

This analysis set out to examine the extent of chest and abdominal injuries to occupants in far side crashes, that is, side impact crashes where the

occupant is seated on the opposite side of the vehicle to the side where it is impacted. This is commonly referred to as the non-struck or far side seating position. The study also aimed to examine a range of potential countermeasures to prevent or mitigate these injuries.

It is clear that side impact collisions are severe events with little room for energy management, compared with frontal crashes. While the current focus on side impact protection is for the nearside occupant, there is clearly a need to address ways of providing greater protection for the far side occupant.

Current restraint systems do not offer optimal restraint for far side occupants. A number of possible opportunities exist for better restraining them in a side impact collision for which more research and development effort is needed.

Limitations

This analysis suffered from small in-depth case numbers in spite of the use of one of the largest in-depth databases available. Combining additional case details from other databases would be useful in addressing this shortcoming.

REFERENCES

Andrea DJ. The effects of age on judgements of vehicle motion, Unpublished PhD thesis, Monash University, Melbourne, April 2003.

Augenstein J. Differences in Clinical Response between the Young and the Elderly. Paper presented at the Ageing and Driving Symposium, Association for the Advancement of Automotive Medicine, Des Plaines, IL. February 19-20, 2001.

Bostrom O. and Haland Y. Benefits of a 3+2 point belt system and an inboard torso side support, Paper No. 451, Enhanced Safety of Vehicles conferences, Nagoya, Japan, May 2003.

Digges KH and Augenstein J. Research to determine the causes of aortic injury in nearside crashes, NCAC, The George Washington University, Virginia, & William Lehman Injury Research Center, Miami.

Fildes BN, Sparke LJ, Bostrom O, Pintar F, Yoganandan N & Morris AP. Suitability of current side impact test dummies in far-side impacts, Proceedings of the IRCOBI Conference, Munich Germany, September 2002.

Fildes BN, Bostrom O, Haland Y. and Sparke L. Countermeasures to Address Far-Side Crashes:

First Results, Paper No. 447, Enhanced Safety of Vehicles conferences, Nagoya, Japan, May 2003.

Fildes BN, Linder A, Douglas C, Digges K, Morgan R, Pintar F, Yoganandan N, Gabler HC, Duma S, Stitzel J, Bostrom O, Sparke L, Smith S, Newland C. Occupant Protection in Far Side Crashes, Paper No. 05-0299, Enhanced Safety of Vehicles conferences, Washington DC, May 2005.

Fildes B, Fitzharris M, Koppel S, & Vulcan P (2002), 'Benefits of seatbelt reminder systems', Report CR 211, Australian Transport Safety Bureau, Canberra.

Fitzharris M, Scully J, Fildes BN and Gabler HC. On the Weighting Of In-Depth Crash Data, Internal MUARC Report, Monash University Accident Research Centre, Clayton, Australia 2005a.

Fitzharris M, Scully J, and Fildes BN. Comparative analysis of Australian and US weighted in-depth crash data, Presentation to ARC Far Side Consortium, George Washington University, June 2005b.

Foret-Bruno J-Y, Trosseille X, Le Coz J-Y, Bendjellal F, Steyer C, Phalempin T, Villeforceix D, Dandres P, & Got C (1998), 'Thoracic injury risk in frontal car crashes with occupant restrained with belt load limiter', 42nd Annual STAPP Car Crash Conference, SAE Paper 983166; Society of Automotive Engineers, Inc., Warrendale, Pennsylvania, USA.

Franklyn, M., Fitzharris, M., Fildes, B., Yang, K., Frampton, R. & Morris, A. (2003) 'A preliminary analysis of aortic injuries in lateral impacts', *Traffic Injury Prevention*, **4** (3), pp263-269

Gabler, H.C., Fitzharris, M., Scully, J., Fildes, B.N., Digges, K. and Sparke, L., Far Side Impact Injury Risk for Belted Occupants in Australia and the United States, Proceedings of the Nineteenth International Conference on Enhanced Safety of Vehicles, Paper No. 05-0420-O, Washington, DC June 2005.

Gibson, T., Fildes, B., Deery, H., Sparke, L., Benetatos, E., Fitzharris, M., McLean, J. & Vulcan, P. *Improved side impact protection: a review of injury patterns, injury tolerance and dummy measurement capabilities*, Report 147, Monash University Accident Research Centre, Clayton, Australia, 2001.

IIHS (2003). Side airbags that protect the head reduce driver fatalities by 45 percent, *Status Report Vol 38* (8), August 26, 2003.

Kent R., Henary B. and Matsuoka F. On the fatal crash experience of older drivers, Proceedings from the 49th Annual AAAM Conference, Boston, Mas., September 12-14, 2005.

Monash University Accident Research Centre 1992. Feasibility of occupant protection measures, Report CR100, Federal Office of Road Safety, Canberra.

Oxley J, Fildes BN, Corben B. and Langford J. Intersection design for older drivers, J. Transportation Research Part F: Traffic Psychology and Behaviour (Special Issue - Older Road Users, **9F (5)**, 335-346.

Resource4accidents, www.resource4accidents.com

Rouhana SW, Kankanala SV, Prasad P, Rupp JD, Jeffreys TA, and Schneider LW. Biomechanics of 4-Point Seat Belt Systems in Farside Impacts, Stapp Car Crash Journal, **Vol. 50** (November 2006), pp.

Welsh R. Morris AP., Hassan A. and Charlton J. Crash characteristics and injury outcomes for older passenger car occupants, J. Transportation Research Part F: Traffic Psychology and Behaviour (Special Issue - Older Road Users, **9F (5)**, 322-334.

Zhou Q, Rouhana S W, Melvin J W, (1996), 'Age effects on thoracic injury tolerance', Proceedings of the 40th STAPP Car Crash Conference, SAE Paper 962421. Society of Automotive Engineers, Inc., Warrendale, Pennsylvania, USA.

INVESTIGATION INTO THE EFFECTIVENESS OF ADVANCED DRIVER AIRBAG MODULES DESIGNED FOR OOP INJURY MITIGATION

Jörg Hoffmann

Michael Freisinger

Toyoda Gosei Europe N.V.

Germany

Mike Blundell

Manoj Mahangare

Faculty of Engineering and Computing, Coventry University

United Kingdom

Peter Ritmeijer

TNO Automotive Safety Solutions

Netherlands

Paper Number 07-0319

ABSTRACT

In accordance with National Highway Traffic Safety Administration (NHTSA) regulations and, in particular the Federal Motor Vehicle Safety Standard (FMVSS) 208 for the protection of vehicle occupants from a deploying airbag, the development of frontal restraint systems is driven by new technologies and technical solutions to cover the challenging out-of-position (OoP) load case. Considering the subject of the driver airbags, traditional module technology addressed only the energy absorption capability to protect the driver occupant while in-position for a severe frontal crash load case. The early unfolding characteristics of the deploying airbag and its physical effects on the environment did not therefore form part of the engineering focus at that time. This paper will discuss an advanced driver airbag (DAB) module devised to deploy in an initially less aggressive mode, thereby exposing occupants seated OoP and close to the airbag's effective working area to less risk. The airbag inflation is divided into a primary and a secondary deployment phase by chambering the cushion with internal gas deflection fabric walls. After reaching an internal threshold pressure, these walls fail at a predetermined energated split line. This leads to full bag deployment to ensure full energy absorption potential for the occupant seated in-position during the crash loading. This sophisticated deployment characteristic is simulated using a numerical approach to represent the actual fluid flow within the airbag to reproduce the airbag's initial unfolding process. Initial simulations

recreate a simple physical (pendulum) laboratory test scenario. Further consideration of the OoP performance of the advanced airbag module is provided by replacing the simple pendulum with the more complex digital female frontal dummy positioned in accordance with the FMVSS 208 standard. Finally, the results obtained using the advanced airbag occupant simulation methodology are compared with the results of OoP occupant tests.

Keywords: Airbag, OoP, MADYMO, CFD, Gasflow

INTRODUCTION

Studies indicate that airbags have reduced deaths in frontal crashes by about 26 per cent for belted drivers and by about 32 per cent for unbelted drivers [1]. Fatalities in frontal crashes have also been further reduced by 14 per cent for belted and by 23 per cent for unbelted passengers [2]. The National Highway Safety Administration (NHTSA) estimates that as of May 1998, airbags had saved nearly 3 000 lives in the United States [3]. Thus, airbags are effective in reducing the risk of death and injury associated with many severe frontal car crashes.

Despite overall effectiveness, real-world experience has shown that some unbelted (OoP) occupants are being injured and even killed by deploying airbags. As of May 1998, NHTSA attributed 99 deaths in low-severity crashes to airbag inflation energy. These deaths include 38 adult drivers, 4 adult passengers (a

belted 98-year-old female and an unbelted 88-year-old female, an unbelted 57-year-old male and an unbelted 66-year-old female, 44 children aged 1-11 and 13 infants (10 restrained in rear-facing infant seats and 3 seated on adult passenger laps). In response to these side-effects of an airbag in low- and moderate-severity crashes, FMVSS 208 issued by NHTSA in May 2000, proposed that static OoP tests should be a mandatory requirement starting in 2003 [4]. These tests include performance requirements to ensure that airbags developed in the future do not pose an unreasonable risk of serious injury to OoP occupants. For the driver side, there are two static OoP test positions using a 5th percentile female dummy as illustrated in the following Figure 1.

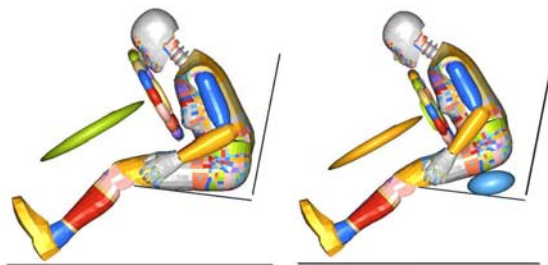


Figure 1. Dummy posture for driver-side OoP test according to FMVSS 208

To achieve occupant protection during a crash using a fully-deployed airbag to dissipate the frontal crash forces experienced by the driver over a larger body area and gradually decelerate the occupant's head and torso to prevent contact with other interior surfaces, the airbag itself must deploy rapidly in less than 50 milliseconds. Consequently, an occupant positioned extremely close to the airbag module at the time the airbag begins to inflate is exposed to highly localised forces [5]. Two phases of airbag deployment have been associated with high, injury-causing localised forces: the punch-out phase and the membrane-loading phase [6]. The punch-out phase occurs before or immediately after an airbag escapes from the module. If this escape is blocked by an unconscious driver slumped over the steering wheel, the resulting high force is concentrated on that part of the driver blocking the airbag's deployment path. The membrane-loading phase occurs after the airbag is out of the module. The injury-causing forces during this phase result from a combination of the airbag's internal pressure and the tension forces arising from the inflating airbag wrapping around the occupant.

To address the low risk deployment requirement of the FMVSS208 standard, the following parameters, which influence the functional design process of restraint systems, should be considered:

- Inflator (dual-stage, mass flow characteristic, diffusers, gas outlets, power) [7],
- Cushion geometry (chambered, vents, straps, mounting) [8],
- Folding pattern [9],
- Airbag door opening (tear seam geometry, material) [10].

To cover the FMVSS208 occupant OoP load case on the driver's side, Toyota Gosei has developed an advanced airbag design that features a cushion geometry which is initially separated into two chambers by internal tethers. Targeting a less aggressive primary deployment (punch-out phase) as well as a less aggressive radial secondary deployment (membrane-loading phase), the following Figure 2 explains the deployment characteristics of the advanced cushion compared to a conventional cushion.

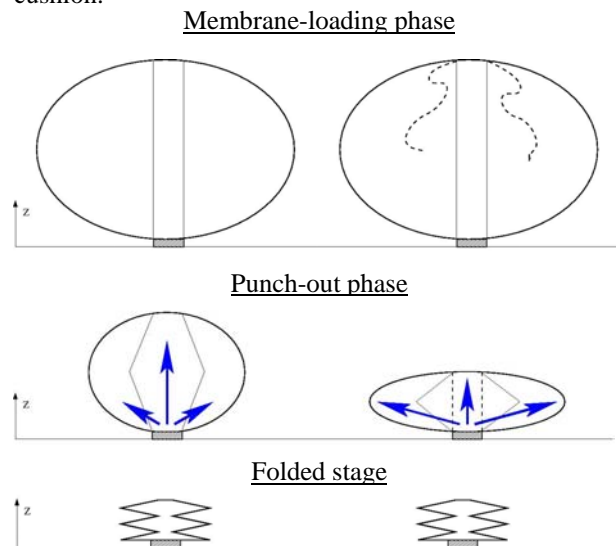


Figure 2. Deployment phases of a conventional airbag design (left) versus the advanced airbag design (right)

On the left, the deployment kinematics of a conventional DAB are shown to be directed mainly towards the occupant. By contrast, the advanced airbag deploys more laterally in the plane parallel to the occupant's head (right). If the internal pressure increases to a certain threshold, the internal chamber walls will rupture. This leads to the full deployment that would be needed to cover the kinetic energy absorption at in-position load cases including the conventional tethers. Because at the same time local low risk deployment and global restraint performance must be guaranteed, the design of the advanced airbag must meet the conflicting objectives of keeping the released energy as low as possible, while

at the same time maintaining acceptable crash protection performance.

The only plausible solution to master this challenge makes use of CAE simulation processes which help to find an optimised compromise between risk and protection as discussed in [11]. For frontal restraint systems, occupant protection CAE methods based on Finite Element Modeling (FEM) and Multi-Body-System (MBS) have evolved into powerful tools with a high degree of maturity. Unlike protection situations where interaction between the airbag and the occupant does not occur until the airbag is fully deployed, in risk situations, the occupant interacts with the airbag at an early stage of deployment. Typical characteristics of an OoP airbag simulation model, which covers the early inflation of a folded airbag, are listed in accordance with [12] as follows:

- highly unsteady phenomenon,
- wide range of gas flow speeds (supersonic to transonic),
- coupled moving boundaries of the airbag interact with gas flow and deform in space and time,
- unfolding of a folded airbag (contact characteristics).

Safety system engineers studied the inflation process of fully folded airbags based on uniform pressure (UP) distribution within the airbag volume [13] at quite an early stage. The implementation of real gas flow computer fluid dynamics (CFD) approaches, combined with improved contact algorithms in the safety system simulation tools Ls-Dyna, Pam-Crash and Madymo, that are commonly used in the industry, was mainly driven by the FMVSS 208 standard issued by NHTSA in 2000 (please refer to [14], [15], [16], [17] and [18]).

As a world-wide standard in restraint system simulation, the study accompanying CFD advanced airbag simulations has been performed with Madymo 6.3.1 release [19]. The underlying numerical airbag model setup has been activated by the state-of-the-art capabilities of the Madymo integrated CFD Gasflow (GF) Module at the start of the presented study (please refer to [20], [21] and [22]). The effectiveness of the advanced airbag technology is investigated with the help of the advanced airbag CAE simulation methodology derived throughout the study and recorded also in [23], [24], [25].

The current paper documents the DAB module model setup and validation, and describes the findings applying the advanced simulation method to the OoP

occupant load case. Using the GF simulation method, the predicted dummy injury values are objectively compared to the ones observed in a real laboratory test. Questioning the quality of prediction, the potential of the CFD advanced airbag simulation method in terms of the development of new future technologies is discussed finally.

DAB MODEL

Analog to the main functional design parameters for finding an optimum solution for low-risk airbag deployment, the implementation of the most important physical properties of an OoP airbag model (inflator characteristics, cushion, folding, airbag door) are explained briefly within this chapter. The deployment characteristics of the advanced initially chambered DAB are discussed based on GF analysis and the model validation to dynamic pendulum deployment tests is explained in the final paragraph.

Inflator

The input to the airbag models is stated in terms of inflator exit gas temperature and mass flow rate. This input was generated using the MADYMO Tank test Analysis (MTA) programme which was used to convert experimental data for the ignition of the inflator in a closed tank to mass flow rate and temperature input (the empirical thermodynamic approach is explained in [26]). This data was validated by carrying out a 3-D tank test simulation (GF and uniform pressure (UP)) which was then compared to the experimental tank test records as shown in Figure 3. Please note that the pressure and time have been normalised to provide dimensionless units on the axis.

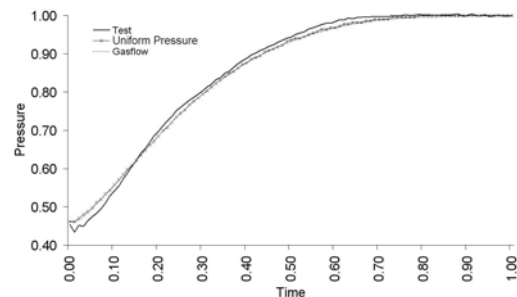


Figure 3. Tank pressure validation (GF and UP)

The above tank validation example shows the GF and UP pressure simulation time history versus the experimental pressure response of a single-stage

inflator output. Dual-stage output was applied for OoP application.

Cushion geometry and material

The fabric of the airbag was constructed using a FEM representation comprising the real geometry of the cushion. The whole airbag was split into two main chambers (2) and (3) during the modeling process (the additional chamber (1) was a dedicated chamber for the inflator). The inner chamber (2) represents the jet control in the early phase of deployment and the chamber (3) represents the remaining ring volume (please also refer to Figure 4 below).

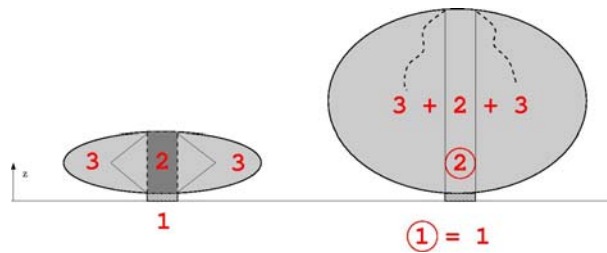


Figure 4. Initially chambered model before (left) and after (right) the rupture of the sacrificial tether

The initial two-chambered airbag evolves into a single-chambered airbag after the rupture of the sacrificial tether structure. Figure 5 shows the flat numerical model compared to the physical airbag.

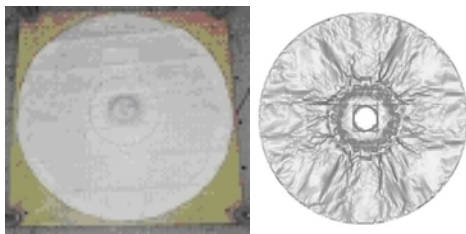


Figure 5. Physical flat airbag cushion (left) and the corresponding CAE model (right)

To cover the warp and weft fabric direction in the FEM model, the orthotropic fabric material model was implemented for the cushion as originally developed within [27]. Elastic fabric tensile material properties of the warp and weft direction were obtained from relevant tensile tests (possible test scenarios can be found in [28], [29]).

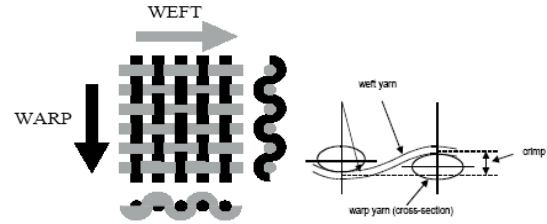


Figure 6. Warp and weft directions in woven fabric construction

Test matrix - The following material tests have been conducted (please refer to Table 1 below).

Table 1. Fabric material test matrix

Test	Static	Dynamic	Remarks
Tensile	X	X	Warp and weft
Bias	X	-	Picture frame

Bias tests were performed to identify the typical shear deformation mechanism that occurs in a plain-woven fabric as shown in Figure 7.

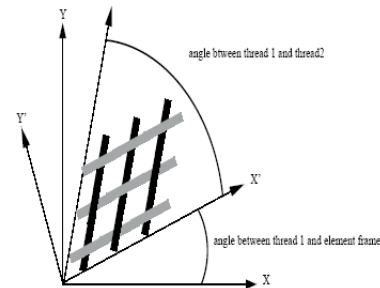


Figure 7. Shear deformation of woven fabrics [30]

The warp and weft yarns typically displace in a trellis-like manner under shear loading with little resistance until the yarn compaction or “lockup” angle has been reached which corresponds to an initial soft response of the fabric. The lockup angle is dependent on the yarn spacing and the geometry of the weave pattern.

Picture frame testing validation - To load the fabric specimen in shear direction, the following test setup with a picture frame was applied (see Figure 8).

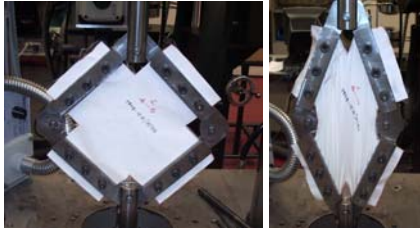


Figure 8. Picture frame test setup

The warp and weft thread properties incorporated from the tensile tests, together with the theoretically derived bias curve, lead to the following simulation of kinematics time history.

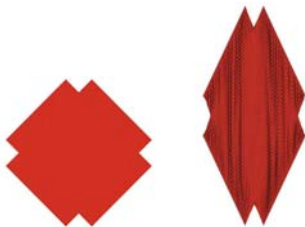


Figure 9. Picture frame simulation time history kinematics – non-deformed (left), deformed (right)

As observed in the test, the wrinkling of the fabric specimen also occurs in the simulated deformed frame. The diagram below shows the force-displacement response measured in the test versus the simulation time history curve.

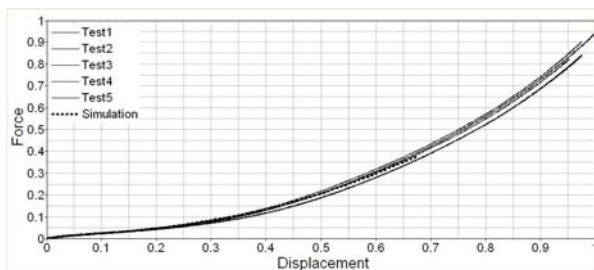


Figure 10. Picture frame force displacement

Although the MBS structure of the frame model was restricted to a determined shear movement, the simulation time history is closely validated to the test response.

Folding pattern

Folding is one of the most difficult tasks in an OoP simulation using CFD techniques. The flat 2-D cushion, which contains the main panels, internal chamber walls and conventional tethers leads to a stack of multiple fabric layers after folding. The

folded package cut view in Figure 11 gives an indication of the challenging folding task to be performed with the Madymo folder software [31].



Figure 11. Folded cushion package cut view with inflator gas opening locations (arrows)

The inflator is modeled with multiple radial jets at the gas opening locations. The bag retainer (turning vane) also deflects gas and is therefore included in the simulation model. It is omitted only initially to implement the inflator jets in a vertical direction, as was previously examined in [32]. To cover the folded package dimensions of the real folded cushion fabric and to increase the surface ratio (initial mesh to reference mesh), a pre-simulation must be performed as described in the next paragraph. Handling folded FEM airbag cushions with the initial metric method (IMM) is further explained in [33].

Folded package pre-simulation - To implement the folded cushion into the bag holder, the dynamic relaxation shown in Figure 12 below is applied as a type of pre-simulation.

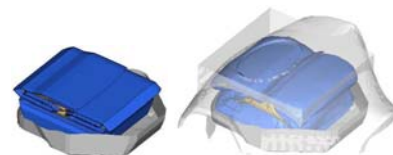


Figure 12. Cushion after folding (left) and the piston method mesh relaxation with boundary surfaces (right)

The dimensions of the folded package are restricted by a quadratic cube, the bag holder and the piston-like moving airbag door structure. The final relaxed mesh state of the pre-simulation leads to the folded cushion, which is finally implemented into the DAB module model.

Assembled DAB module - Figure 13 shows the folded cushion integrated in the bag holder and inflator model, as the assembled DAB module compared to the real hardware.

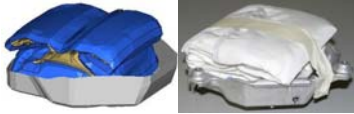


Figure 13. DAB model (left) and the hardware folded cushion package (right)

Airbag door

It is evident that the strength of the airbag door tear seam can have an impact on the punch-out phase of airbag deployment and therefore has a great influence on OoP load generation. Within the virtual state-of-the-art instrument panel development by structural FEM analysis, the airbag door characteristics also play a significant role. Therefore derivation of the elastic-plastic material properties is possible in accordance with the procedures described in [34]. Implicit structural FEM analysis (stress-strain analysis) as explained in [35] is also commonly applied within IP development. This approach was not applied within this study, but derivation of the material parameters with the help of physical tests helped to define practical experiments.

Test matrix - Table 2 provides an overview of the tests conducted.

Table 2. Airbag door material test matrix

Test	Static	Dynamic	Remarks
Tensile	X	X	Injected specimen
Tensile	X	X	Cut specimen
Impact	-	X	Full airbag door

The tensile test response of the injected specimen was used to implement the elastic-plastic properties. The test with the specimen cut from the airbag door identified the properties of the tear line. The airbag door-opening characteristic was then studied when a rigid impactor (simple airbag substitute) opened the tear line dynamically from the back.

Tensile testing validation - injected specimen - As an abstract of the tensile tests, Figure 14 through 16 below illustrate the injected plastic specimen and the static and dynamic test response versus the simulation force-displacement time history.

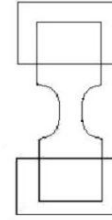


Figure 14. Injected plastic tensile specimen

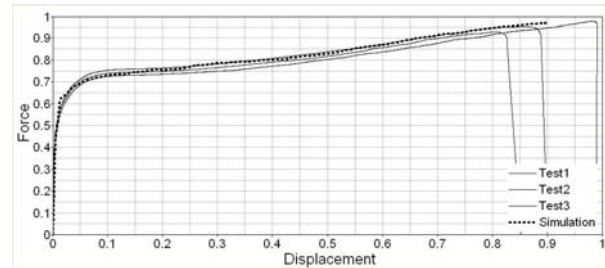


Figure 15. Static tensile force-displacement

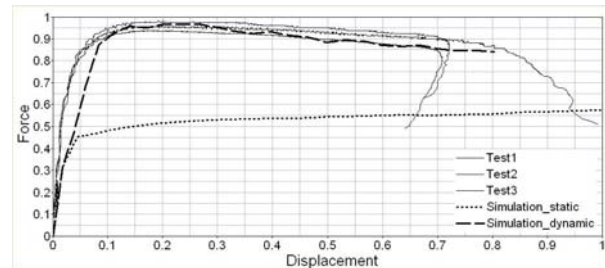


Figure 16. Dynamic tensile force-displacement

The derived plastic material model was then implemented into the full-size FEM model of the airbag door, which was validated in a dynamic impactor scenario as already mentioned above.

Full airbag door impactor testing validation - The dynamic test was conducted at high and low impactor velocities. In Figure 17, the simulation time history (left) and the test response (right) are shown for high velocity at 30 and 40 ms.

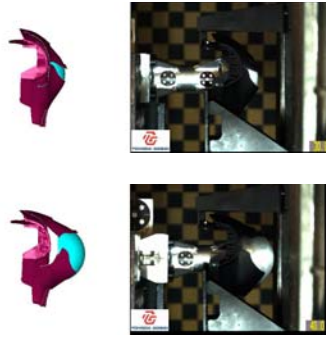


Figure 17. Airbag door-opening model at high impactor velocity; upper plot: at 30 ms; lower plot: at 40 ms

Door-opening kinematics are covered at both time points. To assess the accuracy of the simulation model, the impactor acceleration test response (during the opening process) was compared with the simulation acceleration time history (see Figure 18 below).

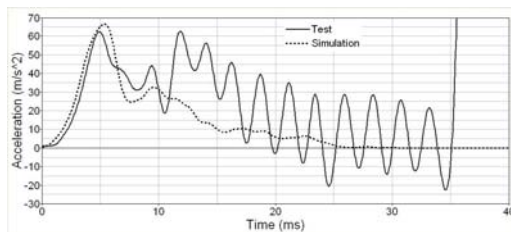


Figure 18. Impactor acceleration – at high velocity

The acceleration peak level at the moment of the tear line rupture – corresponding to the punch-out phase explained earlier – is also covered by the simulation. The further decrease in loading can also be seen, whereas friction between the impactor and the airbag door leads to some differences in test response and simulation time history.

The same scenario was also verified for a lower level impactor velocity. First the simulation time history (left), and then the test response (right), are pictured in Figure 19 at 60 and 70 ms.

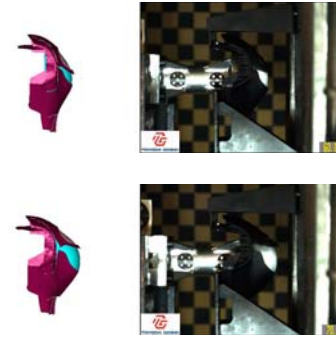


Figure 19. Airbag door-opening model at low impactor velocity; upper plot: at 60 ms; lower plot: at 70 ms

The tear line opening mode and acceleration peak for the lower impactor velocity are again reproduced by the simulation.

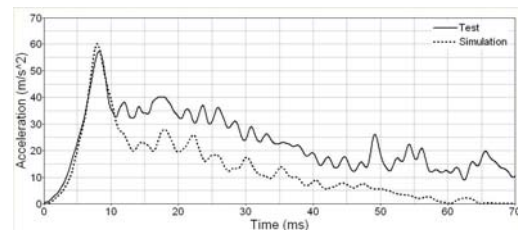


Figure 20. Impactor acceleration – at low velocity

Further, the acceleration peak level at the moment of the tear line rupture is covered by the simulation at the low impactor velocity. The further decrease in loading can be seen again, whereas friction between the impactor and the airbag door leads to some differences in test response and simulation time history.

DAB Simulation validation

Before discussing validation of the advanced DAB module in a simple physical pendulum environment, deployment of the flat airbag will be explained to analyse the real gas flow from the inflator to the initially chambered internal airbag volume. To dynamically validate the simulation model against a physical test, the airbag was made to hit a head form pendulum during the initial inflation (punch-out) phase. The acceleration test response was compared to the simulation time history obtained.

Gas flow control - To obtain an idea of the real gas flow within the chambered airbag volume, the non-folded flat airbag was statically deployed with single-stage inflator output.

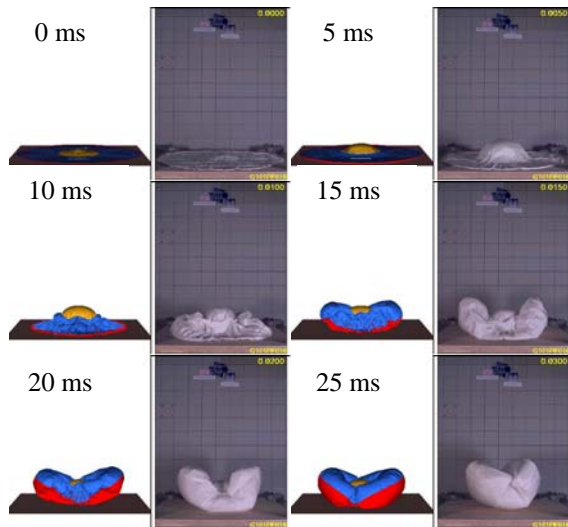


Figure 21. Deployment kinematics comparison for the first 25 ms of the real airbag and the simulation model

The inner tethers restrict the airbag's deployment throughout the 25 ms time. The accumulated internal pressure does not exceed the threshold to allow the sacrificial tether rupture. During the first 10 ms, hardly any gas is transported from the inner to the outer airbag chamber. Between 10 ms and 15 ms, the gas starts to move to the outer chamber, giving the deployed airbag a U-shape form, which is also effected by the outlet geometry between the airbag chambers.

A further academic comparison between the advanced airbag and a virtual conventional airbag (removed inner tethers) model was performed to analyse the gas jet path with the help of CFD result visualization. The calculated gas velocity vector plots are a good indication of the gas path as shown in Figure 22 below.

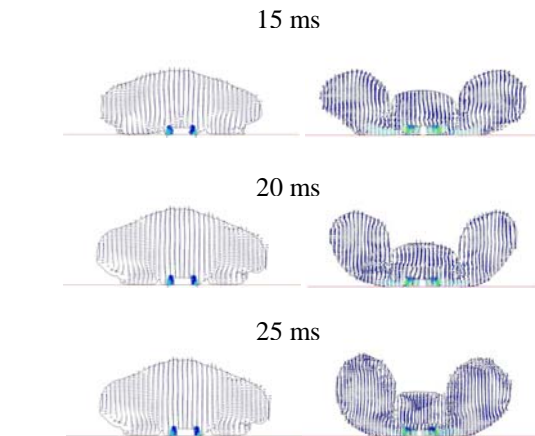
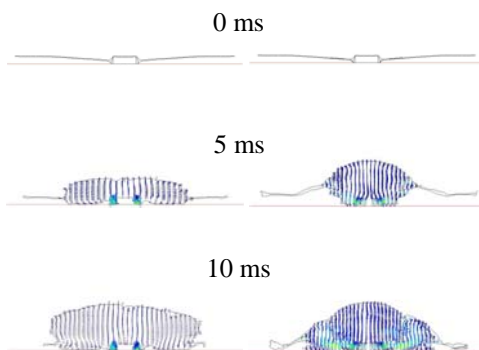


Figure 22. Comparison between the flat conventional (left) and flat advanced airbag (right) deployment kinematics in the first 25 milliseconds – CFD velocity vector plots

During the first 15 ms –indicated here as the punch-out phase - the vector plot clearly illustrates the difference between both airbag designs. Whereas the airbag's inner chamber is filled first and the inflator gas starts to flow to the outer tether at approx. 10 ms, the gas flow is not re-directed in the conventional cushion. If 15 ms to 25 ms could be indicated as the membrane-loading phase, the above plot shows the significant difference of the airbag expansion distance at the centre of both bags.

A brief analysis of the academic example suggests the GF CFD airbag simulation potential to provide detailed evaluation of the real gas flow within, here the chambered airbag volume. This advanced simulation method constitutes a powerful tool to evaluate, features such as orifice geometry and location to further optimise the low risk airbag deployment functionality.

DAB model validation - Dynamic head form pendulum tests were performed to validate the DAB module model with the equipped airbag door. At a defined close distance, the airbag hits the head form during the initial deployment phase. Figure 23 shows the simulation animation (left) versus the test (right).

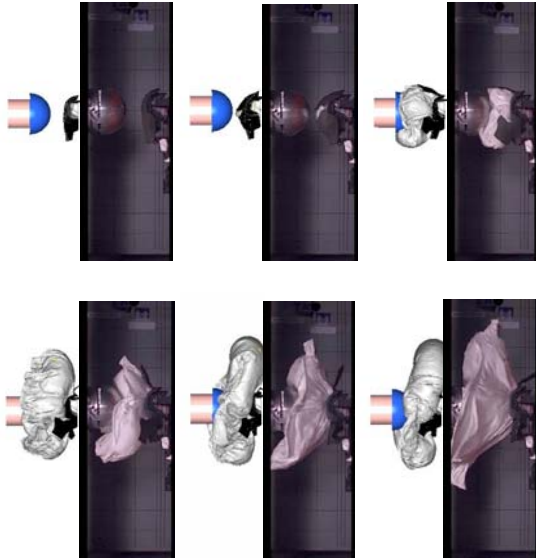


Figure 23. Head form simulation (left) versus test (right) – initial deployment – 0ms to 10 ms in 2ms steps

The simulation supplies a realistic airbag door-opening mode together with reasonable cushion deployment kinematics. The pendulum acceleration time history and the test response are compared in the following diagram (Figure 24).

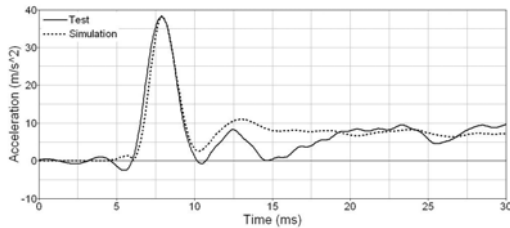


Figure 24. Head form acceleration test response versus simulation time history

The punch-out acceleration peak is covered by the simulation model. The validated DAB module model was applied in the OoP occupant simulation as discussed in the next paragraph. The resulting dummy injury values are expected to provide an indication of the airbag membrane-loading phase explained above.

OOP OCCUPANT TEST

To verify protection in an OoP situation, three different options can be considered in development according to FMVSS 208, whereby the major OoP

option applied by automobile manufacturers is the so-called “low risk deployment”. In the following Table 3, which contains the FMVSS 208 OoP injury value limits, this is referred to as “static”.

Table 3. FMVSS 208 OoP injury value limits

AF05 injury criteria limits		Crash	Static
Head	HIC15 [-]	700	700
Neck	Nij [-]	1.0	1.0
	Tension [N]	4287	3880
	Compression [N]	3880	3880
	Flexion [Nm]	155	155
	Extension [Nm]	67	67
	Max tens. [N]	2620	2070
	Max comp. [N]	2520	2520
Chest	Accel. 3 ms [g]	60	60
	Deflection [mm]	52	52
Femur	Force [N]	6.8	6.8

The static option is verified with static deployment tests where the dummy is positioned close to the airbag module. The OoP test scenario was set up within this study in a generic laboratory environment according to the FMVSS 208-regulated AF05 female dummy positions:

- Position 1: Chin on module
- Position 2: Chin on rim

The following Figure 25 and 26 show the OoP occupant test setup for both positions:



Figure 25. Position 1 – side and front view of test setup

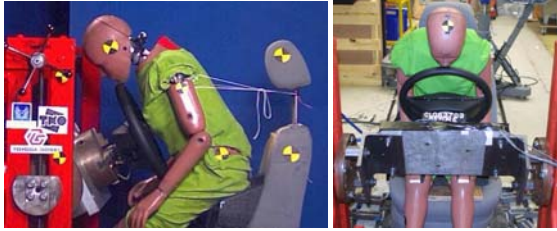


Figure 26. Position 2 – side and front view of test setup

In real vehicle environments, the windshield sometimes affects the dummy position 2. Correcting the steering-wheel angle is therefore a permissible procedure in order to avoid contact between the dummy head and the windshield. In the laboratory test, the steering-wheel angle could be kept constant for both dummy postures. To reproduce the exact dummy position later in the simulation approach, dummy target points were determined using a 3-D measurement device.

OCCUPANT OOP SIMULATION

The validated DAB module, including the airbag door, was inserted into the detailed steering-wheel model as indicated in Figure 27.

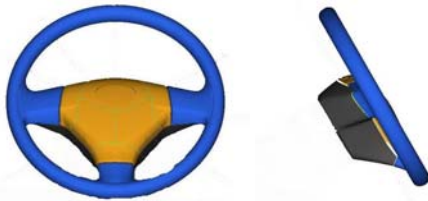


Figure 27. Detailed FEM steering-wheel model – front view and side view

The rim and the back cover were implemented as non-deformable rigid contact surfaces. The following Figures 28 and 29 depict the OoP occupant models for both positions.

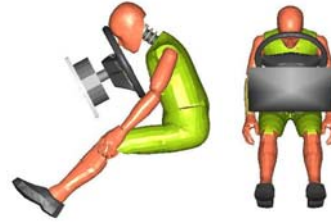


Figure 28. Position 1 – simulation model side and front view

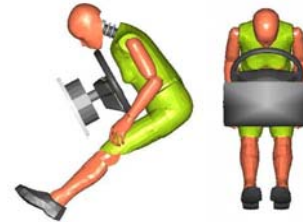


Figure 29. Position 2 – simulation model side and front view

Madymo’s AF05 facet data base dummy posture corresponds to the 3-D target points reported during testing.

Occupant position 1 results

Figure 30 shows the initial airbag deployment kinematics (simulation: left; test: right) at 10, 20 and 30 ms from the side view.

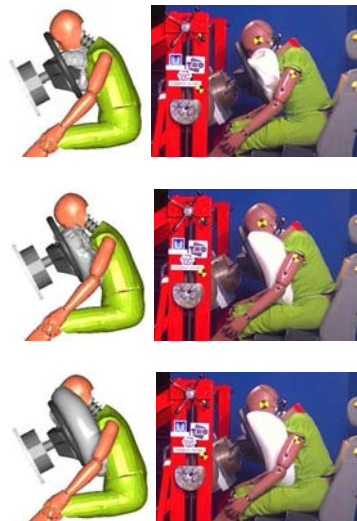


Figure 30. NHTSA position 1, test (right) versus simulation (left) for 10, 20 and 30 ms – side view

In simulation, friction between the airbag and the dummy influences airbag deployment towards the femurs and therefore a slight difference in kinematics

occurs in comparison to the test response. Table 4 lists the injury peak values reached in the test versus the simulation time history.

Table 4. Test and simulation OoP injury values – OoP position 1

AF05 injury criteria OoP position 1		Test average	Simulation
Head	HIC15 [-]	26	11
Neck	Nij [-]	0.24	0.24
	Tension [N]	580	890
	Compression [N]	20	70
	Flexion [Nm]	18	22
	Extension [Nm]	5	1
Chest	Accel. 3 ms [g]	11.0	8.2
	Deflection [mm]	9	7

Because the femur forces play a minor role within the laboratory test (no contact to an instrument panel was possible), they are not discussed further here. Whereas the neck values are overestimated by simulation, the simulated chest values are slightly lower than the test response. To evaluate the punch-out and the membrane-loading phases and their dummy injury cause in more detail, a closer look is taken at the injury curve characteristics below. As for dummy position 1, in which the chin is positioned closely in front of the airbag module, the punch-out phase greatly influences the head and neck dummy body area. Figures 31 to 33 plot the head and neck injuries obtained by the simulation model versus the test response for dummy position 1.

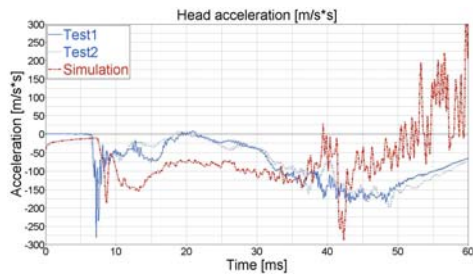


Figure 31. NHTSA position 1, injuries test versus simulation – head X-acceleration

The initial peak can not be correctly covered by the simulation for head acceleration, but is well reproduced for the upper neck force (punch-out effect).

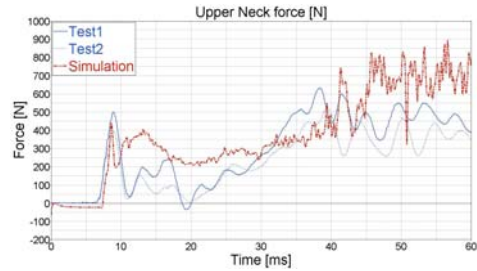


Figure 32. NHTSA position 1, injuries test versus simulation – upper neck Z-force

The membrane-loading phase (here approx. 10 ms to 40 ms) can be seen in the simulation. The released energy is relatively well transferred to the dummy in the simulation.

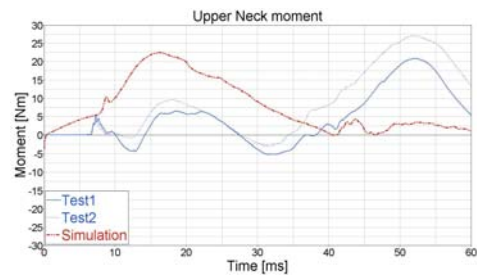


Figure 33. NHTSA position 1, injuries test versus simulation – upper neck Y-moment

Overestimating the neck moment timing, the injury value tendency of the head and neck can be predicted by the GF simulation. Figure 34 indicates the dummy test response versus the simulation time history of the dummy chest acceleration and chest deflection.

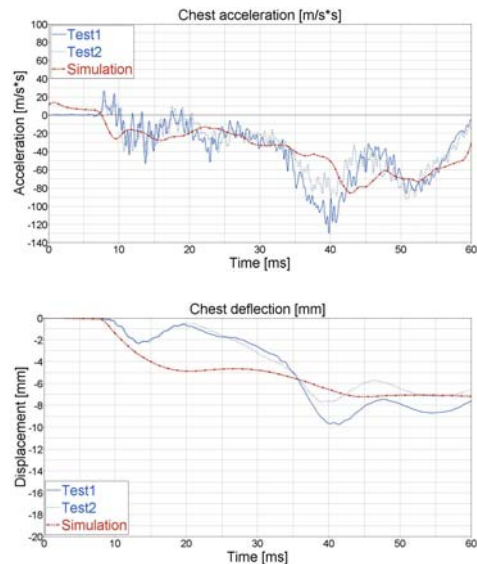


Figure 34. NHTSA position 1, injuries test versus simulation – chest X-acceleration and deflection

With respect to the dummy's measurement tolerance, the chest injury values are predicted by the GF simulation. The curve characteristics of the test response for the chest mark the membrane-loading phase (load increase to 40 ms). A good trend can be obtained by the advanced simulation method.

Occupant position 2 results

Figure 35 indicates the initial airbag deployment kinematics (simulation left versus test right) at 10, 20 and 30 ms from a side view for dummy position 2.

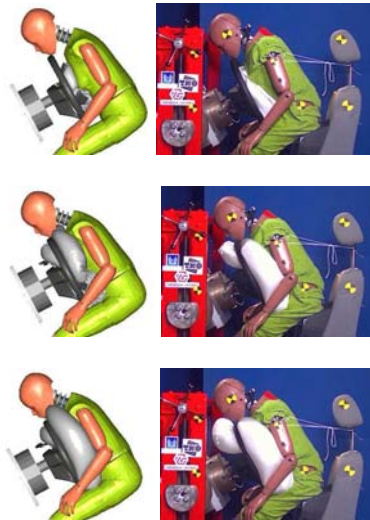


Figure 35. NHTSA position 2, test (right) versus simulation (left) for 10, 20 and 30 ms – side view

In simulation, the airbag mainly deploys below the upper rim of the steering-wheel. The friction between the airbag and the dummy could cause the differences compared to the test. Before the curve characteristics of the injury values are discussed in brief, Table 5 below lists the injury peak values – test versus simulation.

Table 5. Test and simulation OoP injury values – OoP position 2

AF05 injury criteria OoP position 2		Test average	Simulation
Head	HIC15 [-]	7	8
Neck	Nij [-]	0.18	0.33
	Tension [N]	430	570
	Compression [N]	25	30
	Flexion [Nm]	5	7
	Extension [Nm]	10	20
Chest	Accel. 3 ms [g]	11.7	10.7
	Deflection [mm]	20	23

The simulation slightly overestimates all the injury values. Figure 36 to Figure 38 plot the dummy head and neck injuries obtained by simulation versus the test response for dummy position 2.

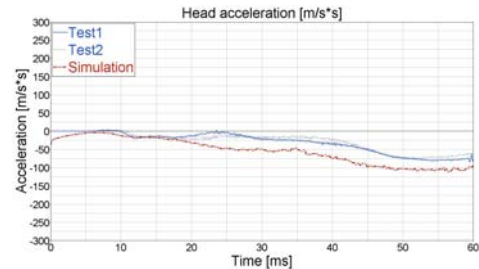


Figure 36. NHTSA position 2, injuries test versus simulation – head X-acceleration

The curve characteristic is followed well by the simulation.

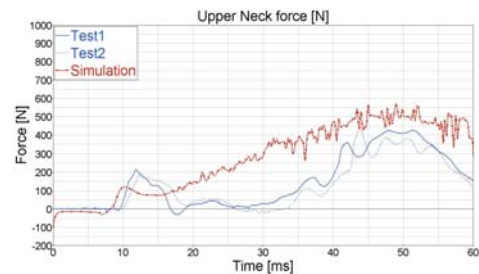


Figure 37. NHTSA position 2, injuries test versus simulation – upper neck Z-force

As already mentioned above, simulation overestimates the upper neck force. The increase of force during full deployment (membrane-loading phase) is covered by tendency.

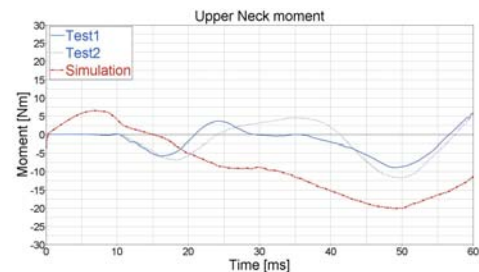


Figure 38. NHTSA position 2, injuries test versus simulation – upper neck Y-moment

The head acceleration and the neck force can be predicted by simulation, whereas differences within the neck moment are obtained. Figure 39 indicates

the dummy chest simulation time history versus the test response.

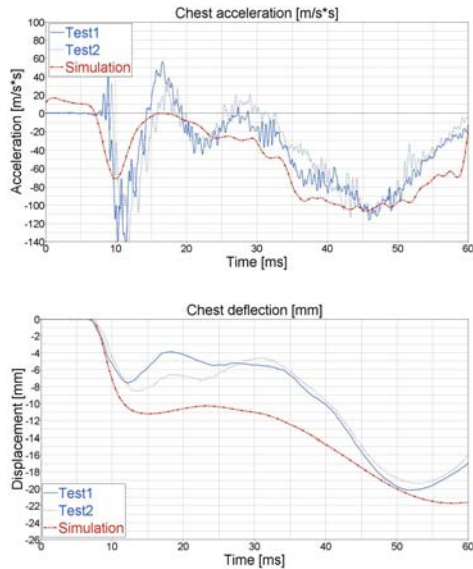


Figure 39. NHTSA position 2, injuries test versus simulation – chest X-accelerations and deflection

For position 2 (chest on module), the airbag punch-out effect affects the dummy chest body area more, whereas the head and neck injury values provide an indication of the membrane-loading phase. The punch-out phase in chest acceleration is covered by tendency but can not match the test response peak value. The load transfer during full airbag deployment (membrane-loading) is reproduced well by the advanced simulation.

DISCUSSION

Identification of the essential parameters by means of the appropriate experiments and CAE methods to model the folded airbag module leads to reasonable airbag validation within the simple one degree of freedom pendulum scenario (punch-out effect). Further replacement of the pendulum by the dummy model with its sophisticated contact surfaces such as head, neck, chest, arms and shoulders increases the numerical complexity. The thermodynamic energy released by the chambered airbag module presented is transferred to the dummy via the CFD gas transport algorithm (fluid-structure interaction) and finally by means of the numerical contact mechanics between the cushion and the dummy surfaces during the early stage of airbag deployment. The different loads measured in the dummy indicate the energy transmission in more detail. The airbag punch-out

and membrane-loading phase tendency observed in the laboratory tests are covered by the OoP simulation as a result of the investigation of the low-risk effectiveness of the initially chambered DAB design. Generally speaking, the FMVSS 208 relevant dummy load levels can be predicted by the advanced GF airbag simulation method using Madymo's facet data base dummy model. Whereas the CFD results are close to experimental response, there are still some differences, e.g. in the dummy neck injuries as also reported in [36] and in deployment kinematics, which need to be analysed further. With the application of the FEM AF05 dummy designed for the OoP load case, a further improvement in result quality is expected. The FEM dummy is equipped with more detailed upper body description (head, neck and chest contact surfaces) and improved soft tissue compliances (material model).

In the automotive industry's product development process, analysis and physical prototyping have co-existed for years. Being the key to a higher level of competitiveness in terms of faster-to-market and cost reduction for OEMs and suppliers, a big push in the direction of 100% virtual prototyping is going to take place in the near future in the area of CAx data management and processes as presented in [37] and [38]. What does this and the above summarised results of the OoP simulation with the advanced chambered airbag mean for the future development and design of new airbag technologies?

Based on the current study experience, it is the author's opinion that 100% virtual airbag prototyping and validation will be difficult to reach in the near future, not only because of the challenges in simulating long-term durability or aging, but also due to the following major hurdles in design disciplines which need to be overcome:

1. Inflator characteristics applied in the study are based on over-simplified assumptions (MTA). Intensive research work and collaboration with inflator suppliers is still required to identify correct inflator gas initial conditions and characteristics for CFD integrated airbag models.
2. Although the folder software and contact algorithm can handle the presented complex 2-D DAB cushion from folding over folded mesh relaxation, it is still a time-consuming process within the industrial design procedure. Further folding process optimisations are necessary which also take into consideration the complex folding of 3-D passenger airbags with internal gas deflection to improve the effective

application of the presented advanced airbag simulation methodology.

3. The accuracy and robustness of constitutive material models for engineering plastics and polymeric foams under high strain rate and large deformations for airbag door modelling as well as for robust response of local airbag dummy interactions (improvement of dummy model robustness).
4. In order to investigate the effects of design parameter variations, a vast amount of computing resources are needed.

CONCLUSION

The presented advanced initially chambered driver airbag performs in reality and virtually far below the injury value limits required by FMVSS 208. The advanced CFD airbag simulation methodology allows a deep insight into better understanding the physical problems. Therefore it is a helpful and powerful tool for pushing the future development of new airbag technologies. For instance by changing the cushion geometry – here the inner control volume of the presented chambered airbag – the effect on risk performance can be studied with numerical simulation. In mathematical terms, an approximation of the inner control volume size to the airbag volume itself leads to a conventional airbag. But shrinking with parallel application of new materials (to avoid burning) could lead to the next generation of advanced airbags designed for the low risk deployment target. Further, the CFD integrated simulation allows investigation into the effectiveness of different folding patterns in order to evaluate the consequences for the gas jet path and for the ensuing dummy injury values. The challenge of solving the airbag risk and protection compromise tells its own tale that further investment into the advanced airbag simulation methodology, as presented in this paper, will be a technically profitable task for the future.

REFERENCES

1. *Driver fatalities in 1985-1994 air bag cars.* Ferguson S.A., Lund A.K., Greene M.A., Insurance Institute for Highway Safety, Arlington, USA, 1995.
2. *Risk of death among child passengers in front and rear seating positions.* Braver E.R., Whitfield R.A., Fergusson S.A., Child Occupant Protection 2nd Symposium Proceedings (P-316), SAE, pp 25-34.
3. *Crash investigation reports.* U.S. NHTSA Department of Transportation, Washington DC, USA, 1998.
4. *5th Percentile Driver Out of Position Computer simulation.* R. Roychoudhury, D. Sun, M. Hamid, C. Hanson, SAE Paper 2000-01-1006.
5. *Driver Fatalities in Frontal Crashes of Airbag Equipped Vehicles: A Review of 1989-1996 NASS Cases, Accident Research and Analysis.* Cammisa X.C., Ferguson S.A., Lund A.K., SAE Paper 2000-01-1003.
6. *Assessment of Airbag Deployment Loads.* Horsch J., Lau I., Miller G., SAE Paper 902324.
7. *Dual-Stage Inflators and OoP Occupants - A Performance Study.* Malczyk A., Franke D., Adomeit H.-P., SAE Paper 982325.
8. *Ringairbag – Smart Driver Airbag Concept.* Krönes W., Schmidt W., 6th International Symposium and Exhibition on Sophisticated Car Occupant Safety Systems, Karlsruhe Germany, December 2002.
9. *Influence of Air Bag Folding Pattern on OOP-injury Potential.* Mao Y., Appel H., SAE Paper 2001-01-0164.
10. *A Math-Based CAE High-Speed Punch Methodology for Polymer Airbag Cover Design.* Lee M.C., Novak G.E., SAE Paper 2006-01-1187.
11. *Out of Position Simulation – Possibilities and Limitations with Conventional Methods.* Beesten B., Hagen S., Rabe M., 6th International Symposium and Exhibition on Sophisticated Car Occupant Safety Systems, Karlsruhe Germany, December 2002.
12. *Development of a Benchmark Problem Set for Assessing Out-of-Position Simulation Capabilities.* Wenyu Lian, SAE Paper 2004-01-1628.
13. *Numerical Simulation of Fully Folded Airbags and Their Interaction with Occupants with Pam-Safe.* Lasry D., Hoffmann R., Protard J.-B., SAE Paper 910150.

14. *Airbag modelling for Out-of-Position: Numerical approach and advanced airbag testing*. Rekveldt M., Swartjes F., Steenbrink S., Madymo User Conference, Como, Italy, October 2002.
15. *Advanced Airbag Fluid Structure Coupled Simulations Applied to Out-of-Position Simulations*. Ullrich P., Tramecon A., Kuhnert J., ESI Distributions, 2000.
16. *Simulation of Airbag Deployment Using a Coupled Fluid-Structure Approach*. Souli M., Olovsson L., Do I., 7th International LS-DYNA Users Conference, 2002.
17. *Evaluation and Comparison of CFD Integrated Airbag Models in LS-DYNA, MADYMO and PAM-CRASH*. Zhang H., Raman S., Gopal M. Han T., SAE Paper 2004-01-1627.
18. *OOP-Simulation – A Tool to Design Airbags? Current Capabilities in Numerical Simulation*. Beesten B., Hirth A., Reilink R., Remensperger R., Rieger D., Seer G., 7th International Symposium and Exhibition on Sophisticated Car Occupant Safety Systems, Karlsruhe Germany, November 2004.
19. *Madymo 6.3.1 Reference / Theory Manual*. TNO Madymo BV. Delft, The Netherlands. August 2006.
20. *Fully Multidimensional Flux-Corrected Transport Algorithms for Fluids*. Zalesak S.T., Journal of Computational Physics Vol. 31, pp 335-362, 1979.
21. *Solution of Continuity Equations by the Method of Flux-Corrected Transport*. Boris J.P., Book D.L., Methods in Computational Physics Vol. 16, Academic Press, 1976.
22. *Numerical Modelling of the Inflation Procedure of an Airbag and the Thermo-Chemical Process in the Gas Generator*. Rieger Doris, Institute of Aeronautics, Technical University Munich, October 2005.
23. *A Simulation Approach for the Early Phase of a Driver Airbag Deployment to Investigate OoP Scenarios*. Mahangare M., Trepess D., Blundell M.V., Freisinger M., Hoffmann J., Smith S., European Madymo User Conference, Cambridge, UK, September 2005.
24. *A Methodology for the Simulation of Out-of-Position Driver Airbag Deployment*. Mahangare M., Trepess D., Blundell M., Freisinger M., Hoffmann J., Smith S., International Journal of Crashworthiness, pp 511-517, November 2006.
25. *Investigation of an Advanced Driver Airbag Out-of-Position (OoP) Injury Prediction with Madymo Gasflow Simulations*. Freisinger M., Hoffmann J., Blundell M., Mahangare M., Smith S., International Madymo User Conference, Detroit, USA, November 2006.
26. *Advances in Airbag Inflator Modelling*. Bosio A.C., Lupker H.A., 4th International MADYMO Users Meeting, Eindhoven, The Netherlands, 1993.
27. *The Development and Validation of the Material Model Fabric_Shear for Modelling Advanced Woven Fabrics*. U. Stein, G. Weissenbach, M. Schlenger, M. Tyler-Street, P. Ritmeijer. 10th International Users Meeting. Amsterdam, The Netherlands. October 2004.
28. *A Study on the Modelling Technique of Airbag Cushion Fabric*. Hong S., Park S., Kim C., 9th International MADYMO Users Meeting, 2002.
29. *An Integrated Testing and CAE Application Methodology for Curtain Airbag Development*. Narayanasamy N., Hamid M., Ma D., Suarez V., SAE Paper 2005-01-0289.
30. *Airbag Fabric Picture Frame Test Manual. Version 1.0*, TNO MADYMO BV, 2005.
31. *Madymo Folder - Folding Airbag Models Version 9.0*. Oasys Limited. London, UK. November 2003.
32. *Capability of Simplified Folded Airbag Models in Gasflow Simulations*. Doris Rieger. 4th European Madymo User Conference. Brussels, Belgium. October 2004.
33. *Airbag Modelling Using Initial Metric Methodology*. Tanavde A., Khandelwal H., Lasry D., Ni X., Haug E., Schlosser J., Balakrishnan P., SAE Paper 950875.
34. *Analytical Design of Cockpit Modules for Safety and Comfort*. Lin J.Z., Pitrof S.M., SAE Paper 2004-02-1481.
35. *Validation/Verification of Hidden Airbag Door Loads and Kinematics*. Coulton J., CAD-FEM Users Meeting – International Congress on FEM Technology, Friedrichshafen, Germany, 2002.
36. *Use of MADYMO CFD for Driver Out of Position Simulation*. Lee W., SAE Paper 2006-01-0825.
37. *Digital Prototypes: Another Milestone for the Improvement of Processes and Cooperation in Vehicle Development*. Breitling T., Dragon L., Grossmann T., International VDI Symposium of Numerical Analysis and Simulation in Vehicle Engineering, Würzburg, Germany, 2006.
38. *Data Management, Process Support and CAx Integration of Engineering at Audi*. Reicheneder J., Gruber K., Wirch, W., Mayer S., International VDI Symposium of Numerical Analysis and Simulation in Vehicle Engineering, Würzburg, Germany, 2006.

REVIEWS OF SIDE KNCAP ON THE VEHICLE STRUCTURES AND OCCUPANT PROTECTIONS

Younghan Youn

Korea University of Technology and Education

Gyu-hyun Kim

Korea Automotive Testing and Research Institute

Sang-do Kim

Won-man Chung

Ministry of Construction and Transportation

Korea, Republic of

Paper Number 07-0423

ABSTRACT

The Ministry of Construction and Transportation of Korea (MOCT) has been conducted the side impact crash tests for the new passenger vehicles as a Korean New Car Assessments Programs (KNCAP) and provided crashworthiness and safety information to the public since 2003. Eleven compact passenger cars, four medium passenger cars and three SUVs and two Van type vehicles were evaluated according to the Korean side impact test protocols. Based on the test results, the most dominant factor for good star rating was the rib deflections of EuroSID-I. The next main factors were abdominal forces and pubic symphysis forces. The least influencing factors were viscous criteria and head injury criteria. Since KNCAP side impact program has been introduced, year after year, the newer vehicles gained the better grades. Especially, all SUVs and Vans with R-point over 700 mm get five stars due to higher side sill heights.

The main purpose of this study is to evaluate the trends of strength of vehicle structure changes, interior package design parameters, protection zone of side impact airbag or type of airbags to add additional counter measurements of side impact performances, such as a pole type impact test.

INTRODUCTION

In 1999, Korean government established the Korean New car Assessment Program (K-NCAP) after 3 years research work. The main purpose of KNCAP is that to not only promote buying a safer car but encourage auto makers to undertake more efforts in building safer cars by publishing test results every year. KNCAP also provide information on proper use of safety devices in order to enhance user's awareness and correct understanding on safety related devices such as

airbag, ABS and seat belts. At the beginning, frontal KNCAP test protocol and evaluation methods were identical to USA NCAP and only passenger car category was tested. In 2005, up to 4.5 tons of small trucks and vans were included in the K-NCAP.

The test items were only the full wrap frontal crash test and braking test until 2002, however, with 55kph impact speed side crash test was added in 2004 then in 2005, static roller and head restraint test were now part of K-NCAP as shown in Table 1. This year, the pedestrian head test will be added to evaluate the protection of pedestrian. Next year, 2008, the pedestrian leg test and dynamic head restraint test will be conducted. Until 2011, the test items will be expanded up to 10 test items.

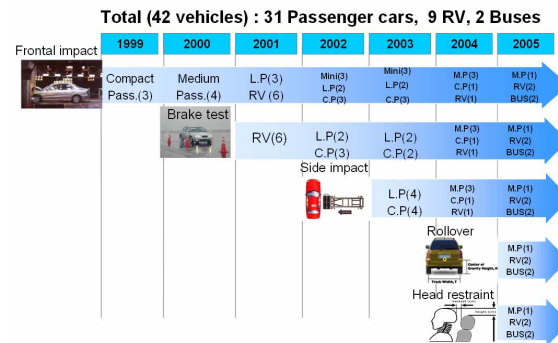


Figure 1. History and progress of KNCAP

ASSESSMENT OF SIDE CRASH ACCIDENTS

Police reported accidents data in 2005 show that 74.3% (159,063 accidents) of all accidents (214,171 accidents) were car-to-car type accidents, the pedestrian accidents were 21.8% and vehicle only involved accidents were 4.0% as shown in Figure 2. According to the police reports, during the fiscal year of 2005, total fatality of car-to-car type accidents was 2,659. Among the car-to-car type accidents fatality, the most serious accident type was side collisions. The side impact type accident's death was 717 (28%). The following higher fatality

was rear collision (25%) and the frontal collision type was about 22% as shown in Figure 3.

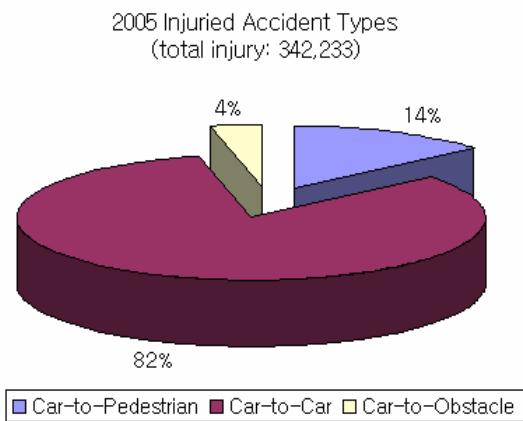
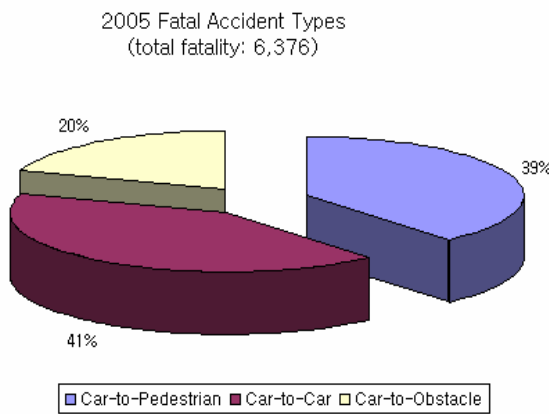
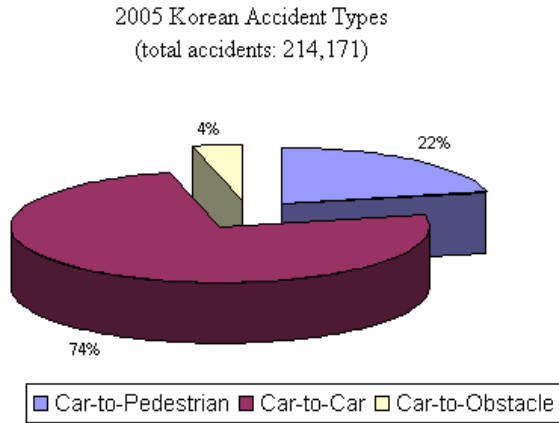


Figure 2. Traffic accidents, fatality and injury in 2005

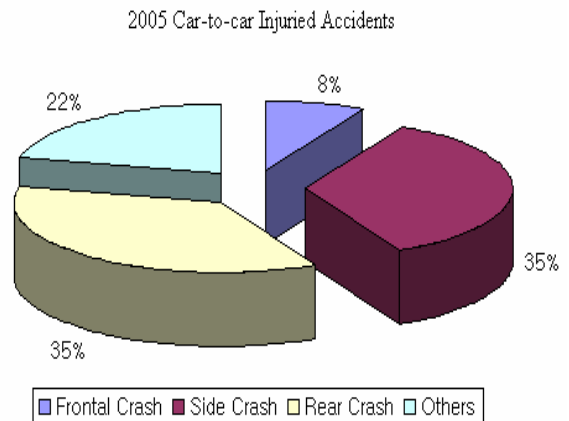
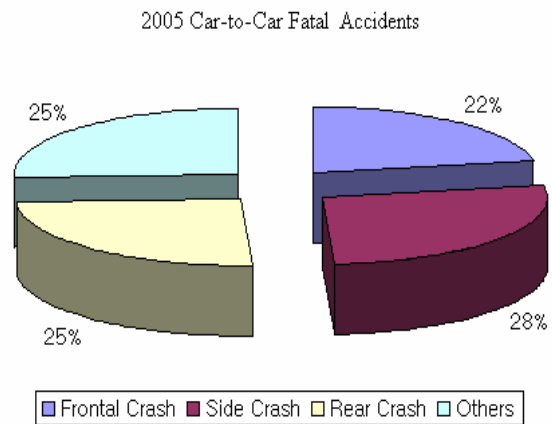
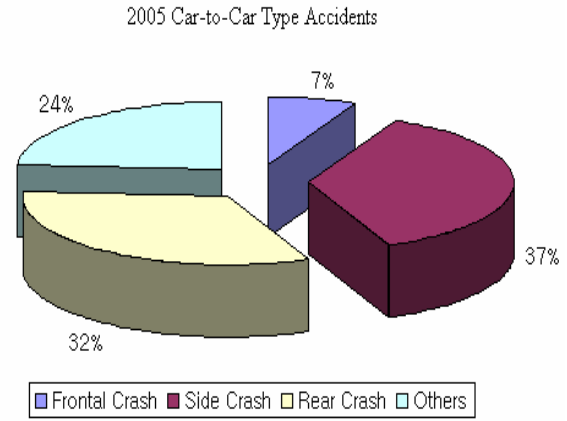


Figure 3. Car-to-Car involved accidents, fatality and injury in 2005

As shown above, the side collision was the most frequent accident type and life threatening accident in domestic traffic environments with rear collisions.

KNCAP TEST AND EVALUATION METHODS

The method of the side crash tests currently conducted by KNCAP is defined and documented in the “Regulation of motor vehicle safety standards” and the detailed test procedures and methods are listed in the bylaw of the regulations.

The test method and evaluation protocol is similar to the EuroNCAP with slightly higher impact speed. As shown in Figure 1, EuroSID-I is seated in the driver side. The reason higher impact speed than EuroNCAP is that the impact speed of Korean side impact regulation is currently set to 50 kph as shown in Figure 4. Currently the moving deformable barrier speed is 55 kph in KNCAP.



Figure 4. The schematic view of KNCAP side impact test

Table 1. Comparison of KMVSS and KNCAP

	Regulation (Act. 102)	KNCAP Side Impact
Type	90° Side Impact	Same
Effect. Date	2003. 1.1	2003.1.1
Speed	50 km/h	55 km/h
Dummy	EuroSID-1	EuroSID-1
Rate	Pass/Fail	5 Star rating

The performance of vehicle safety is evaluated by four items, injury rate, possibility of door opening during the test and door opening ability of after test, and leaking of fuel. The injury rate is calculated by the performance of driver side EuroSID-1. The injuries of head, chest, abdomen and pelvis will be calculated by formulation as

shown in Table 2. Each point of injury can interpolate and the total maximum possible points are 12 points.

Table 2. Side KNCAP injury evaluation methods

	Injury	Criteria	Points	% AIS>3
Head	HPC	650 - 1000	0 - 4	5 - 20
Chest	Rib def, mm	22 - 42	0 - 4	5 - 30
	V*C, m/s	0.32-1.0		5 - 50
Abdomen	Force, kN	1.0-2.5	0 - 2	Abdomen rupture (0)
Pelvis	Pubic Symphysis Force, kN	3.0-6.0	0 - 2	Abdomen rupture (0)
Total			0-12	5 - 50

The safety levels can be divided by 5 steps and the highest level has 5 stars and lowest level of side impact safety can get only 1 star as shown in Table 3.

Table 3. KNCAP star rating system

Star rating	point
★★★★★	10.50 – 12.00
★★★★	9.00 – 10.49
★★★	7.50 – 8.99
★★	6.00 – 7.49
★	0.00 – 5.99

KNCAP RESULTS AND DISCUSSIONS

During the last four years (2003 – 2006), total 21 vehicles were tested. Since small numbers of new vehicles were introduced in the market every year, KNCAP committee decided to selection of test vehicle with same class category as well as consideration of vehicle sales volume. Until recently the Korean new car sales have been dominated by large vehicle that including recreation vehicle (RV) - SUV and Van type cars, mediums size passenger cars as shown in Table 4. The KNCAP uses vehicle categories that align closely with the Code of Korean Vehicle Classifications (CKVC). The RV categories vehicle (SUV and Van) segments are combined in the KNCAP either Medium or Large depended on the engine sizes and vehicle weights.

Table 4. Sales Volume of Korean new car market

	2003	2004	2005	2006
Sub-compact	741 (-0.7)	753 (+1.5)	759 (-0.9)	759 (-0.3)
Compact	3,040 (-5.6)	2,816 (-8.0)	2,630 (-7.1)	2,441 (-7.7)
Medium	4,739 (+9.2)	5,064 (+6.2)	5,493 (+7.8)	5,907 (+7.0)
Large (incl. SUV)	1,750 (-22.3)	1,988 (+12.0)	2,240 (+11.2)	2,502 (+10.5)

Unit: 1,000 vehicles,
(): % of increment or decrement.

Table 5. Total Number of KNCAP side impact tested vehicles

	2003	2004	2005	2006
Compact	8	-	1	1
Medium	-	3	1	2
Large (incl. SUV)	-	1	4	-

Based on the test results listed in Table 6 - 8, the most dominant factor for good star rating was the rib deflections of EuroSID-I. The next main factors were abdominal forces and pubic symphysis

forces. The least influencing factors were viscous criteria and head injury criteria. All tested vehicle have full 4 points in HPC criteria thus the head injury criteria does not influence the overall star rating. In 2005, all tested vehicle have 5 stars due to their higher seating reference point, H-point, over 700 mm. Since the impact point between the moving barrier and vehicle side structures are below the H-points, the influences in chest and abdomen injuries was negligible.

Table 6. Test results and star ratings for compact cars

Year of Test	Maker	Vehicle	Grade
2003	KIA	RIO-SF	★★★
	GM-DAWOO	KALOS	★★
	HYUNDAI	NEW-VERNA	★★★★
	HYUNDAI	CLICK	★★★
	RENAULT- SAMSUNG	SM3	★★★
	GM DAWOO	LACETTI	★★
	HYUNDAI	NEW-AVANTE XD	★★★★
	HYUNDAI	LAVITA	★★★★★
2004	KIA	CERATO	★★★★
2005	KIA	PRIDE	★★★

Table 7. Test results and star ratings for the medium cars

Year of Test	Maker	Vehicle	Grade
2004	KIA	OPTIMA REGAL	★★
	GM-DAWOO	MAGNUS	★★★
	HYUNDAI	NF-SONATA	★★★★★
2005	RENAULT- SAMSUNG	SM5	★★★★

2006	RENAULT- SAMSUNG	SM5	★★★★★
	GM-DAWOO	GENTRA	★★★

Table 8. Test results and star ratings for the SUVs and Vans

Year of Test	Maker	Vehicle	Grade
2004	KIA	X-TREK	★★★
2005	KIA	SPORTAGE	★★★★★
	HYUNDAI	TUCSON	★★★★★
	HYUNDAI	STAREX	★★★★★
	SSANGYONG	RODIUS	★★★★★

The rib deflections and abdomen forces for each test vehicles were shown in Figure 5 through Figure 7. As shown in Figures, if the rib deflections were less than 30mm or the abdomen forces were less than 1.0kN, most of all tested vehicles have at least 4 stars. To get the 5 stars, the rib deflections should be less than 25mm and the abdomen forces are less than 2.0kN.

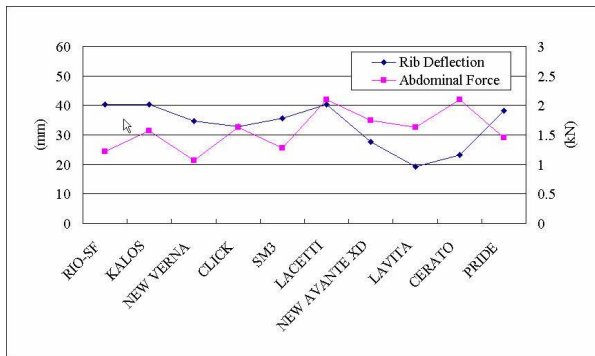


Figure 5. Rib deflection and abdominal force for the compact cars

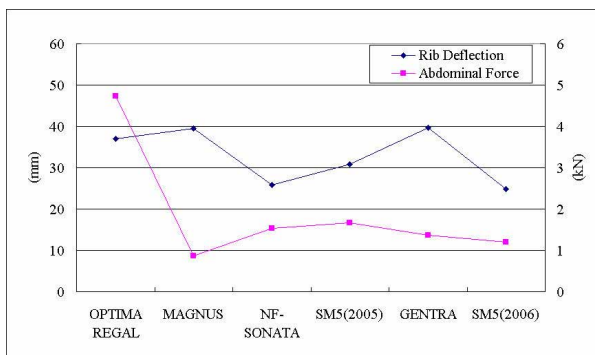


Figure 6. Rib deflection and abdominal force for the medium cars

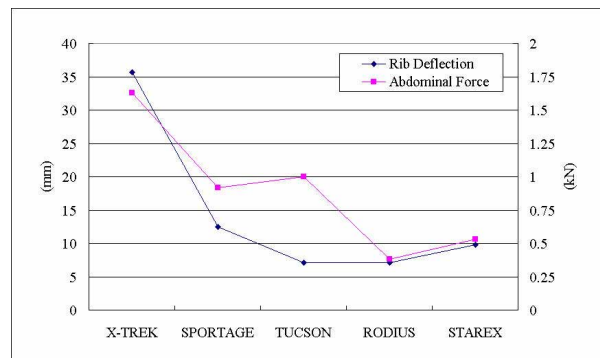


Figure 7. Rib deflection and abdominal force for the SUVs and Vans

As shown below Figures, the vehicle deformation, of course, differs greatly depending on the penetration speed at the door of the struck vehicle, and produces significant differences in the responses of the dummies. The amount of structural deformation of struck side directly influences the injury of rib deformation. To improve side crash safety performances, stiffer door impact beams or reinforced B-pillar structures are adopted recent model year vehicles. As alternative methods, additional proper padding material between door and occupant can protect the occupants. Even though there are no vehicles equipped with side thorax airbag or curtain airbag in domestically manufactured vehicles in the market. But from NHTSA study [], specifically side air bags systems appear to have improved side impact protection. Using a simple comparison of star ratings in the US side New Car Assessment Program (NCAP),

recent model year passenger cars and LTVs equipped with thorax air bags provided better overall thoracic and pelvic protection than vehicles not equipped. The vehicles equipped with thorax air bags may have other structural enhancements that contributed to their improved safety performance.

Figures in below show that the relationships between rib deflections and structural intrusions of the struck side door at the level of armrest.

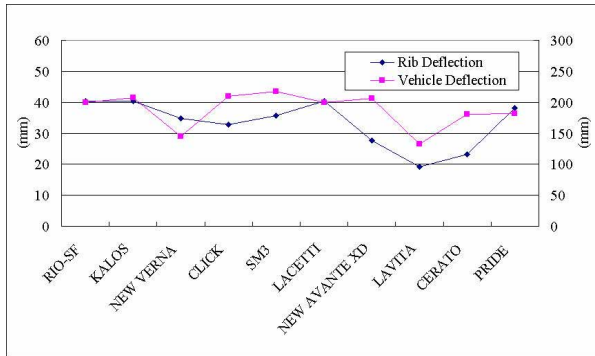


Figure 8. Rib deflection and vehicle deflection at the arm rest for the compact cars.

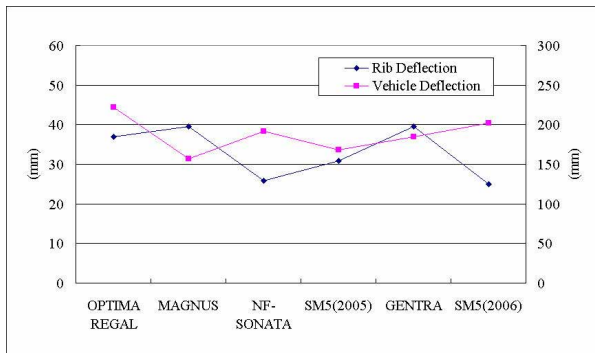


Figure 9. Rib deflection and vehicle deflection at the arm rest for the medium cars.

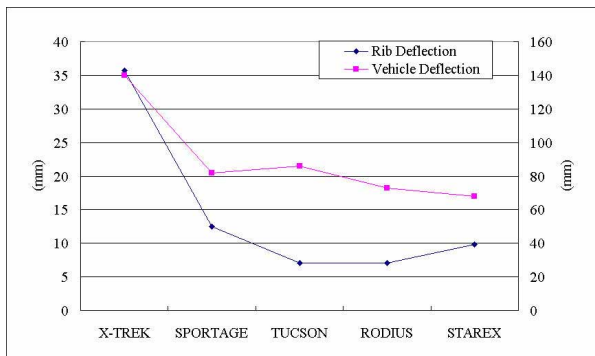


Figure 10. Rib deflection and vehicle deflection at the arm rest for the SUVs and Vans.

the arm rest for the SUVs and Vans.

A correlation was found between door intrusion velocities and chest deflections. The abdominal and pelvis forces become high as the vehicle deformation at the height of SRP is larger. The amount of rib deflections were in proportion to the amount of side structural deformations. The less deformation of side structures improves the chest injury. In addition to the vehicle deformation and intrusion velocity, padding and side airbag can also affect injury criteria in a side impact.

CURRENT PROBLEMS AND FUTURE KNCAP PROGRAMS

From this study, the performances of Korean side impact NCAP system was evaluated with 21 tested vehicles. Even though the evaluation periods was only 4 years test data with the limited test vehicles, this system can promote to improve safety performances in side collisions.

The most influencing factor for better star rating is rib deflection injury criteria. The most of vehicles that achieve the more than 4 stars reveal that their occupant rib deflection were less than 30 mm. If the rib deflection was less than 25mm, it can be a five star rated vehicle. Also, the abdomen force is relatively larger factor effecting in safety rating due to more than 2.0kN force of abdomen receiving a cut in marks. The HPC is the least influencing factor in safety evaluation.

In side impact tests, the injury criteria have been decreased by the side stiffness, B pillar layout, door pad, and airbag. As a result, the side impact score have improved, and the HPC, chest deflection, and pelvis force showed nearly full scores. The scores in the side impact test have become better as the ground height of the seat reference point has become greater, e.g., the MPV due to the height relation between the MDB barrier face and the seat reference point. Since in MDB tests, the contact of the dummy head does not occur in most cases, the risk of head injury which has been frequently observed in real side collisions is difficult to evaluate. Some cars have a new head protection

device like a curtain airbag. Therefore, pole impact and other tests should be introduced to evaluate these kinds of devices and head injury risk.

With close examinations of other NCAP test data such as NHTSA SINCAP, IIHS side impact and EuroNCAP, the KNCAP will be evaluated and updated to present better reproducing severity of the real accidents with adoptions of progressive type MDB and EuroSID-2 dummy.

REFERENCES

1. Yonezawa, H., et al “Japanese Research Activity on Future Side Impact Test Procedures” 17th ESV, Paper Number 267, (2001)
2. Seyer, K.,_International Harmonized Research Activities Side Impact Working Group,” 17th ESV, Paper Number 151, (2001)
3. ECE Regulation No.95,_Uniform provisions concerning the approval of vehicles with regard to the occupants in the event of a lateral collision,” (1995)
4. IIHS Status Report Volume 36, Number 1, (2001) 1. Hobbs, C. A., Gloyns, P. F., Rattenbury, S. J., European New Car Assessment Program – Assessment Protocol and Biomechanical Limits Version 2, May 1999.
5. Seeck, A., Friedel, B., Lutter, G., Appel, H., Das TUB-NCAP, Verfahren und der Vergleich zum Euro-NCAP, Crash-Tech special’98, March 1998.
6. Seeck, A., The Euro-NCAP and the German Ideas for a New Safety Assessment of Cars in Europe, 16th VDIK EuroNCAP Workshop, December 1998.
7. Hofmann, J., Kramer, F., Dausend, K., Side-Collision, Comparison of Dummy Loadings with Injuries of Real Accidents, III. IRCOBI-Conference, Lyon, 1978.

THE EFFECT OF IMPACT ENVIRONMENT ON OCCUPANT RISK AND THE BELTED/UNBELTED DILEMMA

Guy S. Nusholtz

Murthy Kowsika

Jianqing Xue

Yibing Shi

Guglielmo Rabbio

Laura Di Domenico

Fariba Famili

Lynn Byers

DaimlerChrysler Corporation

USA

Paper Number 07-0453

ABSTRACT

The fleet-wide occupant risk for frontal impact is estimated using a previously developed, data-based model. The model is constructed using the National Automotive Sampling System (NASS), the Fatality Analysis Reporting System (FARS), and the New Car Assessment Program (NCAP) databases and evaluated against Insurance Institute of Highway Safety (IIHS) data. The occupant risk is obtained from the NASS and FARS databases. The accident velocity distribution is obtained from the NASS data base. The vehicle impact response characteristics that are incorporated into the model are derived from the NCAP test data. The parameters included in the investigation are “intrusion” and vehicle “stiffness”, for both belted and unbelted conditions. The model is used to demonstrate that these are not independent in terms of overall occupant risk. The optimal level of vehicle stiffness is different for the belted and the unbelted conditions: Vehicle impact response optimized for the belted may be counter-indicated for the unbelted and vehicle impact response optimized for the unbelted may be counter-indicated for the belted. The model is used to study the effects of limiting intrusion, by stiffening the front structure in the current fleet. The results indicate that limiting the vehicle’s intrusion in this manner may reduce fleet wide occupant risk at the high impact velocities; however, it is counter-productive at low impact velocities and, may have no value overall in the current fleet for the current accident velocity distribution.

INTRODUCTION

In an effort to increase occupant safety and reduce fatality rates, the governments of many countries have enacted vehicle safety regulations that

automakers must comply in order to sell their vehicles. NHTSA has been tracking the fatality rates and publishes detailed reports each year, showing trends in vehicle occupant injuries and fatalities. Based on the data shown in Figure 1, the trend appears to be that the fatality rate has been progressively decreasing per 100 million vehicle miles traveled (VMT) for passenger cars (PC) and light trucks and vans (LTV).

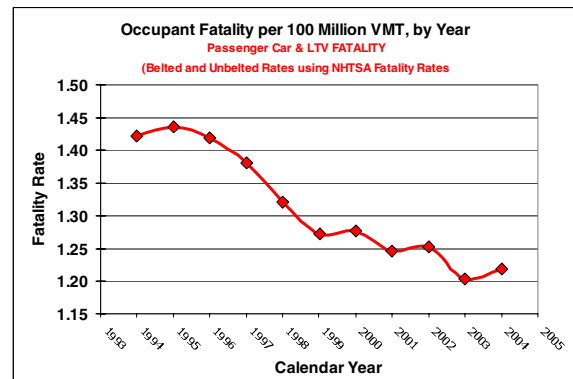


Figure 1. Fatality rate per 100 million miles traveled for PC & LTV.

What does this mean? Is it the result of regulations or ratings tests or something else. Many other factors have changed through the years and contributed to the trends shown above as well. One such change has been in seat belt usage, as reported by the National Occupant Protection Use Survey (NOPUS) which is shown in Figure 2. The reduction in fatality rate shown in Figure 1 could be attributed to the increase usage of belt.

Since there is considerable influence of safety belts on fatality risk, the effect of safety regulations and rating tests need to be ascertained for belted and unbelted cases separately. Using the data shown in Figures 1 and 2, along with the FARS fatality data for belted and unbelted occupants, the adjusted fatality

risk for unbelted and belted occupants are evaluated and are shown in Figures 3 and 4. Figure 3 shows that the fatality rate has been decreasing for belted occupants and Figure 4 shows that the fatality rate has actually been increasing for unbelted occupants.

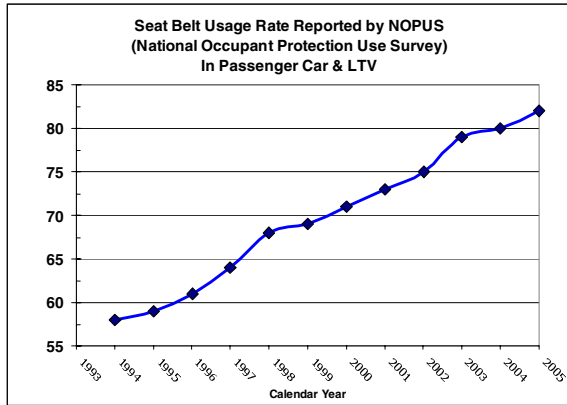


Figure 2. Seat belt usage rate reported by NOPUS for PC & LTV.

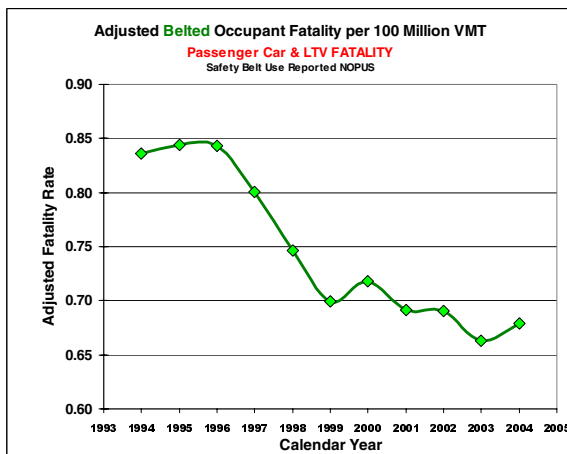


Figure 3. Adjusted belted occupant fatality rate per 100 million VMT.

Consequently, if it is assumed that these results are due to regulations or rating tests, then it appears that the regulations and ratings tests are providing a benefit for the belted and a dis-benefit for the unbelted. However, the foundational data shown in Figure 1, and the adjusted data shown in figures 3 and 4, are contaminated with driver behavior. Driver behavior is a very significant, possibly the most significant, contributing factor in accident and fatality rates. In particular, with the increase in seat belt usage, those who chose to remain unbelted tend to be higher risk takers than those who chose to wear seat belts. With a higher percentage of risk takers in the

unbelted group, it is inevitable that they will experience a higher percentage of accidents, and consequently fatalities (exacerbated by the lack of seat belt usage), per 100 million vehicle miles

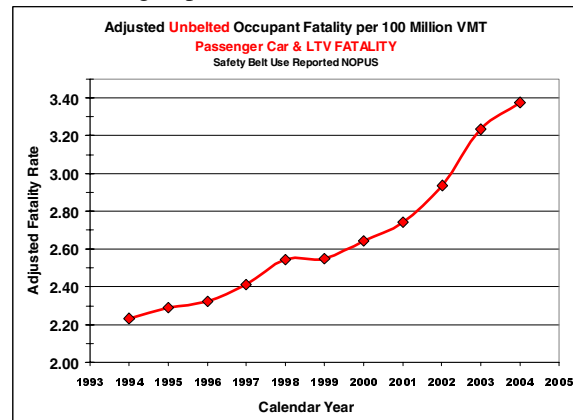


Figure 4. Adjusted unbelted occupant fatality rate per 100 million VMT.

traveled, than their belted counterparts do. Therefore, in this type of analysis, the fatality rates may be too dominated by driver behavior, Evans 2002. to allow the small effects of the regulations and ratings to be evident.

A double pair comparison method which is less sensitive to driver behavior was used by by Kahane [2000] to determine seat belt effectiveness., Using the seat belt effectiveness reported in this study, the fatality risk is once gain estimated for the belted and occupants and these results are shown in Figure 5. This study indicates that there is little change in fatality risk over several years for both the belted and unbelted once seat belts are removed from consideration.

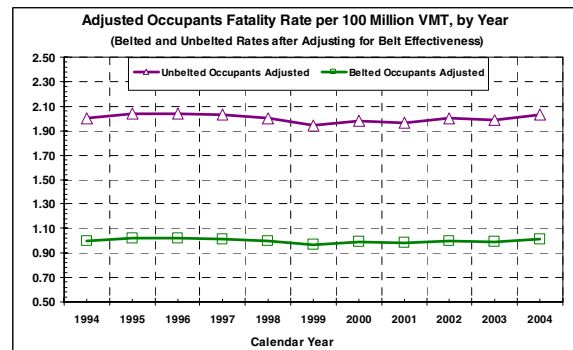


Figure 5. Adjusted occupant fatality rate based on restraint use per 100 million VMT.

Therefore, if we assume that the decrease in fatality rates for 100 million VMT is caused by regulations or ratings tests, then we can conclude that, at a

minimum, current regulations and/or ratings tests for the unbelted are unwarranted and may have negative benefits. However, most likely this assumption is not valid, and driver behavior dominates results to such a degree that the effects of the regulations and ratings tests can not be determined. This is an example of the complexity in trying to interpret the results of experimental tests, regulations, or ratings tests with the effect in the field.

We are going to try to address this complexity with one aspect of crashworthiness, which is the conflict between stiffness versus intrusion in vehicle crashes and the positive and negative effects they have on the belted and unbelted occupants, at slow and high speeds.

Frontal impact vehicle crash tests are conducted by various agencies worldwide to develop “safety” ratings for different vehicles. In The National Highway Traffic Safety Administration (NHTSA) New Car Assessment Procedure (NCAP), a vehicle is impacted against a flat, rigid barrier (RB) at 35 mph. In the Insurance Institute of Highway Safety (IIHS) and the European New Car Assessment Procedure (EuroNCAP) an offset deformable barrier (ODB) is used and the vehicle is tested at 40 mph. In the ODB test, the impact velocity is higher and the entire impact is concentrated on about 40% of the vehicle. As a result, the intrusion into the passenger compartment is generally higher than in the RB test. However, the RB test results in a significant change in velocity (Δv) over a much shorter time than the ODB test, leading to a higher average acceleration for the un-deformed part of the vehicle. Consequently, it is possible that in general, for the undeformed part of the vehicle, intrusion is more important than average acceleration for the ODB test, whereas, average acceleration (deceleration during impact) is more important for the RB test.

The above discussion points to two main issues in frontal impact crashes; i) intrusion and ii) average acceleration (deceleration of the un-deformed part of the vehicle upon impact). Fundamentally these two factors revolve around the amount of available energy to be transferred to the occupant and the rate at which this energy is transferred. The stiffness of the vehicle front end structure is currently an important aspect of energy management in the characterization of the vehicles in ODB and RB tests. A study by Agaram [2000] using different frontal impact excitation pulse shapes (but maintaining the same Δv and displacement) has shown that the simulated peak acceleration response of the unbelted HYBRID III dummy is considerably lower if the “stiffness” is higher in the initial stages of impact in the RB test. There are several theoretical models by Shi et al. [2003] and Wu et al. [2003] that suggest

similar findings. This clearly indicates that the response of the dummy is dependent on the characteristics of the deceleration pulse of the vehicle upon impact. However, based on a separate definition that takes into account the maximum crush and the maximum acceleration and time period of the crash pulse, Park et al. [1999] indicated that LTVs with a lower “overall stiffness” have shown an improvement in the vehicle crash “safety” rating in the RB test. A study by Nolan and Lund [2001], based on vehicles subjected to the ODB test, indicates that vehicle designs that minimize intrusion, by proportionately stiffening the front end structure and occupant compartment, can result in an improvement in the vehicle’s safety rating for that test. However, a report from NHTSA [2003], using an analysis of FARS data and an estimate of stiffness from NCAP tests, indicates that stiffening the front end of a vehicle increases occupant risk in car-to-car crashes. To complicate these results further, stiffness is never well defined, as reported by Nusholtz et al [2004, 2005]: The force-deformation (F-d) response in frontal impact tests is non-linear; the term “stiffness” is an undefined parameter and only relates to a general unspecified trend. Nonetheless stiffness does not seem to be a significant variable in terms of occupant risk. Instead, other parameters such as vehicle mass, belt use, and age are much more significant as reported by Padmanaban [2003] and Kahane [2003]. Occupant risk is also very dependent on crash severity as reported by Malliaris et al. [1985].

Velocity tends to be a good predictor of the severity of a crash: The higher the velocity of the crash the greater the severity and the higher the injury risk. The prediction of severity and injury risk can be further improved by using average acceleration instead of velocity. This assumes that the motion of the un-deformed part of the vehicle contains more of the necessary information than velocity to determine the injury risk and, that other variables such as intrusion contribute indirectly, as a function of average acceleration, and not directly as a function of the motion of the interior structures.

The relationship between intrusion and average acceleration is dependent on several factors, which includes the crash mode, seatbelt usage, and most importantly the severity of the crash. However, when different classes of impact severities are considered, the relationships between these two parameters (acceleration and intrusion) and their influence on injuries/fatalities keep changing. Over the entire range of possible crash velocities, intrusion correlates with average acceleration and both of them correlate with injuries/fatalities in the field; however, for the low crash velocity range, only a weak correlation is

noticed. Finally, in a domain where the velocity is “high”, there is an inverse correlation between the two parameters: Increased average acceleration implies decreased intrusion. In addition, injuries and fatalities can occur without intrusion. Consequently, the relationship of intrusion and injury could be poorly understood. Intrusion may be rightfully accused of causing the majority of the fatalities and injuries in the field, it may be a correlative variable that has little or no relevance, it may be somewhere in the middle, or it could be none of the above. It could be that the rate of intrusion is the critical value and intrusion is just a correlate. Assuming that intrusion is an important factor for causing injuries/fatalities, then some forms of intrusion control are also important. To accomplish this task, an estimator of crashworthiness with respect to intrusion would be needed. However, it is difficult to attribute the complex two-dimensional intrusion profile with a single descriptor that measures the crashworthiness of the vehicle. Nonetheless, several procedures have been developed to rate performance of vehicles based on intrusion (the EuroNCAP and IIHS ODB tests) with a metric that gauges the overall intrusion into the passenger compartment of the vehicle. In this study, a mathematical model is used to assess the influence of parameters that control intrusion on the fatality risk. The fatality risk is evaluated for both belted and unbelted occupants and any differences in the characteristics of the fleet, that influences occupant risk, are highlighted. An attempt is made to estimate the trade-offs inherent in implementing intrusion control. This is accomplished through field data obtained from FARS, NASS, and State databases and a fleet model developed by Nusholtz et al. [2003]. Using this data the correlation between the fatality risk and the intrusion rating obtained from ODB vehicle crash tests is assessed. Two separate analyses are conducted to deal with the IIHS and EuroNCAP test data independently.

THEORETICAL MODEL

A fleet model is developed to investigate the effect of stiffness and intrusion on the fatality risk as a function of impact velocity. The fatality risk for both belted and unbelted restraint conditions is assessed. This model is derived from an existing model originally developed by Nusholtz et al. [2003] that was used to understand the effects of vehicle size and mass on injury outcome. The vehicle is idealized as a mass attached to a non-linear spring, impacting against a rigid barrier at a prescribed velocity. The lumped mass represents the motion of the reaction surface (instrument panel,

steering wheel). A similar type of model is used by Shi [2003] for determining the crush pulse to minimize occupant risk.

For each impact velocity, a Monte Carlo simulation of 1000 crashes is performed, each using a random sample of the fleet populations of mass and the force-deformation response of the spring. The average acceleration (A) of the lumped mass is computed using the model. Using the relationship shown in Equation 1 the fatality risk (R) is evaluated from average acceleration. This equation is obtained by modifying the relationship reported by Evans [1994] which deals with occupant risk and closing velocity.

$$R_{unbelted} = \left(\frac{A}{C}\right)^{3.54} \quad (1a).$$

$$R_{belted} = \left(\frac{A}{C}\right)^{4.57} \quad (1b).$$

The distribution of the mass is obtained from NCAP tests. The force-deformation (F-d) response of the non-linear spring that is used for simulation is derived from 22 NCAP tests. For modeling purposes, instead of using the actual F-d trace of each vehicle, two separate parametric models, a two-step model and a linear elastic model as shown in Figure 6, are used to describe the F-d response. The two-step model is a better representation of the actual F-d response but the linear elastic model is also used to evaluate the effect of the type of F-d model on the fatality risk.

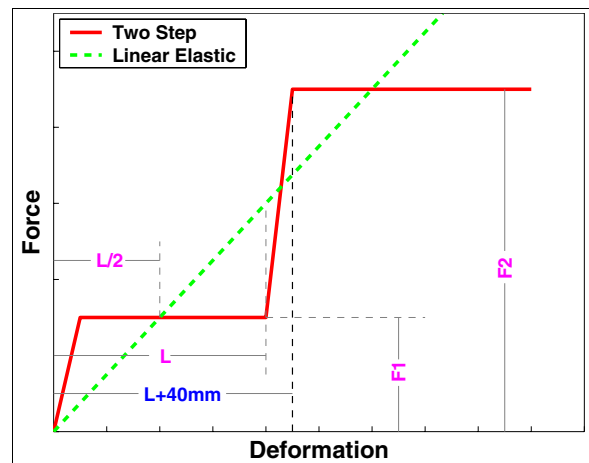


Figure 6. Schematic of the force-deformation response that is used in the mathematical model.

In general, the two-step model has a stiffer response in the initial stages when compared with the linear

model. By using the linear model we are assuming that the two-step model is stiffer than real world crashes and that the linear model is softer than real world. The difference could have an influence on the fatality risk output from the model. It should be noted that even though the F-d response is different between the linear and two-step models, the area under the curve, up to the crush length L, is maintained constant.

The parameters shown in Figure 6 that define the F-d response (for each model) are obtained by curve fitting the data obtained from each NCAP test. The F-d response parameters evaluated from all 22 NCAP tests are used to determine the mean and the standard deviation. This data is used for simulating changes to the stiffness of the fleet. The mass and the parameters (F1, F2 and L) are assumed to be normally distributed in the analysis. The amount of available crush is proportional to the parameter L (L+40 mm is used as available crush). For each run at a given impact velocity, the time (Δt) taken to consume the available crush is determined to estimate the average acceleration. Intrusion is assumed to start after the available crush is consumed. At each pre-selected impact velocity, several simulations are performed by changing the parameters mentioned above using the Monte Carlo procedure to obtain the distribution of the fatality risk. This information is used to calculate the average risk at each velocity. With the accident velocity distribution reported by Malliaris et al. [1997], the cumulative fatality risk up to each impact velocity is then calculated. In order to understand the influence of stiffness change of the fleet on the fatality risk, case studies are conducted in which the F-d response of the fleet is changed, by increasing and decreasing the initial stiffness (F1 in Figure 6) by $\pm 10\%$ and $\pm 20\%$ from its nominal value.

A model validation study is conducted to gain confidence in the mathematical models and their underlying assumptions by comparing the assessed fatality risk with accident data. The results from this study clearly indicated that the model is capable of capturing the fatality risk. The details involved in the model validation and their results can be obtained from a previously published study [Nushlotz, 2006].

RESULTS

One of the main aspects of this study is to evaluate the effect of stiffness (a parameter that controls intrusion) on the fatality risk. This investigation is carried out by changing the stiffness of the fleet by $\pm 10\%$ and $\pm 20\%$ from the nominal value. The results from these case studies are shown in terms of cumulative fatality risk which takes into account both

the fatality risk at a particular impact velocity and the likelihood of accidents at that impact velocity. The accident velocity distribution is obtained from the study by Malliaris et al. [1997] and it is reproduced in Figure 7. A gamma function is fitted through the data to facilitate the analysis.

The results obtained from the linear elastic model are shown in Figure 8. The title at the top of each plot shows the amount by which the stiffness has been changed from the nominal value. For example, a stiff/soft factor of 10% indicates that the fleet stiffness is changed to 90% and 110% from the nominal value and two separate analyses are conducted. As expected the cumulative fatality risk is lower for the belted when compared with the unbelted case. For the unbelted case, the cumulative fatality risk is always lower for a softer vehicle when compared with a relatively stiffer vehicle. However, for the belted case, the cumulative fatality risk for softer vehicles is lower only up to a certain impact velocity. Beyond that point, relatively stiffer vehicles seem to have a lower cumulative fatality risk.

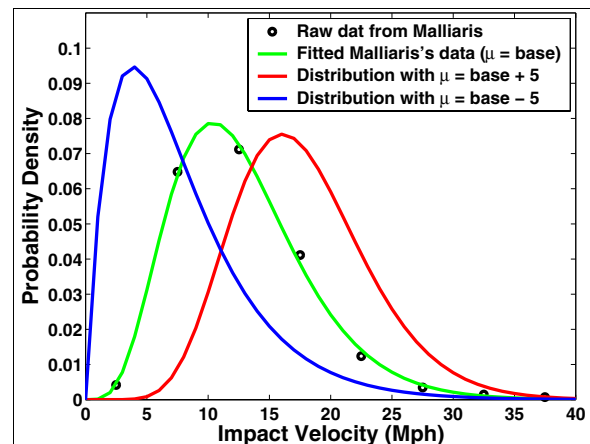


Figure 7. Accident velocity distribution.

Figure 9 shows the cumulative fatality risk obtained from the two-step model. For both belted and unbelted cases, the fatality risk for the softer vehicle is lower than the stiffer vehicles. Unlike the linear model, for the belted case, the results show that there is no cross over from a softer to a stiffer vehicle response, to minimize occupant risk as impact velocity increases, although the gap in fatality risk continued to decrease with an increase in impact velocity. The results clearly indicate that there is considerable reduction in fatality risk if there is a reduction in the stiffness of the fleet, especially at lower impact velocities. Also, the reduction in fatality risk for the unbelted case is much greater than

the belted case. The results shown in Figures 8 and 9 take into account the impact velocity up to a maximum of 40 mph. For numerical reason the model is not able to predict accurately beyond 40 mph. However, since the accident velocity distribution shown in Figure 7 indicates very few accidents beyond an impact velocity of 40 mph, the cumulative fatality risk should not be greatly altered after 40 mph.

The results shown in Figures 8 and 9 indicate that stiffness changes to the fleet influence the cumulative fatality risk to a varying degree depending on the impact velocity. As a result, any change to the accident velocity distribution clearly affects the cumulative fatality risk. A case study is conducted to understand the trends in fatality risk with a change in the accident velocity distribution. If it is assumed that the accident velocity distribution is related to the current driving environment and driving behavior, then changes to factors such as imposed speed limits, driver perception of appropriate speed, road conditions, etc., might have an influence on the velocities at which accidents occur. Assuming that the overall shape of the accident distribution is similar to the distribution reported by Malliaris et al. [1997], two separate distributions are constructed by shifting the mean by an amount of ± 5 mph. The resulting accident velocity distribution obtained by shifting the mean is shown in Figure 7. Only the two-step model is used in this study. The results shown in Figure 10 indicate that the cumulative fatality risk is not only lower at low velocities but the overall risk is also reduced by lowering the mean

accident velocity distribution. For the distribution where the accident velocities are lower, a relatively softer vehicle minimizes the fatality risk. However, upon increasing the mean of the accident velocity distribution, a clear cross over from softer to stiffer vehicles is seen at an impact velocity little over 30 mph. As a result, this case study indicates that the accident velocity distribution plays a significant role in determining the optimum stiffness characteristics of the fleet.

Since, in general, most safety rating tests are evaluated at the higher end of the accident velocity distribution, it is possible that the vehicles designed for higher impact velocities may not be able to provide an increased amount of safety benefit at lower impact velocities. Also, the safety rating obtained from vehicle crash tests puts an emphasis on minimizing the intrusion into the occupant compartment which leads to an increase in the stiffness of the vehicle. Stiffer vehicles that minimize intrusion at higher impact velocities may not provide adequate safety at lower impact velocities. As a result, the overall fatality risk, which is dependent on accidents occurring at lower, intermediate, and higher impact velocities, may not show significant improvement in real world safety. In order to understand whether the inferences from the mathematical model apply to real world vehicle crashes, the intrusion rating obtained from vehicle crash tests is used to see whether there is any correlation with fatalities. The details of this analysis are addressed in the following discussion.

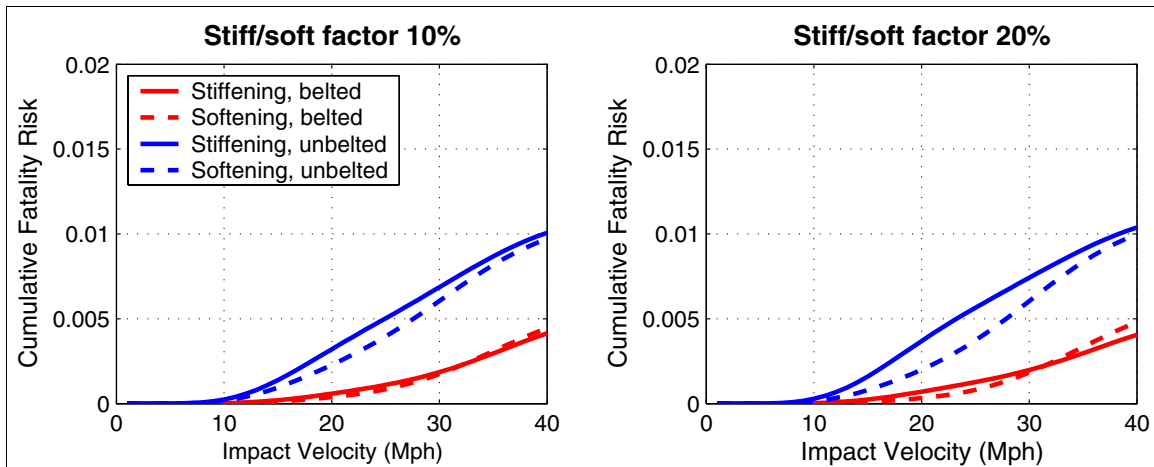


Figure 8. Cumulative fatality results obtained from the linear elastic F-d model.

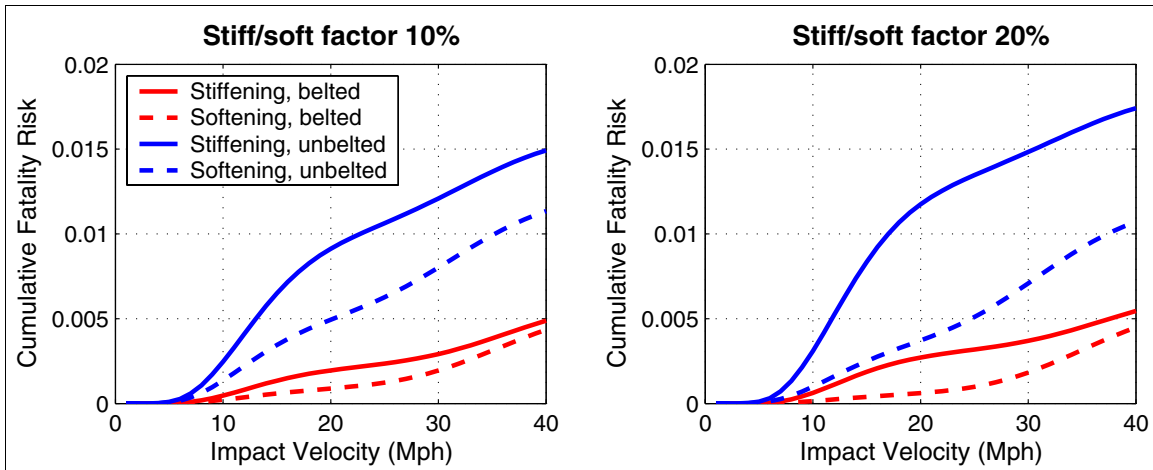


Figure 9. Cumulative fatality results from the two-step F-d model.

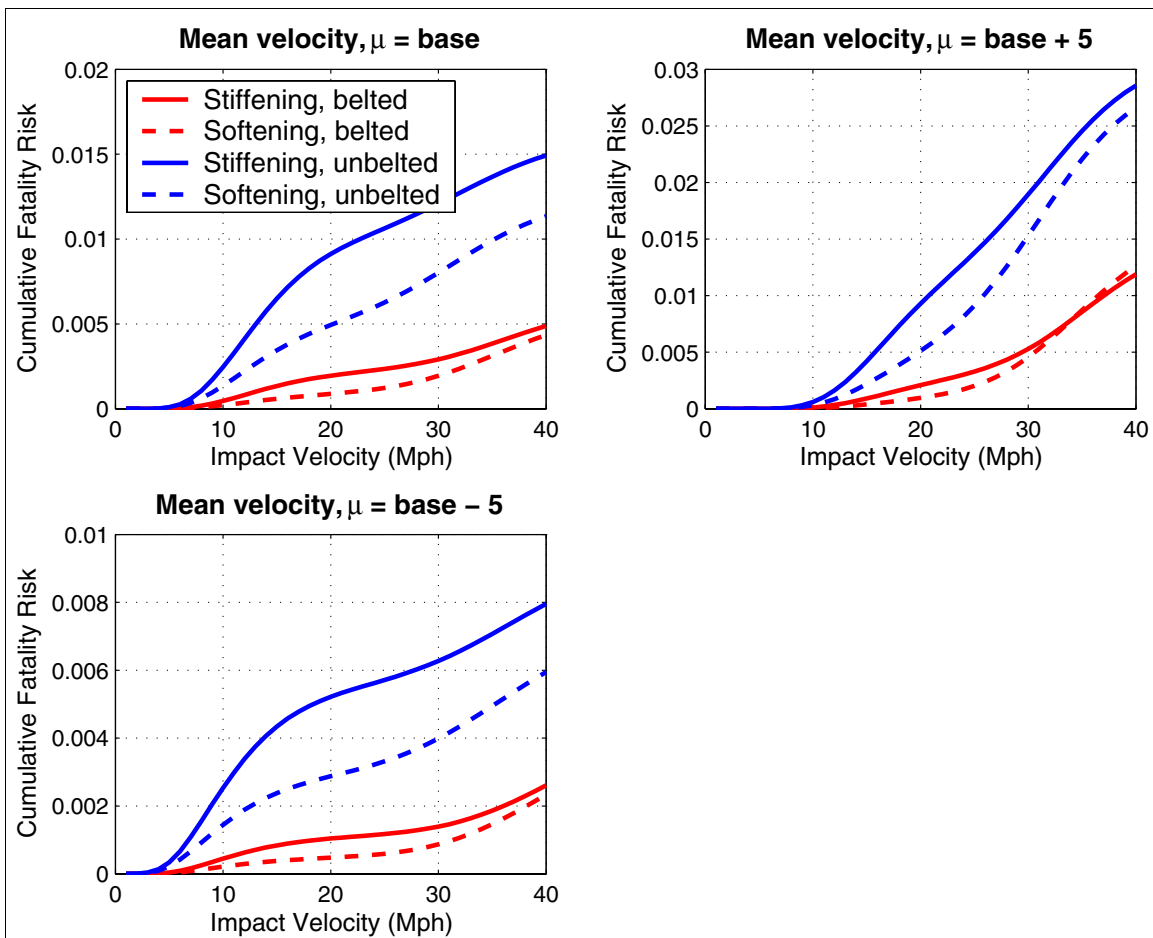


Figure 10. Influence of accident velocity distribution on the cumulative fatality risk (two-step F-d model and variation in stiffness is $\pm 10\%$ from the nominal value).

Analysis of Field Data

Determination of which vehicles are intrusion resistant should come from the accident data. However, a review of the NASS and FARS databases indicates that there is not enough data in NASS for each individual vehicle and not enough information in the FARS records to be able to determine intrusion resistance for the different vehicle make/models. Therefore, it is assumed that the vehicle intrusion ranking obtained from the IIHS ODB tests can serve as a surrogate for vehicle intrusion resistance. To facilitate the analysis, numerical values are assigned to the IIHS intrusion ratings: “good”, “acceptable”, “marginal” and “poor” ratings are mapped to values of 4, 3, 2 and 1, respectively. This integer parameterization can then be used to compare intrusion with fatality risk obtained from State accident databases and the Fatality Analysis Reporting System (FARS). Care is taken to include data from only those vehicles for which enough fatalities are recorded to make the results statistically meaningful. Details involved in the data collection method and subsequent analysis are presented in the following discussion. A discussion on the EuroNCAP rating as an estimate of intrusion and its correlation with fatality risk is also included.

The IIHS Intrusion Rating and Relative Fatality Risk are obtained from the IIHS web site and an analysis of the FARS database, respectively. The analysis of the FARS database includes data between the calendar years 1980-1999 for only car-to-car crashes that resulted in exactly one driver fatality: Therefore, the relative fatality risk for an average vehicle would be 50%. The model year of both vehicles involved in the accident is in between 1981-1998. Only those vehicles that are involved in ten or more accidents are included, but if sufficient data is not available, vehicles that are close to the subject vehicle are considered. Two different types of relative fatality risk are examined: raw and mass adjusted.

In order to adjust for mass, a logistic model developed earlier by Padmanaban [2003] is used. The risk adjustment, as a function of mass, is done for each individual vehicle; then the mass adjusted risk for each group of vehicles (“Good”, “Acceptable”, etc.) is assessed by aggregating the mass adjusted risk from individual vehicles. Vehicles that meet the data collection requirements are arranged as per the intrusion rating (Good, Acceptable, Marginal or Poor) obtained from IIHS ODB tests. Using the data obtained for each rating group, the average and the standard deviation of the relative fatality risk and mass adjusted relative fatality risk are evaluated. Table 1 indicates a

summary of the relative fatality risk for both belted car-to-car and all car-to-car crashes. In some cases, information for the “Marginal” rated group is not provided as it is based on limited data. The correlation between the relative fatality risk and the intrusion rating shown in Figures 11 and 12 indicates very little correlation between the two: R^2 values of 0.074 and 0.13 respectively.

Table 1.
Summary of relative fatality risk (%) for belted and all car-to-car crashes

Crash type	Good (%)	Acceptable (%)	Marginal (%)	Poor (%)
	Avg* (std)	Avg (std)	Avg (std)	Avg (std)
Belted Car-to-car	17.8 (9.8)	33.8 (23.4)	23.5 (---)	35.0 (21.7)
All car-to-car	30.6 (13.9)	38.2 (23.4)	50.7 (15.2)	48.9 (20.6)

*Avg is Average; std is standard deviation

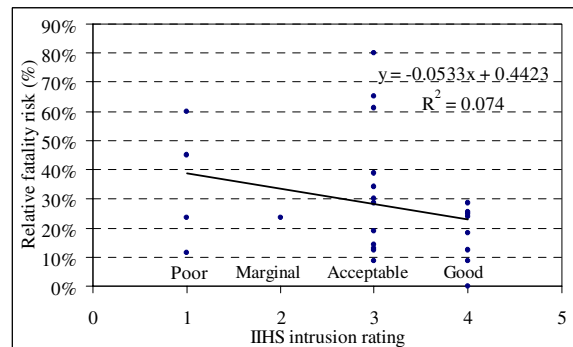


Figure 11. Correlation between relative fatality risk and intrusion for belted car-to-car crashes.

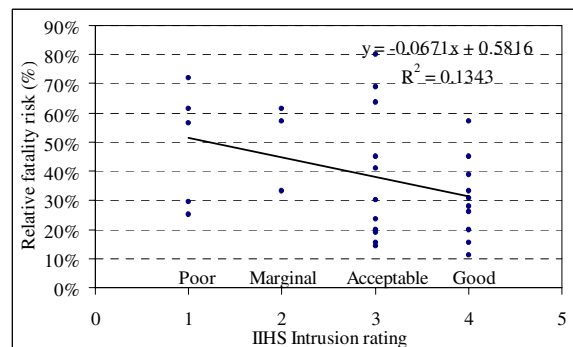


Figure 12. Correlation between relative fatality risk and intrusion for all car-to-car crashes.

A summary of the mass adjusted relative fatality risk for the belted and all car-to-car crashes with respect to each intrusion rating category is shown in Table 2.

Table 2.
Summary of weight adjusted relative fatality risk (%) for belted and all car-to-car crashes

Crash type	Good (%)	Acceptable (%)	Marginal (%)	Poor (%)
	Avg* (std)	Avg (std)	Avg (std)	Avg (std)
Belted Car-to-car	28.8 (14.3)	35.7 (17.8)	22.5 (---)	37.5 (20.8)
All car-to-car	39.2 (15.8)	36.6 (16.0)	40.8 (9.4)	46.2 (19.1)

*Avg is Average; std is standard deviation

It can be ascertained that the mass adjusted relative fatality risk between rating groups (e.g. “Good” and “Poor”) has become less discernable when compared with the relative fatality risk. Figures 13 and 14 show the correlation between the mass adjusted relative fatality risk and the intrusion rating for the belted and all car-to-car crashes, respectively. Comparison of the correlation coefficient (R^2) between Figures 11 through 14 also shows that when the relative fatality risk is adjusted for mass, the correlation between the relative fatality risk and intrusion diminishes further, as depicted by the correlation coefficient.

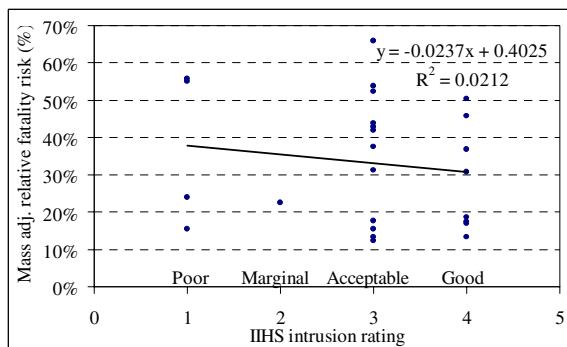


Figure 13. Correlation between mass adjusted relative fatality risk and intrusion for belted car-to-car crashes.

A statistical t-test is conducted to analyze whether the mean relative fatality risk of a particular “intrusion” rating group can be differentiated from the other groups. The t-test is conducted for both the relative fatality risk and the mass adjusted relative fatality risk. The results from the statistical t-test for belted and all car-to-car crashes are shown in Tables 3 and 4 respectively. The confidence level is set at 95% for performing the t-statistical analysis. The critical t-value determined based on sample size and this

confidence level are also listed within brackets in the table. For the belted case, there is limited data for the “Marginal” rated vehicles and it is not considered for analysis.

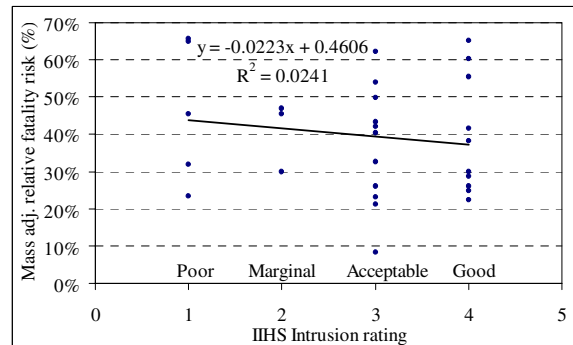


Figure 14. Correlation between mass adjusted relative fatality risk and intrusion for all car-to-car crashes.

Based on the data shown in Tables 3a and 4a, it can be assessed that the differences in the means of the relative fatality risk between “Good” and “Acceptable” as well as “Good” and “Poor” are statistically not significant at the 95% confidence level. However, considering that the computed t-value is closer to the critical t-value, it can be ascertained that there could be a differentiation between groups at lower confidence levels. For example, the t-value estimated between “Marginal” and “Good” ratings for the all car-to-car crashes is close to the critical value, indicating that the means can be differentiated at the 95% confidence level. The mass adjusted relative fatality risk shown in Tables 3b and 4b indicate a much lower t-value when compared with the t-value shown in Tables 3a and 4a, respectively. This indicates that when the relative fatality risk is adjusted for mass, the correlation between the “intrusion” rating and relative fatality risk diminishes considerably. In other words, there is no statistically significant correlation between the “intrusion” rating and mass adjusted relative fatality risk.

Intrusion and Severe Injury Risk obtained from Newstead, et al. [2002] is also used to highlight some aspects concerning the current study. They used the accident data obtained from several State databases (Florida, Ohio, and Pennsylvania). Only car-to-car crashes are considered in their analysis. Basically, this study is included to show whether the trends shown above, using the FARS database, are any different from the accident data collected from the state databases. The correlation between the mass adjusted severe injury risk and intrusion

measurements from IIHS ODB tests is analyzed. The intrusion that affects the driver, which includes the left lower instrument panel and steering column, is considered. The results from this study are shown in Figure 15. It is clear from this figure that vehicles

that show reduced intrusion in IIHS ODB tests do not show any significant difference in the mass adjusted severe injury risk when compared with other vehicles.

Table 3.

The data from t-statistical analysis showing the extent of separation of relative fatality risk between vehicle rating groups for *belted* car-to-car crashes

3a) Relative fatality risk

3b) Mass adjusted relative fatality risk

Intrusion rating	Good	Acceptable	Marginal	Poor	Intrusion Rating	Good	Acceptable	Marginal	Poor
Good	0	1.81 (2.1)	---	1.95 (2.2)	Good	0	0.91 (2.1)	---	0.86 (2.2)
Acceptable		0	---	0.10 (2.1)	Accept		0	---	0.17 (2.1)
Marginal			0	---	Marginal			0	---
Poor				0	Poor				0

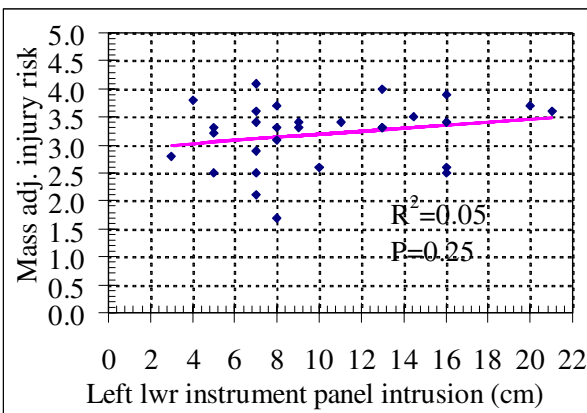
Table 4.

The data from t-statistical analysis showing the extent of separation of relative fatality risk between vehicle rating groups for *all* car-to-car crashes

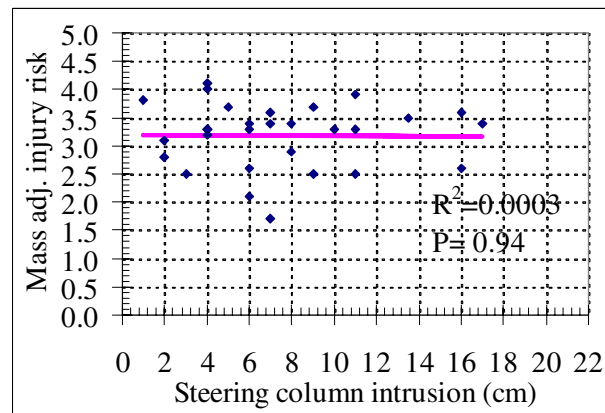
4a) Relative fatality risk

4b) Mass adjusted relative fatality risk

Intrusion rating	Good	Acceptable	Marginal	Poor	Intrusion rating	Good	Accept	Marginal	Poor
Good	0	0.90 (2.1)	2.16 (2.2)	2.06 (2.2)	Good	0	0.37 (2.1)	0.16 (2.2)	0.75 (2.16)
Acceptable		0	0.85 (2.2)	0.87 (2.1)	Accept		0	0.42 (2.2)	1.04 (2.1)
Marginal			0	0.13 (2.4)	Marginal			0	0.45 (2.4)
Poor				0	Poor				0



(15a)



(15b)

Figure 15. Correlation between the mass adjusted severe injury risk and intrusion measurements obtained from IIHS tests: a) left lower instrument panel; b) steering column.

Analysis Using EuroNCAP Test Data is conducted using a similar procedure as mentioned above for the IIHS test data. However, in the FARS database there are fewer numbers of vehicles that have both the EuroNCAP rating and sufficient field accident data (to determine the actual fatality risk) to do a thorough analysis. Based on this limited data set, the results indicate similar trends between the safety rating and fatality risk as observed using the IIHS data mentioned above.

An analysis is also conducted using the data from a recently published study by Lie and Tingvall [2002] that deals with police reported car-to-car crashes in Sweden between the years 1994 and 2000. There are some deficiencies in the analysis process reported by Lie and Tingvall associated with the mass compensation for adjusting the fatality risk (see Appendix). An attempt is made to address these limitations by using the procedure reported by Evans and Frick [1992] and Kahane [2003]. The results from this study indicate that there is no statistically significant correlation between the mass adjusted fatality risk and the EuroNCAP rating.

DISCUSSION

Two different F-d models are used to estimate the effect of average stiffness change on the fleet wide occupant risk response: One that, in general, overestimates the risk as seen in NASS and one that, in general, underestimates the risk as seen in NASS. Both models do not estimate risk over 40 mph. The models are limited in their ability to predict the precise nature of the changes in occupant risk that is seen in the field and only are used for general trends. Occupant risk trends that are seen in both models can be expected to be seen in the field, although not necessarily at the velocities or magnitudes as estimated by the models.

The first observation is that when the vehicle fleet is stiffened there is an increase in risk at the low velocities and a decrease in risk at the high velocities. This is true for both F-d models and, for the range of variation evaluated, is independent of the amount of stiffness increase, velocity distribution, belted and unbelted distribution, and amount of crush available before intrusion begins. This result indicates that stiffening the vehicle to prevent intrusion has a complex relationship with occupant risk and it is dependent on a considerable number of confounding factors. It implies that stiffening the vehicles to prevent intrusion could increase or decrease the fleet wide occupant risk depending on factors such as velocity distribution, belted/unbelted distribution, mass distribution, etc.

Since the model evaluates the fatality risk based on the average deceleration of the vehicle during a crash, the energy absorption characteristics play a dominant role on the estimated fatality risk. Softer vehicles undergo more crush and minimize the average acceleration leading to lower fatality risk for low to medium impact velocities. Even though stiffer vehicles can minimize intrusion for crashes at higher impact velocities, at relatively low impact velocities there is little intrusion but higher average acceleration contributing to an increase in fatality risk. Another reason for relatively minor improvements in cumulative fatality risk for stiffer vehicles at higher impact velocities is attributed to a lower number of accidents at those velocities as per the accident velocity distribution.

Most “safety” vehicle evaluation procedures (NCAP, IIHS, EuroNCAP, etc.) typically assume(implicitly) that when occupant risk in vehicle crash tests conducted at relatively high impact velocities is reduced by stiffening the vehicle to prevent intrusion then there is also a reduction in risk at the lower impact velocities or at a minimum there is no significant increase in occupant risk. However, taking into account the accident velocity distribution and the safety merit offered by relatively softer vehicles at lower impact velocities, this may not be true and those vehicles may not show improvements in overall safety. The models indicate that reducing intrusion at “high” velocities by stiffening the front end of the vehicles should have little effect, or a slight negative effect, on overall risk. Since the models can only give general trends it is not completely unlikely that there is some overall reduction in occupant risk as a result of stiffening. However, The accident data analysis done in this paper using IIHS intrusion ratings as a surrogate for reduced intrusion at high impact velocities indicates that there is no benefit to the current fleet by stiffening the vehicle to reduce intrusion.

Three different case studies are conducted to compare the intrusion/safety rating with actual field data obtained from FARS and State databases. In the first case study, the intrusion rating obtained from the IIHS ODB tests is used. This study has shown that even though there is a fair correlation between the relative fatality risk and intrusion rating, the mass adjusted fatality risk has shown no statistically significant correlation with the intrusion rating. A recent study conducted by Farmer et al. [2005] using a different metric, in which the mass adjusted fatality risk is computed based on the number of vehicle registrations, which involves driver behavior and crash characteristics, also indicates that there is no clear correlation between the overall safety rating and fatality risk. However, a marginal change in the

fatality risk between the “Good” and “Poor” rated vehicles is noticed, which is also seen in the current study.

In the second case study, the data reported by Newstead et al. [2002] is utilized. The correlation between the mass adjusted severe injury risk and the intrusion measurements obtained from IIHS ODB is analyzed. This study deals with the data obtained from State databases and it helps to check the mathematical model predictions using separate databases. The results also indicate that the mass adjusted severe injury risk for the vehicles that have a minimum amount of intrusion (at the left lower instrument panel and steering column), in the IIHS ODB tests, have no statistically significant improvement over other vehicles.

In support of this result, Padmanaban [2003], using a logistic model, indicated that stiffness is not a statistically significant variable with respect to occupant risk. In contrast to that, a study by Kahane [2003] indicates that, for car-to-car crashes, stiffness is important and that “softer” is better, implying that stiffening to reduce intrusion may have an overall negative effect. Either result is consistent with the models and analysis presented here.

The second observation is that there is a difference in the effect of stiffening for the belted and the unbelted occupants. In all of the models presented here there is an overall dis-benefit, or almost no effect, for the unbelted to stiffening. For most of the models there is an overall benefit, or almost no effect to stiffening, for the belted. The implication is that optimized stiffness for the unbelted will be sub-optimized for the belted and optimized stiffness for the belted will be sub-optimized for the unbelted. Consequently, these results indicate that a common design solution in terms of stiffness characteristics of the fleet cannot be obtained for both belted and unbelted occupants. The optimal solution for the fleet will depend on the belted/unbelted distribution and will change with time as the percentage of belt usage increases. As a result the best solution might be to design for the belted only in anticipation of a high belt use in the future.

The third observation revolves around driver behavior. The results obtained from shifting the mean of the accident velocity distribution indicate that stiffness of the fleet needs to be lowered if the velocity distribution mean is reduced from the baseline distribution. On the other hand, fleet stiffness has to be increased to minimize fatality risk for an increase in the mean of the accident velocity distribution. These studies indicate that the optimal stiffness of the fleet is dependent on the accident velocity distribution. If the vehicle driving speed is lowered, then a softer fleet will minimize the

cumulative fatality risk. On the other hand, a stiffer fleet is required if the driving speed increases.

CONCLUSIONS

The results from this study are based on a limited amount of data; with the addition of more data in the future, there could be changes in the observed trends that are reported in this paper. More work is needed before the results can be generalized. With these limitations, the following conclusions can be drawn.

- The mathematical model indicates that limiting the vehicle’s intrusion by stiffening the front end structure may reduce fleet wide occupant risk at the high velocities but it is counter indicated at low velocities.
- The optimal level of vehicle stiffness is different for the belted and the unbelted conditions: Vehicle impact response optimized for the belted may be counter indicated for the unbelted and vehicle impact response optimized for the unbelted may be counter indicated for the belted.
- The model indicates that the crossover (from the softer to a stiffer response) occurs at an impact velocity of approximately 25mph; however, the model is only able to capture the general trend and not able to predict the exact crossover in the field. The actual cross over will depend upon many factors not addressed in the current model and may be higher or lower than 25 mph.
- The model indicates reducing intrusion by stiffening the vehicle has limited value. It reduces occupant risk at the high velocities and increases it at the low velocities with little overall benefit. This is consistent with the field data.

Stiffening the front end of a vehicle to prevent intrusion has a complex effect on occupant risk. The restraint condition, the velocity of impact, the fleet composition, relative stiffness, etc., all play an interacting role in the determination of overall occupant risk. This does not mean that front end stiffness or intrusion reduction is not important, but stiffening the vehicle to reduce occupant risk is a double edged sword: It can in some cases reduce occupant risk and in other cases increase occupant risk.

REFERENCES

- Agaram, V., et al. 2000. "Comparison of Frontal Crashes in Terms of Average Acceleration," SAE 2000-01-0880.
- Evans, L. 1994, "Driver Injury and Fatality Risk in Two-car Crashes Versus Mass Ratio Inferred Using Newtonian Mechanics," Accident Analysis and Prevention, Vol. 26, No. 5, pp. 609-616.
- Evans, L. and M.C. Frick. 1992. "Car Size or Car Mass: Which has greater Influence on Fatality Risk?," Am J Public Health, 82:1105-1112.
- Evans, L. 2002. "Traffic Crashes, Measures to Make Traffic Safer are Most Effective When They Weigh the Relative Importance of Factors Such as Automotive Engineering and Driver Behavior," American Scientist, Vol. 90, No. 3, pp. 244-253.
- Farmer, C. M. 2005. "Relationships of Frontal Offset Crash Test Results to Real-World Driver Fatality Rates". Traffic Injury Prevention, 6:31-37.
- Joksch, H., D. Massie, and R. Pichler. 1998. "Vehicle Aggressivity: Fleet Characterization Using Traffic Collision Data". DOT HS 808679.
- Kahane, C. J. 2003. "Vehicle weight, fatality risk and crash compatibility of model years 1991-99, passenger cars and trucks", DOT HS 809662.
- Kahane, C.J. 2000. "Fatality Reduction by Safety Belts for Front-Seat Occupants of Cars and Light Trucks," DOT HS 809199.
- Malliaris, A. C., R. Hitchcock and M. Hansen. 1985. "Harm Causation and Ranking in Car Crashes," SAE 850090.
- Malliaris, A.C. 1997. "Occupant Exposures and Incidence of Casualties in Light Vehicle Crashes," Final Report - Project funded by AAM conducted for the Ad Hoc Task Group on Advanced Restraint Systems.
- Newstead, S. V., C. M. Farmer, S. Narayan, and Cameron, M. H. 2002. "U.S. Consumer Crash Test Results and Injury Risk in Police-Reported Crashes," Report No. 191, Accident Research Center, Monash University.
- Nolan, J. M. and A. K. Lund. 2001. "Frontal Offset Deformable Barrier Crash Testing and Its Effect on Vehicle Stiffness," 17th ESV, Paper No., 487.
- Nusholtz, G.S., J. Xue, Y. Shi, F. Famili, L. Xu, G. Rabbiolo. 2006. "Effects of Different Vehicle Parameters on Car to Car Frontal Crash Fatality Risk Estimated through a Parameterized Model," Paper # 2006-01-1134, 2006 SAE World Congress, Detroit, Michigan.
- Nusholtz, G. S., L. Xu, Y. Shi, L. DiDomenico. 2005. "Vehicle Mass, Stiffness and their Relationship," 19th ESV, Paper # 05-0413.
- Nusholtz, G. S., L. Xu, Y. Shi, L. DiDomenico. 2004. "Vehicle Mass and Stiffness: Search for a Relationship," SAE 2004, Report No. SP-1878, pp. 69-75.
- Nusholtz, G. S., G. Rabbiolo, and Y. Shi. 2003. "Estimation of the Effects of Vehicle Size and Mass on Crash-Injury Outcome through Parameterized Probability Manifolds", Paper # 2003-01-0905, 2003 SAE World Congress, Detroit, Michigan.
- Padmanaban, Jeya. 2003. "Influence of vehicle size and mass and selected driver factors on odds of driver fatality", 47th Annual AAAM conference proceedings, AAAM, Lisbon, Portugal.
- Park, B. T., et al. 1999. "The New Car Assessment Program: Has It Led to Stiffer Light Trucks and Vans over the Years?," SAE 1999-01-0064.
- Shi, Y., J. Wu, and G. S. Nusholtz. 2003. "Optimal Frontal Vehicle Crash Pulses -- A Numerical Method for Design," 18th ESV Conference, paper number 514, 2003.
- Traffic Safety Facts 2003, A Compilation of Motor Vehicle Crash Data from the Fatality Analysis Reporting System and the General Estimates System, National Highway Traffic Safety Administration. DOT HS 809 775, January 2005.
- Wu, J., S. Bilkhu and G. S. Nusholtz. 2003. "An Impact Pulse-Restraint Energy Relationship and Its Applications," SAE 2003-01-0505.

APPENDIX

One of the major limitations of the study by Lie and Tingvall [2002] is the lack of an adequate explanation for the procedure that is used for adjusting the fatality risk to account for mass compensation. As shown in Equation 2, a mass compensation factor of 7% for every 100 kg change in mass is used in their analysis. However, when Equation 3 is used to match the fatality risk reported by Lie and Tingvall, the value of the mass ratio exponent α , that is used to compensate for mass, is found to be lower than the values reported by other researchers. The value of the mass ratio exponent (α) turned out to be 2.3, which is lower than the values of 3.8 and 5.5 reported by Evans and Frick [1992] and NHTSA [2003], respectively.

$$R_{comp} = R_1 * \frac{1.07^{((M_{case} - M_{avg})/100)}}{1.07^{((M_{opp} - M_{avg})/100)}} \quad (2)$$

$$R_{adj} = R_1 \left[\frac{M_{opp}}{M_{case}} \right]^\alpha \quad (3)$$

where,

- R_1 = Raw fatality risk
- M_{opp} = Mass of the opponent vehicle
- M_{case} = Mass of the case vehicle
- R_{comp} , R_{adj} = Mass adjusted fatality risk

Table 5 shows the adjusted fatality risk for different values of the mass ratio exponent. As mentioned above, the adjusted fatality risk when α is set at 2.3 results in values similar to those reported in the paper by Lie and Tingvall. However, using the same data, but with more widely accepted values of α , Table 5 indicates that there is no significant correlation between the safety rating and fatality risk.

Another limitation in the study by Lie and Tingvall is that variability in mass within each group is not considered in the analysis. The fatality risk is collectively adjusted for mass using the average mass of the struck and striking vehicles. However, there will be a difference in the adjusted fatality risk depending on whether the variation in the mass is considered or not. A case study is conducted to determine the influence of including mass variation, while assessing the adjusted fatality risk.

In this case study, the fatality risk is adjusted for mass by assuming that the variation in mass of the struck and striking vehicles is to be normally distributed. Assuming that the variation in mass is about 8% of the average value, a case study is conducted to determine the influence of mass variation on the adjusted fatality risk. The results are

shown in Table 6. When the variation in mass is taken into account, although at lower values of α the adjusted fatality risk has shown a correlation between the safety rating and severe injury/fatality risk, at higher mass ratio exponent values this relationship is not noticeable. This study indicates that adjusted fatality risk, evaluated using a reasonable spread in mass distribution with an appropriate choice of α , has shown no clear relationship with the safety rating.

Table 5.
Mass adjusted severe/fatality risk for different safety rating groups

Euro NCAP Rating	Severe/fatality risk				
	Actual	Mass adjusted risk			
		Eq.2	Eq. 3, for different α		
			2.3	3.8	5.5
No class	0.92	0.98	0.99	1.05	1.11
2 stars	0.92	0.89	0.87	0.85	0.82
3 stars	0.61	0.75	0.79	0.93	1.13
4 stars	0.63	0.7	0.72	0.77	0.83

Table 6.
Change in adjusted severe injury/fatality risk when the variation in mass is accounted for in the analysis

EuroNCAP rating	Adjusted severe injury/fatality risk			
	Baseline	$\alpha = 1.8$	$\alpha = 3.8$	$\alpha = 5.5$
No class	0.98	1.0	1.15	1.35
2 Stars	0.88	0.90	0.94	0.99
3 Stars	0.75	0.76	1.01	1.36
4 Stars	0.7	0.72	0.84	1.00